Proteolysis and ATP-Independent Disaggregation of Tau Aggregates by the Human Serine Protease HTRA1

Inaugural - Dissertation

zur

Erlangung des Doktorgrades

Dr. rer. nat.

der Fakultät für

Biologie

an der

Universität Duisburg - Essen

vorgelegt von

Simon Pöpsel

aus Schwelm

Juni 2014

Die der vorliegenden Arbeit zugrunde liegenden Experimente wurden am Zentrum für medizinische Biotechnologie (ZMB) in der Arbeitsgruppe Mikrobiologie II, Prof. Dr. Michael Ehrmann, an der Universität Duisburg – Essen durchgeführt.

1. Gutachter:	Prof. Dr. Michael Ehrmann
2. Gutachter:	Prof. Dr. Hemmo Meyer
Vorsitzender des Prüfungsausschusses:	Prof. Dr. Dr. Herbert de Groot
Tag der mündlichen Prüfung:	27.08.2014

Parts of this work are included in the following publications:

*Tennstaedt, A., *****Popsel, S., Truebestein, L., Hauske, P., Brockmann, A., Schmidt, N., Irle, I., Sacca, B., Niemeyer, C.M., Brandt, R., Ksiezak-Reding, H., Tirniceriu, A.L., Egensperger, R., Baldi, A., Dehmelt, L., Kaiser, M., Huber, R., Clausen, T., and Ehrmann, M. *Human High Temperature Requirement Serine Protease A1 (HTRA1) Degrades Tau Protein Aggregates.* Journal of Biological Chemistry *287*, 20931-20941. * shared first authors

Pöpsel, S., Sprengel, A., Sacca, B., Kaschani, F., Kaiser, M., van Oepen, T., Clausen, T., and Ehrmann, M. *ATP-independent disaggregase activity of human serine protease HTRA1* (in preparation)

Acknowledgements

I would like to thank Professor Michael Ehrmann for giving me the opportunity to work on this project, for great mentorship, exceptional support, understanding and so many inspiring discussions on science, scientists and beyond.

I also want to say thank you to all the past and present members of the Ehrmann lab, who have made this group such a comfortable environment to work in - these are Adam, Helmut, Mina, Insa, Svenja, Michael, Sonja, Christiane, Nicolette, Annette, Inga, Nina, Juliane, Melisa, Vanda, Heike, Kamilla, Kathi, Maike, Jens, Jasmin, Juliana, Yvonne, Jenny and all the many short term visitors and students. Thanks for providing guidance, help, discussions, fun, barbecues and special thanks to those who have become friends.

In particular, I would like to thank Melisa for showing me how many reactions and tubes one can put into a single experiment, and for being so helpful any time with whatever problem came up. Thanks Annette and Vanda for helping me getting my project started and for listening to and channeling my ideas from the start. Thank you to Nina, Vera, Olga, Melanie and Peri for their great help with microscopy. I am also very thankful to Barbara and Andreas for their work and patience with the AFM, and to Farnusch for doing mass-spectrometry. It was a great experience to meet Prof. Robert Huber and Prof. Kurt Wüthrich to discuss my project and future plans with them, and I am grateful for their advice and stimulative discussions.

For critically reading the manuscript and helping with formatting issues, I would like to thank Kathi, Vanda and Munisch, I really appreciate your time, effort and constructive feedback.

Thanks Helmut and Melisa for your friendship and fun inside and outside the lab. Thank you Kathi for being a great bench-mate and friend and thank you Kamilla for being an awesome friend, not only when things got tough.

A big thank you goes to my family, whose never-ending support and love helped me so much in all those years and gave me strength and confidence to keep going. Thank you Alex, Achim and Munisch for your great friendship.

Finally, I would like to thank Jule for being the most warmhearted and loveable person I have ever met.

Contents

List of Abbreviations

1°	primary
2°	secondary
A.dest.	distilled water
aa	amino acid
AD	Alzheimer's Disease
AF568	Alexa-Fluor 568
Ap	ampicillin
AP	alkaline phosphatase
APS	ammonium persulfate
ArA	arachidonic acid
BCiP	5-Bromo-4-chloro-3-indolyl phosphate
BSA	bovine serum albumin
Cm	chloramphenicol
CV	column volume
DAPI	4',6-diamidino-2-phenylindole
DMEM	Dulbecco's modified Eagle's medium
DMSO	dimethyl sulfoxide
DTT	dithiothreitol
EDTA	ethylenediaminetetraacetic acid
EtOH	ethanol
FBS	fetal bovine serum
HA	hemagglutinin
HAP	hydroxyl apatite
HCl	hydrogen chloride
HEPES	4-(2-hydroxyethyl)-1-piperazineethanesulfonic acid
Hsp	heat-shock protein
HtrA	high-temperature requirement A
IDP	intrinsically disordered protein
IF	immunofluorescence
IPTG	Isopropyl-β-D-thiogalactosid
MDH	malate dehydrogenase
MeOH	methanol
MES	2-(N-morpholino)ethanesulfonic acid
MOPS	3-(N-morpholino)propanesulfonic acid
MT	microtubule

NaAc	sodium acetate
NBT	nitro blue tetrazolium chloride
NEB	New England Biolabs
NFT	neurofibrillary tangle
Ni-NTA	Nickel-nitrilotriacetic acid
Ni-TED	Nickel-tris(carboxymethyl)ethylene diamine
o/n	over night
PAGE	polyacrylamide gel electrophoresis
PBS	phosphate buffered saline
PCR	polymerase chain reaction
pNA	para-nitroaniline
PTM	posttranslational modification
ROI	region of interest
rpm	rounds per minute
RT	room temperature
SDS	sodium dodecyl sulfate
SEC	size-exclusion chromatography
TAE	Tris-Acetate-EDTA buffer
TBS	Tris-buffered saline
TBS-T	TBS with 0.05% Tween
TCEP	tris(2-carboxyethyl)phosphine
TCEP-HCl	hydrochloride salt of TCEP
ThS	Thioflavin S
ThT	Thioflavin T
Tris	tris(hydroxymethyl)aminomethane
β-ME	β-mercaptoethanol

List of Figures

List of Tables

1. Introduction

1.1. Protein Homeostasis and Protein Quality Control

Proteins are the predominant class of biomolecules making up every living cell, by providing cell shape and plasticity, mediating the synthesis and reproduction of all cellular components, ensuring the energetic homeostasis as well as communication between cells and, ultimately, organisms. This implicates that the structural, metabolic and intercellular integrity of a cell is inseparably dependent on the abundance, localization and structural intactness of its proteome. The process of keeping all these aspects in balance and in agreement with the function of a cell is termed protein homeostasis (Hartl et al., 2011). In order to maintain protein homeostasis, cells have evolved a large number of dedicated factors which work in each life stage of a protein, from its synthesis to its degradation. Except for the synthesis rates, which are determined by the abundance of mRNAs, their stability and the rate of translation, the other aspects of protein homeostasis are controlled by the diverse group of protein quality control factors. Many proteins rely on the assistance of molecular chaperones for acquiring their native conformation which is needed for enzymatic activity and interactions with other biomolecules. For example, 10-20% of newly synthesized proteins in bacteria were found to be associated with chaperones (Ewalt et al., 1997).

The native conformation of a protein is considered one of a vast number of possible three-dimensional arrangements of the polypeptide chain which together represent the folding energy landscape of a protein (Figure 1). In principle, a protein can adopt every possible conformation marking a “dip” of low energy in the folding landscape, each of which may represent a folding intermediate, transition state or alternative conformation. Among these states, a few are productive, i.e. they allow the proper function, activity and interactions, while others may e.g. abort or reduce activity, distort interactions, or favor the assembly of insoluble protein deposits. Such protein aggregates are particularly stable and are thought to be toxic to cells (Dobson et al., 1998). In thermodynamic terms, the dissociation constant of involved protein monomers, K_{off}, is small as compared to the association constant K_{on} favoring their stable association with a preexisting aggregate and making the process of aggregation largely irreversible.

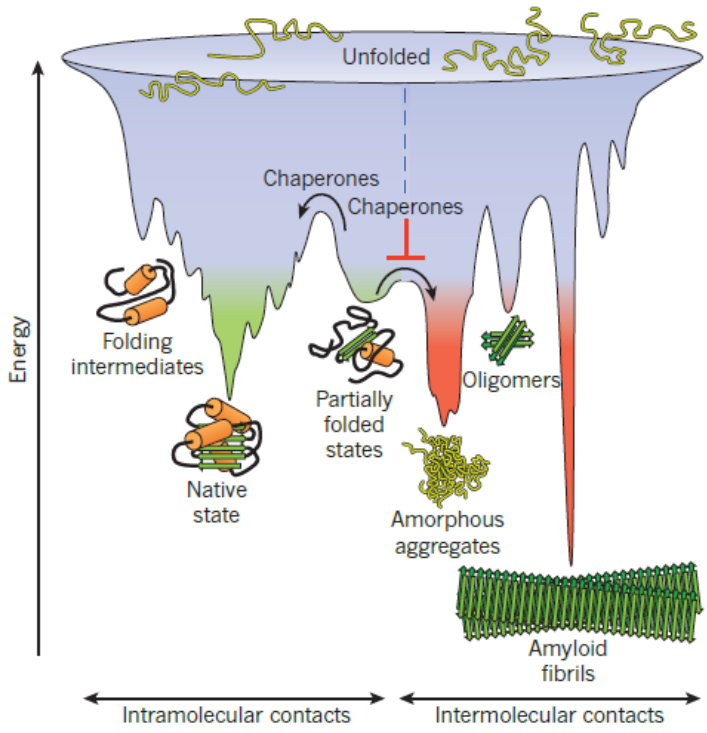

Figure 1 - Energy Landscape of Protein Folding

Simplified representation of the energy landscape of protein folding (adapted from (Hartl et al., 2011)). Minima of free energy represent stable folding states of a protein, with intermolecular interactions possibly giving rise to misfolded or aggregated species (in red). Chaperones facilitate the transition between states and favor the adoption of the native state (green) across barriers of high energy.

Molecular chaperones have evolved in order to lower the energy barrier a protein needs to surmount to transit between intermediate states of folding and at the same time to favor the acquisition of the native conformation over the formation of potentially aggregation-prone folding states (Figure 1). Chaperones can bind nascent polypeptide chains emerging from the ribosome, as well as misfolded proteins or even folded proteins which need to be unfolded for their transit across membranes or for subsequent degradation by the proteasome (Wickner et al., 1999). The accumulation of misfolded protein species represents a threat to cells because of corrupting proper protein function or due to the formation of protein aggregates. The causes may range from an increase in the protein misfolding rate, a decrease in the chaperone capacity or dysfunctional protein degradation.

As protein levels are dynamic, proteolysis targets not only misfolded proteins, but eventually every cellular protein that needs to be removed from the cellular protein pool or truncated for regulatory purposes. Consequently, the following parts will be concerned with the role of chaperones in assisting protein folding, with mechanisms of protein misfolding and in

particular protein aggregation, with the cellular measures operating to prevent and reverse protein aggregation, and with mechanisms of proteolysis.

1.1.1. Molecular Chaperones in Protein Quality Control

The native fold of a protein is referred to as the three-dimensional structure which allows its function, activity and correct localization in the cellular context. The native folding state is one of the energetically most favored states, but every protein can adopt a number of other conformations during the folding process. Moreover, a natively folded protein can misfold as a consequence of biophysical changes in the cellular environment and modifications such as phosphorylation or truncation. Both the initial folding and such influences on the mature protein may lead to misfolded conformations that can be thermodynamically very stable and therefore need to be avoided or reversed. Additionally, the crowded environment of the cell with concentrations of macromolecules exceeding 300 mg/ml (Zimmerman and Trach, 1991) provides conditions favoring protein aggregation, which confirms that faithful protein folding is a formidable challenge for the cell (Ellis and Minton, 2006).

Molecular chaperones employ a variety of mechanisms and act in several phases of protein folding, maturation, refolding and degradation to maintain a pool of structurally intact proteins. In addition to chaperone activity during phases of regular growth and metabolism, there are also regulatory mechanisms allowing the adaptation to conditions of protein folding stress such as elevated temperatures or high concentrations of reactive oxygen species, or the presence of misfolded proteins (Tyedmers et al., 2010) (Figure 2). The importance of these mechanisms is underlined by the observation that during aging, the risk of diseases which are associated with protein misfolding and aggregation, such as sporadic Alzheimer's disease, increases along with a decrease in the capacity of chaperone and proteolytic systems decreases (Morimoto, 2008).

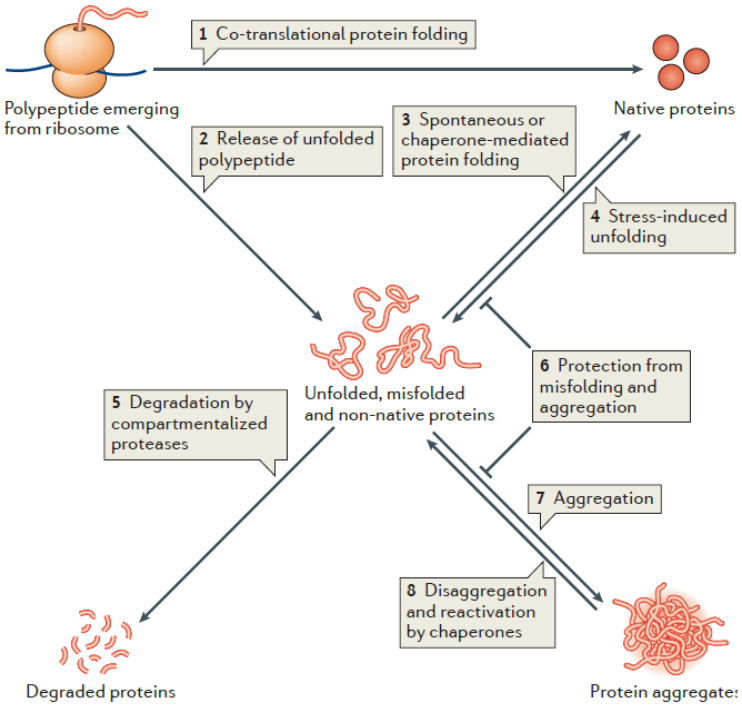

Figure 2 - The Involvement of Protein Quality Control in Protein Homeostasis

Protein quality control factors act at various stages in the life of a protein, including its initial folding (**1**), refolding of unfolded or misfolded species (**3**), the disaggregation (**8**) or degradation (**5**) of aberrantly folded proteins (center) as well as in preventing misfolding and aggregation (**6**). When protein quality control mechanisms are compromised or under stress conditions, unfolding (**4**) and aggregation (**7**) can pose a threat to cellular integrity (Doyle et al., 2013).

The most abundant and best studied chaperones belong to the family of the heat-shock proteins (Hsps), forming a diverse group of proteins that share being upregulated in response to folding stress conditions (Vabulas et al., 2010). They can be divided into classes of functionally and mechanistically related players. Chaperones and associated factors assemble into complexes which catalyze the folding, unfolding and refolding of their client proteins and by these means counteract or reverse misfolding and aggregation. The classic chaperone systems, members of which share a common mechanism of action, are called the HSP60 (also called chaperonins), HSP70, HSP90 and HSP100 systems in eukaryotes. There are many eukaryotic homologs found in each of these groups, giving rise to a total number of ca. 200 chaperones in a eukaryotic cell (Hartl et al., 2011). The core chaperone systems associate with a set of cofactors and co-chaperones conferring substrate recruitment (Kampinga and Craig, 2010) or assisting at individual steps of the chaperone cycle. For example, HSP40s are essential parts of the HSP70 chaperone system and strongly enhance ATP hydrolysis by HSP70. While the detailed mechanism of action and

molecular architecture differs strongly between these groups of chaperones, they share some general features. All of them preferentially bind hydrophobic stretches or patches exposed by their substrates, which is indicative of partial folding or misfolding and signals a risk of aggregation. By sequestering the hydrophobic parts of a client protein, chaperones prevent the formation of thermodynamically stable aggregates and may by these means provide a time-frame for the folding process of complex domains. Chaperonins shield their substrate proteins completely from the cytoplasm by forming a large cage, thereby providing a folding chamber. The structural rearrangement of substrate proteins depends on energy provided by ATP hydrolysis, which is coupled to conformational changes within the chaperone chamber.

Small heat-shock proteins (sHsps) act independently of ATP hydrolysis. However, they do not actively refold their substrates, but rather bind misfolded proteins under conditions of folding stress and by these means avoid their aggregation and keep them in a refolding competent conformation (Ehrnsperger et al., 1997; Lee et al., 1997). SHsps have also been described to be incorporated into aggregates leading to enhanced disaggregation (Mogk et al., 2003; Ratajczak et al., 2009). This implies that they are cofactors of protein quality control with a “holdase” rather than active refolding function (Sun and MacRae, 2005).

In addition to these cytosolic chaperone systems acting on single substrate proteins, there is a number of other mechanisms which mediate the assembly of multi-component macromolecular complexes, e.g. nucleosome assembly which is mediated by chaperone chromatin assembly factor-1 (CAF-1) (Verreault et al., 1996). In subcellular compartments of eukaryotic cells, specific factors have evolved which are related to the classical Hsp systems, such as the endoplasmic reticulum resident chaperone BiP/Grp78, which is a member of the HSP70 family of chaperones (Munro and Pelham, 1986). The extracellular space of eukaryotic cells cannot harbor functional Hsp systems due to the lack of ATP. At the same time, a number of diseases are characterized by the extracellular deposition of protein aggregates, which illustrates the need for extracellular protein quality control. Whereas refolding or disaggregating activities have not been detected in the extracellular space, ATP-independent chaperones which are related to sHsps, are suggested to counteract extracellular protein aggregation. They do so by stabilization of misfolded conformations or oligomers, which facilitates subsequent proteolysis or the uptake by endocytic mechanisms leading to intracellular degradation. Examples of such extracellular chaperones, which are closely related to cytosolic sHsps, are Clusterin, Haptoglobin and α_2-Macroglobulin (Wyatt et al., 2013).

Chaperones also play an important role for proteolytic degradation. HSP70 chaperones, for example, were found to bind misfolded proteins and mediate their interaction with the ubiquitin ligase CHIP to target them for destruction by the proteasome (McClellan et al., 2005). In chaperone-mediated autophagy (CMA), the constitutive HSP70 member HSC70 binds a subset of cytoplasmic protein substrates and mediates their translocation across the lysosomal membrane for proteolytic degradation in the lysosome (Cuervo and Dice, 1998). Thus, the surveillance of the folding states of cellular proteins is important for preventing aggregation, facilitating refolding, the degradation of misfolded proteins and normal protein turnover. Chaperones also participate in the process of disaggregation, in which protein aggregation can be reversed to recover or degrade proteins which have assembled into insoluble deposits, as will be described later (1.2.3).

1.1.2. Proteolysis and Protein Quality Control

Proteolysis is the enzymatic cleavage of peptide bonds by proteases, leading to the truncation or fragmentation of the substrate protein. A nucleophilic attack by the active site of the protease ultimately results in the hydrolysis of the peptide bond. The nucleophilic attack can be performed by several mechanisms, which are the basis of the classification of proteases. In serine, threonine and cysteine proteases, the respective amino acid (aa) residue represents the nucleophile, whereas aspartyl and metalloprotease use an activated water molecule for the nucleophilic attack of the substrate peptide bonds, with an aspartate residue or a complexed metal ion playing a crucial role (Figure 3).

a – Cysteine Proteases b – Aspartyl Proteases c - Metalloproteases

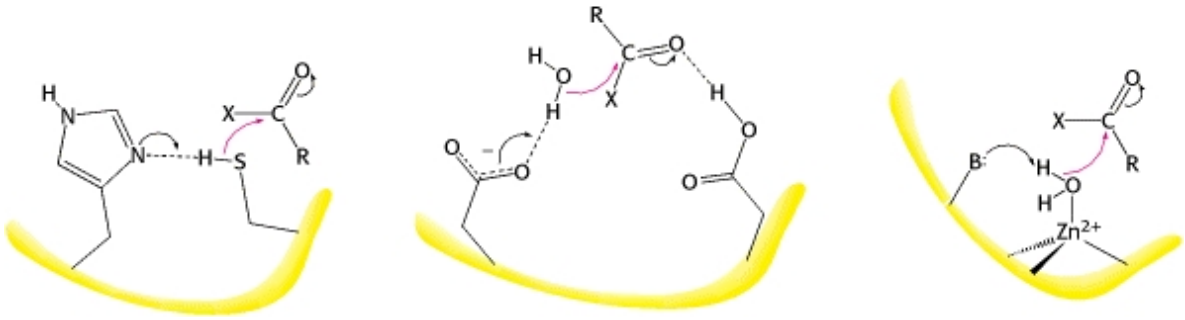

Figure 3 - Catalytic Mechanisms of Three Representative Classes of Proteases

Proteases catalyze the hydrolytic cleavage of peptide bonds by a nucleophilic attack (purple arrow) of the peptide carbonyl group. The nucleophile resides in the active site of the protease, where hydrolysis takes place. **a,** In Cys proteases, the nucleophile is a His activated Cys side chain. Serine proteases use a similar mechanism of the nucleophilic attack, but with a Ser side chain instead of a Cys in the active site. **b,** Aspartyl proteases make use of a water molecule activated by an Aspartate side chain located in the active site. **c,** In metalloproteases, the respective water molecule performing the nucleophilic attack is activated by a metal ion such as Zn^{2+}, which is complexed in the active site (Berg et al., 2002).

The substrate specificity of a protease determines which proteins can be substrates and thus be proteolyzed. The specificities of some proteases such as Caspases can be clearly defined and proteolysis restricted by the presence of recognition sequences, while other proteases are more promiscuous and recognize secondary structures or the charge of amino acid residues. Especially in the latter case, the need for tight spatial and temporal regulation of proteolytic activity becomes obvious. Functionally, proteolysis confers much more than just the degradation of aged and damaged proteins. Instead, proteolytic mechanisms serve regulatory roles in a vast number of cellular processes. Some prominent examples are cell cycle progression (King et al., 1996), the activation of apoptosis by Caspases (Salvesen and Dixit, 1997), and the degradation of extracellular matrix components required for cell migration (Stetler-Stevenson and Yu, 2001). Particularly, the exploration of the ubiquitin-proteasome system has shifted the view of proteases from waste disposal to regulatory devices (Hershko and Ciechanover, 1998).

To maintain protein homeostasis, damaged and aggregation-prone proteins which cannot be refolded have to be targeted for proteolytic degradation (Figure 2). The major degradative pathways of the cell are the ubiquitin-proteasome system and the autophagy-lysosomal pathway, which provide both endpoints of regulated proteolysis and mechanisms of the elimination of misfolded proteins. A large number of experimental studies have established a

close connection between protein quality control, proteolytic mechanisms and the pathogenesis of diseases associated with the accumulation of misfolded and aggregated proteins, such as neurodegeneration (Morimoto, 2008). The first studies pointing at the structure of proteins having an impact on their degradation rate were done in *E. coli* (Goldberg, 1972) and in reticulocytes, where aberrant proteins were shown to have a strongly reduced half-life. It was also shown that the proteasome preferably proteolyzes proteins with modified amino acid side chains (Tarcsa et al., 2000) which might render them more prone to aggregation. In the endoplasmic reticulum (ER), the recognition of damaged proteins leads to their elimination by means of the ER-associated protein degradation pathway (Meusser et al., 2005). The N-end rule ensures that proteins are targeted to protein degradation pathways depending on their N-terminal aa residues, which provides means of distinguishing between substrates which should be refolded and those which should be eliminated (Bachmair et al., 1986; Wickner et al., 1999).

Due to the proposed causal link between protein misfolding and disease, the proteolytic clearance mechanisms of aggregation prone proteins have been in the focus of interest. For example, inhibition of macroautophagy may result in the deposition of insoluble alpha synuclein deposits (Rideout et al., 2004), which are a hallmark of Parkinson's disease (PD). Accordingly, a functional consequence of interfering with autophagic proteolysis can be neurodegeneration (Komatsu et al., 2006), whereas activation of autophagy has a beneficial effect in experimental models of protein misfolding and aggregation diseases (Berger et al., 2006). The co-occurrence of p62, which is involved in autophagy, with intracellular Tau inclusions in Alzheimer's disease gives another hint to a link between proteolytic degradation pathways and the deposition of insoluble aggregates. In PD, deficient proteasomal degradation has been implicated in the pathological process (Dauer and Przedborski, 2003). In contrast to the protective effect in the course of protein quality control, proteolysis can lead to the formation of aggregation prone or toxic protein species. The most prominent example is the successive cleavage of the amyloid precursor protein (APP) eventually giving rise to Aβ peptides which play a central role in the pathogenesis of Alzheimer's disease (Selkoe, 2001). In summary, mechanisms of proteolysis are tightly connected to protein quality control under both physiological and pathological conditions and are therefore linked to protein folding and aggregation diseases.

1.2. Protein Aggregation

1.2.1. Mechanisms of Protein Aggregation

Protein aggregates arise from stable intermolecular interactions between proteins leading to large assemblies that may contain one or more different protein species. Typically, aggregation originates from partially folded states and is caused by the exposure of hydrophobic stretches of the polypeptide chain, which are normally buried in the core of a natively folded protein. The processes leading to intracellular aggregation can be diverse, but the general view is that it occurs when the mechanisms which normally prevent aggregation, i.e. refolding by chaperones or clearance by proteases, are overwhelmed and can no longer keep up with the production of misfolded protein species (Goldberg, 2003). The reasons can be both defects in protein quality control and a dramatic increase of misfolded proteins. The latter situation is frequently observed when heterologous proteins are overexpressed in *E. coli*. Other triggers are mutations leading to folding defects (Conway et al., 2000), the expression of truncated proteins or aberrant modification of aa side chains (Nilsson et al., 2002). In contrast, when protein quality control is boosted, e.g. by chaperone overexpression, the effects of protein aggregation can be often ameliorated (Auluck et al., 2002).

Apart from being a toxic consequence of protein misfolding, the regulated deposition of insoluble protein inclusions, termed aggresomes, might protect the cells against uncontrolled accumulation of misfolded proteins (Johnston et al., 1998). While many protein aggregates are usually believed to be largely unstructured, one exception are amyloids. Amyloids are characterized by a repetitive and clearly defined structure, the formation of which is associated with the pathogenesis of diseases, called amyloidoses. Although amyloid aggregates can be formed from a large number of proteins in vitro, only few proteins aggregate into amyloids in vivo. Thus, the type of protein as well as the location of aggregate deposition is characteristic of the respective disease (Merlini and Bellotti, 2003).

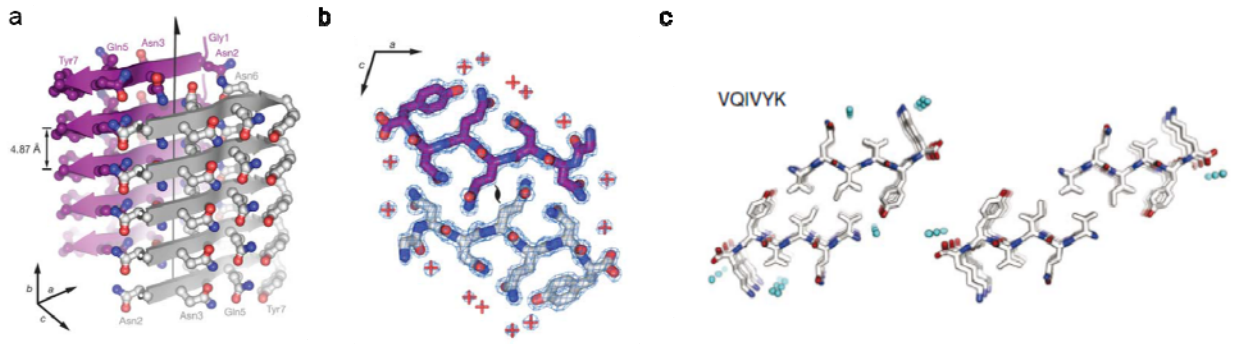

Figure 4 - Atomic Structures of the Amyloid Fibril Core

The classic cross-β structure arises from the regular, parallel stacking of β-strands and the assembly of two resulting sheets into stable, fibrillar aggregates. X-ray diffraction of fibrils composed of peptides derived from the yeast prion Sup35 (**a**, **b**) and Tau (**c**) show a common arrangement of polypeptides in the fibril core. The side chains of the amino acids alternate between pointing to the core or the outside of the fibrils. Interactions between individual β-strands are mediated by the peptide backbone, whereas the interaction of the β-sheets arises from the interdigitating of side chains and is stabilized by the hydrophobic effect. Therefore, water is excluded from the core giving rise to a “steric dry zipper” arrangement. **a**, The side view illustrates the stacking of β-strands with regular spacing and the antiparallel arrangement of sheets. Side chains are shown in ribbon representation. **b**, End on view of the interaction of Sup35 β-sheets with interacting side chains. Water molecules are represented as + symbols. **c**, Two alternative arrangements of Tau fibrils, displayed according to b, except for the water molecules being depicted as cyan spheres. Oxygen atoms are shown in red, nitrogen in blue (Nelson et al., 2005).

Structurally, amyloid aggregates typically form fibrillar aggregates with a tight fibril core. This spine is characterized by a regular alignment of β-sheets, the so-called cross-β structure (Figure 4) (Sunde et al., 1997). Crystallographic studies have allowed a detailed view of the interactions which give rise to this structural pattern (Nelson et al., 2005). While the amide groups of the peptide backbones involved in β-sheet formation interact via hydrogen bonds, the interaction of individual β-sheets require an aa sequence complementarity that allows the aa side chains to intertwine and form a so-called dry steric zipper. The hydrophobic effect resulting from these interactions together with the hydrogen bonds between the polypeptide backbones are considered to be responsible for the stability of amyloid aggregates (Figure 4). Thus, exposure of the peptide backbone is a prerequisite for amyloid formation, which may in part explain why it is favored by partial unfolding and why intrinsically unstructured proteins, like Tau or α-synuclein display a pronounced tendency to assemble into amyloid fibers (Eisenberg and Jucker, 2012). The nature of the interactions within the spine of amyloid fibrils is suggested to account for their kinetic stability as well as for the nucleation dependence of fibril formation (Jarrett and Lansbury, 1993). The mechanism of nucleation says that a template of the amyloid core in the form of small oligomeric species is needed for the subsequent addition of more and more monomers to give rise to a fiber. This feature of

templated aggregation is also thought to be the structural basis of the prion-like propagation of misfolding and aggregation, which has in recent years emerged as a unifying feature of many neurodegenerative disorders (Soto, 2012).

Despite the structural commonalities, there is a considerable complexity of amyloid aggregates, because there are not only different types of steric zippers found in the fibril core, but also a large number of different higher order arrangements of so-called protofibrils into higher order structures, such as paired helical filaments (PHFs) composed of the Tau proteins. Consequently, even for a single protein such as Tau a number of different aggregate morphologies can occur, with potentially different impacts in the cellular environment (Furukawa et al., 2011).

1.2.2. Consequences of Protein Aggregation: Amyloid Diseases

While the links between defective protein quality control, the accumulation of proteins and the association of these processes with the occurrence of protein misfolding diseases are known for a long time (Wickner et al., 1999), the mechanistic consequences of protein aggregation remains enigmatic even today. There are several prominent examples of where the accumulation of insoluble protein deposits is tightly linked to disease, such as AD, PD or Huntington's disease (Dobson, 2003). Additionally, mutations causing hereditary forms of these diseases often lead to a higher aggregation propensity of the respective proteins, as was shown for α-synuclein (Conway et al., 2000), huntingtin (Perutz and Windle, 2001) and Tau (von Bergen et al., 2001). However, it is still a matter of debate if these aggregates play a disease causing role (Ross and Poirier, 2005). For example, in AD there is no clear correlation between Aβ plaques and severity of the disease (Terry et al., 1991). Accordingly, the role of pre-amyloid oligomers has become a focus of research, because oligomers of, for example, Aβ or α-synuclein have been shown to be highly toxic to neurons (Lauren et al., 2009; Winner et al., 2011). Independent of whether aggregates themselves are toxic to cells, the process of aggregation seems to be harmful to cells, and some mechanisms of the toxicity of protein aggregates have been suggested. For example, the aggregates or aggregation-prone forms of huntingtin (Bence et al., 2001) and Tau (Keck et al., 2003) have been shown to inhibit the proteasome, which might in turn lead to increased accumulation of misfolded proteins and, therefore, increased aggregation. Other proposed mechanisms are

the sequestration of important cellular factors in aggregates (Yu et al., 2014), or the disruption of membranes by pre-fibrillar amyloids (Demuro et al., 2005).

In addition to these findings, the prion-like properties of disease-associated aggregates have recently gained increasing attention. It was found that fibrillar protein aggregates composed of huntingtin, α-synuclein and Tau can enter cells and seed the intracellular aggregation (Frost et al., 2009a; Guo et al., 2013; Ren et al., 2009), providing evidence for cell to cell transmission of protein aggregation in neurodegenerative diseases. These observations were substantiated by *in vivo* studies showing that, in disease models of Tauopathy and AD, protein aggregation can be infectious in a way reminiscent of prion diseases (Clavaguera et al., 2013; Eisele et al., 2010). These processes might account for the reproducible temporal spreading of the pathological features of neurodegenerative disease across brain regions of patients (Jucker and Walker, 2013), probably tracing neuronal networks and connectivity (Ahmed et al., 2014). Given these harmful effects of protein aggregates and the process of aggregation, it is no surprise that organisms have evolved mechanisms not only to avoid aggregation, but also to remove aggregates.

1.2.3. Protein Disaggregation

Resistance to proteolytic degradation is considered a defining feature of protein aggregates, in particular amyloids, and is also thought to contribute to their toxicity and irreversible accumulation under pathological conditions. Therefore, disaggregation mechanisms have emerged which allow the extraction of individual protein molecules from aggregates and their subsequent refolding or proteolytic degradation. Today, the mechanisms of disaggregation mediated by ATP-driven chaperones are well characterized for bacterial and yeast disaggregases (Doyle et al., 2013). These mechanisms have in common that disaggregase activity involves the coordinated action of multiple-subunit, ATP-driven molecular machines which use the energy from ATP hydrolysis for the disruption of the tight interactions between the protein subunits of an aggregate. In bacteria, plants and yeast, this task is performed by members of the HSP100 family of chaperones and their co-chaperones.

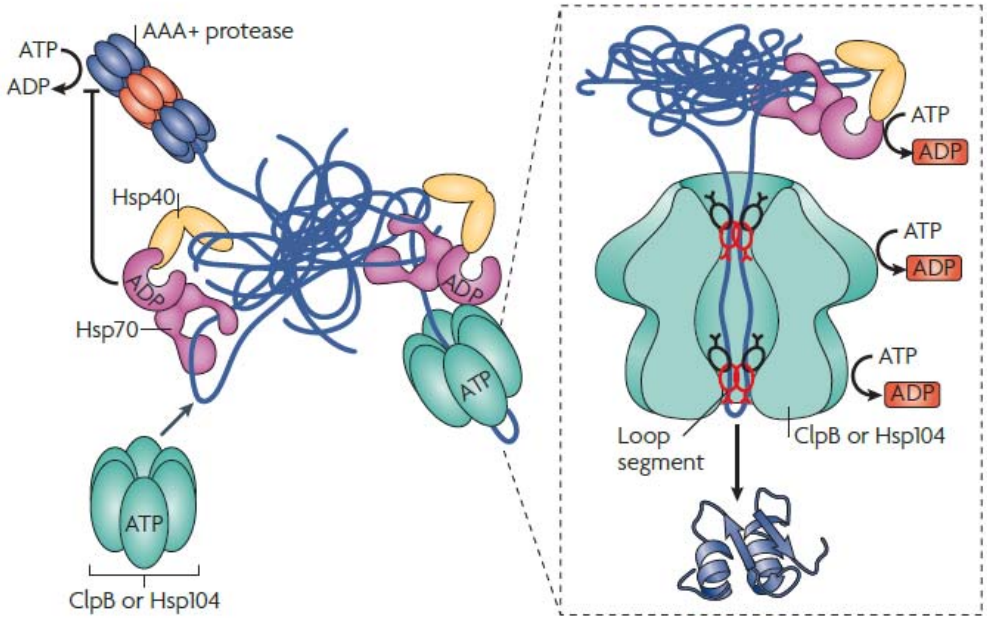

Figure 5 - Protein Disaggregation by the HSP70/Hsp104 Machinery.

Schematic representation of the ATP-dependent disaggregation performed by Hsp104 or ClpB with the respective members of the HSP40/HSP70 families of chaperones. Protein aggregates (dark blue) are bound by HSP40 and/or HSP70 and subsequently targeted for degradation by compartmentalized AAA+ proteases or disaggregation by the Hsp104/ClpB disaggregase machinery. Hsp104/ClpB couples the chemical energy of ATP hydrolysis to the forced threading of individual polypeptide chains through the central pore of the complex. The mechanism involves rearrangements of loop segments residing in the pore, but the exact mechanism of translocation is unknown (Tyedmers et al., 2010).

ClpB from bacteria and Hsp104 from yeast have been studied most extensively with respect to the mechanism of disaggregation. In contrast to many other HSP100 members which associate with protease subunits to form ATP-dependent proteolytic machines, ClpB and Hsp104 are dedicated disaggregases which do not necessarily trigger the proteolysis of their substrates. They are members of the AAA+ family of ATPases and form hexameric complexes with a central pore. Disaggregation depends on the association of HSP100 with members of the HSP40/HSP70 chaperone system, which mediate the binding of substrates and their recruitment to the HSP100 oligomers (Glover and Lindquist, 1998; Winkler et al., 2012). ATP hydrolysis is believed to power conformational changes within the HSP100 subunits that lead to the threading of individual polypeptide chains through the central pore of the complex. Thereby, individual proteins are extracted from the aggregate one by one (Figure 5). The exact mechanism which confers the coupling of ATP hydrolysis and polypeptide threading has not been elucidated yet. However, there are data supporting an active power-stroke mechanism rather than a molecular ratcheting mechanism which relies

on Brownian motion (Maillard et al., 2011). Functionally, the ability to disrupt aggregates by these mechanisms is essential for growth under folding stress conditions such as heat shock (Weibezahn et al., 2004). In yeast, the Hsp104 disaggregase machinery is also important for the inheritance of prion strains by breaking of amyloid fibers composed of the Sup35 prion and by these means allowing their distribution to daughter cells.

Higher eukaryotes lack homologs of Hsp104 and ClpB, and only recently, an alternative mechanism for disaggregation was shown (Rampelt et al., 2012). This mechanism involves the HSP70 member Hsp110 and requires its interaction with the HSP70/HSP40 chaperone system for disaggregase activity. Interestingly, Hsp110 does not have refolding activity but acts as a nucleotide exchange factor for HSP70 members and might be important for the recruitment of HSP70 to protein aggregates. When cooperating with sHsps, such as HspB5, depolymerization even of amyloid aggregates derived from α-synuclein has been shown (Duennwald et al., 2012). So far, only the resolubilization *in vitro* and in *C. elegans* has been reported, but there is no data mechanistically explaining how the interactions described above work together in disaggregation. Even in the more widely studied HSP100 disaggregation system, some central questions remain unanswered. For example, there is only a vague concept of how the initial binding and remodeling of aggregates by HSP40/HSP70 chaperones takes place, or how ATP hydrolysis is translated into mechanical force leading to the dissolution of aggregates.

1.3. The HtrA Family of Serine Proteases

Members of the high-temperature requirement A (HtrA) family of serine proteases are found in all domains of life and are therefore highly conserved. The first description of an HtrA gene in *E. coli* established its essential role for growth at elevated temperatures. This fact already pointed to the potential importance of HtrAs in stress response and protein quality control (Lipinska et al., 1988). HtrAs are targeted to extracytoplasmic compartments and therefore act independent of ATP. In addition to their serine protease activity, members of this protein family have also been shown to act as folding factors in protein quality control (Spiess et al., 1999). Most organisms express more than one homolog, e.g. there are 16 homologs in *Arabidopsis thaliana* and 4 homologs in humans. The important role of HtrA proteases for cellular physiology is supported not only by their evolutionary conservation, but also by their association with pathologic conditions in humans (Clausen et al., 2011). This indicates that

HtrAs generally take part in essential cellular processes and that a modulation in HtrA abundance and activity might be deleterious or advantageous in the genesis or the course of diseases. In bacteria, their association with stress response pathways makes HtrAs good candidates for targets of novel antibiotic substances. The following parts will therefore summarize some important aspects of the functional, structural and regulatory properties of HtrAs.

1.3.1. Structural Conservation of HtrAs

A typical domain architecture is shared by all HtrAs, i.e. the combination of a trypsin-like serine protease domain with at least one C-terminal PDZ domain (postsynaptic density of 95 kDa, Discs large and zonula occludens 1), with varying domains residing in the N-terminal part which may e.g. mediate membrane anchoring (Figure 6).

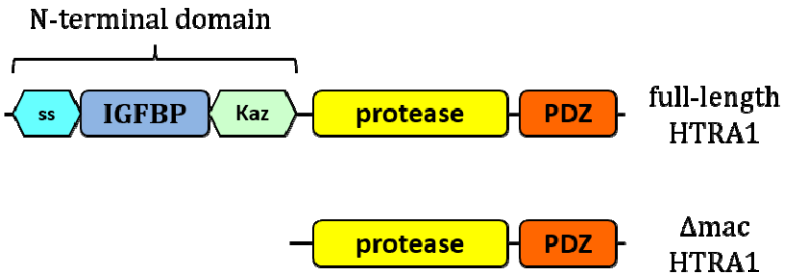

Figure 6 - Primary Structure of HTRA1

The human HtrA homolog HTRA1 shows the typical HtrA domain organization, with a chymotrypsin like Ser protease domain and a C-terminal PDZ domain. In the N-terminal part, the different HtrAs carry varying functional domains. In the case of HTRA1, the N-terminus is the “mac” domain containing a signal sequence for secretion (ss, cyan), an IGFBP7 fragment which contains a Kazal-like protease inhibitor domain (Kaz, green).

PDZ domains are found in a wide range of proteins with various functions, where they mediate the binding of peptides or the interaction between proteins, which may affect their localization, oligomerization or activity. The binding mode of peptides to PDZ domains is conserved and requires binding of the C-terminal three or four residues of the respective ligand, with a free carboxylate group of the last aa typically being a prerequisite for efficient binding. However, in some instances, binding of internal sequences has also been reported (Sheng and Sala, 2001), which was also suggested to be the case for the human HtrAs

HTRA1 and HTRA3, but for internal peptides binding was much less efficient (Runyon et al., 2007).

Apart from the shared domain organization, HtrAs also have in common that the functional HtrA particles are homo-oligomers based on a trimeric building block structure. Structurally, the bacterial HtrAs were the first to be characterized in detail (Krojer et al., 2002; Wilken et al., 2004). These studies have allowed a detailed view of the architecture and mechanistic features of homooligomers. DegS, for example, resides in the periplasm of *E. coli* and is catalytically inactive unless specific, folding stress associated peptides are bound to its PDZ domain (Hasenbein et al., 2007). This binding causes the repositioning of the sensor Loop L3 which eventually leads to the remodeling of the active site into its active conformation and, as a consequence, the highly specific cleavage of the signaling protein RseA.

In contrast, DegP is a periplasmic protease which forms a number of different oligomeric states arising from the association of trimeric building blocks. In this case, oligomerization dynamics reflect the interchange of various functional and activation states of DegP. Crystal structures are available for the hexameric resting state (Krojer et al., 2002), as well as for the large 24mers which represent protease chambers with high proteolytic activity (Krojer et al., 2008), in which misfolded or incompletely folded substrate can be sequestered or degraded. These structures, together with mutagenesis studies, have helped to understand how DegP can switch reversibly between active and inactive states (Merdanovic et al., 2010). The PDZ domains of DegP, PDZ1 and PDZ2, participate in substrate binding, as well as the formation of the active higher order oligomers, such as 12-, 15- and 24mers. Furthermore, they mediate the intramolecular transduction of activating signals from the site of ligand binding to the active site and the concomitant switch from the resting to active oligomeric states. Ligand binding to PDZ1 triggers conformational changes which critically involve the reorientation of both PDZ domains relative to each other, as well as the rearrangement of sensor loop L3 which becomes instrumental in setting up a proteolytically competent active site by interacting with the activation loop LD* of a neighboring subunit. In addition to this allosteric mode of activation, ligand binding to both DegP and DegS has been shown to take place in a cooperative manner. In contrast to the activation of classic serine proteases such as Trypsin, which are activated by proteolytic cleavage of an inactive proenzyme (Stroud et al., 1977), HtrAs can reversibly switch between inactive and active states and therefore have evolved mechanisms of reversible zymogen activation. Taken together, the bacterial HtrAs have proven to be good models for studying the mechanisms of allostery, cooperativity and activation by oligomerization in a detailed manner (Clausen et al., 2011).

1.3.2. Functional Conservation of HtrAs

The involvement of HtrAs in protein quality control has been best characterized for the bacterial members. In the cell envelope of *E. coli* they play diverse roles in the sensing and counteracting of protein folding stress. DegS acts as a stress sensor, and its activation triggers a proteolytic cascade eventually leading to the downstream activation of the transcriptional σ^E stress response pathway (Hasenbein et al., 2007). One of the factors which are upregulated in the course of this response is DegP, which is thus an effector of protein quality control. DegP has little substrate specificity and can encapsulate misfolded proteins after conversion into higher order oligomers. Accordingly, it is allosterically activated by hydrophobic stretches of proteins which become exposed only upon misfolding. Importantly, DegP can act on its substrates either as a protease or as a chaperone and by these means combines two opposing activities in a single polypeptide chain. The switch between proteolytic and chaperone activities has been shown to be temperature dependent, with the protease activity being predominant at high temperatures (Spiess et al., 1999). The ball shaped DegP oligomers are large enough to harbor folded outer membrane proteins, which were actually encapsulated in DegP prepared from *E. coli* as detected by electron microscopy (Krojer et al., 2008). Therefore, DegP might act as a chaperone by providing a folding chamber for its substrates and at the same time preventing their aggregation. It has also be proposed that outer membrane proteins use DegP oligomers for transit through the periplasm, as the dimensions of the DegP 24mer would suffice for spanning the periplasmic space. In accordance with their characterized activities in the course of the protein folding stress response of the cell envelope of *E. coli,* DegS is an essential protein, and DegP is essential for bacterial growth at elevated temperatures or under other conditions causing protein folding stress, such as a change in pH or increased concentrations of H_2O_2 (Pallen and Wren, 1997). In addition to these functions, bacterial HtrAs have been implicated in virulence, as was shown for HtrA members of *Helicobacter pylori* or *Bordetella pertussis.* In plants, the role of some HtrAs in protein quality control is also well established. In the model organism *Arabidopsis thaliana,* for example, various HtrA proteins play important roles in the protein quality control of chloroplasts. Here, DEG1, DEG5, DEG7 and DEG8 take part in the assembly as well as the degradation of photosystem protein complexes (Clausen et al., 2011).

There are 4 human HtrAs, named HTRA1-4, with a variety of postulated functions, many of which go beyond protein quality control. Whereas little is known about the roles of HTRA3

and HTRA4 in humans, the other two HtrA homologs have been studied in more detail. Some studies have shown a connection between HTRA2 and protein quality control of the mitochondrial intermembrane space, to which HTRA2 is localized. When HTRA2 is lost, there is an accumulation of unfolded proteins in mitochondria which ultimately leads to mitochondrial defects and a transcriptional stress response reminiscent of what is observed in the brains of PD patients (Winklhofer and Haass, 2010). Additionally, when HTRA2 is knocked out in mice, they show a PD-like phenotype (Moisoi et al., 2009) and a correlation of a loss-of-function mutation of HTRA2 and PD was observed in humans (Strauss et al., 2005). Together with a possible contribution of the proteolytic activity of HTRA2 to Aβ metabolism, these studies suggest that HTRA2 is important for protein homeostasis in humans and its function might be linked to protein folding diseases. HTRA2 has also been proposed to play a role in apoptotic pathways as it gets released into the cytosol in response to apoptotic stimuli and subsequently degrades Caspase inhibitors, ultimately driving apoptotic processes (Verhagen et al., 2002). However, this was put into question by animal data indicating that when the prime caspase inhibitor XIAP, a postulated substrate of HTRA2, was deleted, no difference in apoptosis was observed (Harlin et al., 2001). Diverse roles have also been suggested for human HTRA1, due to its association with a number of pathological processes as well as the varying subcellular localizations and large number of reported substrates. These implications are discussed below in detail.

1.3.3. HTRA1

The human HtrA family member HTRA1 shares the typical domain organization in combining a trypsin-like serine protease domain with one C-terminal PDZ domain. Additionally, the N-terminus harbors a fragment of the insulin-like growth factor binding protein 7 (IGFBP7) which contains a Kazal-like protease inhibitor motif (Figure 6). So far, no functional role has been attributed to this domain, but it has been shown that the Kazal-motif does not affect proteolytic activity of HTRA1, which questions its relevance for the regulation of HTRA1. Moreover, the N-terminus does not bind IGF1 (Eigenbrot et al., 2012). Thus, it can only be speculated that the N-terminal domain might affect the localization or interactions of HTRA1. The crystal structure of human HTRA1 trimers lacking the N-terminal domain has, along with biochemical characterizations, helped to point out structural features which HTRA1 shares with other HtrAs, as well as some differences (Truebestein et al., 2011) (Figure 7).

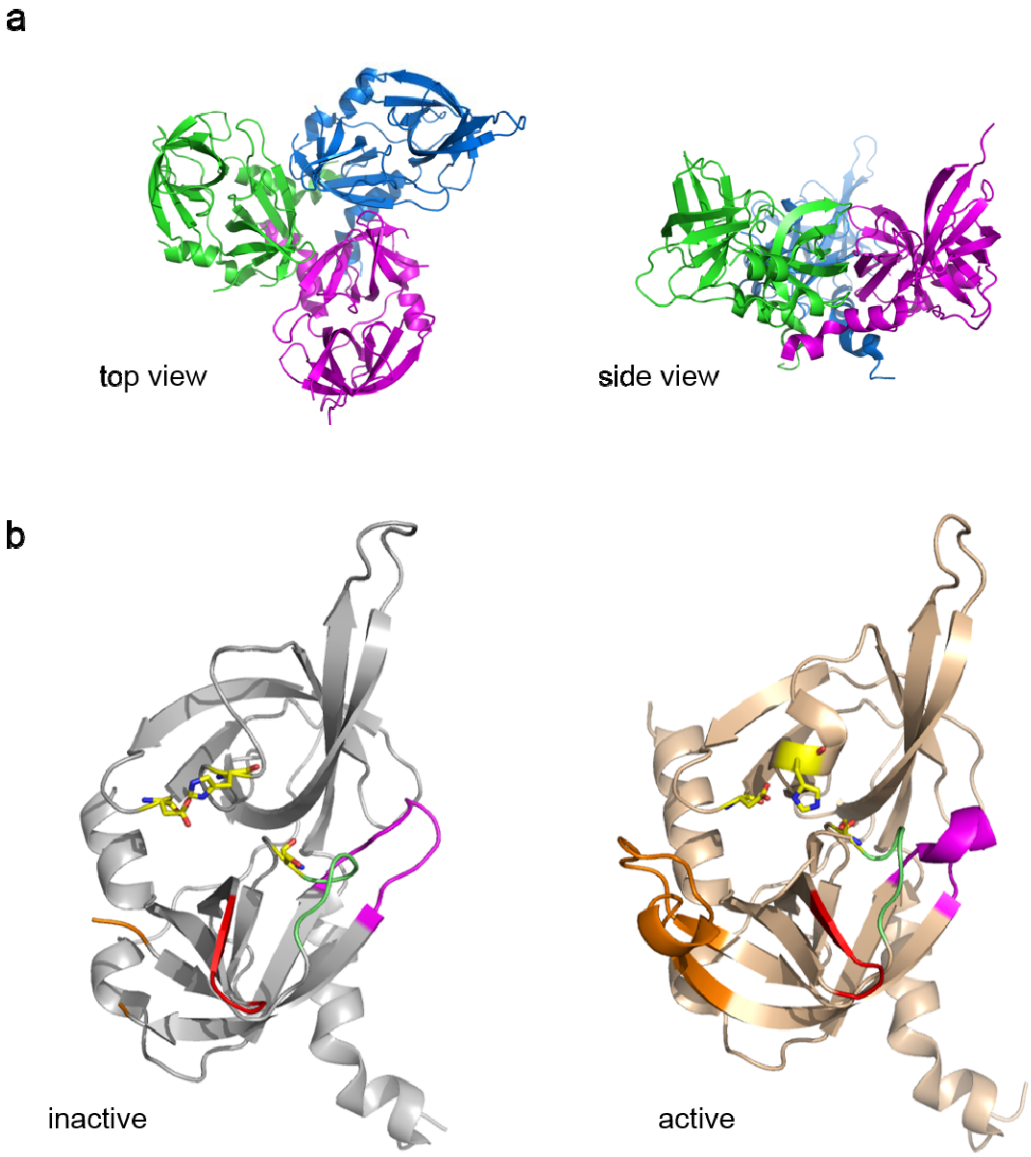

Figure 7 - Crystal Structure of HTRA1 (Truebestein et al., 2011)

a, HTRA1 forms a disc-shaped trimer that is built up by tight interactions of the protease domains. The active sites reside on top of the side view, the PDZ domains were not resolved in the crystal due to their pronounced *en bloc* mobility. The monomers are colored differently to highlight their arrangement within the trimer. **b**, Only the protease domain of one monomer is shown with the active site loops colored differently to highlight their rearrangement during activation. Loop L1 is depicted in green, L2 in red, L3 in orange, and LD in pink. Residues of the catalytic triad His220, Asp250 and Ser328 are shown in yellow. In the inactive conformation, the active site loops are distorted and the setup of a competent catalytic triad prevented. Note that loop LD reaches into the active site of a neighboring monomer upon activation.

In the absence of substrate, the protease domain is in an inactive conformation. In order to track the conformational rearrangements associated with activation, a substrate peptide modified with a boronic acid group, which reversibly binds to the active site and fixes it in a

substrate-bound conformation, was added to HTRA1. This allowed the detailed analysis of the inactive and active conformations and their comparison to the mode of activation of other HtrA proteases.

In brief, the inactive state is characterized by a distorted active site with the essential loops L1, L2, L3 and LD being present in disordered conformations. In contrast, in the substrate-bound, active state, these loops change positions to adopt a defined positioning concomitant with the successful assembly of structural elements needed for proteolysis, i.e. the oxyanion hole, S1 specificity pocket and the catalytic triad composed of aa residues His220, Asp250 and Ser328 (Figure 7 b). This disorder to order transition is reminiscent of what is also observed in the activation process of other HtrAs and classic serine proteases. However, in contrast to the activation mechanism of DegP, HTRA1 can be activated by its substrates even in the absence of the PDZ domain. The sensor loop L3 mediates in DegP the allosteric communication between substrates bound to PDZ domain 1 and the active site. In contrast, L3 is directly involved in the build-up of the active site of HTRA1 by making direct contact to substrate bound to the active site, suggesting an induced-fit rather than an allosteric mechanism of activation. In accordance with this, HTRA1 could be activated by its substrates in activity assays using a PDZ deletion mutant. Moreover, the PDZ domain was not resolved the crystal structures reported, which is indicative of a distinct *en bloc* flexibility of this domain and a lack of stable contacts within the trimer that was crystallized. The loss of the PDZ domain also did not significantly affect the structure of the protease domain, as was shown for the crystal structure of the protease domain alone. Similar to DegP, there are experimental hints to an oligomer conversion of HTRA1 in the presence of substrates, but the exact mode of the oligomeric switch or the stoichiometric composition has not been determined, yet. Analysis of the cleavage products of HTRA1 pointed at a low sequence specificity with a preference for small hydrophobic residues at the P1 site (i.e., the C-terminal residue of the cleavage product) such as Leu, Val or Ala. This fact is again similar to the low sequence specificity of other HtrA proteases. Taken together, the structural and biochemical characterization has so far shown that, while maintaining basic structural features, HTRA1 has evolved different mechanisms of substrate binding and to control proteolytic activity. The role of the PDZ domain seems to have shifted from being a module of allosteric communication to other functions which still have to be fully clarified. It is likely that one of these new roles is the targeting of HTRA1 to its subcellular localizations, which was shown in previous work (dissertation A. Tennstädt, (Chien et al., 2009c)).

Functionally, the implications of HTRA1 are very diverse. HTRA1 is ubiquitously expressed and differentially regulated in development and disease, pointing to essential functions under defined physiological conditions. The association of a number of diseases such as Arthritis, age-related macular degeneration, cerebral small vessel disease, various cancers and neurodegenerative disorders such as Alzheimer's disease (AD) underlines this functional diversity (Clausen et al., 2011). Here, just a few lines of evidence linking HTRA1 and disease in humans will be pointed out. In different cancer types, such as melanoma, HTRA1 is differentially regulated and the levels of HTRA1 correlate with e.g. cell proliferation, migration and the sensitivity of cancer cells towards chemotherapeutic drugs (Baldi et al., 2002; Chien et al., 2006). These and other studies have established HTRA1 as a tumor suppressor and potential target for anticancer treatment (Chien et al., 2009a), with an increase in the proteolytic activity of HTRA1 possibly leading to a decrease in proliferation, migration and resistance to chemotherapeutic interventions. In arthritic disease, where the destruction of the extracellular matrix is central to the pathological process, HTRA1 activity is believed to negatively contribute to disease progression. Consequently, HTRA1 levels are several fold higher in arthritic compared to healthy tissues (Grau et al., 2006).

Evidence linking HTRA1 and protein misfolding and aggregation comes from studies which have shown a physical interaction of HTRA1 with hallmark lesions of AD in histopathological slices from AD patient brains, as well as the cleavage of the amyloid β peptide (Aβ) by HTRA1, which plays a central role in AD pathology. Furthermore, upon HTRA1 inhibition Aβ was found to accumulate in the supernatant of cultured cells (Grau et al., 2005). Several sets of data support the notion that HTRA1 also has an impact on the metabolism of the microtubule-associated protein Tau (Tau), which is critically involved in AD by being excessively modified and forming intraneuronal aggregates (1.4.1). For example, in post mortem brain samples from AD patients, the protein levels of HTRA1 were found to negatively correlate with the extent of Tau pathology as assessed by the number of Tau inclusions or the abundance of the hyperphosphorylated form of Tau (dissertation A. Tennstädt). In the course of that work, it was also shown that HTRA1 can degrade the Tau protein *in vitro* and that the levels of Tau in cultured cells are reduced upon overexpression of HTRA1.

Given these diverse pathological settings, it is not surprising that HTRA1 was found in many different subcellular localizations, including the extracellular space, the nucleus and the cytoplasm (Chien et al., 2009c). The presence of a signal sequence targets HTRA1 for the secretion. However, it was estimated that approximately 20% of the protein resides inside of

the cells, whereas 80% was found extracellular (Grau et al., 2005), but how the localization is regulated and how an intracellular pool of HTRA1 is generated remains unknown. The range of substrates which have been demonstrated to be cleaved by HTRA1 supports the diverse roles and localizations. Many of these substrates are extracellular matrix components (e.g. aggrecan, fibronectin and clusterin) or extracellular signaling molecules (e.g. TGF-β (Launay et al., 2008) and IGFBP5 (Hou et al., 2005)), the proteolysis of which might contribute to the involvement of HTRA1 in development, cell growth and migration. Additionally, HTRA1 was shown to localize to microtubules (Chien et al., 2009c), to degrade tubulins (Chien et al., 2009b) and other cytoplasmic proteins such as the tuberous sclerosis 2 (TSC2) protein (Campioni et al., 2010).

In summary, the diverse functions of HTRA1 require dedicated regulatory mechanisms which ensure the spatial and temporal activation of the protease. These might involve posttranslational modifications and processing mechanisms, as well as regulation on the transcriptional level or on the level of substrate recognition by HTRA1 and the concomitant conformational and oligomeric changes. Only little is known about how these modulations might be brought about, which leads to many potential ways of addressing these open questions. Obviously, HTRA1 has extended its scope of functions during evolution, therefore it would be interesting to see in how far the evolutionarily conserved quality control function of HtrAs is retained by HTRA1.

1.4. The Microtubule-associated Protein Tau

The microtubule-associated protein (MAP) Tau is a member of the MAP2/Tau family of microtubule-associated proteins which generally take part in the regulation of microtubule (MT) dynamics and stability. Like an estimated 20-30% of all cellular proteins, Tau is an intrinsically disordered protein (IDP), which means that it lacks stable secondary or tertiary structures in solution and is therefore highly flexible and soluble. IDPs can adopt a large number of conformations, but frequently become structured upon binding to their interaction partners (Dunker et al., 2008). Tau is expressed specifically in neurons, where it regulates of axonal outgrowth and dendrite development (Dehmelt and Halpain, 2005). In mature neurons, Tau has a characteristic axonal localization, but it was also shown to be localized at the cell membrane (Brandt et al., 1995) and in the nucleus (Brady et al., 1995). Tau is not an essential protein and shows only mild Tau knock-out phenotypes in mice, which is probably

due to functional redundancy with other MAPs (Harada et al., 1994). The protein exerts its functions by binding to MTs via its microtubule binding regions, which are pseudo-repeats located in the C-terminal part of Tau. Although the binding sites within the primary sequence are known, the exact mode of binding is not fully characterized and a matter of debate. It has been suggested that Tau binds to the outer surface of MTs, bridges tubulin subunits of protofilaments and becomes ordered upon binding (Al-Bassam et al., 2002). Functionally, Tau binding increases microtubule stability (Butner and Kirschner, 1991), but it also affects the spacing between MTs and might therefore help regulating the overall spatial organization of the MT network of the cell (Chen et al., 1992). Among other posttranslational modifications (PTMs), regulation of Tau function is critically mediated by phosphorylation, which leads to a decrease in the affinity towards MTs.

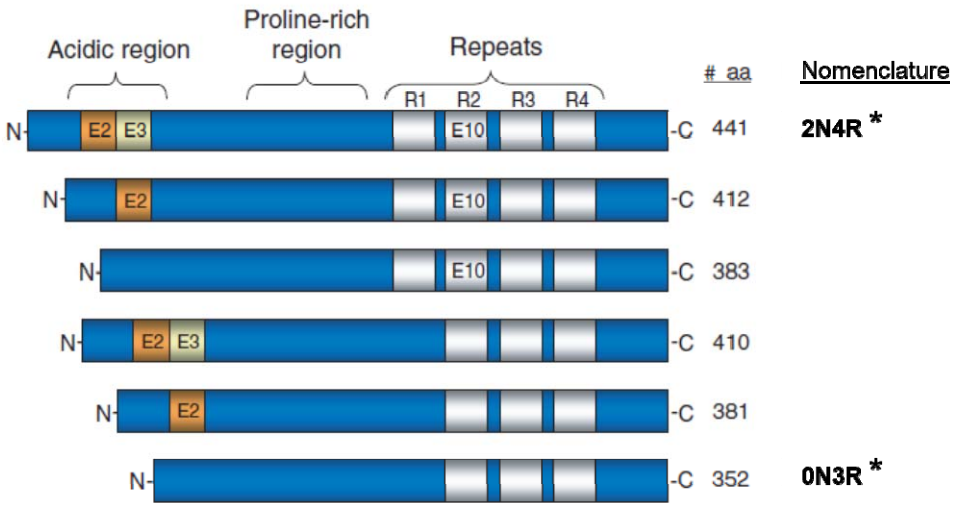

Figure 8 - Overview of the Six Different Tau Isoforms

Alternative splicing of exons 2, 3 and 10 (marked E2, E3 and E10) gives rise to six isoforms of Tau being expressed in the central nervous system. Consequently, the isoforms differ with respect to the number of N-terminal inserts as well as the number of repeats. The repeat region mediates the MT binding of Tau (Figure modified and adapted from (Johnson and Stoothoff, 2004)). * = these isoforms were used in this work.

Alternative splicing of exons 2, 3 and 10 gives rise to six different isoforms of Tau being expressed in the central nervous system which differ in the presence of 0, 1 or 2 N-terminal inserts and 3 or 4 microtubule binding repeats (Figure 8) (Goedert and Jakes, 1990). The isoforms are named accordingly, with 2N4R Tau and 0N3R Tau being the largest and smallest isoforms, respectively, consisting of 441 and 352 aa. Little is known about the functional differences of the individual isoforms, but an intronic mutation which leads to a

change in the ratio of isoforms causes a hereditary form of Tauopathy, indicating that maintaining the correct proportions of Tau isoforms is important (Hutton et al., 1998). The primary sequence of Tau can be divided into two domains, an N-terminal “projection domain” which is formed of an acidic subdomain in the N-terminal half and a proline-rich half in the C-terminal part, and the C-terminal microtubule-binding domain (MTBD) (Figure 8). The projection domain is thought to influence the MT spacing mediated by Tau, as well as the interaction with other cytoskeletal proteins. The MTBD, on the other hand, contains three or four repeats depending on the isoform, each consisting of an 18 residue minimal MT binding sequence a 13-14 aa residue “inter repeat” stretch. This region not only provides the binding region to MTs, but is also responsible for the self-association into aggregates, as discussed below (1.4.4).

Multiple posttranslational modifications have been reported for Tau, including phosphorylation, glycosylation, glycation and ubiquitination. Phosphorylation is the predominant modification, and almost 40 potential phosphorylation sites have been reported, some of which are thought to play a regulatory role in the physiology of Tau (Avila et al., 2004). Excessive phosphorylation is one of the hallmark modifications under pathological conditions with possible consequences for the pathogenesis of AD and other Tauopathies.

1.4.1. Alzheimer’s Disease and the Role of Tau

Tau has been in the focus of research for a long time, because it forms intraneuronal, fibrillar protein inclusions in diseases collectively called tauopathies, among which Alzheimer’s disease (AD) is the most prominent. Since the first description of this type of dementia in 1906 by Alois Alzheimer, significant effort has been put into studies aimed at shedding light on the disease process in order to develop therapeutic strategies. However, till this day we neither understand in detail what the molecular mechanisms are, nor can we effectively prevent let alone reverse the progressive cognitive decline that characterizes AD and inevitably leads to the death of the patient (Chiang and Koo, 2014). Two hallmark lesions are the defining histopathological features in the brains of AD patients. While the senile plaques are found in the extracellular space surrounding neurons, the so-called neurofibrillary tangles (NFTs) predominantly occupy the cell bodies of affected neurons (Figure 9 a,b). NFTs are composed of filamentous aggregates consisting of Tau protein which is phosphorylated to an abnormally high degree. Structural analyses using electron microscopic techniques revealed

that these make up a population of filaments called straight filaments, as well as characteristic paired helical filaments (PHFs) which are formed by the association of two Tau fibrils with a helical twist (Figure 9 c).

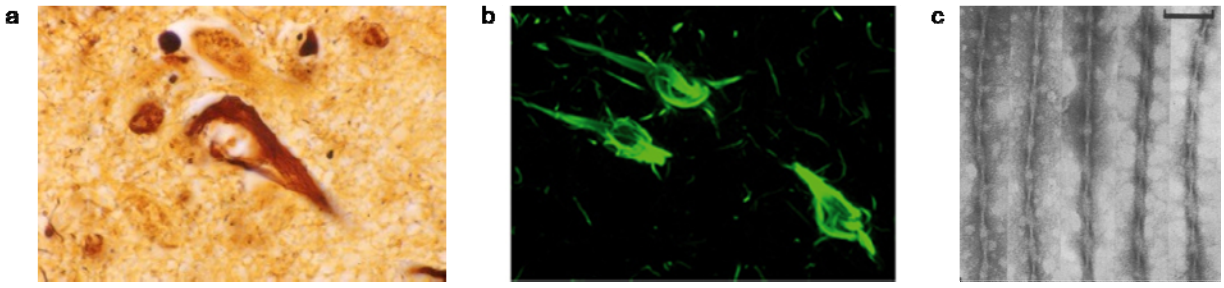

Figure 9 - Neurofibrillary Tangles and Paired Helical Filaments in Alzheimer's Disease

Representative images showing NFTs in brain sections from AD patients (**a**, **b**) and isolated PHFs (**c**). Histological silver staining (**a**) and immunofluorescence staining using Tau-specific antibodies (**b**) illustrate the presence of large aggregates within the cell bodies of affected neurons. Bundles of aggregates essentially fill the whole somatodendritic compartment. After isolation from post mortem brain tissue of AD patients and negative stain transmission electron microscopy, isolated filaments display the characteristic arrangement of two fibres which are regularly twisted around each other. Images were adapted from (Marcus and Jacobson, 2003)(**a**), (Helbecque et al., 2003)(**b**) and (Wischik et al., 1988)(**c**).

Initial research has focused on the senile plaques, which are aggregates composed of Aβ peptides. They are produced by sequential processing of the amyloid precursor protein (APP), eventually leading to the secretion of APP fragments composed of 40 or 42 amino acids, called $A\beta_{40}$ and $A\beta_{42}$, respectively. The amyloid hypothesis which had placed the aggregation of Aβ in the center of the disease process (Hardy, 2009) was abandoned after only a poor correlation between the abundance of senile plaques and regions of neuronal degeneration was found (Terry et al., 1991). At the same time, progress in the field of Tau research led to an increased acceptance of the pathological importance of Tau in AD. After years of scientific debate by researchers seeing either Aβ or Tau and their dysfunction or aggregation as the causative agents of AD, present hypotheses favor an interaction of both pathological processes making up the “amyloid cascade” (Ittner and Gotz, 2011). These assumptions are based on a more detailed understanding of pathological processes which has been gained by studies with transgenic mice serving as models for Aβ and Tau pathologies. Further progress has led to the notion that soluble oligomers rather than aggregates are the toxic agents and aggregation might be protective by sequestering toxic oligomers and thus rendering them less harmful to neurons. Current models claim that Aβ oligomers of unknown structural identity exert their neurotoxic effect on synapses (Selkoe, 2001). Interestingly, Aβ induced toxicity leading to the loss of neurons and cognitive decline

requires the presence of the Tau protein, as was shown in various studies (Gotz et al., 2001; Jin et al., 2011; Roberson et al., 2007; Zempel et al., 2013). These studies not only suggested pathological events upstream of Tau pathology, but they also collectively support the hypothesis of an essential role of Tau for neurodegenerative processes observed in AD. In accordance with this observation, and considering recent failures of Aβ targeting drugs, drug discovery efforts in AD have shifted towards tau based therapeutics. These include compounds aimed at reducing the degree of Tau phosphorylation as well as Tau aggregation inhibitors and agents that target physiological or pathological effects of Tau, such as MT stabilization or increased excitotoxicity upon missorting of Tau (Chiang and Koo, 2014). The pathological changes of Tau as well as the mechanisms of Tau misfolding and aggregation, and how these processes might contribute to disease will be discussed in more detail in the following section.

1.4.2. Pathological Changes of the Tau Protein

The assembly of inclusions composed of Tau (neurofibrillary tangles, NFTs) is the defining and most striking feature of tauopathies. The formation of NFTs in neurons follows the same pattern across the cortex of AD patients as does the neuronal loss and concomitant dysfunctions of the respective brain regions, which manifest as a characteristic sequence of clinical symptoms (Arriagada et al., 1992). Although this does not necessarily demonstrate a causal role of Tau aggregation for neurodegeneration, it shows how closely neuronal death and Tau aggregation are connected. Furthermore, hereditary tauopathies, termed frontotemporal dementia with parkinsonism linked to chromosome 17 (FTDP-17), are caused by missense mutations in the gene encoding for Tau, which lead to neurofibrillary degeneration in the absence of Aβ pathology (Spillantini et al., 1998). Many of these mutations have been shown to increase the tendency of Tau to aggregate, adding more evidence to the relevance of Tau aggregation. Considering that there are also other forms of tauopathy like Pick's disease or progressive supranuclear palsy, it becomes clear that Tau pathology can be caused by a variety of upstream events and may lead to phenotypically diverse disorders, which all have in common neurodegeneration as well as misfolding, aggregation and various molecular changes of the Tau protein.

In tauopathies, the Tau molecules which constitute the intraneuronal inclusions are phosphorylated to an abnormally high degree. This hyperphosphorylation is an early event in

AD pathology depending on the sites (Augustinack et al., 2002) and is believed to be important for both a loss of function as well as the potential toxic gain of toxicity due to Tau oligomerization and aggregation. Under physiological conditions, phosphorylation of a small number of defined aa residues negatively regulates MT binding. Consequently, aberrantly high phosphorylation impairs normal function of Tau which might lead to defects in the transport of molecules and organelles across axonal MTs (Ballatore et al., 2007). In addition, the dissociation of Tau from MTs leads to an increased cytoplasmic pool of free, hyperphosphorylated Tau potentially favoring aggregation. This effect might be further aggravated by an increased aggregation propensity which has been observed for hyperphosphorylated Tau (Chang et al., 2011).

Phosphorylation of Tau can occur at over 40 different sites, and numerous kinases have been reported to phosphorylate Tau, which makes this process very complicated and the causes and effects hard to dissect experimentally. Glycogen synthase kinase 3 β (GSK3β) is considered to be important for Tau phosphorylation under pathological conditions, particularly since Aβ was shown to induce GSK3β activity leading to higher phosphorylation levels, providing another possible link between Aβ and Tau in AD (Avila et al., 2006). Phosphorylation of Tau by GSK3β has also been shown to promote Tau aggregation in cells (Cho and Johnson, 2003). However, there are more potential kinases which might contribute to Tau pathology (Johnson and Stoothoff, 2004). The fact that Tau can be posttranslationally modified in various other ways adds up to the complexity of pathological changes in the Tau protein. For example, acetylation of Tau was shown to prevent its degradation and might have an aggravating effect on tauopathy (Min et al., 2010). Truncation of Tau by caspases (Gamblin et al., 2003), Calpain (Park and Ferreira, 2005) or lysosomal proteases (Wang et al., 2009) might lead to neurotoxic fragments or those with increased aggregation propensities (Kovacech and Novak, 2010). Other modifications including glycosylation, which is associated with AD and might lead to stabilization of fibrils (Wang et al., 1996) or prevent aggregation by excluding phosphorylation of the respective residues (Chiang and Koo, 2014), as well as non-enzymatic glycation (Munch et al., 2002), nitration (Smith et al., 1997) and sumoylation (Dorval and Fraser, 2006), have been described. While it has been possible to link some of the modification to the process of neurodegeneration, as in the case of hyperphosphorylation which might be induced by Aβ oligomers, the involvement and possible causative roles in the disease process of most modifications are not well established (Gong et al., 2005).

Recent studies have also drawn the attention to the importance of aberrant subcellular localizations of Tau in the process of neuronal dysfunction and neurodegeneration (Hoover et al., 2010). For example, effects of Tau on chromatin structure and consequent DNA damage and oxidative stress have been shown (Frost et al., 2014). Another study was able to link Aβ-induced Tau missorting to dendrites with pathological processes such as dendritic spine loss (Zempel et al., 2013). It is very likely that there is extensive interplay between these modifications, and complex causative relationships between the physiological roles of Tau, its modifications and possible effects on neuronal function and viability *in vivo*. Thus, it was not possible so far to establish a model that meets this complexity and at the same time explains the sequence or interaction of molecular changes of Tau leading to neurodegeneration.

1.4.3. Proteolysis of Tau

Although elevated protein concentrations are a risk factor for their aggregation, increased overall concentrations of Tau were not observed at early stages of AD (Khatoon et al., 1994). When determinants favoring the aggregation of Tau are to be addressed, the intracellular pool of “free” Tau should be considered instead of the total levels, together with posttranslational modifications (PTMs) which might influence the folding state of the protein in a way promoting or inhibiting Tau aggregation. Therefore, it is important to learn about the process of Tau aggregation in as much detail as possible, the effects by PTMs, as well as about mechanisms of Tau clearance, since the degradation of soluble, misfolded or aggregated Tau provides potential means of curbing the accumulation of aggregates.

The cleavage by Caspases and Calpain which has been reported is unlikely to confer the physiological turnover of Tau, because only limited proteolysis has been shown in the respective studies (Gamblin et al., 2003; Garg et al., 2011). However, under conditions where the proteasomal degradation of Tau is inhibited, Calpain might function as a degradative Tau protease (Delobel et al., 2005). The lysosomal proteolytic system has also been suggested to contribute to Tau degradation, but probably with outcomes favoring the aggregation of Tau (Wang et al., 2009). Several studies argue that Tau is a substrate of the ubiquitin proteasome system both under physiological and pathological conditions. The ubiquitin ligase CHIP has been shown to catalyze the ubiquitination of Tau upon interaction with the HSP70/90 system and by these means target Tau to proteasomal degradation

(Petrucelli et al., 2004). In accordance with these results, Tau and Tau inclusions were shown to be ubiquitinated (Iqbal and Grundkeiqbal, 1991; Love et al., 1988). Another mechanism of targeting Tau to the proteasome might be the binding of polyubiquitinated Tau by p62, which is supported by the observation of p62 colocalization with NFTs (Babu et al., 2005). Studies suggesting a role of the proteasome in the clearance of Tau are supported by findings showing that proteasomal degradation is impaired in AD (Keller et al., 2000) and inhibited by aggregates (Bence et al., 2001). Additionally, a ubiquitin-independent mechanism of Tau degradation by the proteasome has been suggested (David et al., 2002). These data give hints to candidate pathways of Tau proteolysis, and the enrichment of e.g. CHIP or polyubiquitinated Tau in NFTs indicates that the accumulation of Tau in aggregates might reflect failure to effectively clear the cells of harmful Tau species. However, no proteolytic degradation of Tau aggregates has been reported so far, which would provide means of restoring the protein homeostasis of Tau.

1.4.4. Mechanisms of Tau Aggregation

The early characterization of PHFs isolated from human post mortem brain samples has, apart from the identity of the component proteins, aimed at clarifying the biochemical properties and structure of the Tau aggregates. Ultrastructurally, the aggregates appeared to be bundles of filaments, composed of two proteinaceous filaments forming a helix (Kidd, 1963; Wisniewski et al., 1976). Resistance of the isolated aggregates to harsh treatments suggested that *in vivo* the aggregates might be further compacted and perhaps covalently cross-linked (Selkoe et al., 1982). *In vitro* proteolysis using pronase revealed that these aggregates, which were then known to be composed of Tau, were made up of a protease resistant core and an loose, “fuzzy coat” which was readily proteolyzed (Wischik et al., 1988). Closer analyses of the core fragment located this region to aa residues 266-368 of the Tau protein (Jakes et al., 1991).

Insights into the mechanism of Tau aggregation were greatly facilitated by the finding that the fibrillization of recombinant Tau, which hardly forms aggregates spontaneously, can be induced by incubation with anionic cofactors, such as heparin, fatty acids or RNA (Goedert et al., 1996; Kampers et al., 1996; Wilson and Binder, 1995). Using this *in vitro* system has led to a more detailed characterization of the process of Tau aggregation, showing for example, that Tau filaments are formed by a nucleation elongation mechanism, in which a lag phase

with slow formation of an aggregation nucleus, is followed by a phase of rapid elongation of fibrils (Friedhoff et al., 1998b). Although many studies using polyanionic inducers of aggregation have been performed, the exact mechanism of the induction of fibrillization is unknown (Kuret et al., 2005b). It was shown, however, that truncation of the Tau protein to the MTBD increases the efficiency of aggregation *in vitro* (Barghorn et al., 2004). The fibril core was reported to be rich in β-sheets, with the fibril formation being dependent on the β-propensity of two hexapeptide sequences in the repeat region, VQIINK (aa275-280) and VQIVYK (aa306-311) (von Bergen et al., 2000). Further studies have substantiated the assumption that Tau aggregates reminiscent of those found in tauopathies represent amyloid aggregates. For example, fibrils were shown to have the characteristic cross-β structure (Berriman et al., 2003) and they can be detected and quantified by the amyloid specific dyes Thioflavin S and Thioflavin T (Friedhoff et al., 1998a). The most detailed characterization comes from recent studies using X-ray diffraction of microcrystals derived from Tau fibrils composed of the hexapeptide VQIVYK, showing the typical amyloid structure (Figure 4, c) (Sawaya et al., 2007; Wiltzius et al., 2009).

While the mechanism of induction of aggregation remains unclear, it was postulated that the overall negative charge of the inducer helps to overcome the repulsive electrostatic forces between individual Tau molecules which are largely positively charged (Kuret et al., 2005a). A similar mechanism was suggested for the effect of hyperphosphorylation on the aggregation behavior of Tau, with an accordant neutralizing effect of the negative charges of the phosphate groups (Gong et al., 2005). At the same time, phosphorylation of certain sites has also been shown to inhibit aggregation (Schneider et al., 1999). Therefore, the notion is that there are no unambiguous data on the effect of phosphorylation on Tau aggregation. Similarly, the formation of a dimer which is stabilized by a disulfide bond was proposed to be a prerequisite for the efficient formation of aggregates (Schweers et al., 1995), which was recently challenged by other work (Huvent et al., 2014). For the other possible PTMs of Tau, the effect on aggregation efficiency was not determined in detail, leaving the question unanswered, which modifications affect the aggregation and toxicity of Tau significantly.

Another difficulty in studying Tau aggregation even under controllable and reproducible conditions *in vitro* is the heterogeneous nature of the resulting aggregates. Based on AFM studies, a large number of fibril morphologies including straight and twisted filaments of various widths was described (Furukawa et al., 2011; Wegmann et al., 2010). How the conditions of fibrillization determine the various conformations remains largely unknown, in particular it has not been possible to isolate a defined and stable subpopulation of fibrils,

oligomers or other intermediates to study their toxicity in cells. To determine the *in vivo* impact of certain Tau species is an even harder task, because of the dynamic and heterogeneous nature of Tau oligomers and aggregates. The conformational diversity seen for Tau fibrils is reminiscent of Prion aggregation, and is one of the features that AD and other neurodegenerative diseases were recently shown to share with Prion diseases (Brundin et al., 2010). Another biochemical feature of prion-like misfolding is the seeding of protein misfolding, by which soluble and natively folded proteins can be induced to adopt a conformation leading to their addition to preexisting oligomers or fibrils. Characteristically, this misfolding can spread across cell membranes and is thus propagated from cell to cell and within a given tissue. These features were all shown to apply to the Tau protein (Clavaguera et al., 2009; Frost et al., 2009a; Frost et al., 2009b) and might explain how Tau pathology can spread from its region of initiation across the brain in a highly reproducible manner. Evidence for this model was obtained in a mouse model in which transgenic overexpression in a restricted brain region induced Tau pathology in a distinct sequence of regions, leading to co-aggregation of the transgenic protein with endogenous Tau (de Calignon et al., 2012). Notably, this pathological pattern recapitulated the classical spatiotemporal progression of histopathological changes in AD (Braak and Braak, 1991).

1.4.5. Experimental Models of Tau Aggregation

While the *in vitro* aggregation was very helpful for elucidating mechanistic details of the self-association of Tau proteins into fibrillar aggregates and the resulting structures, work restricted to these questions does not lead to insights into the cellular implications. Therefore, a cellular model of Tau aggregation, in which basic processes such as hyperphosphorylation or aggregation of Tau can be observed and manipulated is indispensable. Compared to mouse models, cultured cells are particularly well suited in that they are easy to manipulate and avoid suffering of animals. Modeling Tau aggregation in cells has proven problematic in some ways. One of the reasons is that expression even of high levels of Tau does not lead to the formation of intracellular aggregates, and the stable overexpression is toxic to cells, probably due to the induction of apoptosis (Delobel et al., 2003).

This has been overcome by the induction of aggregation by small molecules stimulating Tau aggregation such as Congo Red (Bandyopadhyay et al., 2007) and by the overexpression of Tau variants containing mutations which are known to cause hereditary Tauopathy by

increasing aggregation propensity (Khlistunova et al., 2006; Vogelsberg-Ragaglia et al., 2000). For example, the induced expression of an aggregation-prone fragment comprising the MTBD with a Lys deletion found in FTDP-17 led to the spontaneous aggregation of this protein with toxicity which was ascribed to the process of aggregation itself (Wang et al., 2007), providing a hint to the aggregation of Tau being toxic to cells. In a similar model using cultured neuroblastoma cells differentiated into neurons it was possible to induce the aggregation of overexpressed Tau by treatment with Aβ aggregates, suggesting a possible link between Aβ and Tau pathologies (Ferrari et al., 2003). The concomitant overexpression of Tau and induction of hyperphosphorylation induced by either increasing phosphorylation by kinase overexpression (Sato et al., 2002) or inhibition of dephosphorylation e.g. by okadaic acid (Lim et al., 2010) led to intracellular Tau pathology. These experimental models, however, complicate the analysis by possible side effects of the elevated kinase activity and of the compounds due to the effects on target proteins unrelated to Tau. Recently, experimental models have made use of the propagation of misfolding and aggregation, which made possible the intracellular seeding of overexpressed Tau by fragments of fibrils prepared by induced aggregation *in vitro* (Frost et al., 2009a; Guo and Lee, 2011). These models have so far been used to study the seeding and uptake mechanism itself, rather than addressing questions of the cellular response or clearance pathways (Wu et al., 2013).

1.5. Aim of This Work

This work explores the ability of human HTRA1 to proteolytically degrade Tau aggregates *in vitro* and in a cellular model of Tau aggregation to provide insight into the role of HTRA1 in protein quality control (PQC) and to expand the functional and mechanistic repertoire of the HtrA family of serine proteases.

The association of HTRA1 with hallmark lesions in Alzheimer's disease (AD) was the first hint of HTRA1 serving PQC functions similar to other HtrA members (Grau et al., 2005). Previous work has further established that HTRA1 can proteolyze Tau *in vitro* and in cells. Additionally, it was shown that HTRA1 also degraded Tau protein compacted by cross-linking by formaldehyde, and that the HTRA1 protein levels negatively correlate with the abundance of pathological Tau and Tau inclusions in AD brain samples (dissertation A. Tennstädt). This suggested a potential role of HTRA1 in the disease process of AD. To establish a mechanistic basis of these results, the proteolytic activity of HTRA1 towards Tau aggregates will be examined *in vitro*, because Tau forms insoluble inclusions in AD which are considered to be resistant to proteolysis. Therefore, the preparation of Tau aggregates resembling the pathologically relevant forms is to be established using recombinant human Tau. In particular, the mechanism of proteolytic degradation of fibrillar by HTRA1 will be in the focus, because so far, no cellular proteases have been shown to proteolyze Tau aggregates in a physiologically relevant setting.

Moreover, a cellular model of Tau aggregation should be established to experimentally address the proteolytic degradation of Tau fibrils by HTRA1 in living cells. To allow a controlled manipulation of intracellular HTRA1 levels, spontaneous uptake of recombinant protein from the extracellular space will be explored and its association with Tau aggregates will be assessed using laser-scanning confocal microscopy.

Ultimately, the combination of biochemical, structural, molecular and cell biological approaches will be used to generate data leading to a first model of mechanism of ATP-independent degradation of fibrillar Tau aggregates.

2. Materials and Methods

2.1. Materials

2.1.1. Buffer Components

Chemical used for the preparation of buffer solutions and media were obtained from Sigma, Fluka, Roth, Riedel de Haen or Merck.

2.1.2. Enzymes and Other Proteins

Malate dehydrogenase from prorcine heart	Roche Applied Sciences, Mannheim, Germany
Restriction Enzymes	New England Biolabs, Ipswich, MA, USA
Antarctic Phosphatase	New England Biolabs, Ipswich, MA, USA
Calpain-1, from human erythrocytes	Calbiochem, Merck Chemicals Inc., Darmstadt, Germany
Caspase 3, recombinant, human	BD Biosciences, Franklin Lakes, NJ, USA
Polymerase (Phusion)	Thermo Fisher Scientific, Rockford, IL, USA

2.1.3. Kits and Reagents

Alexa Fluor 568 carboxylic acid, succinimidyl ester	Life Technologies, Carlsbad, CA, USA
Cell Line Nucleofector Kit V	Lonza Inc, Basel, Switzerland
Complete protease inhibitor tables	Roche Applied Sciences, Mannheim, Germany
Gel Extraction kits	Qiagen, Hilden, Germany

(QIAquick)	
NucleoSpin PCR Clean-Up Kit / NucleoSpin Plasmid / NucleoBond Midi	Macherey – Nagel, Düren, Germany
Pierce Pro-Ject Protein Transfection Reagent	Thermo Fisher Scientific, Rockford, IL, USA
Rapid DNA Ligation Kit	Roche Applied Sciences, Mannheim, Germany
Thioflavin S	AAT Bioquest, Sunnyvale, CA, USA
Roti Nanoquant Bradford Reagent	Carl Roth GmbH, Karlsruhe, Germany

2.1.4. Equipment

Agarose Gel Chambers	Peqlab, Erlangen, Germany
Äkta FPLC	GE Healthcare, Little Chalfont, UK
Buffer Exchange Columns (PD SpinTrap G-25)	GE Healthcare, Little Chalfont, UK
Cell Culture Incubator (Thermo Forma Series II)	Thermo Fisher Scientific, Rockford, IL, USA
Concentrators (Vivaspin 500, 2, 20; 3,000, 10,000 or 50,000 MWCO PES membranes)	Sartorius Stedim, Göttingen, Germany
Dynamic Light Scattering (Malvern Zetasizer nano ZS)	Malvern Instruments Ltd, Worcestershire, UK
ELISA plates (Immulon 4 HBX)	Thermo Fisher Scientific, Rockford, IL, USA
Eppendorf Shakers and Benchtop Centrifuges	Eppendorf, Hamburg, Germany
FPLC (BioLogic DuoFlow)	Bio-Rad Laboratories, Hercules, CA, USA
French Pressure Cell (FrenchPress SLM AMINCO)	SLM Instruments Inc., Rochester, NY, USA
Gel Documentation	Intas, Göttingen, Germany

Hemocytometer	Assistent, Karl Hecht GmbH, Sondheim, Germany
Hydroxyapatite Bio-Gel HT	Bio-Rad Laboratories, Hercules, CA, USA
Incubator Shaker (Innova44)	Edison, NJ, USA (now Eppendorf Group)
Laminar Flow Sterile Hood (HeraSafe)	Heraeus, Hanau, Germany
Laser Scanning Confocal Microscope (Leica TCS SP5)	Leica Microsystems, Wetzlar, Germany
Leica HyD GaAsP detection system	Leica Microsystems, Wetzlar, Germany
Microfuge Tube Polyallomer	Beckman Coulter, Brea, CA, USA
Microplates (clear flat-bottom or half-area black, clear flat-bottom)	Greiner Bio-One, Frickenhausen, Germany
Nanodrop Micro Volume Spectrophotometer (ND1000)	PeqLab, Erlangen, Germany
Ni-NTA Superflow Resin	Qiagen, Hilden, Germany
Nucleofection Device (Amaxa Nucleofector II)	Lonza Inc, Basel, Switzerland
Power Supply (PowerPac 200)	Bio-Rad Laboratories, Hercules, CA, USA
Rotor (JA-25.50)	Beckman Coulter, Brea, CA, USA
Rotor (JLA 9.1000)	Beckman Coulter, Brea, CA, USA
Rotor (TLA-55)	Beckman Coulter, Brea, CA, USA
Semi-Dry Electrophoretic Transfer Cell (Trans-Blot SD)	Bio-Rad Laboratories, Hercules, CA, USA
Size Exclusion Column (HiLoad 16/60 Superdex 75 PG)	GE Healthcare, Little Chalfont, UK
Size Exclusion Column (Hiload 26/60 Superdex 200 PG)	GE Healthcare, Little Chalfont, UK
Sonication Water Bath (Bioruptor)	diagenode, Seraing, Belgium
Spectrophotometer (SmartSpec Plus)	Bio-Rad Laboratories, Hercules, CA, USA

Tabletop ultracentrifuge	Beckman Coulter, Brea, CA, USA
Tabletop Ultrcentrifuge (Optima MAX-XP)	Beckman Coulter, Brea, CA, USA
Thermocycler	Biometra, Göttingen, Germany
Thermomixer	Eppendorf, Hamburg, Germany
Ultacentrifgue (Avanti J-E)	Beckman Coulter, Brea, CA, USA
UV/Vis Spectrophotometer (SpectraMax M5e)	Molecular Devices, Sunnyvale, CA, USA

2.1.5. List of Bacterial Strains

Strain	**Genotype**	**Source**
DH5α	F-, supE44, ΔlacU169, [Φ80lacZΔM15], hsdR17, recA1, endA1, gyrA96, thi-1, (res-, mod+), deoR (Hanahan, 1983)	
BL21 (DE3) Rosetta	F- *ompT hsdS*$_B$(r_B^- m_B^-) *gal dcm* (DE3) pRARE[1] (Cam^R)	Novagen

[1] pRARE contains the tRNA genes *argU, argW, ileX, glyT, leuW, proL, metT, thrT,tyrU, and thrU*. The rare codons AGG, AGA, AUA, CUA, CCC, and GGA are supplemented.

2.1.6. Mammalian Cell Lines

Cell Line	**Specification**	**Culture Medium**	**Source**
SHSY-5Y	human neuroblastoma	DMEM:F12; 10% FCS, 1% P/S	American Type Culture Collection (ATCC), Manassas, VA, USA
N2A	mouse neuroblastoma	DMEM, 10% FCS, 1% P/S	ATCC
U373	human astrocytoma	DMEM, 10% FCS, 1% P/S	ATCC

HEK-293T	human embryonic kidney	DMEM:F12; 10% FCS, 1% P/S	ATCC

2.1.7. List of Oligonucleotides for Cloning

All nucleotides used in this work were ordered from Sigma-Aldrich, St. Louis, MO, USA.

Denotation	**Sequence (5' -> 3')**	**For Cloning of Plasmid**
4RTau_NcoI_fwd	AATTATCCATGGCTGAGCCCCGCC	pSP01
4RTau_BamHI_rev2	TACTATGGATCCTCACAAACCCTGCTTGGCCAG	pSP01
F3_NcoI_fwd	AATTATCCATGGCTTCCAAGATCGGCTCC	pSP02
F3_BamHI_rev2	AGTCTTGGATCCTCAGATATTGTCCAGGGAC	pSP02
4RFLHA_Bam_fwd	TATATTGGATCCACCATGTACCCATACGATGTTCCAGATTACGCTGCTGAGCCCCGCC	pcDNA3_P301L_HA
4RFLHA_Xho_rev	CGGTCGCCTCGAGTCACAAACCCTGCTTGG	pcDNA3_P301L_HA

2.1.8. List of Plasmids

Empty Vectors and Vector Backbones

denotation	**description**	**resistance**	**manufacturer**
pET3d	vector for protein expression in bacteria, no tag	Amp	Novagen
pET21d	vector for protein expression in bacteria, 6 x His tag, C-terminal	Amp	Novagen

pcDNA3.1	vector for protein expression in mammalian cultured cells	Amp	life technologies

Bacterial Expression Plasmids

denotation	description	backbone	resistance
pSP01	wt 4R Tau	pET3d	Amp
pSP02	MTBD Tau	pET3d	Amp
pPET-HtrA1_helix1	wt HTRA1, 6 x His-tag, C-terminal	pET21d	Amp
pPET-HtrA1 SA-helix1	HTRA1 S328A, 6 x His-tag, C-terminal	pET21d	Amp
Protease_HtrA1_wt-pET	HTRA1 ΔPDZ	pET21d	Amp
Protease_HtrA1_SA-pET	HTRA1 ΔPDZ S328A	pET21d	Amp

Mammalian Expression Plasmids

denotation	description	backbone	resistance
pcDNA3_P301L_HA	P301L Tau	pcDNA3.1	G418

2.1.9. Denotations and Acronyms of Proteins

Tau	MAPT, microtubule-associated protein tau
4R wt Tau	longest human tau isoform, 441 aa; conventionally, numberings of all tau isoforms refer to this isoform of human tau
3R Tau	fetal isoform of human Tau, 352 aa

3R PHP Tau	pseudohyperphosphorylated 3R Tau, mutations: S198E, S199E, S202E, T231E, S235E, S396E, S404E, S409E, S413E, and S422E (Eidenmüller, 2000)
MTBD Tau	aa 258-360, mutation ΔK280 (denoted F3 in Wang et al., PNAS 2007)
P301L Tau	4R Tau with the mutation P301L
wt HTRA1	HTRA1 Δmac, lacking the N-terminal domain, aa 158-480 of HTRA1
HTRA1 S328A	proteolytically inactive HTRA1 Δmac, lacking the N-terminal domain, aa 158-480 of HTRA1
HTRA1 ΔPDZ	HTRA1ΔmacΔPDZ, lacking the N-terminal domain and PDZ domain, aa 158-375 of HTRA1
HTRA1 ΔPDZ S328A	proteolytically inactive HTRA1ΔmacΔPDZ, lacking the N-terminal domain and PDZ domain, aa 158-375 of HTRA1

2.1.10. Antibodies

Primary Antibodies

Antigen	Specifications	Supplier
HA-tag	mouse monocloncal, HA11 clone 16B12	Covance, Princeton, NJ, USA
Tau repeat region	ab-64193, rabbit polyclonal, epitope KIGSTENL (aa 258-262 in 2N4R Tau)	Abcam, Cambridge, UK
actin	mouse monoclonal, clone C4	MP Biomedicals, Santa Ana, CA, USA
αtubulin	mouse monoclonal, T5168, clone B-5-1-2	Sigma-Aldrich, St. Louis, MO, USA
human Tau	mouse monoclonal, Tau-5, RefNo. AHB0042	Life Technologies, Carlsbad, CA, USA
human Tau	mouse monoclonal, biotinylated, clone HT7, RefNo., MN1000B	Thermo Fisher Scientific, Rockford, IL, USA

Secondary Antibodies

For Immunoblotting

Antigen	Specifications	Supplier
mouse IgG (Fc specific)	AP-coupled, goat polyclonal, RefNo. A1418	Sigma-Aldrich, St. Louis, MO, USA
rabbit IgG	AP-coupled, goat polyclonal, RefNo. D0487	Dako, Glostrup, Denmark

For Immunoflurescence

Antigen	Specifications	Supplier
mouse IgG	goat polyclonal, Alexa Fluor 488 coupled, RefNo. A11015	Life Technologies, Carlsbad, CA, USA
mouse IgG	goat polyclonal, Alexa Fluor 594 coupled, RefNo. A11032	Life Technologies, Carlsbad, CA, USA
mouse IgG	goat polyclonal, Alexa Fluor 633 coupled, RefNo. A21052	Life Technologies, Carlsbad, CA, USA
rabbit IgG	donkey polyclonal, Alexa Fluor 488 coupled, RefNo. A21206	Life Technologies, Carlsbad, CA, USA
rabbit IgG	goat polyclonal, Alexa Fluor 594 coupled, RefNo. A11012	Life Technologies, Carlsbad, CA, USA
rabbit IgG	goat polyclonal, Alexa Fluor 633 coupled, RefNo. A21071	Life Technologies, Carlsbad, CA, USA

2.1.11. Software

Software	Purpose	Company / Reference
Leica Application Suite Advanced Fluorescence (LAS AF)	Image Acquisition	Leica Microsystems, Wetzlar, Germany
imageJ	Image Processing and Analysis	open source (Schneider et al.)
NanoScope Analysis	AFM image processing	Bruker, Billerica, MA, USA
GraphPad Prism 5	Statistical analysis and generation of graphs	GraphPad Software, Inc., LaJolla, CA, USA
Zetasizer Software	Dynamic Light Scattering Data Acquisition and analysis	Malvern Instruments, Worcestershire, UK

2.2. Molecular Biology Methods

2.2.1. Buffer Solutions

50 x TAE Buffer

component	per 1000 ml
Tris base	2.42 g
Acetate	57.1 g
0.5 M EDTA, pH 8	100 ml
A.dest.	ad 1000 ml

1 x TAE buffer was prepared by 1:50 dilution with A.dest.

10 x TBS

component	concentration
Tris/HCl, pH 7.5	200 mM
NaCl	1.5 M

1 x TBS buffer was prepared by 1:10 dilution with A.dest.

for 1 x TBS/T, 0.05% Tween was added

10 x PBS

component	concentration
Na-phosphate, pH 7.5	200 mM
NaCl	1.5 M

200 mM Na-phosphate were prepared according to Gomori by a mixing mono- and dibasic Na-phosphate salts, using 161.9 ml 1 M Na_2HPO_4 and 38.1 ml 1 M NaH_2PO_4 per L.

AP Reaction Buffer

component	concentration
Tris/HCl, pH 9.5	100 mM
NaCl	100 mM

$MgCl_2$	5 mM

AP Substrate Solution

The substrate solution for developing AP immunoblots was freshly prepared by diluting BCiP and NBT with AP reaction buffer to a final concentration of 167 µg/ml and 333 µg/ml, respectively. BCiP was prepared as a 300 x stock solution in A.dest. (i.e., 50 mg/ml), NBT as 150 x stocks in 70% dimethylformamide (50 mg/ml).

10 x Transfer Buffer

component	concentration
Tris/HCl, pH 8.3	150 mM
Glycine	1.2 M

6 x DNA loading dye

component	per 100 ml
Glycerol	30 ml
0.5 M EDTA, pH 8	30 ml
Bromophenol blue	30 mg
A.dest.	ad 100 ml

5 x SDS Loading Dye

component	concentration
Tris/HCl, pH 6.8	0.3 M
SDS	10%
Glycerol	40%
Bromophenol blue	0.001%

10x SDS Running Buffer

component	concentration
Glycine	1.92 M
Tris/HCl, pH 8.3	333 mM
SDS	1%

Antibiotics

Antibiotics were added to *E.coli* culture media by dilution of 1000 x stocks:

antibiotic	concentration of 1000 x stock	prepared with
ampicillin	200 mg/ml	A.dest.
chloramphenicol	30 mg/ml	70% EtOH
kanamycin	100 mg/ml	A.dest.

NZA medium

amounts per L medium

component	g/L medium
yeast extract	5
NZ amine A	10
NaCl	5
A. dest.	ad 1 L

LB (Luria Bertani) Medium

component	g/L medium
Bacto/tryptone	10
yeast extract	5
NaCl	10
A. dest.	ad 1 L

LB (Luria Bertani) Agar

LB Agar plates were prepared with 15 g/L agar in LB medium, antibiotics were added in final concentrations as listed above.

2.2.2. Polymerase Chain Reaction (PCR)

For PCR, Phusion polymerase was typically used due to its high fidelity, high processivity and fast polymerization activity. Ca. 10 pg template DNA (plasmids) were used in a typical reaction, as well as 200 µM dNTPs and 200 nM of each primer. To initially test the optimal

conditions of the PCR reaction depending on the particular template and pair of primers, 3 annealing temperatures (typically 55, 60 and 65 °C) as well as 0, 3 and 5% DMSO were used in test reactions. A typical PCR reaction is shown as an example:

Reaction	
5 x Buffer	10 µl
dNTPs	1 µl
fwd	1 µl
rev	1 µl
template	1 µl
DMSO	0/1.5 µl
Phusion	0.5 µl
H_2O	34 µl
ad	50 µl

A PCR program was typically set as follows:

Cycle	Temp (°C)	Duration	→	#	step
1	98	2’			init. denat
2	98	15’’			denat
3	55/60/65	20’’			anneal
4	72	20’’	2	30	elong
5	72	5’			final elong
6	4	-			pause

The success of each PCR reaction was checked by agarose gel electrophoresis and Midori green staining. For the optimal conditions, the PCR was repeated with a larger reaction volume (100 µl), followed by agarose gel electrophoresis and gel extraction for subsequent cloning steps.

2.2.3. Gel Extraction

Extraction of pure DNA from agarose gels, e.g. after PCR or restriction digests, was performed with Qiagen DNA extraction kits according to the manufacturer’s instructions.

2.2.4. Restriction Digest

Restriction digests were performed at 37 °C using the recommended buffers by New England Biolabs, or in the case of two enzymes used simultaneously with the buffer in which both enzymes retain most of their activity. PCR products were digested o/n at 37 °C, whereas plasmid DNA was typically digested for 2 h only. Before ligation, the digested DNA was cleaned up with PCR DNA clean-up kits or by agarose gel electrophoresis and subsequent gel extraction, followed by agarose gel electrophoresis in order to estimate the relative amounts of plasmid and insert DNA to be used the ligation reactions.

2.2.5. Ligation

For the ligation of e.g. PCR fragments into the target vector after the respective restriction digests, the plasmid was dephosphorylated followed by ligation of PCR fragment and plasmid at a molar ratio of ca. 5:1. Typically, several ratios between 2:1 and 10:1 were tested for each pair of insert and target vector. Ligation was performed using the Rapid DNA Ligation kit (Roche) which allows Ligation at RT within 5 min and immediate transformation following the ligation reaction.

2.2.6. Chemically Competent Cells

An overnight culture of the bacterial strain (DH5α or BL21 DE3 pLysS Rosetta II) was added to 100 ml NZA medium to a final OD_{600} of 0.1, the culture was grown until the phase of exponential growth was reached (ca. OD_{600} = 0.5). The culture was cooled down on ice for 10 – 15 min, transferred to 50 ml tubes and spun down at 3,000 x g, 4 °C for 15 min. The supernatant was discarded and the pellet was carefully resuspended with 1/3 of the original culture volume of RF1 buffer (100 mM RbCl, 50 mM $MnCl_2$, 10 mM $CaCl_2$, 30 mM potassium acetate 15% glycerol pH 5.8, adjusted with acetic acid), followed by incubation on ice for 15 min and centrifugation at 3,500 x g, 4 °C for 15 min. The resulting pellet was carefully resuspended with 1/12.5 of the original culture volume of buffer RF2 (10 mM MOPS, 10 mM RbCl, 75 mM $CaCl_2$, 15% glycerol, pH 6.8, adjusted with NaOH), incubated on ice for 15 min, flash frozen as 100 µl in liquid N_2 and stored at -80 °C until usage.

2.2.7. Transformation

Transformation of chemically competent cells was done by incubating and aliquot of competent cells (typically 200 µl) with 1 ng – 1 µg plasmid DNA on ice for 10 – 20 min, followed by a heat-shock at 42 °C, 350 rpm, 1 min, incubation on ice for 1 min and addition of 800 µl LB medium without antibiotics. After a period of phenotypic expression for 45 – 60 min at 37 °C, the cells were plated on LB agar plates or added to the indicated amount of NZA medium for selection and growth.

2.2.8. Agarose Gel Electrophoresis

Agarose gels were freshly prepared by boiling 0.8 – 2% agarose (depending on the size of the DNA to be analysed) in 100 ml TAE buffer (see 2.2.1) and addition of 2 µl of Midori Green DNA staining solution. Electrophoresis was carried out at constant current of 110 V for ca. 30 – 45 min before further staining and gel documentation.

2.3. Protein Biochemical Methods

2.3.1. SDS-PAGE

Sodium dodecyl polyacrylamide gel electrophoresis (SDS-PAGE) is the standard method for the separation and analysis of proteins in solution according to their molecular mass. Treatment with the sodium salt of the detergent dodecyl sulfate followed by boiling leads to the denaturation of proteins and allows their electrophoretic separation because of the resulting overall negative charge. The unfolding and even charge distribution minimize the effects of tertiary structures on the migration of proteins through the polyacrylamide matrix to the anode and therefore results in the size, i.e. the MW, of the macromolecules being the principal determinant of retention in the gel. Accordingly, the MW of the respective proteins can be estimated by comparing the position of the respective protein bands with the position of protein standards of known MW after the appropriate staining of the gels. The reducing agent DTT was added to the sample buffer to a final concentration of ca. 50 – 100 mM in order to reduce possible disulfide bridges. Polyacrylamide gels used in this worked were

prepared essentially according to the classical protocol by Laemmli (Laemmli, 1970), with minor modifications. Depending on the MW range to be separated, the separating gel contained 10%, 12% or 15% polyacrylamide. For the silver stained gels, pre-cast 10% Bis-Tris or 8-13% Tris-Acetate gels (Life Technologies) were used, with the running buffers recommended by the manufacturer. In case of subsequent silver staining, the sample buffer contained ca. 50 mM TCEP instead of DTT to avoid interference with the following silver staining.

2.3.2. Bradford Determination of Protein Concentration

The determination of protein concentration of the recombinant protein samples was performed colorimetric Bradford method (Bradford, 1976), which is based on the shift in absorbance of the dye Coomassie blue, resulting in an absorption proportional to the protein concentration in solution. For the assays performed in this work, the reagent Roti Nanoquant (Carl Roth GmbH) was used in the 96 well plate format, with 50 µl of the diluted protein samples mixed with 200 µl of the reagent. As a standard, a serial dilution of bovine serum abumin (BSA) with known concentrations was prepared.

2.3.3. Coomassie Blue Staining

For detection of proteins by coomassie staining, the gels were heated in Buffer A (25% isopropanol, 10% acetic acid, 0.05% Coomassie blue), rocked for 5-10 min, followed by successive heating in the microwaves in Buffers B (10% isopropanol, 10% acetic acid, 0.005% Coomassie blue), C (10% acetic acid, 0.002% Coomassie blue) and destaining buffer D (10% acetic acid), followed by incubation for 30 min at RT. Buffer D was exchanged until destaining was complete. For documentation of the gels, they were converted to digital images using a Canon office image scanner.

2.3.4. Thioflavin T Fluorescence

In order to detect the formation of amyloid specific cross-beta structures, the amyloid specific dye Thioflavin T (ThT) was used, which is known to specifically shift its emission maximum

towards λ = 480 nm upon binding to amyloid protein aggregates (Friedhoff et al., 1998a; Levine, 1993). For the measurement of ThT fluorescence, 10 µl or 5 µl duplicates of the samples at a Tau concentration of 20 µM were added to 90 µl or 45 µl, respectively, of a 12 µM ThT solution in 50 mM glycine, pH 8.5, using black clear-bottom 96-well microtiter plates for a total of 100 µl measurements and half-area black clear-bottom plates for 50 µl measurements. After incubation at 37 °C, 900 rpm, for 1 min, the fluorescence was measured with a spectrophotometric microplate reader. For emission spectra, the excitation wavelength was kept constant at 440 nm with emission wavelengths ranging from 450 to 520 nm in 5 nm intervals. Single measurements were performed at an excitation and emission wavelength of 440 and 480 nm, respectively. The cutoff filter was set to 450 nm in all cases.

2.3.5. Silver Staining

Silver staining of pre-cast SDS gels was performed for the detection of proteins following digests of soluble Tau and Tau fibrils because of its high sensitivity. The staining protocol was done according to established protocols (Heukeshoven and Dernick, 1988; Merril et al., 1981)(Merril 1981, Heukeshoven 1988). All the steps of the staining protocol were done at RT on a shaker. Gels were fixed 40% EtOH (v/v), 10% acetic acid (v/v), 500 µl/L 37% (v/v) formaldehyde, for 30 min, washed 3 x 10 min with 30% EtOH followed by incubation in A.dest. for 10-60 min. After incubation with a solution containing 0.02% sodium thiosulfate (w/v), the gels were washed 3 x 20 s with A.dest. and incubated with freshly prepared silver nitrate solution (0.2% $AgNO_3$ (w/v), 75 µl 37% formaldehyde per 100 ml). Again, the gels were washed 3 x 20 s with A.dest. and incubated in the developing solution (3% sodium carbonate (w/v), 0.0004% sodium thiosulfate (w/v), 500 µl/L 37% (v/v) formaldehyde) until staining was regarded sufficient. The staining reaction was stopped by washing with A.dest. and incubation with stopping solution (5% acetic acid (v/v)). As for Coomassie stained gels, the gels were documented with a Canon office image scanner.

2.3.6. Immunoblotting

For the specific detection of proteins after SDS PAGE, gels were equilibrated in 1 x transfer buffer containing 10% MeOH at RT for 15 min, blotted using a semi-dry blotting apparatus at 400 mA constant current for 60 min, followed by blocking with 10% skim milk / TBS-T at RT.

All the antibodies used here were diluted as indicated with 5% skim milk / TBS-T. 1° antibody incubation was performed for 1 h at RT or o/n at 4 °C as indicated, followed by washing 3 x with 5% skim milk / TBS-T for 5 min. Incubation with the 2° antibodies was done at RT for 1 h, followed by 3 x washing with TBS-T, equilibration with 1 x AP reaction buffer for 5 min and incubation with the AP substrate solution, until developed sufficiently.

2.3.7. Purification of 3R wt and 3R PHP Tau

3R wt and 3R PHP Tau were purified by boiling of cleared bacterial lysates followed by ammonium sulfate ($(NH_4)_2SO_4$) precipitation. BL21 DE3 Rosetta II cells were transformed with pET 3d vectors containing the respective Tau sequences, grown as 250 ml o/n cultures that were used to inoculate expression cultures of 2 L each starting at an OD_{600} of 0.05. The expression cultures were grown to an OD_{600} of 0.6 – 0.8 and induced with 0.1 mM IPTG for expression. After 5 h expression at 37 °C, the cells were harvested at 8.000 x g, 4 °C for 12 min and the pellets were stored in one 50 ml Falcon tubes at -80 °C until lysis with a microfluidizer in lysis buffer lysis buffer (33 mM Tris-HCl, pH 8, 100 mM KCl). The lysate was cleared by centrifugation (50,000 x g, 4 °C, 40 min), boiled in the water bath for 30 min using 2 ml tubes (ca. 1.5 ml lysate per tube). Tau remains soluble, whereas the precipitated bacterial proteins were cleared from the lysate by centrifugation (35,000 x g, 40 min). For further purification of the 3R Tau variants, the supernatant was incubated with $(NH_4)_2SO_4$ at 30% saturation for 30 min, 4 °C, followed by centrifugation at 20,000 x g, 30 min. Tau was precipitated from the supernatant with 40% saturated $(NH_4)_2SO_4$. Purified Tau was suspended in 80 mM PIPES/KOH, pH 6.8, 1 mM EGTA, 1 mM $MgCl_2$. Due to its low staining by Bradford reagent, the concentration of Tau was determined by comparison of Coomassie stained bands after SDS PAGE with bands of a serial dilution standard of BSA.

2.3.8. Preparation of Soluble and Insoluble Tau Fractions

For the proteolysis of soluble versus aggregated Tau species by HTRA1, purified and AS precipitated 3R wt Tau was ultracentrifuged (100,000 x g, 4 °C, 1 h) to obtain samples of aggregated vs. soluble Tau. The insoluble protein was resuspended from the resulting pellet and the protein concentration determined by Bradford quantitation.

2.3.9. Cloning and Purification of 4R wt and MTBD Tau

The coding sequences of wt full-length 4R Tau and MTBD Tau (aa 258-360 ΔK280 of human 4R Tau) were cloned into pET3d vectors using PCR, restriction digest of PCR products with *Nco*I and *Bam*HI and ligation. 4R wt and MTBD Tau were purified by boiling of cleared bacterial lysates followed by hydroxyapatite (HAP) chromatography and size-exclusion chromatography (SEC) as follows. BL21 DE3 Rosetta II cells were transformed with pET 3d vectors containing the respective Tau sequences, grown as 250 ml o/n cultures that were used to inoculate expression cultures of 2 L each starting at an OD_{600} of 0.05. The expression cultures were grown to an OD_{600} of 0.6 – 0.8 and induced with 0.1 mM IPTG for expression. After 5 h (4R wt) or 2 h (MTBD Tau) at 37 °C, the cells were harvested at 8.000 x g, 4 °C for 12 min and the pellets were stored in one 50 ml Falcon tubes at -80 °C until lysis with a French pressure cell in HAP equilibration buffer (100 mM HEPES, 10 mM KPO_4, 2 mM DTT, pH 7.6). The lysate was cleared by centrifugation (50,000 x g, 4 °C, 40 min), and the lysate was transferred to 2 ml tubes (ca. 1.5 ml per tube) for boiling in the water batch for 20 min. The boiling step was followed by centrifugation (35.000 x g for 40 min) and recovery of the supernatant containing Tau protein and little amounts of contaminating proteins. The supernatant was further purified by HAP chromatography, where Tau was loaded onto the column with HAP equilibration buffer, washed with equilibration buffer (4 CV) followed by Tau elution by an NaCl gradient (0-100% 100 mM HEPES, 10 mM KPO_4, 1 M NaCl, 2 mM DTT, pH 7.6). Typically, Tau eluted at an NaCl concentration of ca. 240 mM NaCl. Usually, the flow-through from the HAP chromatography purification was applied 1-2x after the first purification step to increase the total yield of protein, because of large amounts of Tau being the flow-through after the first rounds of HAP chromatography. Full-length Tau and MTBD Tau were concentrated with centrifugal concentration devices and further purified by SEC using Hiload 26/60 Superdex 200 and HiLoad 16/60 Superdex 75 preparation grade size exclusion columns for 4R wt and MTBD Tau, respectively, with the size exclusion buffer in 10 mM HEPES, 50 mM $(NH_4)_2SO_4$, 2 mM TCEP, pH 7.5. Following SEC, the samples were concentrated to ca. 10 – 25 mg/ml storage concentration, flash-frozen in liquid N_2 and stored at -80 °C until usage. Due to its low staining by Bradford reagent, the concentration of Tau was determined by comparison of Coomassie stained bands after SDS-PAGE with bands of a serial dilution standard of BSA.

2.3.10. Purification of HTRA1

Human recombinant HTRA1 was purified as described (Truebestein et al., 2011) except that an hydroxyapatite column (Bio-Rad) was added after the Ni-NTA purification step.

For expression of HTRA1, BL21 DE3 Rosetta II cells were transformed with pET vectors containing the respective Tau sequences and grown in a 250 ml o/n culture before inoculation of expression cultures (2 L per flask) starting at an OD_{600} of 0.05 and growth to an OD_{600} of 0.6 – 0.8 before induction with 0.2 mM IPTG. 1 h before induction, the cultures were transferred to 25 °C, expression was carried out for 5 h, 25 °C, 180 rpm. The cells were harvested at 8.000 x g, 4 °C for 12 min and - the pellets were stored in one 50 ml Falcon tube at -80 °C until lysis with a French pressure cell in Ni-NTA equilibration buffer (100 mM Tris/HCl, pH 7.5, 150 mM NaCl, 5 mM β-ME). The lysate was cleared by centrifugation (50,000 x g, 4 °C, 40 min). Purification was performed with an Äkta FPLC system, the purification via the 6xHis-tag of HTRA1 was carried out on a pre-equilibrated Ni-NTA column by applying the lysate and successive washing steps with 6 column volumes (CV) equilibration buffer (100 mM Tris/HCl, pH 7.5, 150 mM NaCl, 5 mM β-ME), 8 CV NaCl wash buffer (100 mM Tris/HCl, pH 7.5, 1 M NaCl, 5 mM β-ME), 5 CV 100 mM Tris/HCl, pH 7.5, 1 M NaCl, 5 mM β-ME, 25 mM imidazole and 10 CV 100 mM Tris/HCl, pH 7.5, 300 mM NaCl, 5 mM β-ME, 30 mM imidazole. The protein was eluted with 100 mM Tris/HCl, pH 7.5, 300 mM NaCl, 5 mM β-ME, 150 mM imidazole, 5 x concentrated and diluted with hydroxyapatite (HAP) equilibration buffer (50 mM HEPES, 10 mM KPO_4, pH 7.8) before HAP chromatography for proper binding to the column resin. HAP chromatography was performed by binding with 50 mM HEPES, 10 mM KPO4, pH 7.8, and successive washing steps with 0% (2 CV), 10% (5 CV), 15% (5 CV), 17%, 18% and 19% (2 CV each) of 500 mM KPO_4 elution buffer (50 mM HEPES, 476.6 mM K_2HPO_4, 23.4 mM KH2PO4, pH 7.8), followed by gradient elution from 19-50% 500 mM KPO_4 elution buffer. After HAP chromatography, the protein was further purified by size exclusion chromatography using Superdex 200 preparation grade columns (GE Healthcare) in 10 mM HEPES, 50 mM $(NH_4)_2SO_4$, pH 7.5. Protein concentrations were determined by Bradford assays and SDS-PAGE.

2.3.11. Fluorescence-labeling of HTRA1 S328A

Recombinant human HTRA1 was labeled with the amine reactive fluorescent dye Alexa Fluor 568 carboxylic acid, succinimidyl ester (Life Technologies), by incubating 200 µM of

HTRA1 with 2 mM of the reactive dye in 100 mM sodium bicarbonate, pH 8.3, at room temperature and constant agitation for 1 h. Prior to the labeling reaction, HTRA1 solution was adjusted to the labeling buffer using desalting columns (PD SpinTrap G-25). After completing the labeling reaction, the labeled protein was separated from the free dye using desalting columns and stored at -80 °C in single-use aliquots.

2.3.12. Arachidonic Acid Induced Aggregation of 3R Tau

To induce the aggregation of 3R Tau, arachidonic acid (ArA) was used as based on protocols that have been published before (King et al., 1999). 3R Tau was pre-incubated with 5 mM DTT for 10 min at RT in order to reduce the protein before using it in the aggregation reaction. For the aggregation, 4 µM Tau were incubated in 10 mM HEPES, 100 mM NaCl, pH 7.6 with 150 mM arachidonic acid at 37 °C, 400 rpm for 72 h. Arachidonic acid was added to the reaction from 15 mM stocks in DMSO which had been prepared under argon gas and stored as single-use aliquots at -20 °C.

2.3.13. Heparin-Induced Fibrillization of 4R Tau and MTBD Tau

Aggregation of human full-length Tau was performed as described (Li and Lee, 2006) with minor modifications. In short, Tau at a concentration of 20 µM was incubated in aggregation buffer (100 mM sodium acetate, 2 mM DTT, pH 7) at 55 °C, 800 rpm for 10 min, followed by addition of 1 mM fresh DTT and 50 µM heparin. After fibrillization at 37 °C, 900 rpm for 48 h up to 5 days, with addition of 1 mM of fresh DTT every 24 – 48 h, the extent of aggregation was checked by ultracentrifugation and Thioflavin T fluorescence as indicated. The resulting aggregates were used in disaggregation experiments as explained above. For the proteolysis experiments with HTRA1, the Tau fibrils were sedimented by ultracentrifugation at 186,000 x g, 4 °C for 1 h and resuspended with HTRA1 proteolysis buffer, in order to remove heparin and soluble Tau species from the reaction. Concentrations of the aggregates were determined by SDS PAGE, Coomassie staining and comparison with BSA samples of known concentration. Fibrils composed of MTBD Tau were assembled accordingly, except that the duration of fibrillization was reduced to 24 h.

2.3.14. Dynamic Light Scattering

Dynamic light scattering measurements for size analysis of insoluble 3R Tau and arachidonic acid induced 3R Tau aggregates were performed using a Malvern Zetasizer Nano ZS and the associated software for data acquisition and analysis. The manual run mode was used, with the pre-set refractive index values for proteins and water as solute. 3 measurements were done per sample with constant values for attenuation factors and number of runs to ensure reproducibility of measurements. The temperature was kept at 25 °C with 2 min equilibration time before each measurement. The insoluble Tau samples after ultracentrifugation were diluted to 0.05 mg/ml with 50 mM NaH_2PO_4, 150 mM NaCl, pH 8 with 200 µl measured in disposable DTS1061 cuvettes. For dilution of arachidonic acid induced 3R Tau aggregates, the aggregation buffer 10 mM HEPES, 100 mM NaCl, pH 7.6, was used. To assess the particle size in the respective samples, the mean hydrodynamic radius was calculated.

2.3.15. Chromogenic Activity Assay of HTRA1

For determination of the proteolytic activity of recombinant HTRA1, two synthetic substrates were employed in this work, consisting of the peptides PGGGNKKIETHKL and VFNTLPMMGKASPV coupled to para-nitroaniline (pNA) groups at their C-terminus. 50 µg/ml HTRA1 (i.e., 1.35 µM) were incubated with 500 µM of the respective substrate and the indicated molar proportions of WT or PHP 3R Tau in a total volume of 100 µl, 50 mM Tris/HCl, pH 8, at 37 °C. The release of free pNA upon proteolysis was monitored by measuring the absorption at λ = 405 nm every minute for a total reaction time of 90 min. The reactions were performed in 96-well microplates using a Molecular Devices SpectraMax M5 Microplate Reader. For calculation of the specific activity, a time segment of linear increase in absorption was used to quantify the turnover of the substrate by employing the specific molar absorption coefficient of pNA, 8,800 M^{-1} x cm^1.

2.3.16. Activity Assays of Calpain-1 and Caspase-3

The proteolytic activity of Caspase-3 was assayed by a pNA based chromogenic activity assay corresponding to the assay described for recombinant HTRA1 (2.3.15), with the

following alterations. The substrate Ac-DEVD-pNA was cleaved by 0.5 Units/µl, i.e. 0.33 nM, human recombinant Caspase-3 in the presence of WT and PHP 3 wt Tau in the concentrations corresponding to the indicated molar ratios. The assay buffer used here was 50 mM HEPES, pH 7.4, 100 mM NaCl, 0.1% CHAPS, 1 mM EDTA, 10% glycerol, 10 mM DTT, as described before. For the determination of Calpain activity, a fluorimetric assay was performed as described before using the fluorogenic peptide substrate N-Succinyl-Leu-Leu-Val-Tyr-7-Amido-4-Methylcoumarin (Suc-LLVY-AMC) (Croce et al., 1999). Upon proteolysis, the highly fluorescent AMC moiety is released and can be quantified as a measure of substrate turnover. The assays were performed at 23 °C in 100 µl assay buffer, 50 mM TriS/HCl, 100 mM NaCl, 2 mM $CaCl_2$, 1 mM DTT, pH 7.5 using 96-well microtiter plates. Substrate and Calpain-1 concentrations were 200 µM and 0.1 Units/µl (0.52 µM), respectively. Recombinant wt or PHP 3R Tau was added to the reaction at the indicated molar ratio, and fluorescence was monitored by performing single measurements in duplicates every minute for 90 min with an excitation wavelength of 380 nm and en emission wavelength of 450 nm. The measurements were done with a Molecular Devices SpectraMax M5 Microplate Reader, the cutoff-filter was set to 435 nm. From the initial, linear increase in fluorescence, the concentration of free AMC was quantified using an AMC standard curve generated under the according conditions. The specific activity of Calpain-1 was calculated as the ratio of substrate turnover and amount of enzyme.

2.3.17. Disaggregation of Tau Fibrils by HTRA1 *in vitro*

For disaggregation of full-length Tau fibrils, 6.8 µM Tau aggregates from 48 h fibrillization reactions as described above, were incubated with buffer or equimolar amounts of HTRA1 S328A or the mutants or control proteins as indicated in 100 mM 2-(N-morpholino)-ethanesulfonic acid (MES), 100 mM NaCl, pH 6 at 37 °C, 350 rpm, for 16 h. Analysis of solubility was performed by ultracentrifugation of 20 µl of the samples at 186,000 x g, 4 °C for 1 h. As controls, HTRA1 or the proteins indicated were incubated under the same conditions without Tau, but with the respective volume of aggregation buffer (100 mM sodium acetate, 2 mM DTT, pH 7) with 2 mM DTT instead. The supernatants were mixed with loading buffer containing DTT at a final concentration of 80 mM, the pellets were solubilized with the respective amounts of loading buffer and DTT by thorough vortexing and resuspending. Total samples were removed before ultracentrifugation and treated accordingly. The amounts of Tau in the individual fractions were assessed by SDS-PAGE

followed by Coomassie staining. For AFM analysis of the disaggregation samples, the samples were diluted with PBS, pH 7.4 to 2 µM final Tau concentration as according to the full-length monomer molecular weight of 45.8 kDa. Disaggregation of MTBD Tau fibrils was done in the same way except that 13.7 µM Tau was used, and a 5-fold excess of HTRA1 or MDH, and the disaggregation buffer was 100 mM Tris/HCl, 150 mM NaCl, pH 9, in this case. MTBD Tau was detected by immunoblotting with a polyclonal antibody against the repeat region of Tau, whereas HTRA1 and MDH were analyzed by SDS-PAGE and Coomassie staining of 1:10 diluted total, supernatant and pellet fractions because of the high protein concentrations in the original samples.

2.3.18. Proteolysis of Soluble and Insoluble 3R Tau by HTRA1, Calpain-1 and Caspase-3

Tau from the soluble and insoluble fractions which were prepared as described above was diluted to the assay concentration with the respective assay buffers, which were 50 mM Tris/HCl, pH 8 for HTRA1, 50 mM TriS/HCl, 100 mM NaCl, 2 mM $CaCl_2$, 1 mM DTT, pH 7.5 for Calpain-1 and 50 mM HEPES, pH 7.4, 100 mM NaCl, 0.1% CHAPS, 1 mM EDTA, 10% glycerol, 10 mM DTT for Caspase-3. Before addition of the protease, Tau was diluted with the assay buffer to the final concentration, which was for Calpain-1 and HTRA1 20 ng/µl and for Caspase-3 1.8 ng/µl. After incubation of the Tau solutions at assay temperature for 2 min, the protease was added, so that the molar ratio of protease to substrate was 1:10 based on the Tau monomer MW of 37 kDa. The samples were incubated at 37 °C (HTRA1 and Caspase-3) or 23 °C (Calpain-1) with agitation, aliquots were taken at the indicated time points. The aliquots were mixed with SDS loading dye and a final concentration of 40 mM of the reducing agent TCEP and immediately frozen with liquid N_2. Prior to SDS-PAGE using Novex NuPage 10% Bis-Tris gels (Life Technologies) and MES running buffer, the samples were heat-treated at 75 °C for 10 min. Protein bands were visualized by silver staining.

2.3.19. Proteolysis of 4R Tau and Tau Fibrils

Proteolysis of Tau and Tau fibrils by HTRA1 was performed at protein concentrations dependent on the mode of analysis. Typically, digests of Tau fibrils was performed at low protein concentrations followed by SDS PAGE and the sensitive method of silver staining in

order to use less recombinant protein. For these experiments, Tau fibrils were obtained from heparin induced aggregation as described above, followed by ultracentrifugation in order to remove residual soluble Tau and heparin. 680 nM Tau were incubated with wt HTRA1 at a molar protease:substrate ratio of 1:2.5, i.e., with 272 nM wt HTRA1 in 50 mM Tris/HCl, 5 mM tris(2-carboxyethyl)phosphine (TCEP), pH 8 at 37 °C, 350 rpm. Aliquots were taken at the indicated time points, mixed with loading dye and 50 mM TCEP, flash frozen in liquid nitrogen and kept frozen until analysis by SDS PAGE. For disaggregation followed by proteolysis, Tau fibrils or soluble Tau was incubated with a 10x excess of HTRA1 S328A, or the mutants indicated, as compared to wt HTRA1 (i.e., 2.72 µM) or buffer at 37 °C for 2 h before addition of wt HTRA1. Samples were boiled at 96 °C for 10 min and subjected to SDS PAGE using pre-cast 10% Bis-Tris polyacrylamide gels (Life Technologies).

2.3.20. Disaggregation and Proteolysis Analyzed by Atomic Force Microscopy (AFM)

For proteolysis followed by atomic force microscopy (AFM), the same protocol as described above was used except that 2 µM fibrillar Tau was used, with the other protein concentrations adjusted accordingly to obtain the same molar ratios. Before AFM, the ultracentrifugation step was omitted in order to keep the fibrils intact for reliable analysis. Disaggregation samples were diluted 1:3 (to gain ca. 2 µM final Tau concentration) before AFM analysis. Acquisition of AFM images and operation of the atomic force microscope were done by Barbara Sacca and Andreas Sprengel. Without previous treatment, 5 µl samples were deposited on a freshly cleaved mica surface and adsorbed for 3 min at RT. After addition of 15 µl 40 mM Tris, 20 mM acetic acid, 2 mM EDTA, 12.5 mM Mg acetate, pH, the sample was scanned on a MultiModeTM 8 microscope (Bruker, Germany) equipped with a Nanoscope V controller, using the ScanAsyst® PeakForce TappingTM operational mode. Silicon nitride probes with 0.7 N/m nominal spring constant and sharpened pyramidal tips (ScanAsyst Fluid+, Bruker) were used for scanning. At least three images (3x3 µm) were acquired from random locations of the mica surface for statistical analysis of the results. Recorded views were 3rd order flattened and exported as TIFF files using the NanoScope 6.14 software (Bruker). Fibril lengths were analyzed with imageJ (Schneider et al., 2012) by creating a collection of ROIs using the freehand selection tool and measuring the sets of ROIs of individual images. The sums of the lengths of fibrils in the images of each sample were

statistically analyzed using the two-sided t-test for unpaired samples with Welch's correction using the statistical analysis software Prism 5 (GraphPad).

2.3.21. Proteolysis and Sample Preparation for Subsequent Mass-Spectrometric Analysis (LC-MS/MS)

For the mass-spectrometric analysis of cleavage sites by HTRA1, proteolysis of soluble Tau and Tau fibrils was performed for the indicated duration after 2 h incubation time with buffer proteolysis buffer or HTRA1 S328A as indicated. Buffers and concentrations were the same as described above for the proteolysis with subsequent analysis by SDS-PAGE. At the respective time points after addition of wt HTRA1, 20 µl samples were directly added to 120 µl ice-cold acetone for acetone precipitation for 2 h at -80 °C. The precipitated protein was spun down at 20,000 x g, 4 °C for 60 min. The supernatant containing the peptidic cleavage products was dried, resuspended with PBS and prepared and cleaned up prior to LC-MS on homemade StageTips. The StageTips were prepared using the protocol by Rappsilber et al. (Rappsilber et al., 2007).

2.3.22. Mass-Spectrometry (LC-MS/MS)

The mass-spectrometric analysis and operation of the instruments were performed by Dr. Farnusch Kaschani, University Duisburg-Essen. Experiments were performed on an Orbitrap Elite instrument (Thermo Scientific) that was coupled to an EASY nLC 1000 (Thermo Scientific) liquid chromatography (LC) system (Michalski et al., 2012). The LC was operated in the one-column mode. The analytical column (75 µm × 15 cm, packed in-house with Reprosil-Pur 120 C18-AQ 1.9 µm resin, Dr. Maisch) was linked to a stainless steel emitter (4 cm, OD. 150 µm, I.D. 30 µm) via a Microtight® union (Upchurch, P-771) and hooked up to a nanospray flex ion source (Thermo Scientific). The LC was equipped with two mobile phases: solvent A (0.1% formic acid (FA) in UPLC grade water) and solvent B (0.1% FA in acetonitrile (ACN)). Peptides were delivered directly to the analytical column via the integrated autosampler at a flow rate of 0.7-0.9 µl/min in 100% solvent A. Peptides were subsequently eluted from the column by running a 20 min gradient of solvent A and solvent B (start with 2% B; gradient 2% to 35% B for 10 min; gradient 35% to 100% B for 2 min; 100% B for 8 min) at a flow rate of 300 nl/min.

The Orbitrap Elite mass spectrometer was operated using Xcalibur software (version 2.2 SP1.48). The mass spectrometer was set in the positive ion mode. Precursor ion scanning was performed in the Orbitrap analyser (FTMS) in the scan range of m/z 300-2000 and at a resolution of 30000 with the internal lock mass option turned on (lock mass was 445.120025 m/z, polysiloxane)(Olsen et al., 2005). Product ion spectra were recorded in a data dependent fashion in the ion trap (ITMS) in a variable scan range and at a normal scan rate. The ionization potential (spray voltage) was set to 1.6 – 2.0 kV. Peptides were analyzed using a repeating cycle consisting of a full precursor ion scan (1.0 × 106 ions) followed by five product ion scans (1.0 × 104 ions) where peptides are isolated based on their intensity in the full survey scan (threshold of 500 counts) for tandem mass spectrum (MS2) generation that permits peptide sequencing and identification. CID collision energy was set to 35% for the generation of ms2 spectra. During MS2 data acquisition dynamic ion exclusion was set to 30 seconds with a maximum list of excluded ions consisting of 500 members and a repeat count of one. Ion injection time prediction, preview mode for the FTMS, monoisotopic precursor selection and charge state screening were enabled. Only charge states bigger than 1 were considered for fragmentation.

The recorded RAW files were processed in ProteomDiscoverer 1.3 (PD13, Thermo). MS2 spectra were extracted using the Spectrum Selector node. Precursor selection was set to “use MS1 precursor”. The mass range was set between 350 – 5000 Da with a minimum peak count of 1. Mass analyser was set to “any” and MS order to “MS2”. Activation type was set to “is CID” and Scan type was defined as “full” with ionization source set to “is nanospray”. Selected spectra were submitted to the in house MASCOT server (version 2.4.1) (Perkins et al., 1999) using the PD13 MASCOT node. MS2 spectra data were searched against an E. coli K12 reference protein database downloaded from Uniprot (www.uniprot.org/taxonomy/complete-proteomes) (4574 protein sequences, download date 25.10.2013) and supplemented with the sequence of interest for Tau. To evaluate the degree of contamination MS2 spectra were also searched against a database comprising known MS contaminants (used as implemented in MASCOT, 262 protein sequences). Mascot searches allowed for oxidation of methionine residues (16 Da) but no static modifications (cysteine residues were not alkylated with iodoacetamide). In accordance with our aim to detect endogenous cleavage sites no enzyme was specified. The instrument type was set to ESI-TRAP and the mass tolerance was set to ±10 ppm for precursor mass and ±0.8 Da for product ion masses. MS2 spectra matches were then evaluated using the peptide validation node of PD13 with the standard settings (search against decoy database, target false

discovery rate (FDR, strict): 0.01 and target FDR (released): 0.05). The reported results were further filtered. On peptide level only peptides with a minimum confidence ‘medium’ were reported and on protein level only proteins with a minimum of at least two peptide hits were reported. The detected peptides were mapped to the primary sequence of full-length 4R Tau, and the P1 sites were derived from their N- and C-terminal residues. Assignment of the cleavage site to equal sized sections of the Tau primary sequence was done with Excel.

2.4. Cell Biological Methods

2.4.1. Maintenance and Passaging of Cells

All cell lines were maintained at constant temperature (37 °C), CO_2 concentration (5%) and humidity, maintenance cultures were grown in 10 cm (diameter) plastic cell culture dishes. All cell lines used in this work were maintained in DMEM (Dulbecco’s modified Eagle’s medium) supplemented with 10% fetal calf serum (FCS) and 1% Penicillin / Streptomycin, except for SHSY-5Y cells, which were maintained with DMEM:F-12 medium with 10% FCS and 1% Penicillin / Streptomycin. Cells were passaged regularly to avoid postconfluent growth, the frequence of passaging depending on the rate of cell division. For detachment of adherent cells from the culture dish, the culture medium was removed, the cells were washed once with PBS, and 1.5 ml 0.025% Trypsin / EDTA was added per 10 cm dish. For smaller area cell culture dishes, the volume of Trypsin used was adjusted accordingly. After incubation at 37 °C for 5 min, Trypsin was inactivated by addition of 8.5 ml culture medium containing FCS. The cells remaining adherent to the dish were mechanically detached from the dish by repeated pipetting, which also led to separating groups or clumps of cells. A part of this cell suspension was transferred to a new culture dish with fresh medium to gain the desired dilution of the maintenance culture. 293T HEK cells were passaged every 3 – 4 days with a dilution of 1:12 to 1:15. SHSY-5Y cells were passaged in the same intervals at a dilution of 1:8 to 1:10.

2.4.2. Cryoconservation of Mammalian Cells

For the long-term storage of mammalian cell lines, cells were trypsinized as described in (2.4.1), and counted. 1-2 x 10^6 cells were stored per vial for cryo-conservation. The respective number of cells was centrifuged at 1,100 rpm for 5 min, washed with PBS to remove remaining cell culture medium and resuspended with 500 µl FCS per 1-2 x 10^6 cells. 500 µl per cryo-vial 20% DMSO in FCS were added dropwise to the suspension to gain a final concentration of 10% DMSO. The resulting suspension was transferred to vials and stored in cryo-containers with isopropanol at 80 °C that allow a slow decrease in temperature of ca. 5 °C per hour in order to ensure a gentle freezing process.

2.4.3. Cell Counting

For any application that requires the use of defined numbers of cells, a hemocytometer was used. 20 µl of the cell suspension to be quantified were applied to the clean hemocytometer, followed by counting of the cell in 4 squares á 0.1 µl. The mean number of cells per square equals the number of cells x 10^4 per ml.

2.4.4. Nucleofection

Cultured cells were transiently transfected with mammalian expression plasmids using the Nucleofection method by Lonza Amaxa, which is based on the principle of electroporation. The procedure involved trypsinization of the cells, mixing them with the desired amount of DNA (here, 4 µg of plasmid DNA were used for each nucleofection reaction) in 100 µl of the Nucelofector solution and the electroporation step. After the electroporation, the cells were carefully resuspended with 500 µl preconditioned culture medium containing 10% FCS and transferred to culture dishes in the dilution needed to seed the desired amount of cells. For the cell lines tested in this study, the Cell Line Nucleofector Kit V was used, and the recommended preset programs for the respective cell lines were applied. The appropriate number of cells per nucleofection was tested in preliminary experiments for each cells line. Eventually 3.2 x 10^6 HEK-293T cells were nucleofected using program Q-001, 3 x 10^6 SHSY-5Y cells with program A-023, 1.5 x 10^6 N2A cells with program T-024, and 2.5 x 10^5 U373 cells with program T-020.

2.4.5. Seeding of Tau Aggregation in 293T HEK Cells

The seeding of intracellular Tau aggregation in 293T HEK cells was done according to a protocol that was published before (Guo and Lee, 2011) with some modifications and the additional analysis of the effect of HTRA1 internalization from the extracellular space.

Preparation of MTBD Aggregate Seeds

Fibrils seeds composed or MTBD Tau were prepared by fibrillization for 24 h as described above, followed by ultracentrifugation at 186,000 x g, 4 °C for 1 h. The pellets were thoroughly resuspended with PBS, pH 7.4, vortexed, and the extent of fibrillization was checked by SDS PAGE of samples from the supernatant and pellet. Typically, all of the MTBD Tau was found in the pellet after 24 h of fibrillization. The MTBD Tau aggregates were sonicated in the water bath 2 x 2 min with 1 min interruption before performing protein transfection.

Transient Transfection of 293T HEK Cells and Seeding of Aggregation

For Sarkosyl extraction experiments, 293T HEK cells were transiently transfected by nucleofection (Lonza Inc., Basel, Switzerland) with a pcDNA3.1 plasmid for overexpression of HA-tagged full-length human Tau with the point mutation P301L. 4 x 10^5 cells were grown in each well of a 6-well plate for expression of P301L Tau for 24 h to reach about 50% confluency. Cell culture dishes were poly-L-lysine coated prior to seeding. Freshly prepared MTBD Tau aggregate seeds were transfected into the cells at a final concentration of 17.5 µg/ml using 10 µl per well of the cationic lipid based protein transfection reagent Pro-Ject, followed by 4 h incubation with DMEM culture medium without serum and 20 h of incubation with 0.5% fetal bovine serum (FBS). For HTRA1 internalization experiments, cells were washed twice with serum-free DMEM medium, followed by addition of 2 ml of medium conditioned with either PBS or HTRA1 at a final concentration of 150 µg/ml, i.e. 5.54 µM, and incubated at 37 °C for 20 h before performing Sarkosyl extraction and immunoblotting.

2.4.6. Sarkosyl Extraction from Cultured Cells

After seeded aggregation, Sarkosyl extraction was performed in order to assess the extent of aggregated versus soluble, HA-tagged P301L Tau. The Sarkosyl extraction was done essentially as described before (Guo and Lee, 2011) with some modifications as follow. The

cells were detached from the culture dish by trypsinization, and washed thoroughly with PBS to remove all residual trypsin from the cell pellet. The pellet was resuspended with lysis buffer containing Sarkosyl, 10 mM Tris/HCl, 150 mM NaCl, 1 mM EGTA, 5mM EDTA, 1% Sarkosyl, pH 7.4 with protease inhibitor (Roche complete protease inhibitor tablet), and incubated on ice for 15 min. For cell lysis, the suspension was 10 x syringe sheared with a 27G needle, followed by incubation on ice for 15 min, 2 x 2 min sonication in the water bath and incubation at 25 °C for 20 min. The samples were ultracentrifuged at 186,000 x g, 4 °C for 60 min, the supernatant was saved as Sarkosyl soluble fraction, the pellet was resuspended with the corresponding amount of SDS loading buffer containing 1% SDS by vigorous vortexing and resuspending. Equal amounts of the individual samples were be subjected to SDS PAGE and immunoblotting based on the Sarkosyl supernatant concentrations determined by absorption at 280 nm using a NanoDrop micro volume spectrophotometer (Peqlab, Germany). Volumes of the Sarkosyl insoluble fractions were adjusted accordingly. The samples were loaded onto 10% SDS gels followed by immunoblotting against Tau, HTRA1 and actin. The bands were detected by alkaline phosphatase (AP) coupled secondary antibodies, followed by chromogenic detection of AP activity.

2.4.7. Internalization of Recombinant, Labeled HTRA1 by HEK-293T Cells

To study the spontaneous internalization of recombinant HTRA1 protein from the extracellular space, 8 x 10^5 HEK-293T cells were seeded in poly-D-lysine coated 6 cm cell culture dishes and grown for 24 h to reach ca. 50-60% confluency at the time of treatment with HTRA1 conditioned medium. Cells were washed twice with PBS before addition of 4 ml serum-free medium containing recombinant, labeled HTRA1 in the concentration indicated. After a period of incubation time as indicated, the cells were detached from the culture dish by trypsin / EDTA treatment, centrifuged, and the cell pellet was washed thoroughly with PBS to remove all residual trypsin from the sample. The resulting pellet was lysed with RIPA buffer with protease inhibitor (Roche), the protein concentration was determined by absorption at λ = 280 nm, and equal amounts of 150 µg total cell lysate were analyzed by SDS PAGE followed by immunoblotting. Alternatively, 1.5 x 10^5 cells were seeded in each well of a 24 well plate on poly-D-lysine coated glass coverslips, treated with 500 µl serum-free DMEM medium per well containing 50 µg/ml Alexa Fluor 568 labeled HTRA1 S328A, grown for 24 h, methanol fixed and stained for immunofluorescence as described above. As

a control for the uptake of labeled HTRA1, the amine reactive dye by itself was saturated by 1:5 dilution with 100 mM Tris, pH 8.42, and the same concentration as assessed by absorption at λ = 578 nm of the labeled protein and isolated dye was used in the experiment.

2.4.8. Immunofluorescence Staining and Confocal Laser Scanning Microscopy

For seeding of Tau aggregation and HTRA1 internalization experiments to be analyzed by confocal laser-scanning microscopy, the cells were transfected as done before Sarkosyl extraction except some modifications. Following transfection with Tau P301L expression plasmids, 1.6 x 10^5 cells were transferred to each well of 24 well plates with poly-D-lysine coated glass coverslips and grown for 24 h before transfection with MTBD seeds which were prepared as described above. For transfection in 24 well plates, only 2.5 µl of the transfection reagent were used per well. Where indicated, treatment with labeled HTRA1 was done as described above except that 50 µg/ml, i.e. 1.85 µM labeled HTRA1 was used in a final volume of 500 µl. After an incubation period of 20 h as described above, the cells were fixed with ice-cold methanol, permeabilized with 0.5% Triton X-100 for 5 min, and washed with PBS before further staining was performed. For the detection of amyloid aggregates, Thioflavin S (ThS) staining was performed as described (Guo and Lee, 2011), by incubation with 0.005% ThS, dissolved in PBS and sterile filtered, for 8 min at RT, followed by 5 x washing with 50% ethanol for 5 min. The samples were then blocked with 5% bovine serum albumin (BSA) for 30 min before antibody staining was done with primary antibodies as indicated, using Alexa Fluor 633 labeled secondary antibodies. The anti HA antibody and secondary antibodies were diluted 1:500, the polyclonal anti HTRA1 PDZ antibody was used in 1:50 dilution in 3% BSA/PBS. Before mounting the samples with ProLong Gold antifade mounting solution (Life Technologies), they were washed with PBS 3 x for 15 min at RT. Where used, DAPI was added in 1:10,000 dilution together with the secondary antibody solutions. The nuclear counterstain To-Pro 3 iodide (Life Technologies) was used diluted 1:500 from a 1 mM stock solution. When To-Pro 3 staining was done, the samples were treated with 100 µg/ml RNAse A at 37 °C for 20 min to eliminate unspecific staining of cytoplasmic RNA. Microscopy was done with a Leica TCS SP5 Confocal Laser Scanning Microscope equipped with Leica HyD Gallium Arsenide phosphide hybrid detection systems. Image acquisition was performed with the same detector sensitivity settings for samples and controls. Images of the different channels were acquired individually in serial acquisition

mode to avoid fluorescent bleed-through. Images of single focal planes using 60 µm pinhole width are shown.

3. Results

3.1. Purification of HTRA1

For studying the proteolytic activity of HTRA1 and its ability to proteolyse various forms of soluble and insoluble recombinant human Tau protein, recombinant human HTRA1 was expressed and purified from *E. coli.* Full-length HTRA1 is comprised of an N-terminal partial IGFBP7 domain, a protease resembling chymotrypsin and a C-terminal PDZ domain. While the function of the N-terminal domain is yet to be identified, the other two domains are characteristic of HtrA proteases (See 1.3.1). Purification of the full-length protein from *E. coli* is limited which is probably due to the large number of Cys residues and therefore potential disulfide bonds residing in the N-terminal part of the protein. In previous work (dissertation by L. Trübestein and (Truebestein et al., 2011)), the testing of a number of constructs with varying N-termini has yielded best results for a construct comprising aa residues 158-480 and aa 158-375 for the constructs with and without the PDZ domain, respectively. The former protein will be referred to as HTRA1, whereas the latter is termed HTRA1 ΔPDZ in the following. In addition to the proteolytically active HTRA1, mutants which have the active site serine mutated to an alanine residue (S328A) were also purified and will be referred to as HTRA1 S328A and HTRA1 ΔPDZ S328A. The expression and purification protocol has been established earlier in the group, comprising the IPTG induced expression of the protein in *E. coli* BL21 DE3 pLysS at 25 °C for 5 h and 3 successive chromatographic purification steps as described (2.3.10). Affinity chromatography making use of the 6 x His-tag was followed by Hydroxyapatite (HAP) and size-exclusion chromatography (SEC) steps. To give an overview of the stepwise expression, lysis and purification steps, Coomassie stained SDS gels of the purification of HTRA1 S328A are shown here (Figure 10). The chromatograms as well as the purification steps of the other constructs are omitted for simplicity. They have yielded essentially the same results and highly pure protein as shown in Figure 10.

a

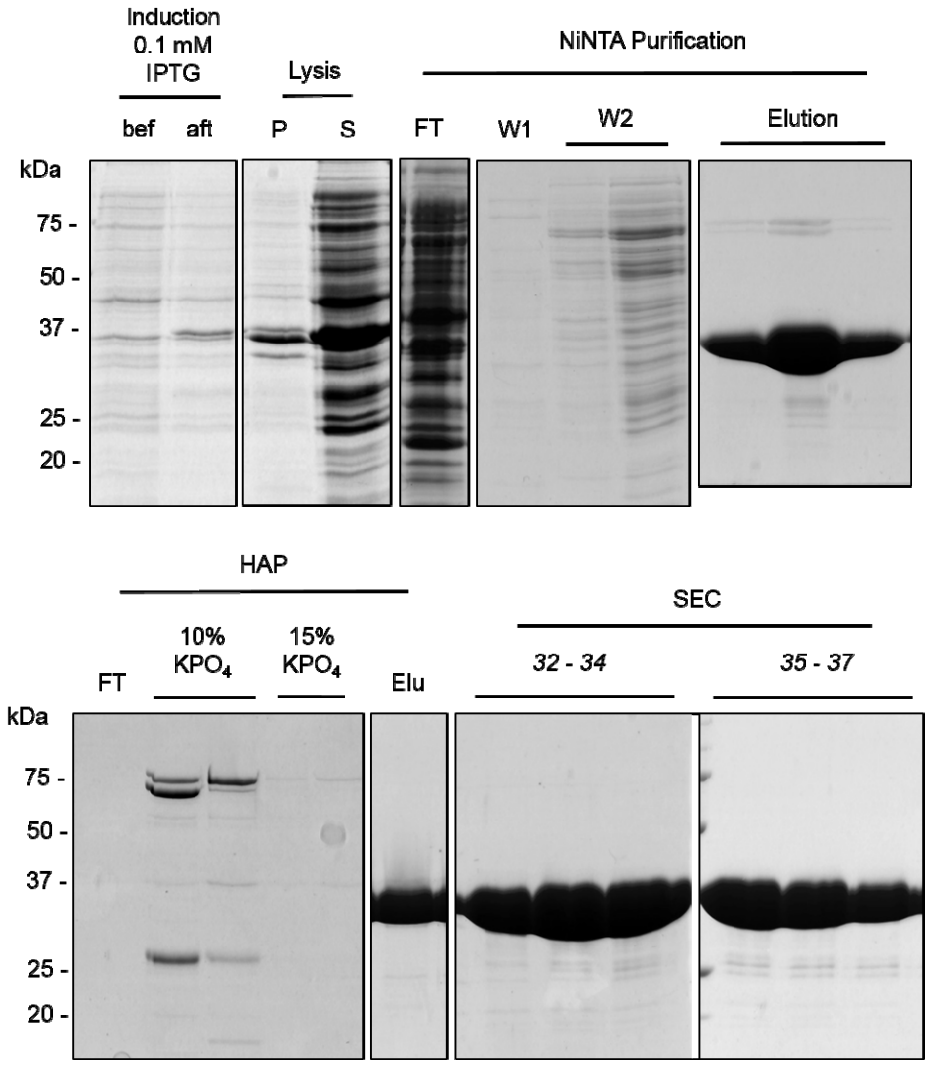
Induction
0.1 mM
IPTG
Lysis
NiNTA Purification
bef
aft
P
S
FT
W1
W2
Elution
kDa
75 -
50 -
37 -
25 -
20 -
HAP
SEC
FT
10%
KPO4
15%
KPO4
Elu
32 - 34
35 - 37
kDa
75 -
50 -
37 -
25 -
20 -

b

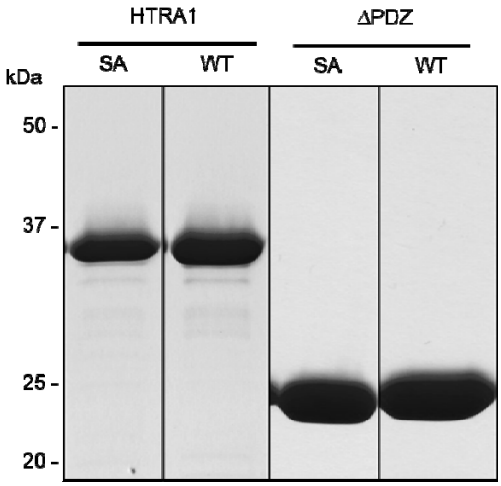

Figure 10 - Purification of Recombinant HTRA1, HTRA1 S328A, HTRA1 ΔPDZ and HTRA1 ΔPDZ S328A

Recombinant HTRA1 was expressed in *E.coli* BL21 DE3 pLysS Rosetta II and purified by successive purification by NiNTA affinity chromatography, HAP chromatography and SEC. **a**, Exemplary purification of HTRA1 S328A with SDS-PAGE of samples from each purification step. Samples are shown to illustrate successive purification are shown. **b**, Samples of wt HTRA1, HTRA1 S328A, HTRA1 ΔPDZ and HTRA1 ΔPDZ S328A were analyzed by SDS PAGE followed by Coomassie blue staining to assess their purity. bef = before induction; aft = after induction with 0.1 mM IPTG; P = pellet; S = supernatant; FT = flow-through; W1 = washing step 1, equilibration buffer containing 1 M NaCl; W2 = washing step 2, equilibration buffer with 30 mM imidazole; Elu = elution; numbering of SEC samples corresponds to the collected fractions.

The induction of HTRA1 expression with 0.1 mM IPTG gave rise to a new band of an apparent MW just below 37 kDa corresponding to HTRA1 (calculated theoretical MW = ca. 36.8 kDa). Some HTRA1 seemed to be lost in the lysis and NiNTA loading steps. Still, large amounts of largely pure protein could be eluted with imidazole (150 mM) from the NiNTA resin, containing some minor contaminants with an apparent MW of approximately 75 kDa and some impurities at around 20-25 kDa apparent MW. In particular, the high MW impurities were efficiently eliminated in the HAP chromatography step when washing with 10% KPO_4 (i.e. ca. 60 mM), leading to further purification of protein. In the following SEC run, the HTRA1 was detected primarily in its trimeric state as reported (Truebestein et al., 2011). This fraction of the eluate corresponding to an elution volume of 170-190 ml, as shown in the bottom right panel of Figure 10, contained pure HTRA1 as assessed by Coomassie blue staining and was chosen for further experiments. Typically, the described purification procedure yielded 8-10 mg/l culture.

3.2. Proteolysis of Soluble and Aggregated 3R wt Tau by HTRA1

3.2.1. Purification of Human 3R Tau

The microtubule-associated protein Tau belongs to the large and diverse group of intrinsically disordered proteins (IDP) which can adapt a plethora of conformations that is not restricted to a defined set of secondary or tertiary structures. As such a protein, Tau is characterized by pronounced solubility, even at high temperatures, which is frequently made use of for the purification of IDPs. Boiling of cleared lysates from bacterial cultures expressing human Tau has therefore proven a convenient first purification step that eliminates the bulk of bacterial proteins from the lysate by heat-induced precipitation (Hagestedt et al., 1989). This strategy was complemented by an ammonium sulfate (AS) precipitation step, where the successive precipitation of contaminants by 30% saturated AS was followed by precipitation of the Tau protein by AS at 40% saturation. Precipitated Tau could be resuspended with the desired buffer to yield soluble protein. The strategy described above has been established before (dissertation A. Tennstädt). Exemplary results of the successive expression and purification steps are shown in Figure 11. The isoform used in this part of the study was the fetal form of Tau, which consist of 351 aa with none of the two possible N-terminal inserts and 3 repeat motifs (0N3R, termed 3R wt Tau here).

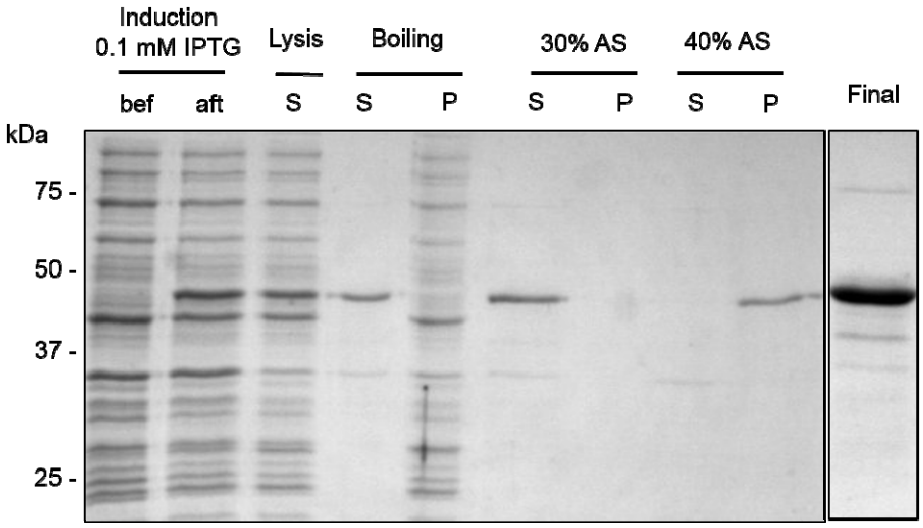

Figure 11 - Purification of 3R wt Tau

Recombinant 3R wt Tau was expressed in *E.coli* BL21 DE3 pLysS Rosetta II and purified by boiling of the cleared bacterial lysate followed by centrifugation and ammonium sulfate (AS) precipitation. Samples from each purification step are shown to illustrate the individual steps of the purification procedure. Aliquots were taken of each step and subjected to SDS-PAGE followed by Coomassie blue staining. bef = before induction; aft = after induction with 0.1 mM IPTG; P = pellet; S = supernatant; AS = ammonium sulfate.

IPTG induced expression of 3R wt Tau caused in the appearance of a prominent band of ca. 45 kDa, corresponding to full-length 3R Tau, which has a theoretical MW of 36.8 kDa. It should be noted that Tau proteins show a characteristic shift towards a higher apparent MW when analyzed by SDS PAGE, which accounts for the discrepancy between theoretical and apparent MW (Grundkeiqbal et al., 1986). Boiling of the cleared bacterial lysates led to the precipitation of most of the bacterial proteins, which were therefore found in the pellet fraction after centrifugation. While the Tau protein remained soluble after incubation with 30% saturated AS, it was successfully precipitated at 40% AS saturation, whereas a contaminant band with an apparent MW of ca. 35 kDa was still soluble at this concentration of AS and could therefore be eliminated from the solution. As shown the right panel of Figure 11, the purification yielded recombinant human 3R Tau protein of high purity, with some residual contamination bands at 75 kDa and between 30-40 kDa. The latter were shown to be Tau fragments by immunoblotting (data not shown), probably caused by degradation during expression in *E. coli*.

3.2.2. Isolation and Characterization of 3R tau Aggregates

Recombinant human 3R wt Tau purified as described above was present as a mixture of aggregated and soluble Tau, which was concluded from the fact that significant amounts of the protein were insoluble after reconstitution of the pellets, subsequent incubation at RT under reducing conditions and ultracentrifugation. Analysis of the resulting pellets and supernatants by SDS PAGE and Bradford quantitation (data not shown) showed that the Tau protein was present in both fractions. To test for β-sheet-rich structures typical for amyloid aggregates, Thioflavin T (ThT) fluorescence spectra of both the soluble and insoluble fractions were recorded as described (2.3.4).

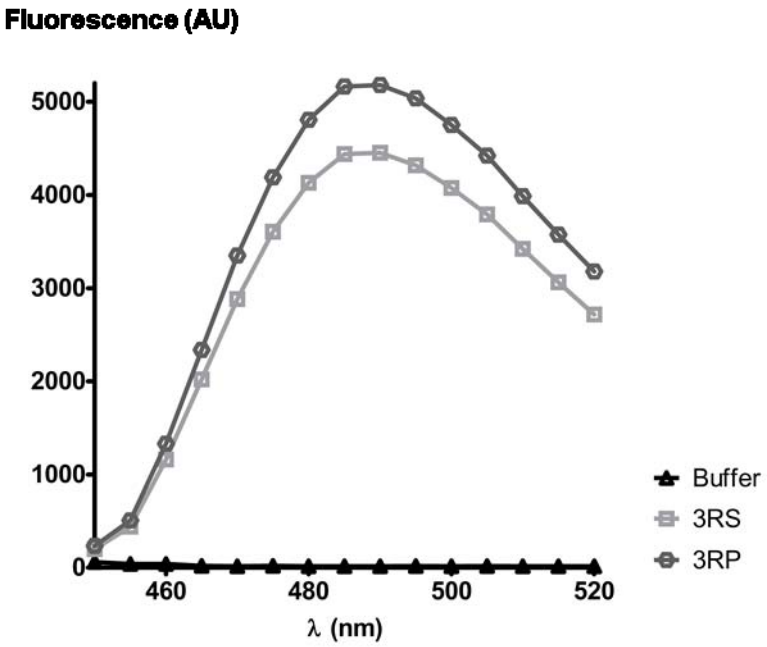

Figure 12 - ThT Fluorescence of Soluble and Insoluble 3R wt Tau Fractions

10 µl of a 20 µM solution of the soluble and insoluble fractions of 3R wt Tau were mixed in a 96-well plate with 90 µl of 12 µM ThT in 50 mM glycine, pH 8.5, at 900 rpm, 37 °C before fluorescence measurement was carried out. The excitation wavelength was kept constant at 440 nm, whereas the detected emission was recorded from 450 – 520 nm in 5 nm increments. 3RS = soluble fraction; 3RP = insoluble fraction of 3R wt Tau.

The fluorescence spectrum showed an emission maximum at an approximate wavelength of λ = 490 nm as reported previously (Friedhoff et al., 1998a). This result was indicative of an enrichment of cross β-sheets in both the soluble and insoluble fractions, the latter showing a higher fluorescence intensity, which is in accordance with the assumption that aggregated

Tau protein might be enriched in amyloid aggregates. However, based on the ThT fluorescence, protein species with similar characteristics could also be detected in the soluble Tau fraction. To further assess the features of insoluble versus soluble Tau with respect to its particle size and composition, dynamic light scattering (DLS) measurements were performed. DLS relies on the increased scattering of particles in solution as the hydrodynamic diameter increases and is frequently used for the assessment of the homogeneity of particle suspensions and protein solutions, as well as for the detection of protein aggregates in solution. Based on the intensity of scattered light (determined as counts per second or cps or kcps) and considering the relevant refractory indices of the solute and the substance to be measured, an approximation of the average MW and the hydrodynamic radius (R_H) of the particles can be calculated. However, due to the influence of the radius on the scattering intensity (to the 6^{th} power), this method is not suitable for the exact determination of quantitative size distribution in heterogenic particle solutions or suspensions. Here, the scattering intensity and mean R_H of both the soluble and insoluble fractions of 3R wt Tau were calculated to obtain an approximation of the extent of aggregation in the samples.

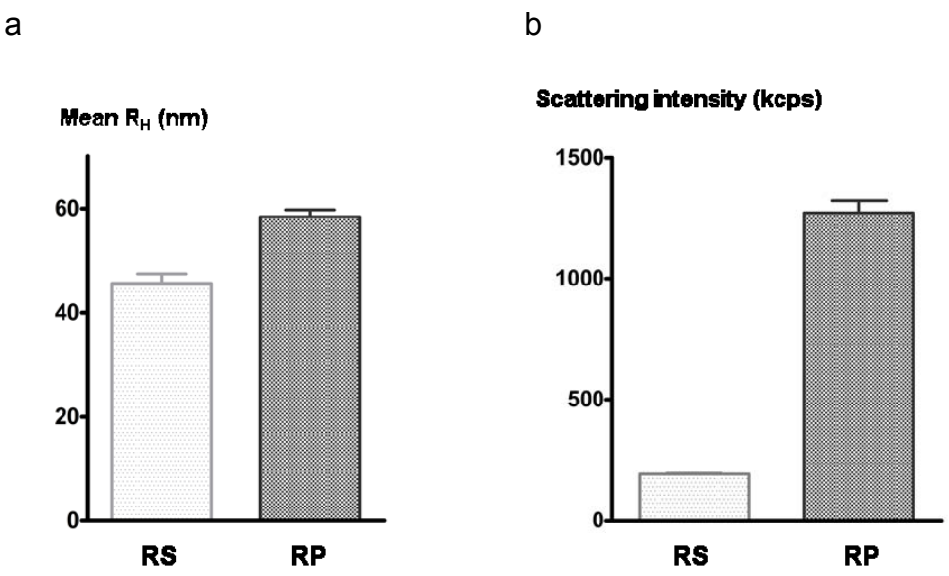

Figure 13 - Characterization of Particle Sizes of Soluble and Insoluble 3R wt Tau by DLS

DLS measurements were conducted with 200 µl of 0.05 mg/ml solutions containing 3R wt Tau from the insoluble (RP) or soluble (RS) fraction in 50 mM NaH_2PO_4, 150 mM NaCl, pH 8. **a,** The mean R_H was calculated as a measure of the mean particle size in solution. **b,** The recorded scattering intensities increased with the size of the detected particles.

In accordance with the ThT fluorescence measurements presented above, the mean R_H determined by DLS indicated that the insoluble 3R wt Tau samples contained more protein aggregates as compared to the soluble 3R wt Tau samples as characterized by a 25% increase in the hydrodynamic radius R_H (Figure 13 a). This finding was substantiated by the scattering intensity, which was sevenfold increased for the insoluble as compared to the soluble samples, supporting the assumption that Tau aggregates are particularly enriched in the pellet fraction after ultracentrifugation (Figure 13 b).

Typical amyloid aggregates have a fibrillar structure, in which the tight interaction of the constituent molecules in the fibril core in a cross β-sheet arrangement give rise to rod-like or filamentous shapes that can assemble into helical filaments. To test whether the aggregated, ThT fluorescence positive 3R wt Tau preparation examined here shows a similar morphology, samples from the insoluble and soluble Tau fractions were analyzed by atomic force microscopy (AFM). The acquisition of AFM images as well as the quantitative analysis with the image analysis software ImageJ was performed by Barbara Sacca.

a

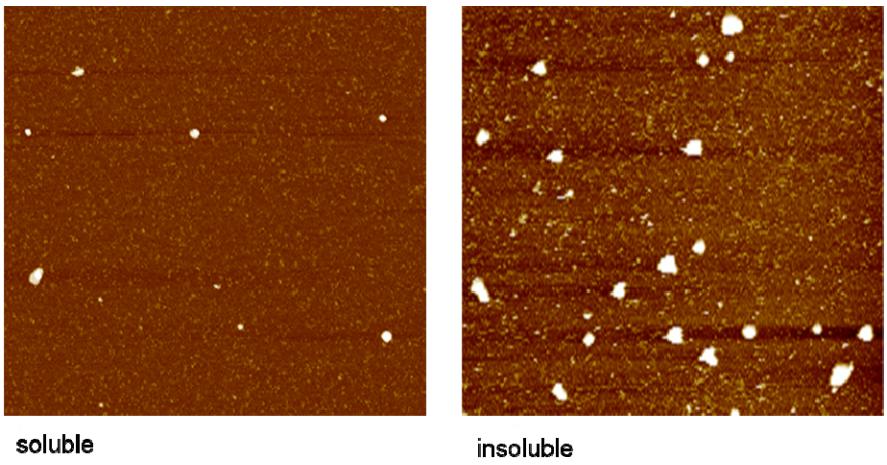

b

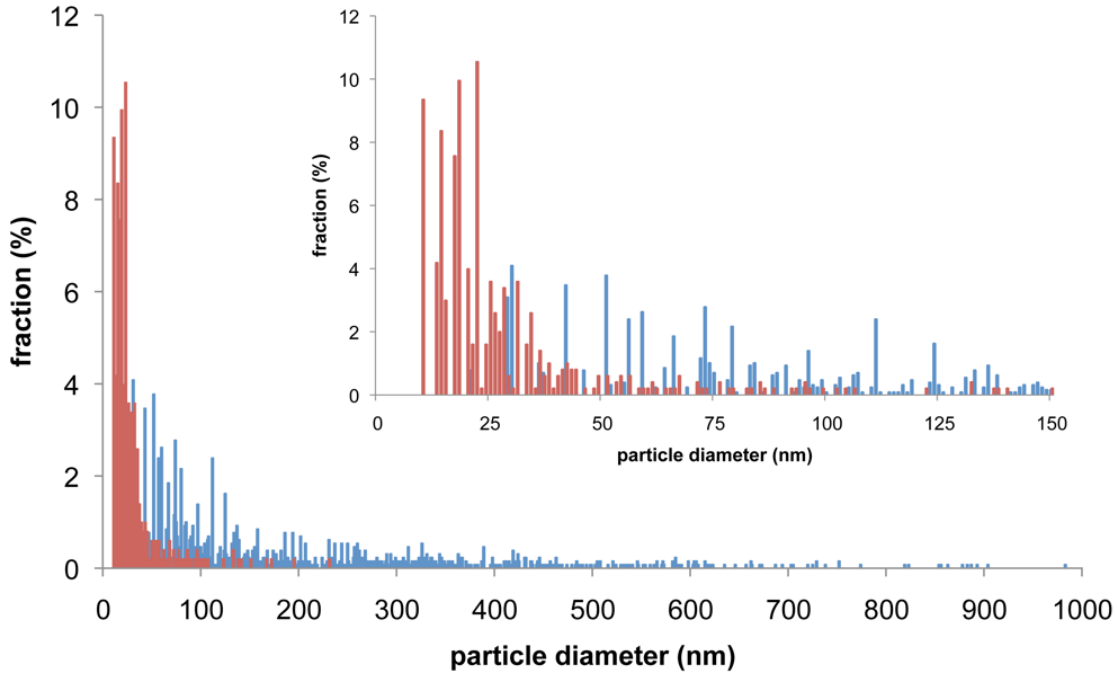

Figure 14 - AFM and Statistical Analysis of Soluble and Insoluble 3R wt Tau Fractions

a, Representative AFM images of soluble and insoluble 3R wt Tau and **b**, the distribution of particle sizes in samples from the soluble (red) and insoluble (blue) 3R wt Tau fractions. The inlet in **b** shows an enlarged part of the diameter range 0 – 150 nm. Statistical analysis was performed with imageJ.

In the AFM images, the presence of round, globular, and irregularly shaped particles can be seen, with these particles being more prominent in size and abundance in the insoluble as compared to the soluble 3R wt Tau samples (Figure 14 a). In accordance with this observation, the quantitative analysis of the relative distribution of particle sizes by ImageJ

indicated that the sizes of the particles were more broadly distributed in the insoluble Tau samples and contained much larger particles. While the soluble Tau fraction mostly contained particles with a diameter between 10 and 40 nm and only few particles were bigger than 100 nm, a large number of insoluble Tau particles were distributed between 10 and 150 nm with a significant number of particles showing diameters of up to 500 nm or sometimes even 1000 nm. These data indicate the presence of aggregates in the insoluble Tau fraction isolated by ultracentrifugation. However, the typical, fibrillar shape of amyloid aggregates did not seem to be present in these samples.

3.2.3. Proteolysis of Soluble 3R Tau and FL 3R Tau Aggregates by HTRA1, Calpain-1 and Caspase 3

Proteolysis of protein aggregates is hampered by their size and compact structure, and their resistance to proteolytic degradation is thought to be central to the continuous deposition of aggregates associated with many protein folding diseases (1.2.2). So far, HtrA proteases have so far not been shown to be able to degrade protein aggregates. The proteolysis of soluble and aggregated Tau was tested in this study to further characterize the proteolytic activity of HTRA1 with a particular emphasis on aggregated substrates and the potential for acting as a protein quality control factor through of this activity. Proteolytic digests of samples from the soluble and insoluble fractions of 3R wt Tau that had been prepared as described above were performed by incubating the respective Tau protein with wt HTRA1 and taking aliquots at the indicated time points.

a

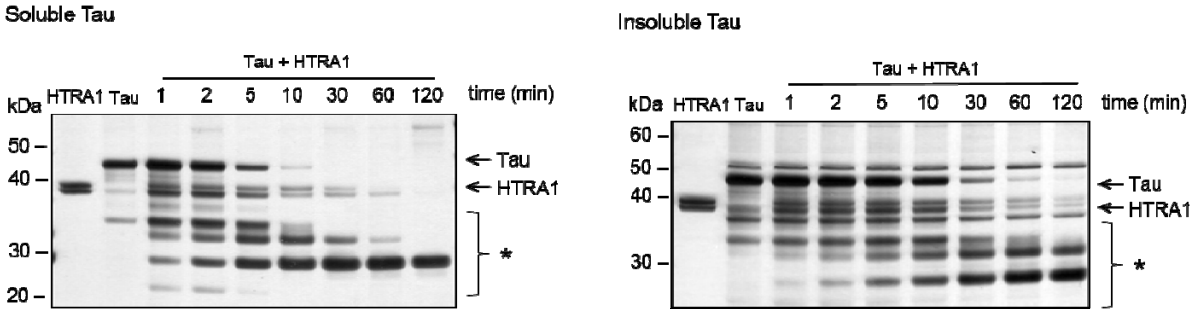

b

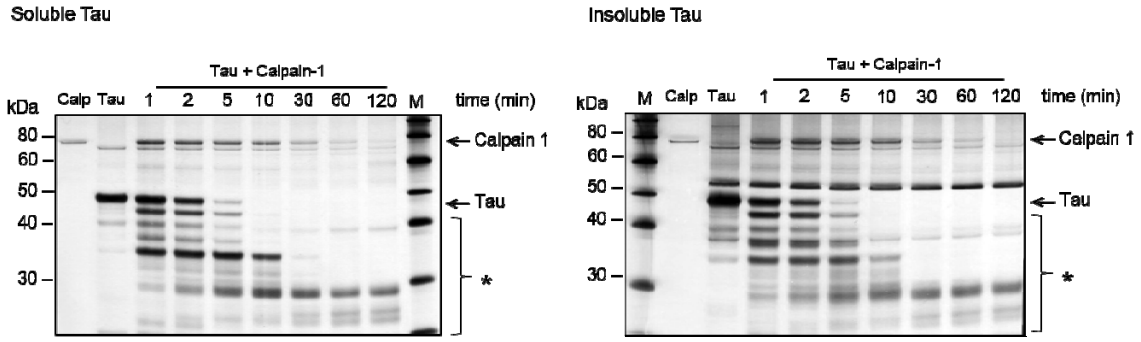

c

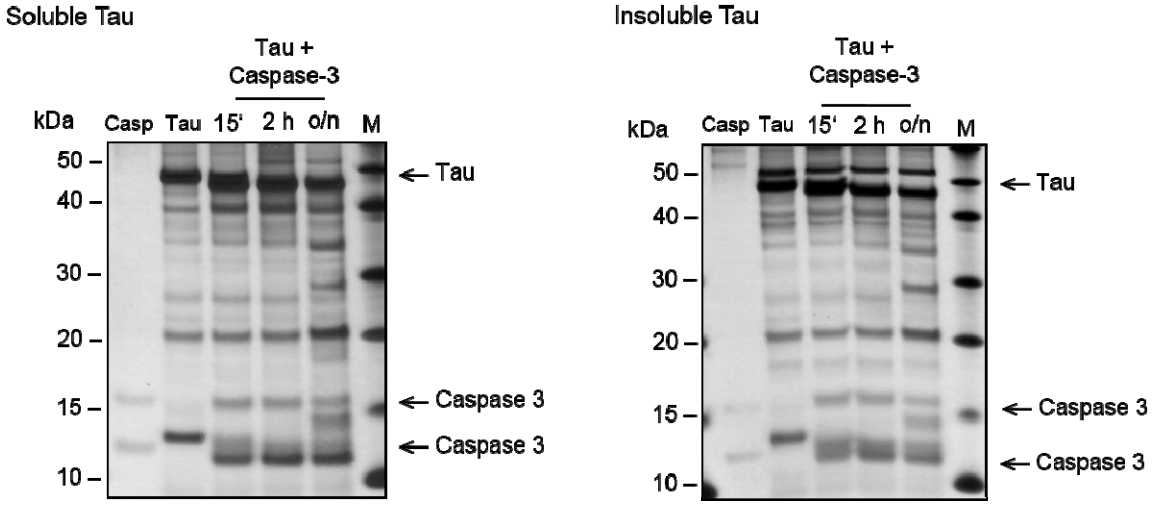

Figure 15 - Proteolysis of Soluble and Insoluble 3R wt Tau by HTRA1, Calpain and Caspase

Human recombinant 3R wt Tau was separated into soluble and insoluble (aggregated) fractions by ultracentrifugation and digested by **a**, HTRA1 at 37 °C, **b**, Calpain-1 at 23 °C and **c**, Caspase-3 at 37 °C for the time periods indicated. Tau was used in a 10-fold molar excess as compared to the respective protease. Aliquots were taken at the indicated time points, heat-treated and subjected to SDS-PAGE. The gels were silver stained. Each lane corresponds to 200 ng Tau of the initial reaction. HTRA1 = sample containing HtrA1 only, Calp = Calpain-1 only, Casp = Caspase-3 only, Tau = 3R wt Tau incubated without protease in the reaction buffer. M = Marker, * = degradation products.

According to SDS PAGE analysis of the proteolytic digest of soluble and insoluble 3R wt Tau, HTRA1 was able to proteolyze the Tau protein in its soluble and its aggregated state. The soluble protein was degraded by HTRA1 within 30 min, as indicated by the disappearance of the band migrating at ca. 48 kDa, corresponding to the full-length 3R wt Tau. It took longer for HTRA1 to degrade aggregated Tau, where full-length Tau could be detected by SDS-PAGE up to 60 min after addition of the protease (Figure 15 a). Calpain-1 and Caspase-3 have been reported to be involved in the proteolytic degradation of Tau (Gamblin

et al., 2003; Garg et al., 2011). Therefore, proteolysis experiments were performed with these proteases analogously to HTRA1 (Figure 15 b, c). Human Calpain-1 could degrade both soluble and insoluble Tau in these experiments, even with a higher efficiency than HTRA1, as can be seen from the shorter time frame of the disappearance of Tau bands. In this experimental setting, Calpain-1 degraded soluble and insoluble 3R wt Tau approximately 2 and 10 times faster, respectively. Caspase-3 was not able to completely degrade the Tau protein, even after overnight (o/n) incubation. Instead, only large fragments were detected by SDS-PAGE, which was in accordance with the well-characterized, pronounced substrate specificity of Caspases based on their recognition sequences which restrict proteolytic activity to precise cleavage sites in their substrate proteins (Salvesen and Dixit, 1997).

3.2.4. Proteolytic Activity of HTRA1, Calpain-1 and Caspase-3 in the Presence of Tau

The proteolytic activity of recombinant HTRA1 can be quantified by monitoring the cleavage of model peptides containing a C-terminal para-nitroaniline (pNA) group as described (2.3.15). As previously reported, HTRA1 is activated by its substrate through an induced-fit mechanism which essentially involves the active site of the protease and, in contrast to other HtrAs such as DegP, does not depend on allosteric activation via the PDZ domain (Truebestein et al., 2011). To test whether recombinant Tau is able to activate, which would be indicative of Tau being a natural substrate of HTRA1, the activity of HTRA1 in the presence of 3R wt Tau and pseudohyperphosphorylated (PHP) Tau was tested, using both HTRA1 and HTRA1 ΔPDZ. PHP Tau is a mutant variant of 0N3R Tau, in which a total of 10 Serine and Threonine residues have been exchanged to Glutamate to mimic the phosphorylation at the respective positions by introducing negative charges. These mutations have been shown to resemble pathologically elevated phosphorylation levels of Tau in cultured cells and the mutant has been used as a model of hyperphosphorylation *in vitro* (Fath et al., 2002). As controls, activity assays were also performed using Calpain-1 or Caspase-3. Based on the absorbance and fluorescence measurements, the calculated specific activities and activation by the respective Tau forms are listed in Table 1.

			- fold Activation by					
			wt 3R Tau			PHP 3R Tau		
	Molar ratio Tau:protease	0	0.5	1	2	0.5	1	2
Protease	Substrate							
HTRA1	PGGGNKKIETHKL-pNA	A	5.6	5.7	5.5	5.9	5.0	5.0
HTRA1	VFNTLPMMGKASPV-pNA	B	4.5	4.4	3.9	4.3	4.2	3.9
HTRA1ΔPDZ	PGGGNKKIETHKL-pNA	C	22.4	23.0	21.7	21.2	20.5	21.1
HTRA1ΔPDZ	VFNTLPMMGKASPV-pNA	D	10.2	9.6	8.8	10.6	10.1	9.2
Calpain-1	Suc-LLVY-AMC	E	1.2	1.3	1.3	1.2	1.3	1.4
Caspase-3	Ac-DEVD-pNA	F	1.0	1.0	1.0	1.0	1.0	1.0

Table 1 - Proteolytic Activities of HTRA1, Calpain-1 and Caspase-3 in the Presence of Tau

The specific activities of the indicated proteases were determined by colorimetric or fluorimetric protease assays as described (2.3.15). PGGGNKKIETHKL-pNA is derived from Tau (dissertation A. Tennstädt), VFNTLPMMGKASPV-pNA is a previously introduced synthetic HTRA1 substrate (Truebestein et al., 2011). The values shown represent means of 4 to 9 independent experiments for each protease with an SEM of < 10%. A – D: specific activities of the proteases without Tau protein, which were set to 1 for the calculation of the activation factors. A = 2.7 nmol x mg^{-1} x min^{-1}; B = 6.5 nmol x mg^{-1} x min^{-1}; C = 1.3 nmol x mg^{-1} x min^{-1}; D = 4.7 nmol x mg^{-1} x min^{-1}; E = 2.6 nmol x mg^{-1} x min^{-1}; F = 12.6 µmol x mg^{-1} x min^{-1}. The Amido-4-Methylcoumarin (AMC) coupled peptide Suc-LLVY-AMC is a synthetic substrate for the determination of Calpain activity by means of the fluorescence of the released AMC moiety upon proteolysis of the substrate.

The proteolytic activity of HTRA1 as measured by the turnover of the synthetic substrates PGGGNKKIETHKL-pNA and VFNTLPMMGKASPV-pNA was enhanced 5 to 6-fold and ca. 4-fold, respectively, in the presence of 3R wt Tau or PHP Tau. HTRA1 ΔPDZ was activated by a factor of 20 – 23 and 9 – 10 when using PGGGNKKIETHKL-pNA and VFNTLPMMGKASPV-pNA as a substrate, respectively. This indicates that both full-length wt Tau and PHP Tau were capable of activating HTRA1. At the same time, neither of the Tau proteins tested had an activating effect on Calpain-1 and Caspase-3 activity, indicating that the observation is specific for HTRA1 activation by its substrate Tau.

3.2.5. Proteolysis of Arachidonic Acid-Induced Tau Aggregates

Due to the finding that the insoluble fractions of 3R wt Tau contained predominantly amorphous aggregates and were isolated without further induction of fibrillization, which was reported to be necessary for efficient aggregation of recombinant wt Tau *in vitro* (Goedert et al., 1996), the aggregation of 3R wt Tau from the soluble fraction was induced by arachidonic acid (ArA). The formation of SDS- and heat-resistant oligomers, which is indicative of the formation of tightly interacting aggregates, was monitored by analyzing aliquots taken from the aggregation reaction at the indicated time points. The samples were heated with sample buffer containing SDS prior to subjecting them to SDS-PAGE.

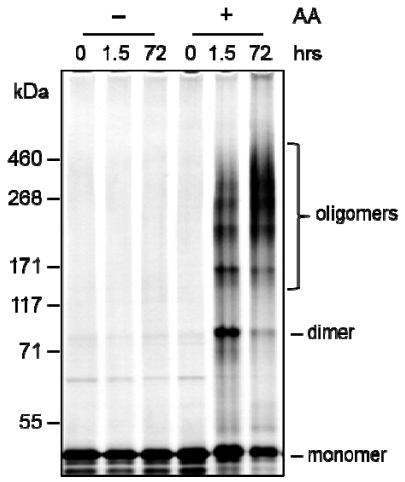

Figure 16 - Arachidonic Acid-Induced Tau Aggregation

3R wt Tau forms heat- and SDS-resistant oligomers in the presence of arachidonic acid (ArA). 4 µM 3R wt Tau were incubated without or with 0.2 µM ArA (- AA and + AA, respectively). Aliquots were heat-treated in SDS sample buffer and subjected to SDS-PAGE followed by silver staining. After 1.5 h, stable dimers have formed which further assembled into higher order oligomers resistant to heat-treatment and denaturing electrophoresis within 72 h.

While there were no SDS-resistant oligomers or aggregates in the samples containing the soluble 3R wt Tau protein and aggregation buffer only, already after 1.5 h of incubation with ArA, there were Tau dimers and higher order oligomers which could not be resolved by heating in the SDS sample buffer and subsequent SDS-PAGE. The apparent MW of these aggregates increased upon further incubation at 37 °C in the presence of the aggregation inducer ArA. After 72 h, the monomer band contained less Tau as compared to the control, whereas a significant amount of the protein was found to be aggregated, with a large fraction forming SDS-resistant oligomers of an apparent MW of ca. 180 – 480 kDa (Figure 16). In the following, these aggregates were incubated with HTRA1 in order to test the ability of HTRA1

to proteolyze these aggregates that are packed tightly enough to resist denaturation by detergents. The respective experiment was also performed with Calpain as described above (3.2.3).

a

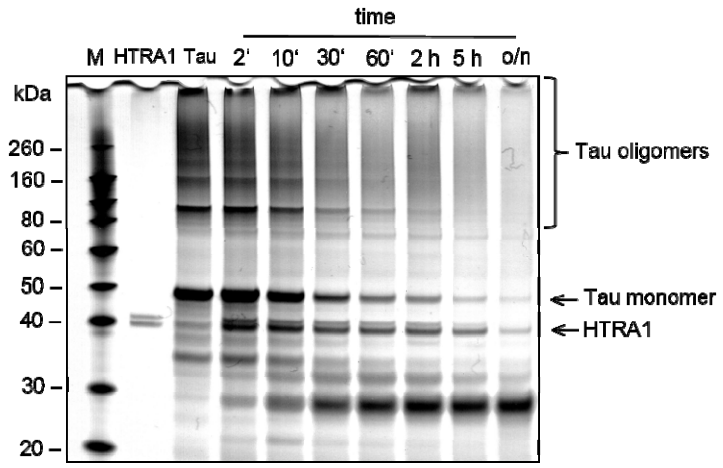

b

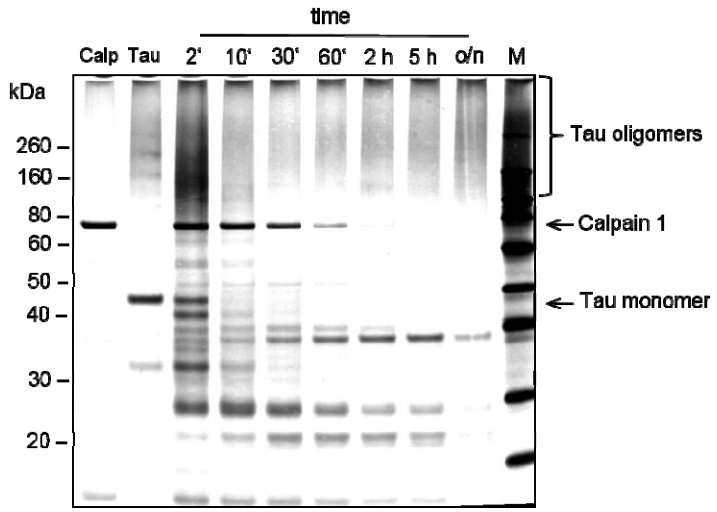

Figure 17 - Proteolysis of Arachidonic Acid-Induced Tau Aggregates by HTRA1 and Calpain-1

Fibrillization of 3R wt Tau was induced by ArA for 72 h. The aggregates were incubated with or without **a** HTRA1 or **b** Calpain-1 over night with a 5-fold excess of Tau. Aliquots were taken at the indicated time points, heat-treated and subjected to SDS-PAGE. The gels were silver stained. Each lane corresponds to 100 ng Tau according to the initial reaction. HTRA1 = sample containing HTRA1 only, Calp = Calpain-1 only, Tau = 3R wt Tau incubated o/n without protease in the reaction buffer. o/n = overnight.

Compared to the proteolysis of the soluble and insoluble 3R wt Tau samples shown above (3.2.3), ArA-induced aggregates were proteolyzed by HTRA1 much more slowly. However, HTRA1 was able to degrade the Tau protein, even the SDS-resistant Tau oligomers, which presumably represent particularly tightly packed aggregates. The bands corresponding to detergent-resistant aggregated Tau disappeared within 5 h of incubation with HTRA1,

whereas the monomeric band could still be detected after o/n incubation, showing that under these conditions, not all of the Tau protein was completely digested by HTRA1. Again, proteolysis of Tau by Calpain-1 was more efficient as compared to proteolysis by HTRA1. The monomeric Tau band was no longer detectable after 2 h, whereas a fraction of the ArA-induced aggregates were apparently still present in the sample as indicated by a high MW smear visible on the gel after o/n incubation with Calpain-1. However, the aggregates induced by ArA, did not show a marked increase in ThT fluorescence, as would be expected for amyloid aggregates, nor were any fibrillar aggregates detected by AFM (data not shown). Therefore, the purification strategy of Tau was optimized as pointed out in the following chapters.

3.3. Proteolysis of Fibrillar 4R wt Tau Aggregates

3.3.1. Purification of 4R wt Tau and MTBD Tau

The purification strategy described above for 3R wt Tau and PHP Tau yielded large amounts of protein of high purity by a convenient and fast procedure. However, it turned out that the protein batches contained a mixture of aggregated and soluble Tau with significant ThT fluorescence in both fractions and amorphous aggregates in the insoluble fraction (3.2.2). Furthermore, there were no fibrillar structures following ArA induced aggregation. These data led to efforts of optimizing the purification conditions for full-length Tau. Also, instead of 3R wt Tau, 4R wt Tau (i.e. 2N4R MAPT) was purified and used for further experiments. To obtain Tau protein that would form fibrillar aggregates, a fragment of Tau termed MTBD Tau was also purified. This fragment essentially comprised the microtubule-binding region of Tau and has a deletion of the residue K280, a mutation which is also found in hereditary forms of Tauopathy (Spillantini et al., 1998). The production in cells and aggregation behavior of this Tau construct *in vitro* was described previously (Wang et al., 2007), which further supports the suitability of MTBD Tau for this study.

The expression and initial purification strategy including the boiling step of the cleared bacterial lysate was maintained as described above (3.2.1). After boiling and centrifugation of the cleared lysate, the supernatant was subjected to two further purification steps including HAP chromatography and SEC. Tau is a very basic protein with a theoretical pI of 8.24 and

9.7, as calculated for 4R wt Tau and MTBD Tau, respectively, using ProtParam (Gasteiger, 2005). Hence, it was assumed that the protein would be best eluted from the HAP column by means of a NaCl gradient. Following HAP chromatography, the protein was further purified by SEC in order to eliminate higher order oligomers and Tau fragments from the samples, both of which could potentially inhibit the self-assembly into fibrillar aggregates.

a

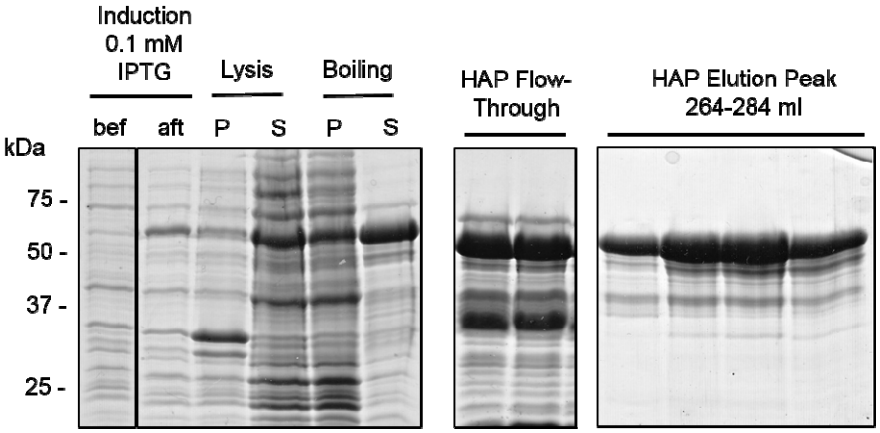

b

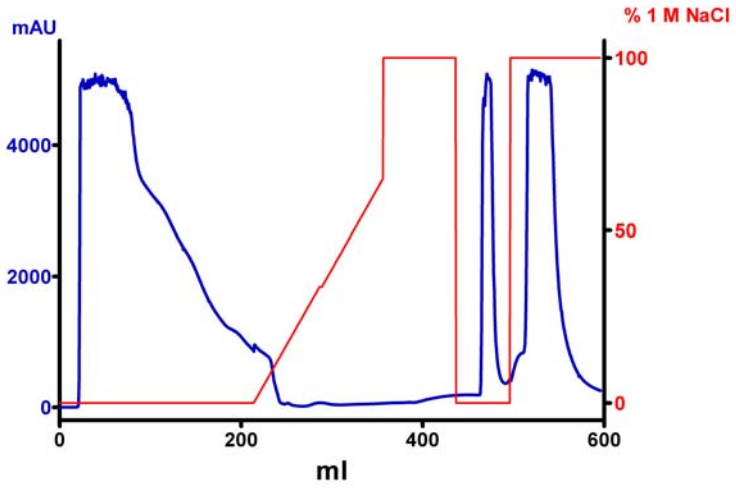

c

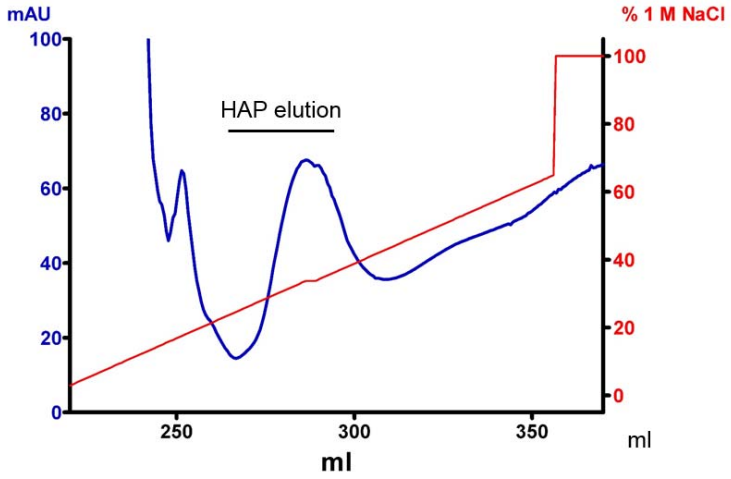
mAU
% 1 M NaCl
100
80
60
40
20
0
HAP elution
250
300
350
ml
ml

d

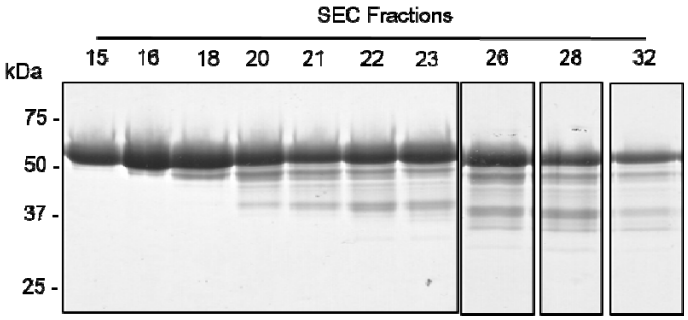
SEC Fractions
kDa
15
16
18
20
21
22
23
26
28
32
75
50
37
25

e

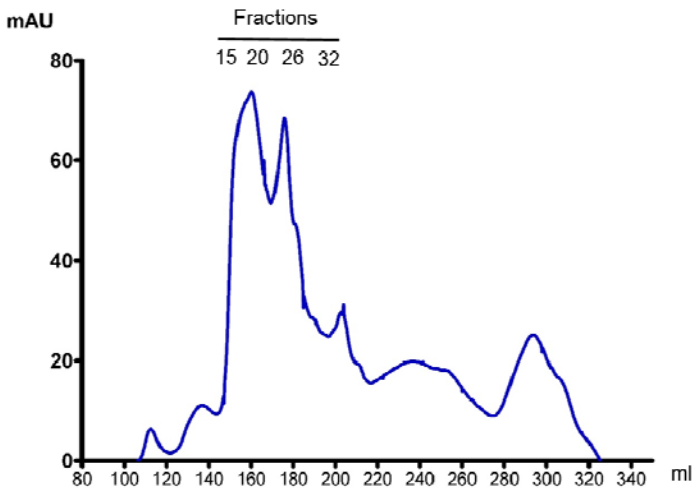

Figure 18 - Purification of 4R wt Tau

Overview of the successive purification steps of 4R wt Tau with representative samples after SDS PAGE. **a,** Samples from the expression, lysis and initial boiling steps, as well as flow-through and elution from the HAP column. bef = before induction; aft = after induction with 0.1 mM IPTG; P = pellet; S = supernatant; UV absorption profile of a HAP chromatography run **b,** as an overview over the complete run and **c** zoomed in into the Tau peak, which has a very low UV signal as compared to the impurities due to the low intrinsic UV absorption coefficient of Tau. **d** Representative samples from fractions of the SEC purification step containing the bulk of purified Tau protein. Aliquots were subjected to SDS PAGE followed by Coomassie blue staining. **e,** UV absorption profile of a representative SEC run of 4R wt Tau. The position of fractions shown in **d,** are indicated in the elution profile.

IPTG induced expression of 4R wt Tau gave rise to a new band with an apparent MW of ca. 58 kDa, corresponding to the 4R wt Tau monomer. Boiling led to the precipitation of the majority of bacterial proteins as was the case when purifying the 3R Tau variant. However, a significant amount of contaminants, particularly those with a MW below that of 4R wt Tau, was still present after boiling (Figure 18 a). A large fraction of these impurities, together with a substantial amount of Tau, was found in the HAP flow-through, indicative of inefficient binding of the Tau protein to the HAP resin. To reduce the loss of Tau in this purification step, the flow-through was re-applied to two additional runs of HAP chromatography after the first step, thereby increasing the overall yield. The UV absorption profile of the HAP run showed that proteins causing a substantial UV signal were present both in the flow-through, as well as in the fractions collected after the NaCl elution, when the column was washed with 0.5 M KPO_4 elution buffer (Figure 18 b). Whereas the flow-through contained large amounts of Tau, the fractions collected after the NaCl elution did not contain any Tau detectable by SDS-PAGE followed by Coomassie blue staining. The bulk of the 4R wt Tau protein was

eluted with 200 – 400 mM NaCl and gave rise to a very low UV absorption peak as compared to the contaminant fractions before and after the NaCl elution (Figure 18 c). The low UV absorption is due to the lack of Trp residues within the Tau protein and the presence of only one Tyr residue. Therefore, it was difficult to distinguish the UV absorption signal of even large amounts of pure Tau protein from contaminating proteins showing high UV absorption. Accordingly, the UV profile of the SEC elution was characterized by a low UV absorption signal, with the major UV peak present between 140 – 190 ml. 4R wt Tau eluted as a peak approximately corresponding to a 4-6 mer of Tau (147-160 ml), and a Tau dimer and monomer peak (160-180 ml) (Figure 18 e). Typically, the fractions containing these peaks were combined and stored at -80°C for further experiments. It should be noted, that the bands below the MW of the Tau monomer were detectable by immunoblotting using antibodies against Tau (data not shown), indicating that they represent Tau degradation products and not other impurities. Only some of the early elution fractions (#15-18 in Figure 18 d,e) seemed to be devoid of these Tau fragments. MTBD Tau was purified accordingly, except that for the SEC purification step, a different column resin suitable for the separation of lower MW proteins was used (2.3.9).

a

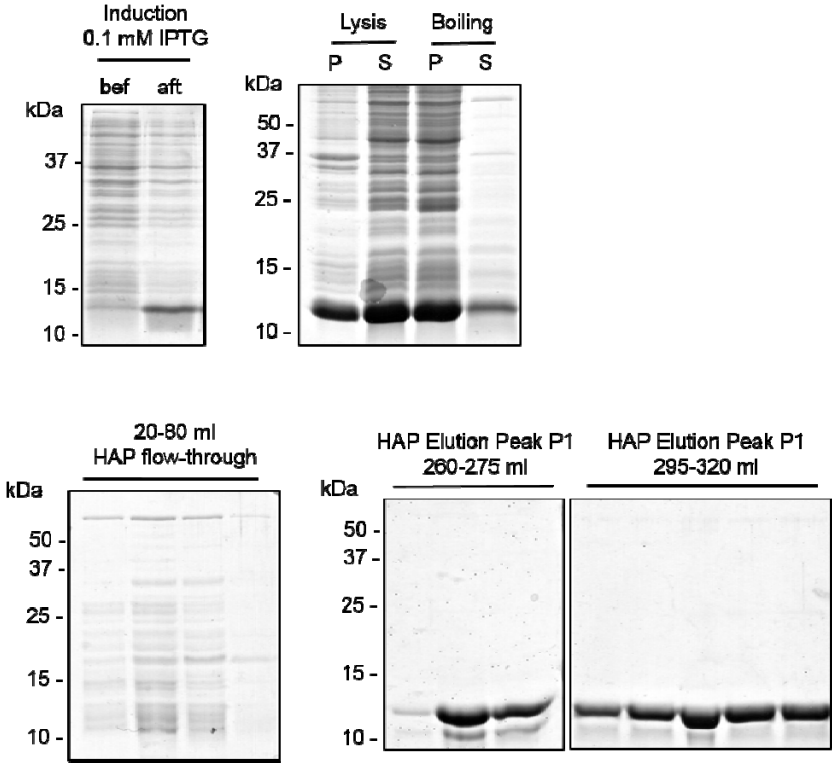

b

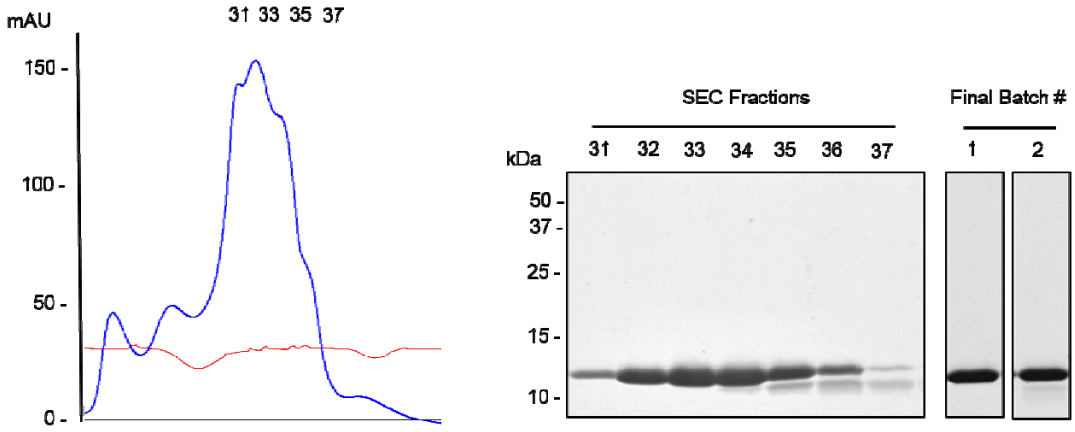

Figure 19 - Purification of MTBD Tau

Overview of the successive purification steps of MTBD Tau with representative samples after SDS PAGE. **a** Samples from the expression, lysis and initial boiling steps, as well as flow-through and two elution peaks (P1 and P2) from the HAP column. bef = before induction; aft = after induction with 0.1 mM IPTG; P = pellet; S = supernatant; **b** UV absorption profile of an SEC run and the respective SDS gel for assessing the purity of the protein. Exemplary fractions shown on the SDS gel are also marked as numbers in the chromatogram. Aliquots were subjected to SDS-PAGE and gels followed by Coomassie blue staining.

As expected from its high theoretical pI of 9.58, MTBD eluted from the HAP column at higher NaCl concentrations (400 – 500 mM) as compared to 4R wt Tau. A substantial amount of contaminating proteins could be separated from the MTBD Tau, as indicated by the HAP flow-through samples in Figure 19 a. The first two peaks collected during the SEC run did not contain any detectable amounts of Tau protein, whereas the almost all of the Tau protein was found in the 3-4 combined peaks after that (60-72 ml), which were not well resolved and supposedly contained fractions of 4-6meric, dimeric, and monomeric MTBD Tau in accordance with the SEC elution profile of full length 4R wt Tau. In analogy to the 4R WT Tau, fractions containing MTBD Tau were combined, concentrated and stored at -80°C as 4-6mer (batch #1 in the right panel of Figure 19, b) as well as dimer plus monomer fractions (batch #1 in the right panel of Figure 19, b). The resulting protein showed negligible ThT fluorescence and was completely soluble (data not shown).

3.3.2. Heparin-Induced Aggregation of Tau

The aggregation of recombinant Tau, which is otherwise a highly soluble protein, can be induced by incubation with fatty acids or polyanions such as heparin, RNA or polyglutamate (1.4.4), which has been reported to yield aggregates that closely resemble paired helical filaments (PHFs) found in Alzheimer's disease (AD) with respect to aggregate morphology and their staining with amyloid specific fluorescent dyes such as Thioflavins. To establish an *in vitro* system for testing hypotheses relevant for pathophysiological conditions, in which amyloid aggregates composed of the Tau protein play a central role, the preparation of PHF-like aggregates from recombinant Tau protein is essential. Therefore, recombinant 4R wt Tau, which had been purified as described above, was incubated after adding heparin with agitation at 37 °C and the potential emergence of cross-β structures was monitored by measuring the Thioflavin T (ThT) fluorescence at various time points. Before the addition of aggregation inducer heparin, the solution containing 4R wt Tau in aggregation buffer was heated to 55 °C for 10 min in order to reduce potential disulfide bonds and denature the Tau protein and thus to obtain aggregation competent protein and dissolve conformations which might inhibit the conversion into β-sheet rich amyloid aggregates.

a

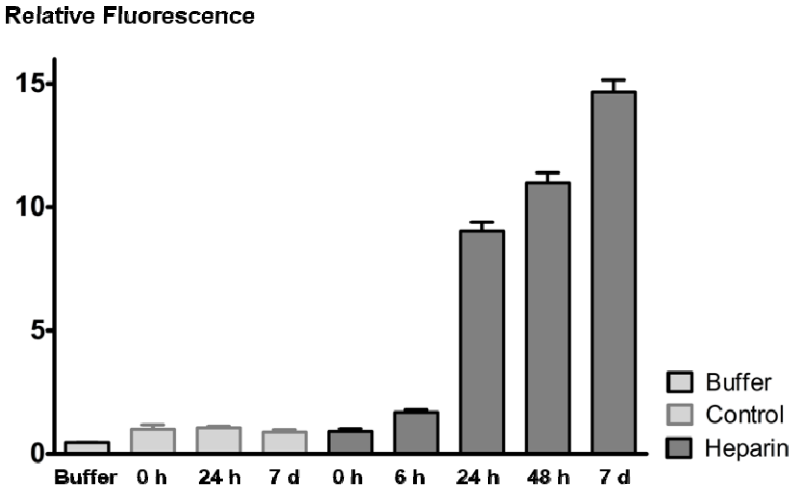

b

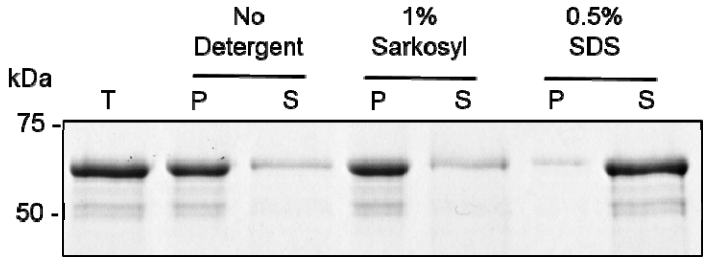

Figure 20 - Heparin-Induced Aggregation of 4R wt Tau – ThT Fluorescence and Insolubility

20 µM 4R wt Tau was incubated for 7 days in the presence of 50 µM heparin. **a** ThT fluorescence was measured at the indicated time points. Relative values as compared to fluorescence intensity measured at time point 0 h are shown. **b** Samples were analyzed regarding their insolubility by incubation with detergents as indicated and subsequent ultracentrifugation followed by SDS-PAGE of the pellet and supernatant fractions. Gels were Coomassie blue stained. Buffer = no protein, background fluorescence; Control = Tau incubated without heparin. Heparin = Tau incubated with heparin. T = total sample before ultracentrifugation; P = pellet fraction; S = supernatant fraction.

Upon incubation with heparin, there was a 10-fold increase in the ThT fluorescence of the samples as compared to the values determined before addition of heparin, which were only slightly higher than the buffer background values. The ThT fluorescence increased over the course of the aggregation reaction up to 7 days, which is indicative of a continuous emergence of amyloid aggregates under these conditions (Figure 20 a). This assumption was supported by ultracentrifugation experiments illustrating that, after aggregation in the

presence of heparin, the protein was almost completely insoluble. This was still the case after incubation with the mild detergent Sarkosyl. Sarkosyl insolubility is a characteristic feature of amyloid aggregates, which can typically only be solubilized by stronger detergents such as SDS. This was also the case for the heparin-induced 4R wt Tau fibrils examined in this experiment (Figure 20 b). To test if this process was concomitant with the formation of morphologically characteristic Tau fibrils, samples after 7 days of aggregation were examined by AFM.

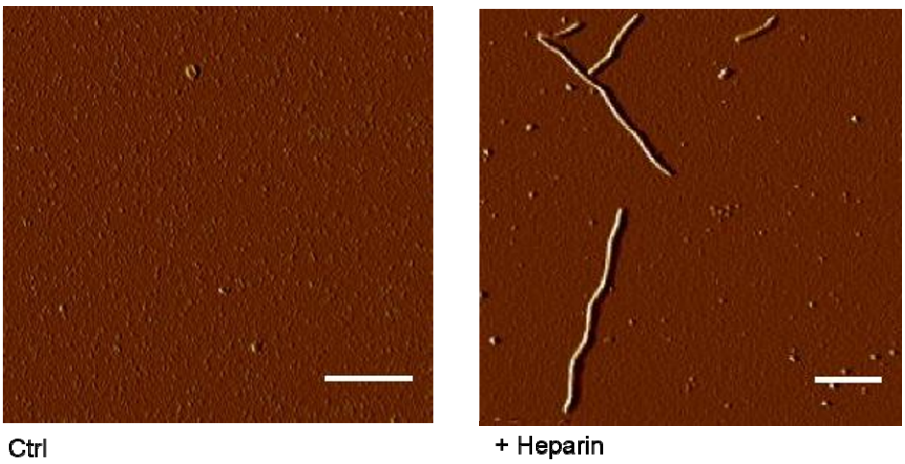

Figure 21 - AFM Images of Heparin Induced 4R wt Tau Aggregates

The morphology of heparin induced 4R wt Tau aggregates was analyzed by AFM, showing the typical, PHF-like fibrillar appearance of Tau aggregates after incubation with heparin for 72 h (+ Heparin), whereas there were no such particles when 4R wt Tau was incubated without heparin (Ctrl). Scale bar = 300 nm.

In the control samples containing 4R wt Tau protein and aggregation buffer only, there were no larger structures detectable by AFM. In contrast, in the samples with heparin to induce Tau fibrillization, there were long, fibrillar aggregates, which seemed to have a helical twist (Figure 21). According to size measurements (data not shown), these fibrils had a width of 20 – 25 nm and lengths varying between 100 nm and up to 2 µm, which is in accordance with aggregate dimensions previously reported for PHFs generated *in vitro* and those isolated from AD tissue (Crowther, 1991).

3.3.3. Proteolysis of Tau Fibrils by HTRA1

On the basis of the morphological and spectroscopic data supporting the PHF-like character of the Tau aggregates prepared *in vitro*, these fibrils were subjected to proteolysis by recombinant HTRA1 in order to test its ability to proteolyze amyloid aggregates. As described above (3.2.3), Calpain-1 was also tested because it is another candidate protease for the degradation of Tau and Tau aggregates in cells.

a

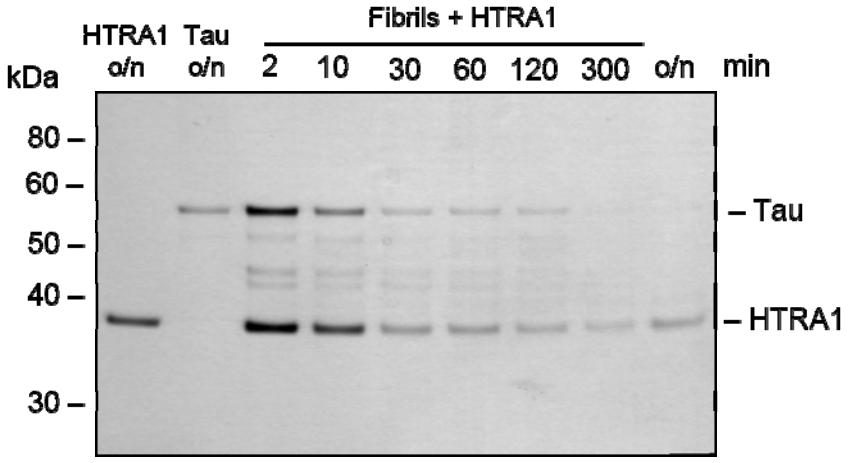

b

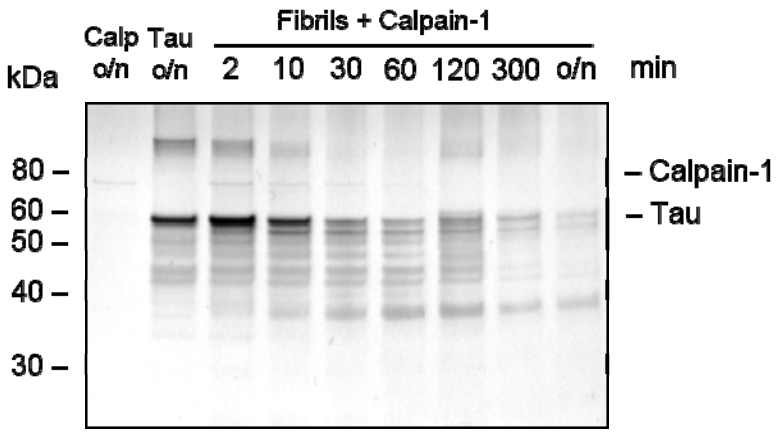

Figure 22 - Proteolysis of Heparin-Induced 4R wt Tau Aggregates by HTRA1 and Calpain-1

Fibrillization of 4R wt Tau was induced by heparin for 72 h. The aggregates were isolated by ultracentrifugation and incubated with or without HTRA1 (**a**) or Calpain 1 (**b**) overnight with a 2.5-fold molar excess of Tau. Aliquots were taken at the indicated time points, heat-treated and subjected to SDS-PAGE. The gels were silver stained. Each lane corresponds to 200 ng Tau according to the initial reactions. Fibrils = heparin-induced aggregates; HTRA1 o/n = sample containing HTRA1 only, Calp o/n = Calpain-1 only, Tau = 4R wt Tau aggregates incubated over night without the respective protease in the reaction buffer. o/n = overnight.

Under these conditions, HTRA1 completely degraded fibrillar Tau aggregates within 5 hours (Figure 22 a). This showed that the proteolysis of Tau fibrils took more time as compared to the proteolytic degradation of soluble Tau protein (Figure 15 a), which is supposedly due to the decreased accessibility of cleavage sites to the active site of HTRA1. Soluble tau is unstructured and displays a high degree of conformational flexibility allowing it to undergo dynamic interactions with binding partners and also proteases. In contrast, aggregates are characterized by strong intermolecular interactions leading to the occlusion of potential cleavage sites and stiff conformations that possibly prevent their productive degradation by proteases. The proteolysis of Tau fibrils was accomplished by Calpain-1 in a comparable time frame (Figure 22 b)

3.4. Disaggregase Activity of HTRA1

The ability of HTRA1 to proteolyze Tau aggregates, which are widely considered to be protease resistant, led to the hypothesis that HTRA1 might have a distinct activity allowing the dissolution of aggregates. This disaggregase activity would act on aggregated proteins and render them more susceptible to proteolysis by loosening tight interactions within the

aggregate or by the extraction of fragments or monomers from the bulk aggregate structure. We hypothesized that upon disaggregation, the disintegration of aggregates would be detectable by assessing fundamental features of amyloid aggregates such as insolubility and fibrillar morphology. To test for disaggregase activity, the inactive mutant HTRA1 S328A was used, which allowed us to assess the effects on fibril integrity independently of the proteolytic activity of HTRA1.

3.4.1. Effects of HTRA1 S328A on the Insolubility of Full-length Tau Aggregates

Initially, the inherent insolubility of 4R wt Tau aggregates was tested by incubation of heparin-induced 4R wt Tau fibrils (3.3.2), with equimolar amounts of HTRA1 S328A. Initially, disaggregation was followed in various buffers by assaying Tau insolubility after o/n incubation at 37 °C with HTRA1 S328A (data not shown). As controls, Tau aggregates were incubated with the aggregation buffer alone to rule out a spontaneous dissolution of aggregates under the tested conditions, and with an unrelated protein which was not expected to specifically interact with Tau or Tau aggregates. The latter control was chosen to make sure that the presence of proteins do not exert an unspecific solubilizing effect on the aggregates simply by their polyanionic properties in solution. A number of different proteins were tested, malate dehydrogenase (MDH) is shown here as an exemplary control.

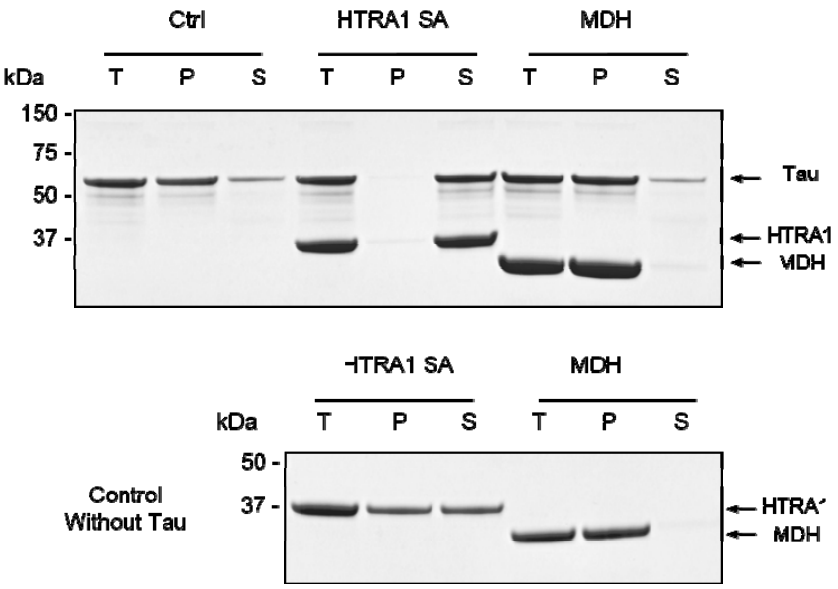

Figure 23 - Solubilization of Tau Fibrils by HTRA1 S328A.

Fibrils were soluble after incubation with HTRA1 S328A but with not the control protein malate dehydrogenase (MDH). Heparin-induced fibrils (6.7 µM) composed of full-length Tau were incubated with equimolar amounts of proteolytically inactive HTRA1 S328A or MDH at 37°C for 16 h, followed by ultracentrifugation and SDS-PAGE of samples. Gels were Coomassie blue stained. T = total, before centrifugation; P = pellet; S = supernatant.

Most of the 4R wt Tau protein was found in the pellet fraction after ultracentrifugation, which supports the stability of aggregates under the buffer conditions tested. After incubation with HTRA1 S328A, Tau was exclusively found in the supernatant together with the protease. In contrast, Tau remained insoluble upon incubation with the control protein MDH, which was also found in the pellet fraction both after incubation with Tau fibrils and following incubation in the disaggregation buffer by itself (Figure 23, bottom panel). Notably, about half of the HTRA1 S328A protein was insoluble after o/n incubation in the disaggregation buffer without Tau aggregates, whereas all of HTRA1 S328A was found to be soluble, as it was found in the supernatant after incubation with Tau fibrils. Taken together, these findings indicated that HTRA1 S328A was able to solubilize amyloid aggregates prepared *in vitro* from recombinant full-length human Tau protein independently of its proteolytic activity. These data also suggested that HTRA1 might have an intrinsic disaggregase activity which might contribute to efficient proteolysis of Tau fibrils.

3.4.2. Effects of HTRA1 S328A on the Insolubility of MTBD Tau Aggregates

Tau fibrils consist of a tightly packed fibril core containing the characteristic cross β-sheet arrangement which is made up primarily of the microtubule binding region of the protein and a “fuzzy coat”, with the largely unstructured N- and C-terminal parts of the protein protruding outwards from the aggregate core (Wischik et al., 1988). The microtubule binding domain (MTBD) of Tau has been shown to be both essential and sufficient for the formation of fibrils, whereas the N- and C-termini displayed inhibitory effects on the *in vitro* aggregation process. We wanted to test whether HTRA1 needed to bind to these flexible parts of the Tau fibrils first to act as a disaggregase. Therefore, the MTBD Tau fragment was used to produce fibrils *in vitro* as described (2.3.13) and incubated with proteolytically inactive HTRA1 S328A.

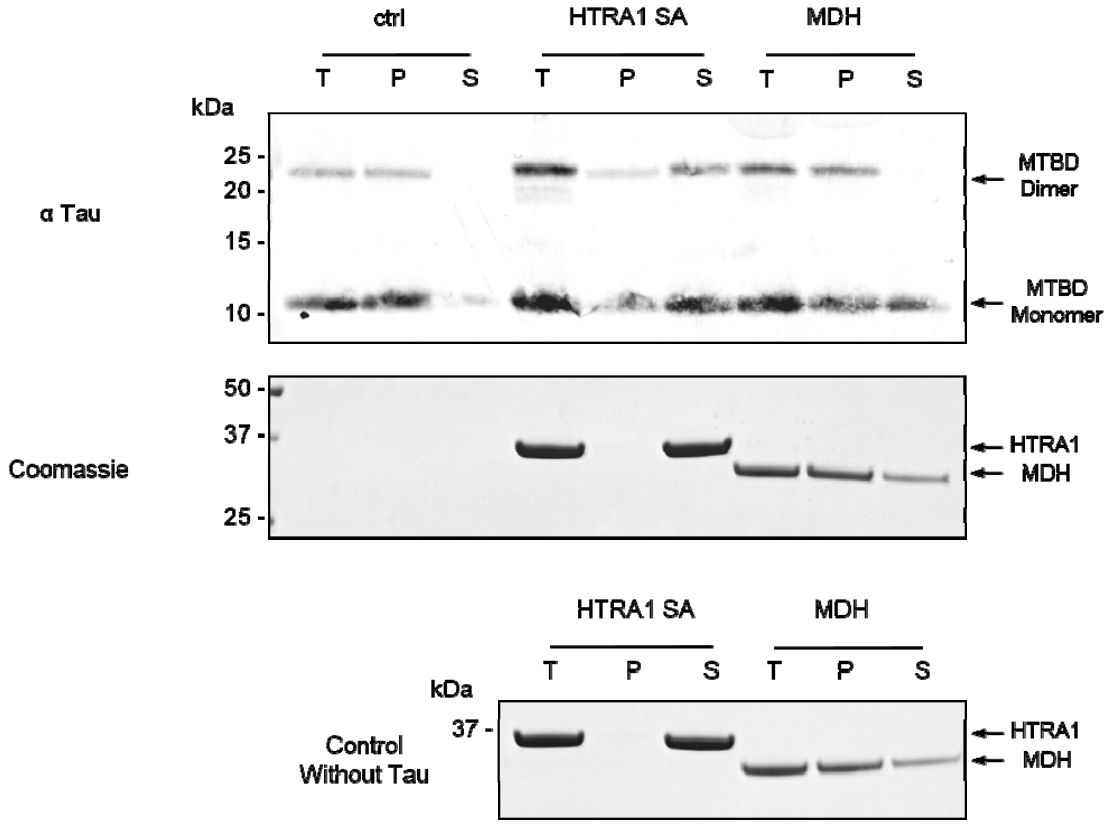

Figure 24 - Solubilization of Fibrils Composed of MTBD Tau by HTRA1 S328A.

Fibrils obtained from the aggregation of the MTBD region of Tau were treated with HTRA1 S328A according to full-length 4R wt Tau fibrils except that the concentration of Tau was 13.7 µM and HTRA1 or MDH were applied in a 5-fold molar excess. MTBD was detected by immunoblotting with a polyclonal rabbit anti Tau antibody, whereas for the detection of HTRA1 and the MDH control, the samples were diluted 1:10 and subjected to SDS PAGE followed by Coomassie blue staining. T = total, before centrifugation; P = pellet; S = supernatant.

After o/n incubation and when incubated with buffer only, MTBD Tau was found almost exclusively in the pellet fraction after ultracentrifugation, whereas incubation with a 5-fold molar excess of HTRA1 SA caused a majority of the protein to be soluble (ca. 75%, Figure 24, top panel). In contrast, incubation with respective amounts of MDH led only to a small increase in the amount of soluble MTBD Tau protein. Notably, all of the SDS-resistant Tau dimers, which supposedly represented aggregates or parts of aggregates which were particularly stable, were found in the pellet after incubation with buffer or with MDH, whereas most of them were soluble after incubation with an excess of HTRA1 SA. This indicates that HTRA1 can disassemble aggregates in the absence of the “fuzzy coat” parts of the Tau aggregates, which might be relevant when considering pathophysiological conditions where the Tau protein was found to be truncated and might therefore lack certain parts residing outside the aggregate core structure.

3.4.3. Analysis of Disaggregation by AFM

It should be possible to track the dissolution of fibrils morphologically, i.e. by AFM, which might help substantiating and further characterizing the disaggregase activity of HTRA1. Disaggregation should not only lead to increased solubility of the Tau protein, but also to a detectable decrease in fibril abundance and a change in the dimensions or shape of Tau aggregates. To address these questions, fibrils prepared from full-length 4R wt Tau were incubated as described above with equimolar amounts of HTRA1 S328A, followed by AFM imaging. As a control, the experiment was repeated with the isolated PDZ domain of HTRA1 (cloned and purified by Vanda Lux) to rule out unspecific effects which could be caused the presence of protein in solution rather than specific effects exerted on the aggregates by HTRA1. Also, the PDZ domain might in principle exert disaggregating effects on its own.

a

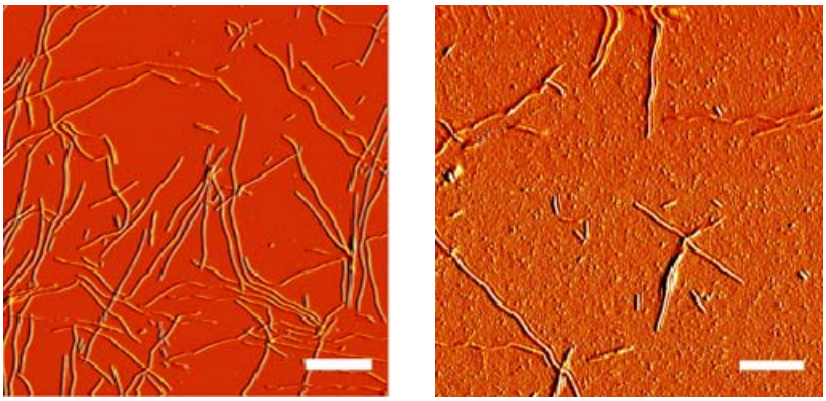

b

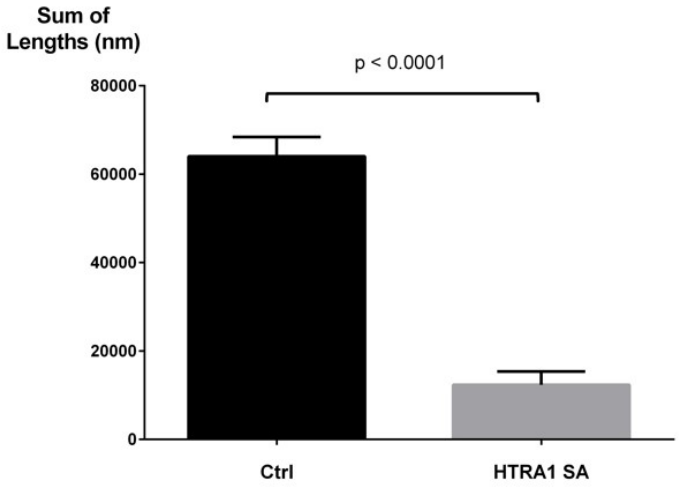
Sum of
Lengths (nm)
p < 0.0001
80000
60000
40000
20000
0
Ctrl
HTRA1 SA

c

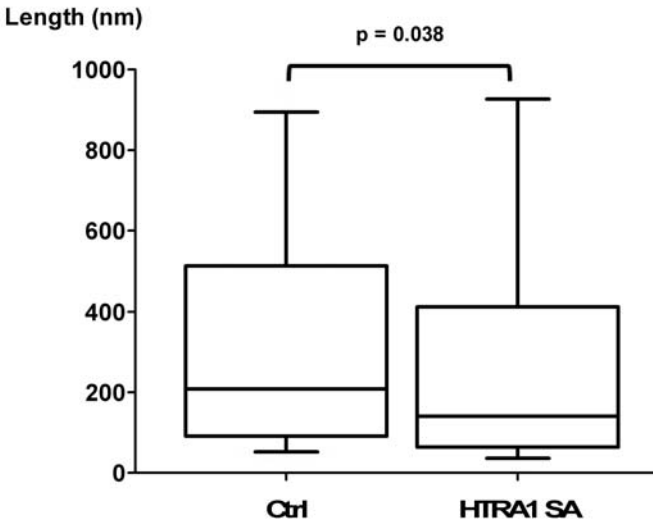
Length (nm)
p = 0.038
1000
800
600
400
200
0
Ctrl
HTRA1 SA

d

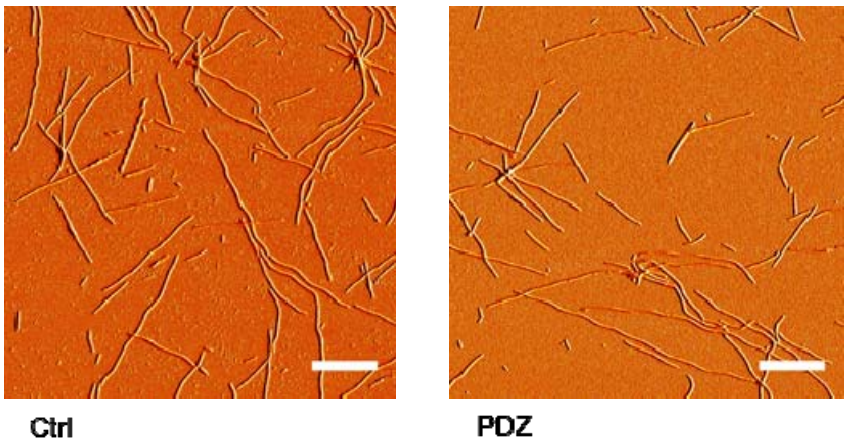
Ctrl
PDZ

e

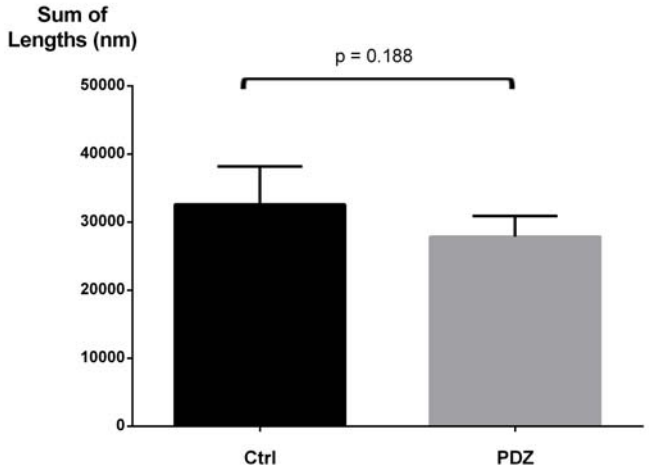
Sum of Lengths (nm)
p = 0.188
50000
40000
30000
20000
10000
0
Ctrl
PDZ

f

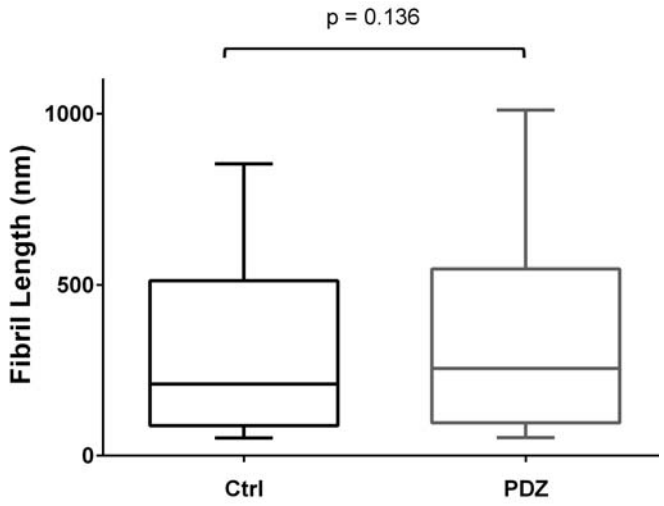

Figure 25 - AFM Analysis of the Disaggregation of 4R wt Tau Fibrils by HTRA S328A

Disaggregation of full-length Tau fibrils by HTRA1 S328A as assessed by atomic force microscopy (AFM). To quantify the effect of disaggregation on the abundance of Tau fibrils, full-length fibrillar Tau was incubated with equimolar amounts of **a** – **c** HTRA1 S328A or **d** – **f** the PDZ domain of HTRA1 o/n, followed by AFM imaging. **a**, **d** Representative AFM images as used for quantification. Scale bar = 500 nm. **b**, **e,** 4 images acquired at random locations in the samples were analyzed with ImageJ. The individual lengths of fibrils were measured and added up for each image as a measure of the total amount of Tau aggregates per image. Error bars indicate the SEM for the respective samples. The p-values were calculated according to Student's t-test with Welch's correction. **c**, **f,** The lengths of individual fibrils was measured with ImageJ and their distribution is represented as box plots. The bars indicate the 1st and 4th quartile ranges, the boxes mark the 2nd and 3rd quartiles. The median is indicated as a bar within the boxes. P-values were calculated according to Mann-Whitney.

The images of the samples in which Tau fibrils were incubated with HTRA1 S328A show a decreased amount of fibrils as compared to the buffer control. In order to quantitate the fibril abundance and the effect of HTRA1 S328A, four images of each sample were analyzed using the image analysis tool ImageJ. For each image, the fibrils were marked separately and measured with respect to their length. Subsequently, the sum of lengths per image was used as a measure of fibrils abundance, and the statistical distribution of fibril lengths in each image was calculated in order to assess the effect of HTRA1 S328A on the lengths of individual fibrils. Based on these analyses, it was demonstrated that HTRA1 S328A caused a significant decrease in the total abundance of fibrils as compared to the buffer control (Figure 25 b), whereas there were only minor changes following incubation with the PDZ domain of HTRA1, which were not statistically significant (Figure 25 e). Concerning the lengths of individual fibrils, a significant reduction in fibril lengths was observed when incubating the aggregates with HTRA1 S328A (Figure 25 c), whereas there were no significant changes

when the PDZ domain was used as a control (Figure 25 f). The analyses of the distribution of lengths indicated that disaggregation led to a shift of fibril lengths towards shorter fibrils, but at the same time to a large number of remaining long fibrils, as can be concluded from the position of the upper quartile bar in Figure 25 c. The overall effect on fibril lengths was less dramatic than it could have been expected for a fibril severing disaggregation mechanism, which will be discussed later. As an additional measure of the abundance of amyloids in solution, ThT fluorescence was determined. However, the disaggregation of Tau aggregates under the same conditions described above did not yield a consistent decrease in the intensity of ThT fluorescence (data not shown). This indicates that there were still amyloid structures present in solution, even in the absence of insoluble or morphologically distinct fibrillar Tau aggregates. These might be soluble, amyloid oligomers which were too small for detection by AFM or sedimentation by ultracentrifugation.

3.4.4. Combined Disaggregase and Protelytic Activity of HTRA1

Given that HTRA1 ultimately acts on Tau aggregates as a protease, it can be expected that disaggregation and proteolysis are performed by HTRA1 in concert. If so, disaggregation would be supportive of proteolysis, i.e. disaggregation of Tau fibrils should enhance proteolytic degradation. This hypothesis was experimentally addressed by sequential disaggregation and proteolysis. Therefore, Tau fibrils were incubated with an excess of proteolytically inactive HTRA1 S328A for 2 h at 37 °C before the addition of active HTRA1 to start the proteolytic degradation of the aggregates.

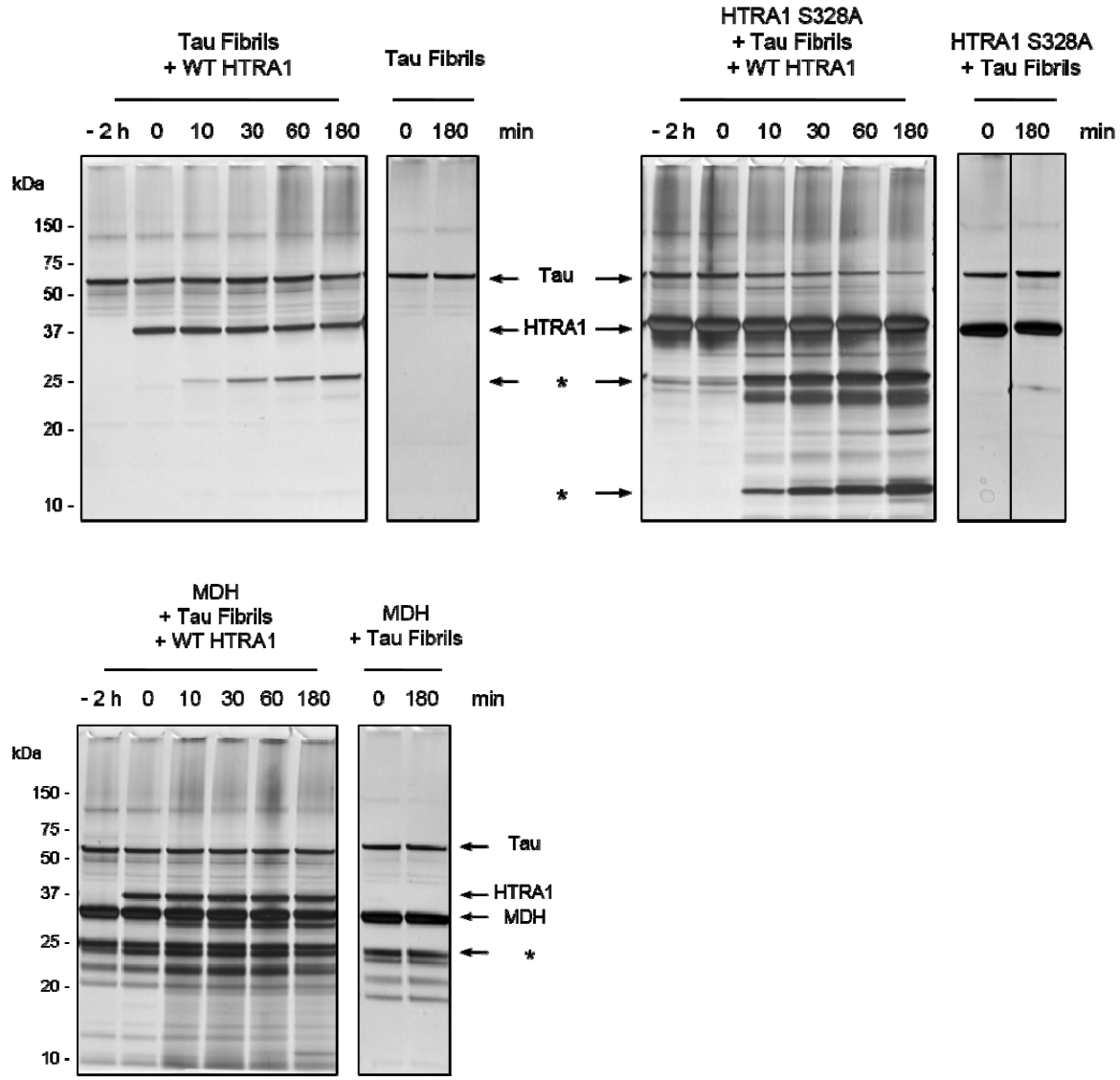

Figure 26 - Effect of Disaggregation on Subsequent Proteolysis of Tau Fibrils by HTRA1

Tau fibrils were incubated with wt HTRA1 after 2 h of incubation with buffer (left panel), with a 10-fold molar excess of HTRA1 S328A as compared to the concentration of wt HTRA1 (right panel), or with the respective concentration of MDH as a control (bottom panel). Aliquots were taken and flash frozen in liquid N_2 when starting the disaggregation (-2 h) or at the indicated time points after addition of wt HTRA1. All samples were subjected to SDS PAGE followed by silver staining. * = degradation products of HTRA1, Tau or MDH.

Proteolysis of Tau aggregates by HTRA1 was very slow under the conditions chosen, as indicated by the continuous presence of the Tau band in Figure 26 top left panel. However, preincubation of Tau fibrils with HTRA1 S328A (10-fold molar excess as compared to the amounts of wt HTRA1) lead to enhanced proteolysis, resulting in clearly visible Tau degradation within 3 h (Figure 26 top right). In contrast, preincubation with the control protein

MDH did not cause an increase of the proteolysis of Tau fibrils. All of the Tau was still detectable on the gel after 3 h of incubation (Figure 26 bottom panel).

The observed improved degradation of fibrils could be explained by two models i.e. disaggregation or activation of HTRA1 by HTRA1 S328A. To distinguish between these models, two additional experiments were performed. First, proteolysis of soluble 4R wt Tau protein with and without preincubation with a 10-fold molar excess of inactive HTRA1 S328A and second, proteolysis of soluble Tau by a 10-fold increased amount of active HTRA1.

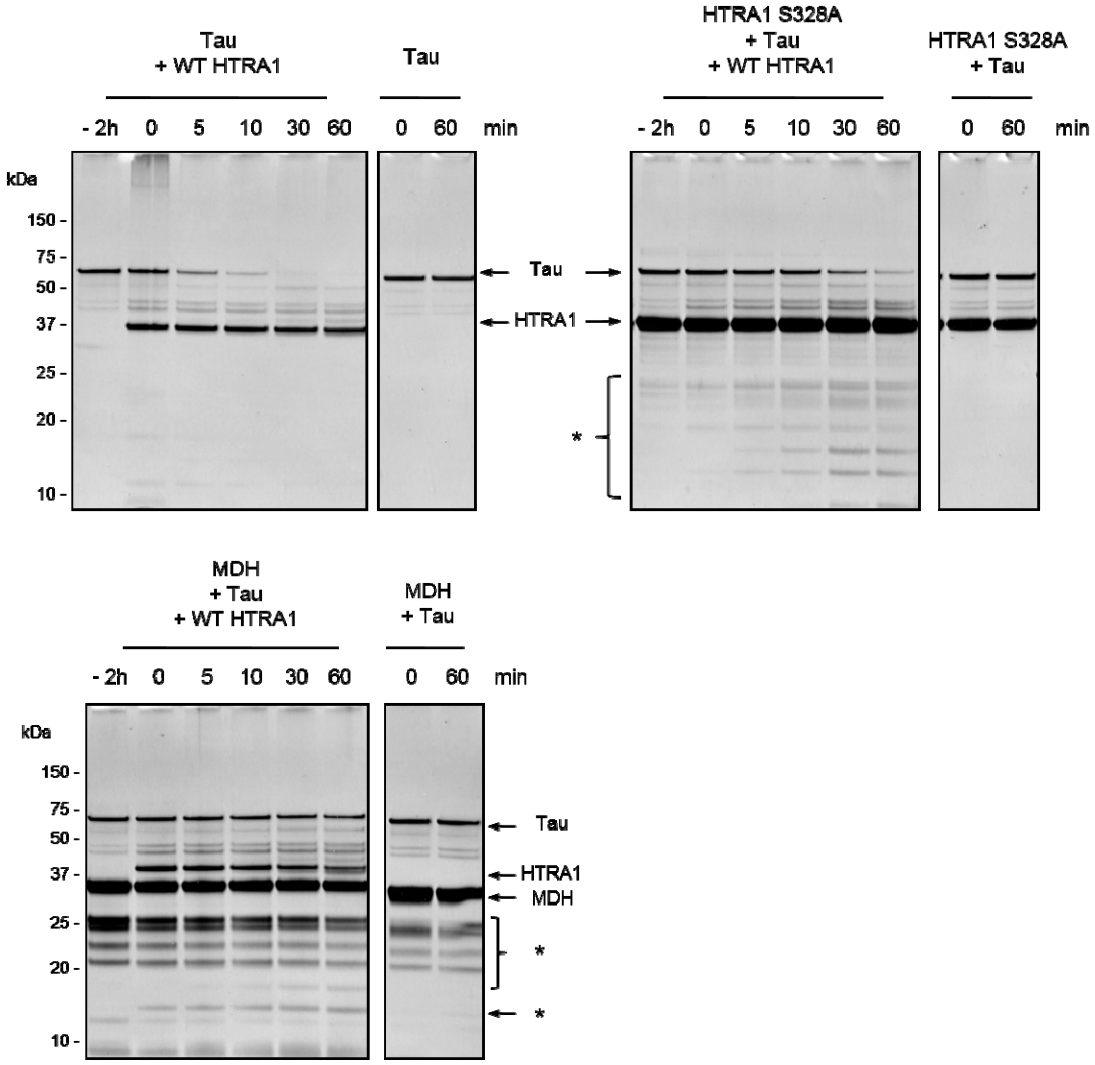

Figure 27 - Proteolysis of Soluble 4R wt Tau after Incubation with HTRA1 S328A or MDH

Soluble 4R wt Tau was incubated with wt HTRA1 after 2 h of incubation with buffer (left panel), with a 10 fold molar excess of HTRA1 S328A as compared to the concentration of wt HTRA1 (right panel), or with the respective concentration of MDH as a control (bottom panel). Aliquots were taken and flash frozen in liquid nitrogen when starting the preincubation (-2 h) or at the indicated time points after addition of wt HTRA1. All samples were subjected to SDS PAGE followed by silver staining. * = degradation products of HTRA1, Tau or MDH.

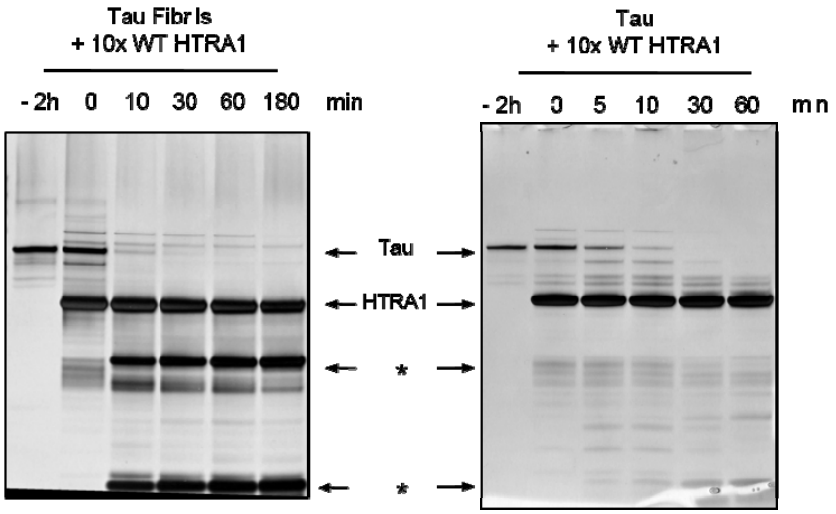

Figure 28 - Proteolysis of Tau by an Excess of wt HTRA1

Tau fibrils (left panel) or soluble Tau were proteolyzed by wt HTRA1 present in the concentration corresponding to HTRA1 S328A in (Figure 26 and Figure 27). Aliquots were taken and all samples were subjected to SDS-PAGE followed by silver staining. * = degradation products of HTRA1 or Tau.

As expected, proteolysis of soluble Tau by HTRA1 without previous incubation with HTRA1 S328A was much more efficient as compared to aggregated Tau (Figure 27 top left). Preincubation of Tau with HTRA1 S328A or MDH did not cause an enhanced proteolysis. Instead, it even slowed down the degradation of 4R wt Tau by active HTRA1 (Figure 27 top right and bottom panels). These findings support the assumption that the enhanced proteolysis after disaggregation is an effect which is seen specifically with Tau fibrils but not the soluble protein, which is in line with a disaggregation activity during the preincubation step. When the concentration of wt HTRA1 was increased 10 fold instead of preincubating the substrate proteins with a 10 fold excess of inactive HTRA1, the proteolysis of Tau fibrils was considerably enhanced. Within 10 min of incubation with wt HTRA1, all of the Tau in the sample with Tau fibrils was degraded, exceeding the enhancement of proteolysis by previous disaggregation (Figure 28 left panel). However, soluble Tau was not degraded considerably faster by 10 fold higher HTRA1 concentration (Figure 28 right panel). These data support the hypothesis that HTRA1 possesses an intrinsic disaggregase activity towards Tau fibrils that enhances proteolysis.

3.4.5. Effects of Disaggregation and Proteolysis on Fibril Abundance

Both the proteolysis itself as well as the enhancement of proteolysis through disaggregation were expected to be assessable by means of AFM. In this way, it should also be possible to distinguish between complete degradation of aggregates and that HTRA1 only degrades parts of the easily accessible and flexible N- and C-terminal parts of the protein. The latter could not be excluded from monitoring degradation by the decreased intensity of Tau containing bands after SDS-PAGE, as these only reflect the intact and not partially degraded Tau species in solution. Therefore, the previous AFM analyses performed to address the process of disaggregation (Figure 26), were repeated including a preincubation step of the fibrils with buffer, HTRA1 S328A or the PDZ domain of HTRA1.

a

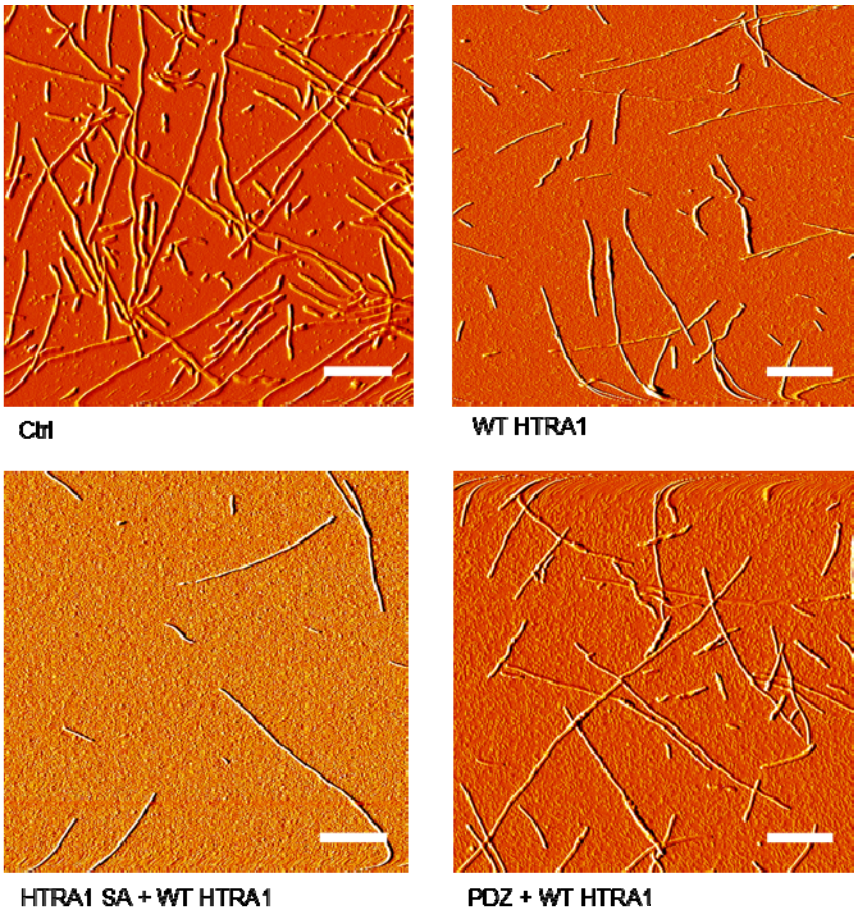

b

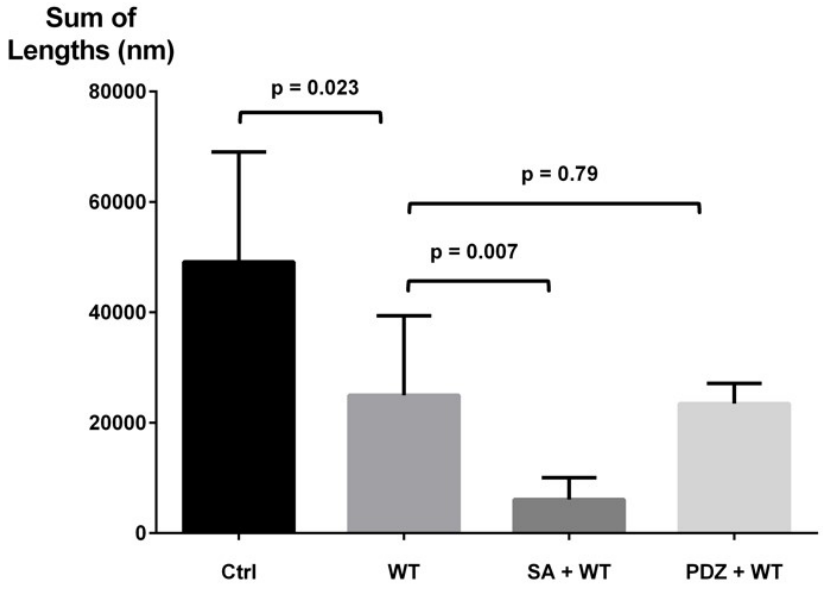

Figure 29 - Disaggregation and Proteolysis of Tau Fibrils as Assessed by AFM

Tau fibrils were incubated with buffer, HTRA1 S328A or the PDZ domain of HTRA1 for 2 h at 37°C before the addition of buffer (Ctrl) or wt HTRA1 and subsequent incubation for another 3 h. Protein concentrations and molar ratios correspond to the proteolysis experiments shown in Figure 26. **a** Representative images of the samples are shown as well as **b** quantification of the abundance of Tau fibrils, which was done in the same way as in Figure 25. Columns show the mean of the sum of fibril lengths of 4-8 random 3 x 3 µm views, error bars indicate the SEM. p-values indicate statistical significance according to t-test for unpaired datasets with Welch's correction. Scale bars in **a** = 500 nm.

When comparing the control samples, which contained only Tau fibrils incubated in buffer for 5 h, with the samples to which wt HTRA1 was added for degradation of the Tau aggregates after 2 h, there was a significant reduction in the abundance of fibrils, indicating that proteolysis of aggregates and not only the "fuzzy coat" had taken place (Figure 29 a). The previous disaggregation by HTRA1 S328A strongly enhanced this proteolysis, leading to a statistically significant decrease in the abundance of fibrils detected per image. Using the isolated recombinant PDZ domain as a control, proteolysis of fibrils was not enhanced compared to using wt HTRA1 alone (Figure 29 b), which underlines that the observed effects can be assigned to a specific disaggregase activity of HTRA1 rather than to unspecific effects arising from the presence of additional proteins in solution only. Furthermore, these results show that the binding of aggregates by the PDZ domain alone did not lead to a disruption of fibrillar integrity with a subsequently enhanced proteolysis. Concerning the lengths of the fibrils, the distribution did not change significantly after the addition of active

HTRA1 or when comparing preincubated vs. not preincubated samples (data not shown). The potential consequences for the mechanism of disaggregation and proteolysis will be discussed later.

3.4.6. Effect of Disaggregation on Cleavage Site Accessibility

The disaggregase activity of HTRA1 facilitated the proteolysis of Tau aggregates by HTRA1 after preincubation of fibrils with proteolytically inactive HTRA1 S328A. Improved proteolysis could be caused by either a loosening of the overall aggregate structure or by a weakening or disruption of the Tau-Tau interactions within the aggregate core. These mechanisms would result in different cleavage patterns by HTRA1 within the primary sequence of Tau. To test this, Tau fibrils or soluble Tau were proteolyzed by wt HTRA1 after an incubation period of 2 h with either an excess of HTRA1 S328A or buffer as control, as was done in the experiments described above. At defined time points as indicated below, the proteolysis reactions were stopped and the resulting cleavage products were isolated by acetone precipitation and subsequently analyzed by mass spectrometry in order to identify the cleavage sites under these conditions. These sites were then mapped to the primary sequence of 4R wt Tau to illustrate their relative position in the Tau protein.

a

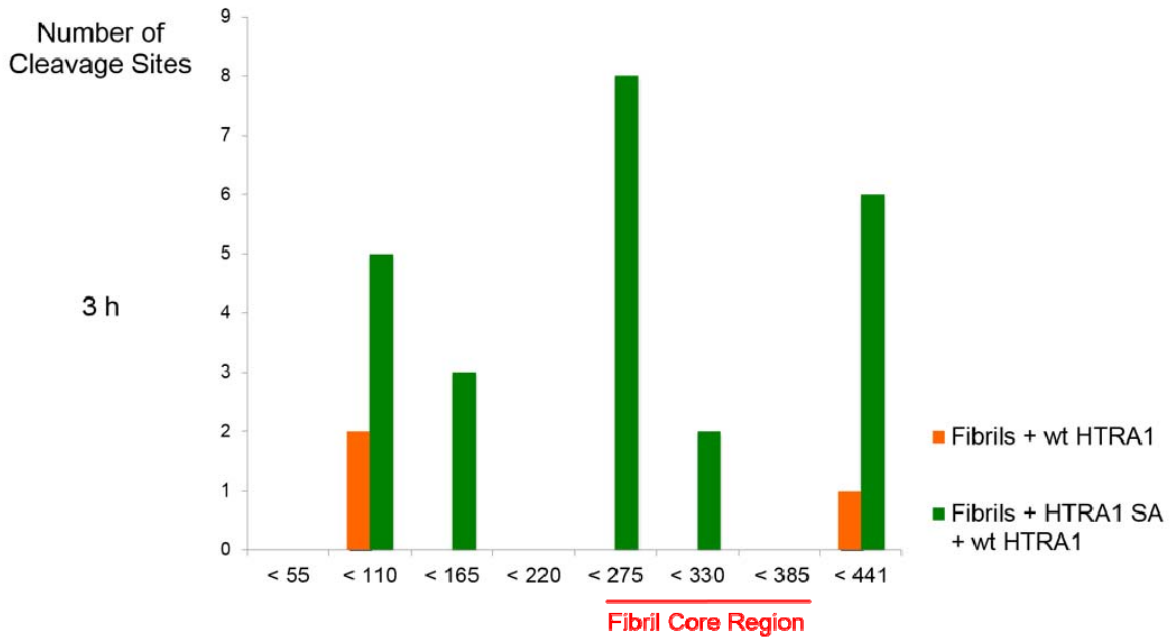
Number of Cleavage Sites
3 h
9
8
7
6
5
4
3
2
1
0
< 55
< 110
< 165
< 220
< 275
< 330
< 385
< 441
Fibril Core Region
Fibrils + wt HTRA1
Fibrils + HTRA1 SA + wt HTRA1

b

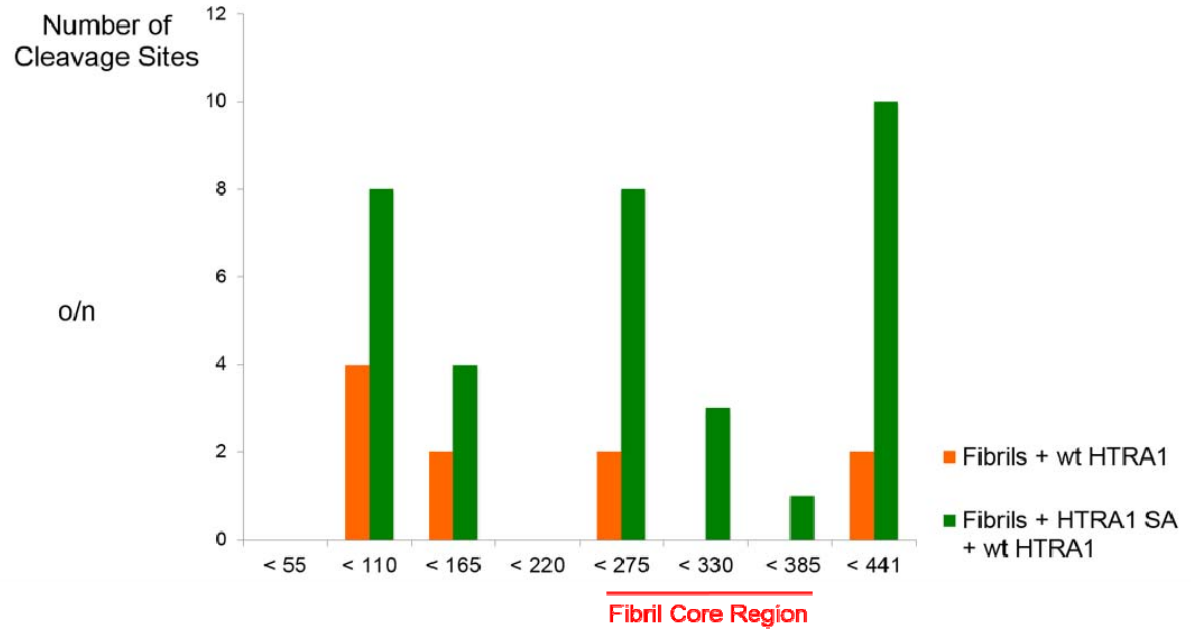
Number of Cleavage Sites
o/n
12
10
8
6
4
2
0
< 55
< 110
< 165
< 220
< 275
< 330
< 385
< 441
Fibril Core Region
Fibrils + wt HTRA1
Fibrils + HTRA1 SA + wt HTRA1

c

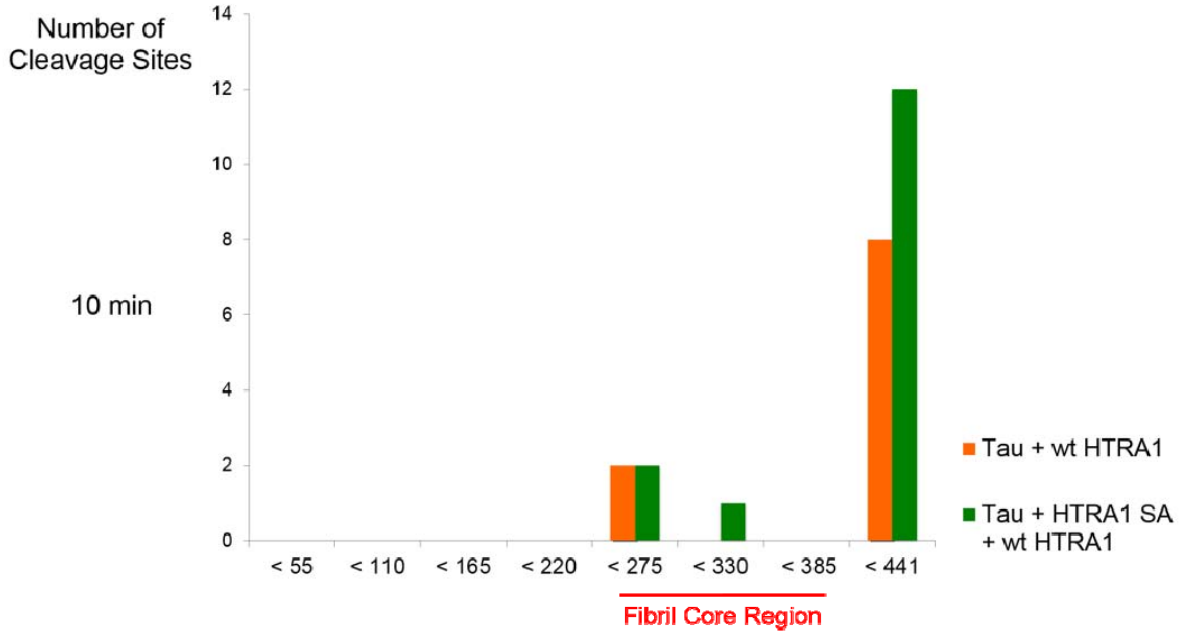
Number of Cleavage Sites
10 min
14
12
10
8
6
4
2
0
< 55
< 110
< 165
< 220
< 275
< 330
< 385
< 441
Fibril Core Region
Tau + wt HTRA1
Tau + HTRA1 SA + wt HTRA1

d

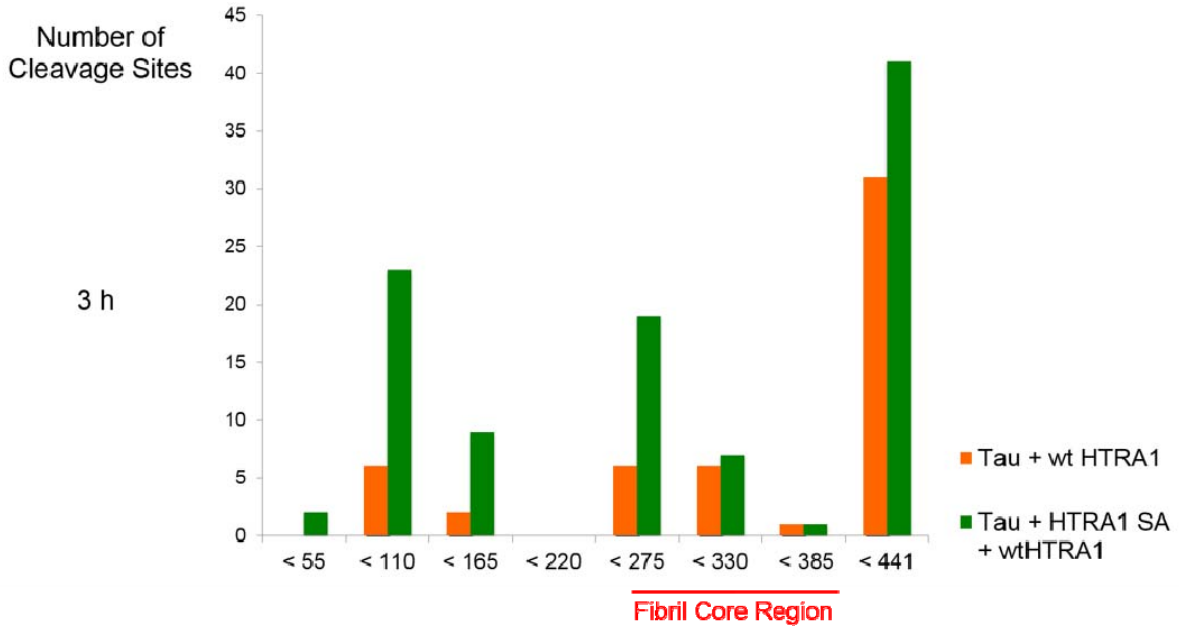

Figure 30 - Determination of HTRA1 Cleavage Sites in Tau

a, **b,** Tau fibrils or **c**, **d**, soluble Tau were proteolyzed by wt HTRA1 for the indicated periods of time after the incubation with buffer (orange bars) or an excess of HTRA1 S328A (green bars) for 2 h. The same molar ratios were used as in the disaggregation and proteolysis experiments described above. At the respective time points, the samples were acetone precipitated to isolate peptidic cleavage products, which were subsequently analyzed by mass spectrometry. The cleavage sites derived from the C- and N-termini of the detected peptides were mapped to regions of the primary sequence of Tau as indicated by the x-axis labeling of the graphs. The tightly packed core region of Tau fibrils is highlighted in red.

The analysis of the cleavage sites in Tau indicated an increased number of proteolytic products following preincubation compared to proteolysis without preincubation with an excess of HTRA1 S328A (Figure 30 a, b). Furthermore, Tau cleavage occurred at earlier time points when the Tau fibrils were preincubated with HTRA1 S328A. Most importantly, proteolysis within the fibril core region was observed within 3 h of incubation only when disaggregation had taken place. Even after overnight incubation, there was significantly enhanced proteolysis particularly in the fibril core when comparing the preincubated samples with the buffer control (Figure 30 b). Soluble Tau was degraded much more efficiently by HTRA1 as was shown in previous experiments (3.3.3), and the differences between preincubation with HTRA1 S328A as compared to the buffer control were not as distinct as compared to proteolysis of Tau fibrils. Moreover, the region corresponding to the fibril core in aggregated Tau were readily cleaved in soluble Tau by wt HTRA1 alone without the need of a previous disaggregation step (Figure 30 c, d).

Taken together, these data illustrate that proteolysis in the fibril core region is strongly restricted at the concentrations of wt HTRA1 used in this proteolysis experiment, probably due to the tight interactions characterizing this part of the aggregates. This resistance to hydrolysis by HTRA1 was shown to be abolished with HTRA1 S328A.

3.4.7. Potential Role of the PDZ Domain for the Disaggregase Activity of HTRA1

PDZ domains are widespread protein-protein interaction modules that have been shown to play important roles in substrate binding and recognition as well as the allosteric regulation of HtrA proteases. In HTRA1, however, the role of the PDZ domain remains largely elusive. Recent data indicate that this domain is not needed for the activation of the proteolytic activity of HTRA1 ((Truebestein et al., 2011) and 3.2.4), but might instead function in targeting HTRA1 to its correct subcellular localization (Dissertation A. Tennstädt, (Chien et al., 2009c)). Due to its pronounced *en bloc* mobility it might be instrumental in the process of disaggregation by providing additional substrate binding sites within HTRA1 homo-oligomers. To address the impact of the loss of the PDZ domain on the disaggregase activity of HTRA1, disaggregation and proteolysis experiments were performed as described above (3.4.1). First, HTRA1 ΔPDZ S328A was incubated with 4R wt Tau fibrils generated *in vitro*, followed by ultracentrifugation in order to test for disaggregase activity in the absence of the PDZ domain.

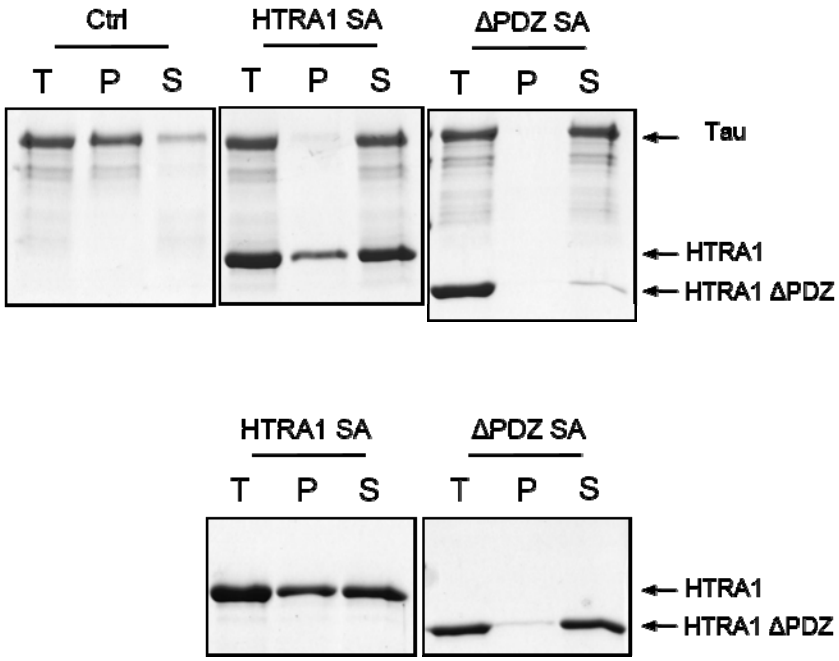

Figure 31 - Disaggregation of Tau Fibrils by HTRA1 ΔPDZ S328A

Tau fibrils were incubated with HTRA1 S328A or HTRA1 ΔPDZ S328A as described before at 37°C for 16 h, followed by ultracentrifugation and SDS-PAGE of the samples. Gels were Coomassie blue stained. T = total, before centrifugation; P = pellet; S = supernatant.

Similarly to HTRA1 S328A, all of the 4R wt Tau fibrils were found in the supernatant after o/n incubation with HTRA1 ΔPDZ S328A. This indicates that HTRA1 was able to dissolve Tau fibrils without the PDZ domain.

To assess the ability of HTRA1 ΔPDZ to proteolyze Tau aggregates and of inactive HTRA1 ΔPDZ S328A to enhance subsequent proteolysis after a disaggregation period, Tau fibrils were incubated with an excess of HTRA1 ΔPDZ S328A before the addition of HTRA1 or HTRA1 ΔPDZ, followed by taking aliquots and analyzing the samples by SDS-PAGE as described above (3.4.4).

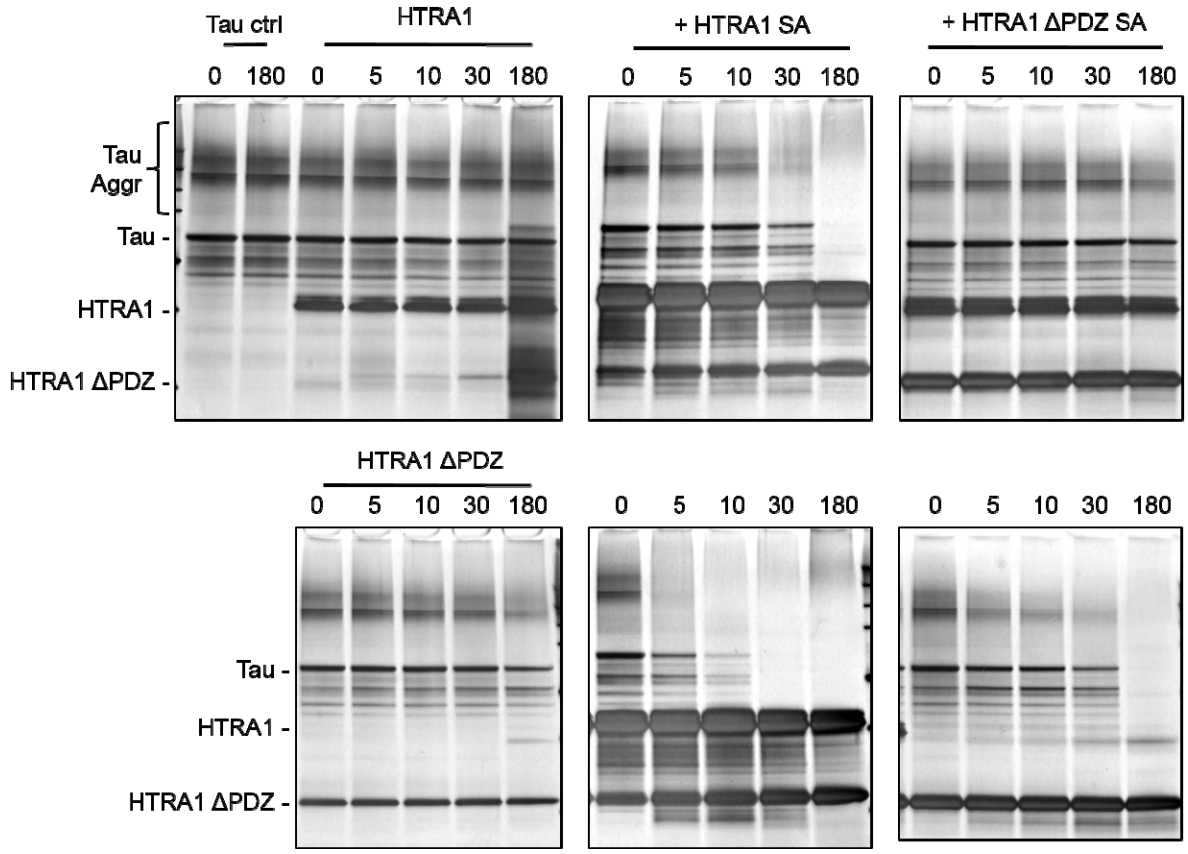

Figure 32 - Disaggregation and Proteolysis of Tau Fibrils by HTRA1 and HTRA1 ΔPDZ

Heparin induced Tau fibrils were proteolyzed by HTRA1 (upper row) or HTRA1 ΔPDZ (lower row) after 2 h of incubation with buffer (left panels), with HTRA1 S328A (middle panels) or HTRA1 ΔPDZ S328A (right panels) at 37 °C as described above. Aliquots were taken and flash frozen in liquid N_2 when starting the disaggregation (-2 h) or at the indicated time points after the addition of wt HTRA1. All samples were subjected to SDS PAGE followed by silver staining. Each lane corresponds to 200 ng of Tau according to the concentration when starting the reaction.

In accordance with previous results, the proteolysis of Tau fibrils after incubation in proteolysis buffer only is a slow process which can be enhanced by preincubating the Tau aggregates with HTRA1 S328A (Figure 32 top left and middle panels). In contrast to the effect of HTRA1 S328A there was no enhancing effect of HTRA1 ΔPDZ S328A on the proteolytic degradation of Tau (Figure 32 top left and right panels). This indicates that the PDZ domain is necessary for disaggregation in this context. Using HTRA1 ΔPDZ as the active protease, degradation with low efficiency as for wt HTRA1 was observed with buffer preincubation only, whereas the proteolysis was strongly enhanced upon disaggregation by HTRA1 S328A (Figure 32 bottom left and middle panels). The effect of disaggregation by HTRA1 ΔPDZ S328A, however, was less pronounced than disaggregation by HTRA1 with

the PDZ domain (Figure 32 bottom middle and right panels), further underlining the potential implication of the PDZ domain in the disaggregase activity of HTRA1.

3.4.8. Impact of the Presence of Inactive HTRA1 on the Proteolytic Activity

HTRA1 S328A was used in a 10-fold molar excess as compared to the active protease in the disaggregation experiments. To address the formal possibility that HTRA1 S328A might activate the proteolytic activity of wt HTRA1, a protease activity assay using the synthetic chromogenic substrate VFNTLPMMGKASPV-pNA was performed to determine the proteolytic activity of HTRA1 and HTRA1 ΔPDZ in the presence of HTRA1 S328A or HTRA1 ΔPDZ S328A both in equimolar and 10-fold higher concentrations as compared to the active protease.

a

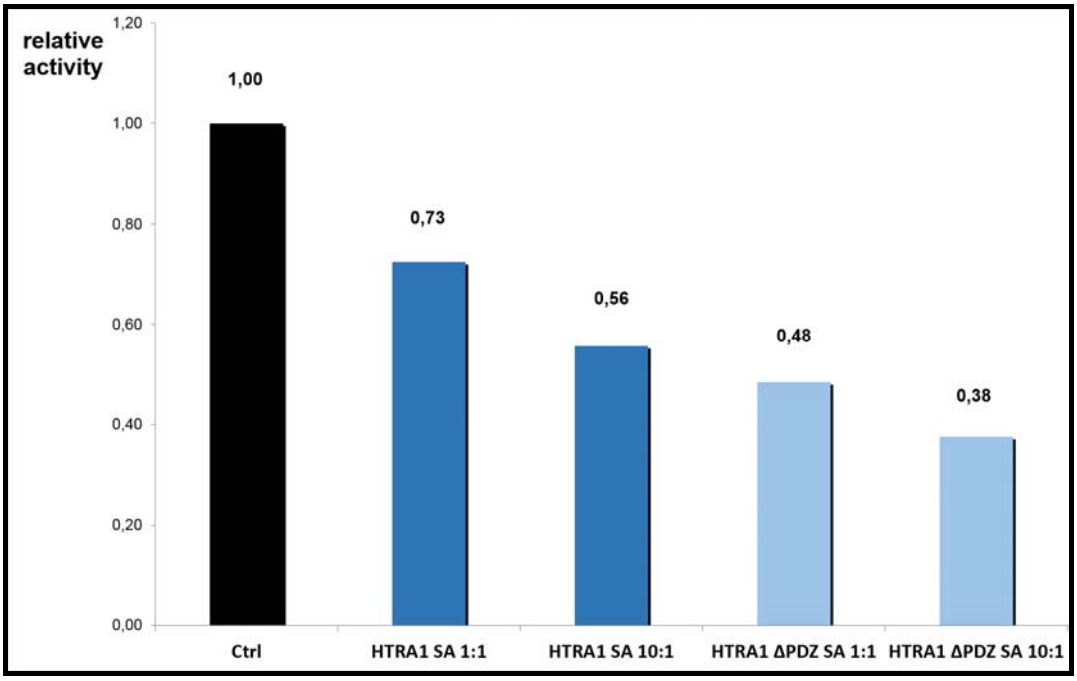

b

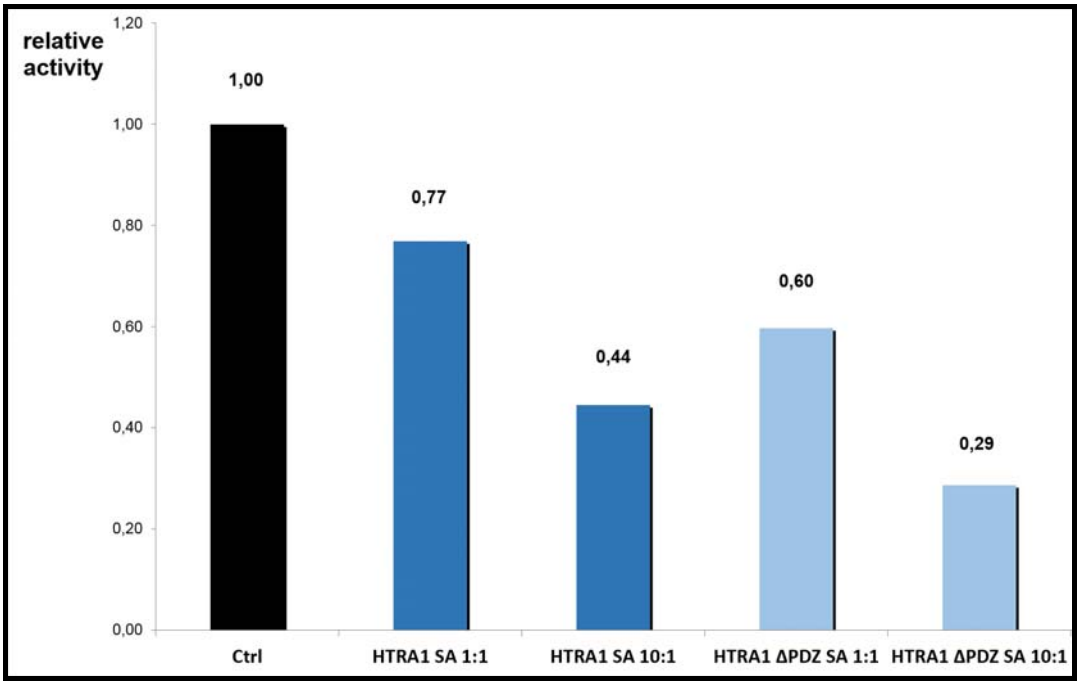

Figure 33 - Specific Activities of HTRA1 and HTRA1 ΔPDZ in the Presence of HTRA1 S328A and HTRA1 ΔPDZ S328A.

The specific activities of **a** HTRA1 and **b** HTRA1 ΔPDZ were determined by a colorimetric pNA assay using the synthetic substrate VFNTLPMMGKASPV-pNA. The assay was performed in the presence of buffer, HTRA1 S328A, or HTRA1 ΔPDZ S328A in molar ratios of 1:1 and 10:1 as indicated. The specific activities were normalized to the values for the basal activities of HTRA1 (7.8 nmol x min^{-1} x mg^{-1}) or HTRA1 ΔPDZ (12.4 nmol x min^{-1} x mg^{-1}).

These data indicate that the proteolytic activity of both HTRA1 and HTRA1 ΔPDZ was not enhanced in the presence of any of the proteins tested (Figure 33). HTRA1 was inhibited by 44% and 62% in the presence of a 10 fold molar excess of HTRA1 S328A and HTRA1 ΔPDZ S328A, respectively (Figure 33 a), while HTRA1 ΔPDZ was inhibited by 56% and 71% in the presence of a 10 fold molar excess of HTRA1 S328A and HTRA1 ΔPDZ S328A, respectively (Figure 33 b). These observations indicate that the previously observed enhanced proteolysis upon preincubation was not due to an enzymatic activation caused by the presence of an excess of the inactive protease. Moreover, the inhibition of proteolytic activity, which was more pronounced for incubation with HTRA1 ΔPDZ S328A as compared to HTRA1 S328A was used, could explain the lower effect of preincubation on the proteolysis of Tau fibrils described above (3.4.7). It should be noted that the basal activity of HTRA1 ΔPDZ as determined in this assay was about 60% higher than the activity measured for HTRA1 (12.35 and 7.73 nmol x min^{-1} x mg^{-1} for HTRA1 ΔPDZ and HTRA1, respectively), which might

account for the more effective proteolysis of Tau fibrils by HTRA1 ΔPDZ after disaggregation with HTRA1 S328A compared to wt HTRA1.

3.4.9. Analysis of the Disaggregase Activity of Point Mutations in the PDZ Domain and the Activation Loop L3

So far, an instrumental role of certain functional elements within HTRA1 for the disaggregase activity could not be shown unambiguously. HTRA1 mutants lacking the entire PDZ domain might obscure mechanistic effects because of being artificial constructs which, for example, show a higher basal activity that HTRA1 containing the PDZ domain (3.4.4). Therefore, it was reasoned that the introduction of point mutations into two potentially important structural elements, namely the activation loop L3 and the PDZ domain, could be helpful in addressing their role for disaggregase activity. On the basis of their position within crystal structures of the HTRA1 protease domain and the PDZ domain (Runyon et al., 2007; Truebestein et al., 2011), two point mutations were chosen, R302L in loop L3 of the protease domain and I383A in the PDZ domain. Site-directed mutagenesis and small scale purification using gravity-flow affinity chromatography columns were performed by Till van Oepen. R302 has been predicted to interact with the substrate and to be important for setting up the active conformation of the active site, whereas I383 has been shown to be important for ligand binding to the PDZ domain.

To test whether these point mutants have retained their proteolytic activity, the activity was determined with a chromogenic protease activity assay using the substrate VFNTLPMMGKASPV-pNA as described above (3.4.8).

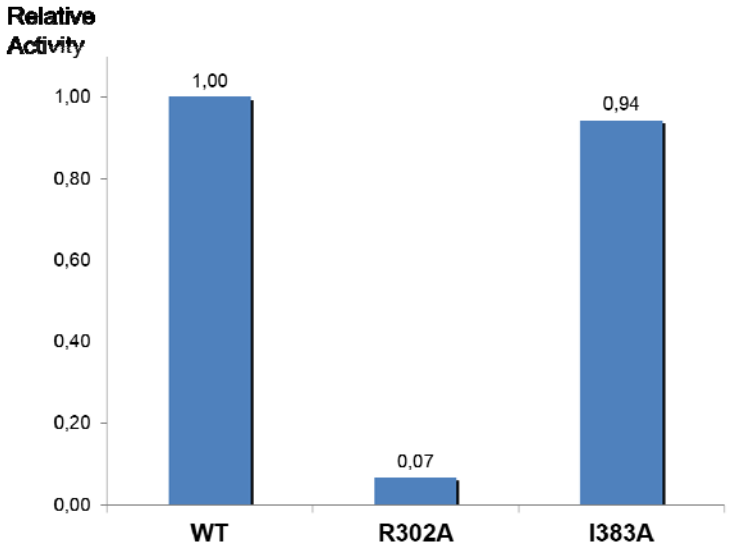

Figure 34 - Specific Activities of the HTRA1 Mutants R302A and I383A.

The specific activities of wt HTRA1, HTRA1 R302A and HTRA1 I383A were determined by a pNA assay using the synthetic substrate VFNTLPMMGKASPV-pNA as described above. The specific activities were normalized to the values for the basal activities of wt HTRA1 2.6 nmol x min^{-1} x mg^{-1}.

The proteolytic activity of the HTRA1 R302A with a mutation in loop L3 was almost completely abolished, the protease only showed a residual activity of 7% (Figure 34). Considering the little increase of the absorption at 405 nm, which had been used for the calculation of the specific activity, there was no reasonable increase in absorption (data not shown), suggesting that this mutant is essentially proteolytically inactive. This finding shows that interfering with substrate binding to loop L3 prevented the arrangement of a proteolytically competent active site. In contrast, mutating I383 to an Ala residue did not interfere with proteolytic activity, which was retained at 94%, which represents only a small reduction.

3.4.10. Disaggregase Activity of HTRA1 R302A and I383A

The effect of the point mutations on the disaggregase activity was initially tested by assessing the solubility of 4R wt Tau fibrils after o/n incubation with equimolar amounts of the mutants or active HTRA1. The control sample contained Tau fibrils prepared *in vitro* from recombinant 4R wt Tau and buffer only. Notably, proteolytically active HTRA1 (including HTRA1 I383A) could be used in this assay because the disaggregation buffer had a low pH (pH 6) and therefore almost completely inhibited proteolytic activity of HTRA1, as confirmed by pNA assays and the proteolysis of full-length Tau (data not shown).

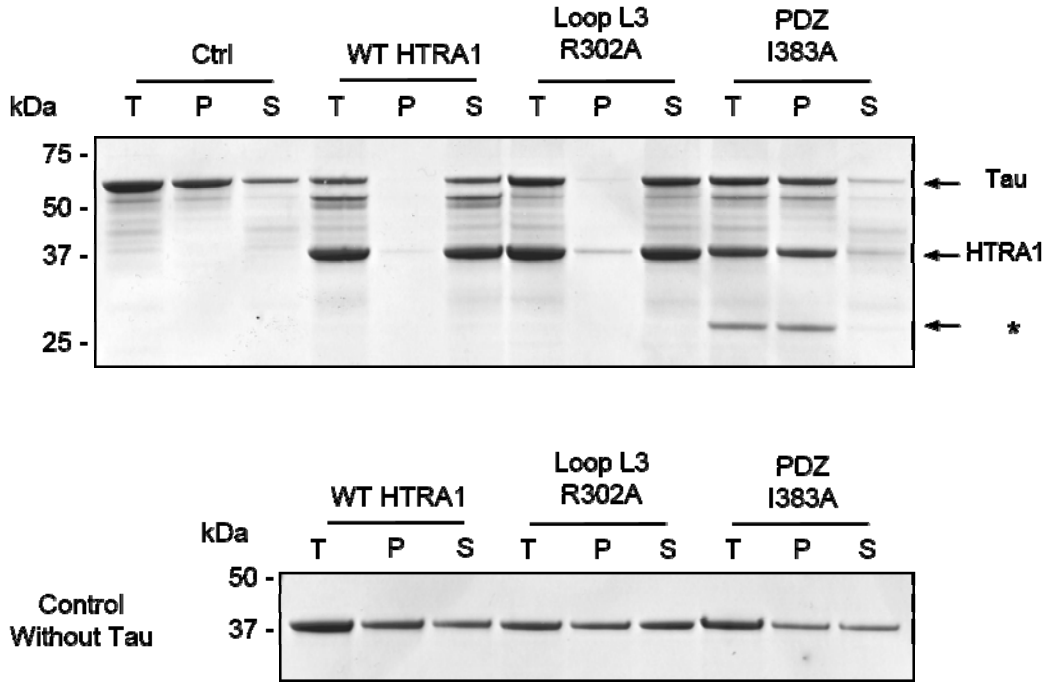

Figure 35 - Disaggregase Activity of wt HTRA1, HTRA1 R302A and I383A.

The disaggregase activities of wt HTRA1 and the HTRA1 mutants R302A and I383A were assessed on the basis of Tau insolubility after ultracentrifugation as described above (3.4.1). Heparin induced 4R wt Tau fibrils were incubated with equimolar amounts of the HTRA1 mutants as indicated at 37 °C o/n, followed by ultracentrifugation and SDS-PAGE of samples before ultracentrifugation as well as the insoluble and soluble fractions. T = total, before ultracentrifugation; P = pellet; S = supernatant. SDS gels were Coomassie blue stained. * = degradation product of HTRA1 or Tau due to residual proteolytic activity of HTRA1 I383A in the disaggregation buffer.

Based on Coomassie blue stained SDS gels, wt HTRA1 as well as HTRA1 R302A were able to solubilize Tau fibrils, whereas the Tau aggregates remained insoluble after incubation with the PDZ mutant I383A (Figure 35). These data suggest that, according to this assay, the I383A mutation inhibited disaggregase activity, whereas the point mutation in loop L3 did not interfere with disaggregation. As shown before, disaggregation enhanced subsequent proteolysis of Tau fibrils by active HTRA1 (3.4.4). Measuring the proteolysis of fibrils and the effect of the preincubation of Tau fibrils with proteolytically inactive HTRA1 therefore provides additional means of assessing the disaggregase activities of HTRA1 mutants. HTRA1 I383A almost completely retained proteolytic activity as determined by a chromogenic activity assay (Figure 34). Therefore, it was not possible to incubate Tau fibrils with this mutant in proteolysis buffer prior to the addition of wt HTRA1 and at the same time prevent proteolysis by HTRA1 I383A. To test the ability of this mutant to degrade Tau fibrils and by these means

test for a potential defect in disaggregase activity, the proteolysis of Tau fibrils was compared to wt HTRA1.

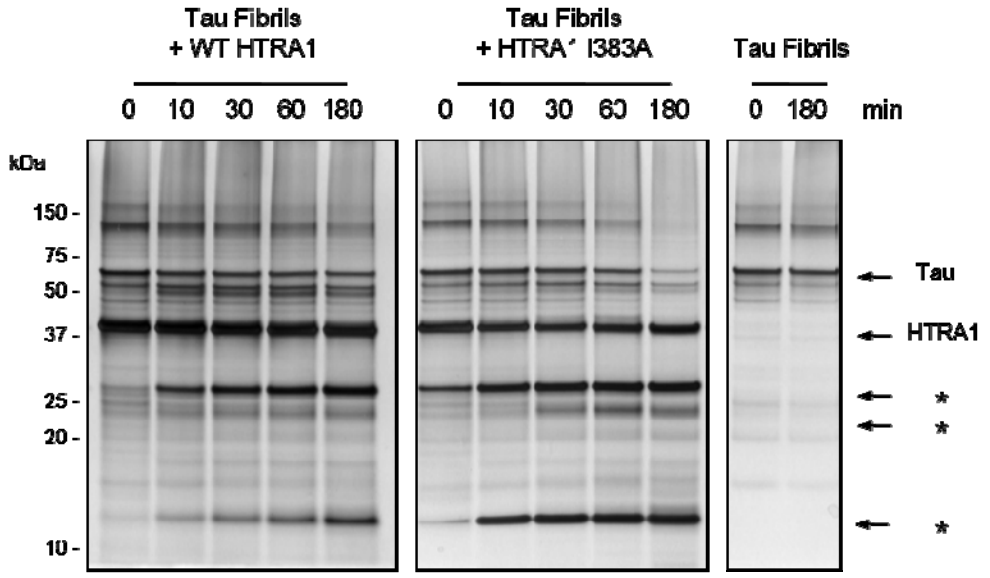

Figure 36 - Proteolysis of Tau Fibrils by HTRA1 I383A

To assess the ability of HTRA1 I383A to proteolyze Tau fibrils, proteolysis experiments were performed at 37 °C as described before except that a molar ratio of HTRA1:Tau = 1:1 was used to allow a better resolution of the differences in proteolysis. Aliquots were taken at the indicated time points and subjected to SDS PAGE followed by silver staining. * = degradation products of Tau or HTRA1.

Surprisingly, HTRA1 I383A showed an even enhanced degradation of Tau fibrils as compared to wt HTRA1. While wt HTRA1 proteolysis led to a small decrease in the Tau bands, a large amount of Tau protein was degraded after 3 h of incubation of with HTRA1 I383A (Figure 36). These observations indicate that the mutation I383A did not interfere strongly with the proteolysis of Tau fibrils, in spite of its lack of disaggregase activity as suggested by ultracentrifugation experiments. In the solubility assays, this mutant did not proteolyze Tau fibrils because of the low pH conditions which preclude proteolytic activity by HTRA1.

HTRA1 R302A did not show any significant proteolytic activity in the quantitative pNA assays (Figure 34), which implicates that it can be used for preincubation of Tau fibrils before the addition of wt HTRA1. Therefore, in order to test the disaggregase activity of HTRA1 R302A, fibrils derived from full length 4R wt Tau were preincubated with HTRA1 R302A for 2 h before starting the proteolysis, which was subsequently monitored by taking samples at the indicated time points.

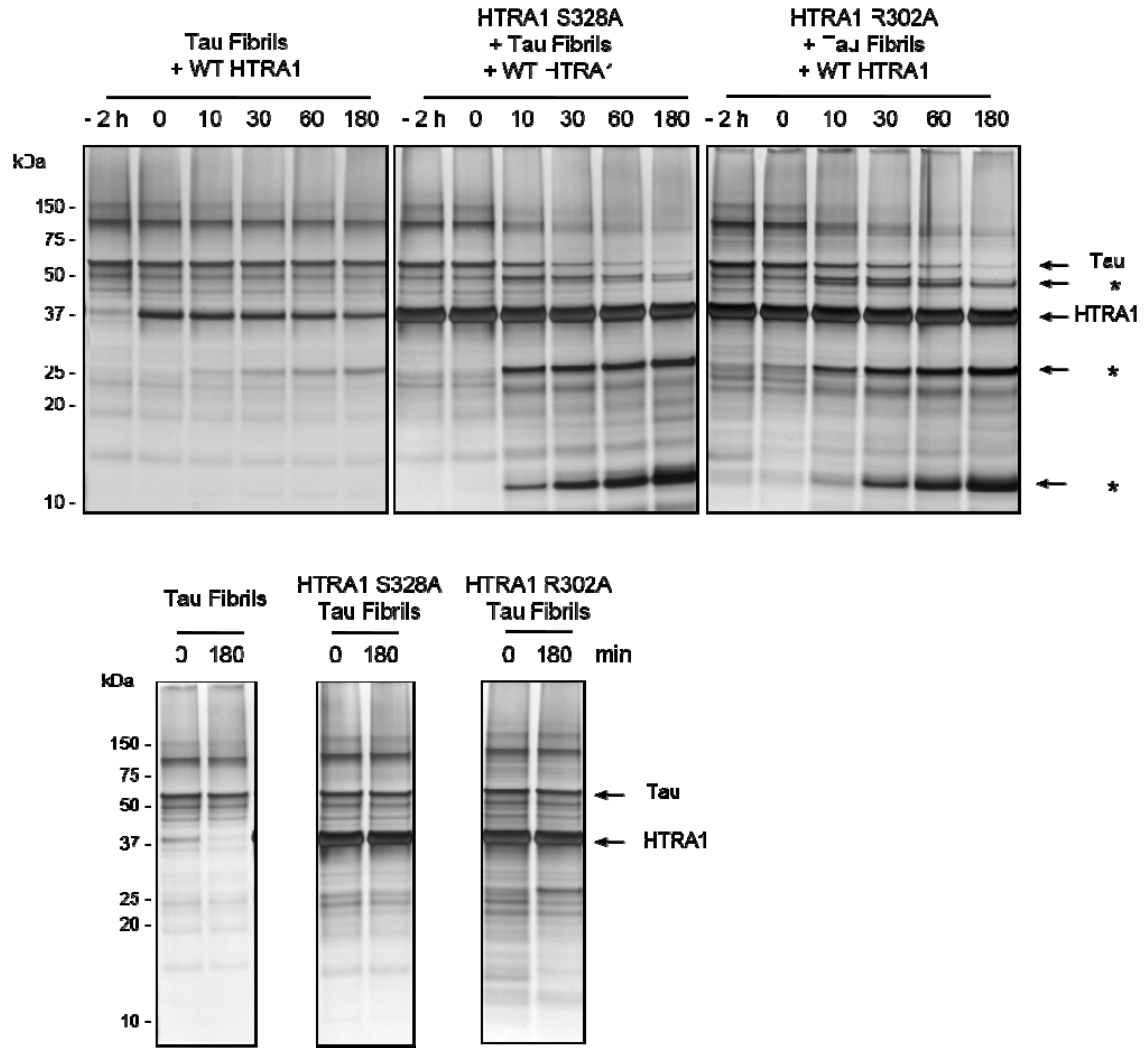

Figure 37 - Disaggregation of Tau Fibrils by R302A and Subsequent Proteolysis by wt HTRA1

To assess the disaggregase activity of HTRA1 R302A, Tau fibrils were incubated with buffer, HTRA1 S328A or R302A for 2 h at 37 °C before the addition of wt HTRA1 with a 10 fold molar excess of HTRA1 S328A and HTRA1 R302A as compared to the wt HTRA1 protein. Samples were taken when starting the disaggregation reaction (-2 h) and at the indicated time points after the addition of wt HTRA1. The bottom panels show the controls, without the addition of wt HTRA1. * = degradation products of HTRA1 or Tau.

In agreement with previous experiments, Tau fibrils were poorly degraded by HTRA1 under the conditions tested here, if no previous disaggregation was performed (Figure 37 left panel). In contrast, preincubation with HTRA1 S328A led to a pronounced decrease in the amounts of Tau within 30 – 60 min after the addition of wt HTRA1. HTRA1 R302A had the same effect on Tau fibril proteolysis, leading to the degradation of Tau fibrils within 30 – 60 min (Figure 37 middle and right panels). This suggests that HTRA1 R302A and HTRA1

S328A were able to disaggregate the Tau fibrils with comparable efficiencies, which means that the mutation in loop L3 did not hamper disaggregase activity.

3.5. Cell Biological Studies of HTRA1 and Tau Aggregation

For the investigation of the potential implications of HTRA1 disaggregase and protease activities in the cellular context, an experimental model of Tau aggregation in cultured cells had to be established. The soluble nature of the Tau protein makes the studying Tau aggregation in the time course available for laboratory experimentation a difficult task. Under pathological conditions, Tau aggregation involves a plethora of posttranslational modifications and interactions which are poorly understood, but which probably take a long time to eventually result in the deposition of insoluble Tau aggregates in neurons. For studying the *in vitro* aggregation behavior of the Tau protein, the induction of aggregation by heparin or other factors is frequently utilized. Yet, this approach cannot be applied in the complex environment of cultured cells. For both *in vitro* and cellular studies, the use of mutations which are the basis of hereditary tauopathies and have been shown to enhance the aggregation propensity of Tau has helped to set up experimental systems in which the aggregation of Tau could be studied in a reasonable time frame (Wang et al., 2007).

In the course of this work, a number of different approaches was tested with the aim of establishing a model in which the generation or the clearance of cytoplasmic Tau aggregates could be monitored in cultured human cells. The spontaneous uptake of insoluble MTBD Tau derived from protein purified by boiling and ammonium sulfate precipitation (see 2.3.7) was discarded because of the amorphous nature of these aggregates and data suggesting that the aggregates might reside in vesicles and therefore be shielded from the cytoplasm by membraneous structures (data not shown). When fibrillar aggregates were added to the culture medium of adherent human neuroblastoma cells, they were not taken up, but instead seemed to stick to the cell surface, as was assessed by immunofluorescence microscopy (data not shown). As an alternative, a recently published model was chosen, which is based on the prion-like propagation of Tau misfolding and aggregation (Guo and Lee, 2011). In this model, the aggregation of cytoplasmic, transiently overexpressed Tau protein is seeded by the transfection of aggregate seeds into the cytoplasm of cultured cells. The seeds were derived from recombinant Tau protein which was aggregated in the presence of heparin followed by the isolation of the fibrils by ultracentrifugation. The aggregates were sonicated in

order to disrupt the fibrillar structures into small fragments which can subsequently serve as templates for the conversion of soluble Tau into amyloid aggregates. The seeds used in this study were prepared using MTBD Tau, which has the ΔK280 mutation rendering the protein highly susceptible to aggregation and seeding. For the transient overexpression of Tau, the P301L mutant form of Tau was chosen which has also been reported to have an increased aggregation propensity (von Bergen et al., 2000). Furthermore, overexpressed Tau had an HA tag, which allowed the distinction of endogenously expressed Tau from the seeds composed of recombinant protein by using specific anti HA tag antibodies.

3.5.1. Identification of a Suitable Cell Line for the Seeding of Tau Aggregation

In order to find conditions suitable for the seeding of cytoplasmic Tau aggregates, overexpression and subsequent transfection of MTBD Tau seeds or the incubation of cells with seeds was tested in four different cell lines. These cell lines were a human neuroblastoma cell line (SHSY-5Y), a mouse neuroblastoma cell line (N2A), a human astrocytoma cell line (U373) and a human embryonic kidney cell line (HEK-293T). The cells were transiently transfected with an expression plasmid encoding full-length human 4R P301L Tau, grown for 24 h, treated or transfected with MTBD Tau protein aggregate seeds, followed by another incubation for 24 h before performing Sarkosyl extraction in order to determine the amount of aggregated, intracellular Tau. It has previously been reported that MTBD Tau can enter cultured cells spontaneously and seed the aggregation of endogenous Tau (Guo and Lee, 2011), which is why the treatment of cells with MTBD seeds conditioned culture medium was also included in the experiment. The MTBD Tau seeds were prepared by aggregating MTBD Tau in the presence of heparin for 24 h, purifying the aggregates by ultracentrifugation and sonicating the pellet to generate small seeds capable of serving as a template for seeded aggregation of full-length Tau. The conditions for sonication and subsequent seeding were determined *in vitro* by seeding of recombinant 4R wt Tau with MTBD aggregates sonicated under various conditions and with different intensities. ThT fluorescence was determined as a measure of successful aggregation (data not shown). After transfection of the seeds into P301L Tau overexpressing cells, the cells were lysed and incubated with the detergent Sarkosyl to solubilize all cellular protein except for aggregates. Following ultracentrifugation of the Sarkosyl treated lysates, the pellet and supernatant fraction were tested for the presence of Tau protein by SDS PAGE and immunoblotting using anti Tau antibodies.

Endogenous Tau was distinguished from the transfected seeds on the basis of the higher apparent MW of P301L Tau versus MTBD Tau (ca. 60 kDa and 15 kDa, respectively).

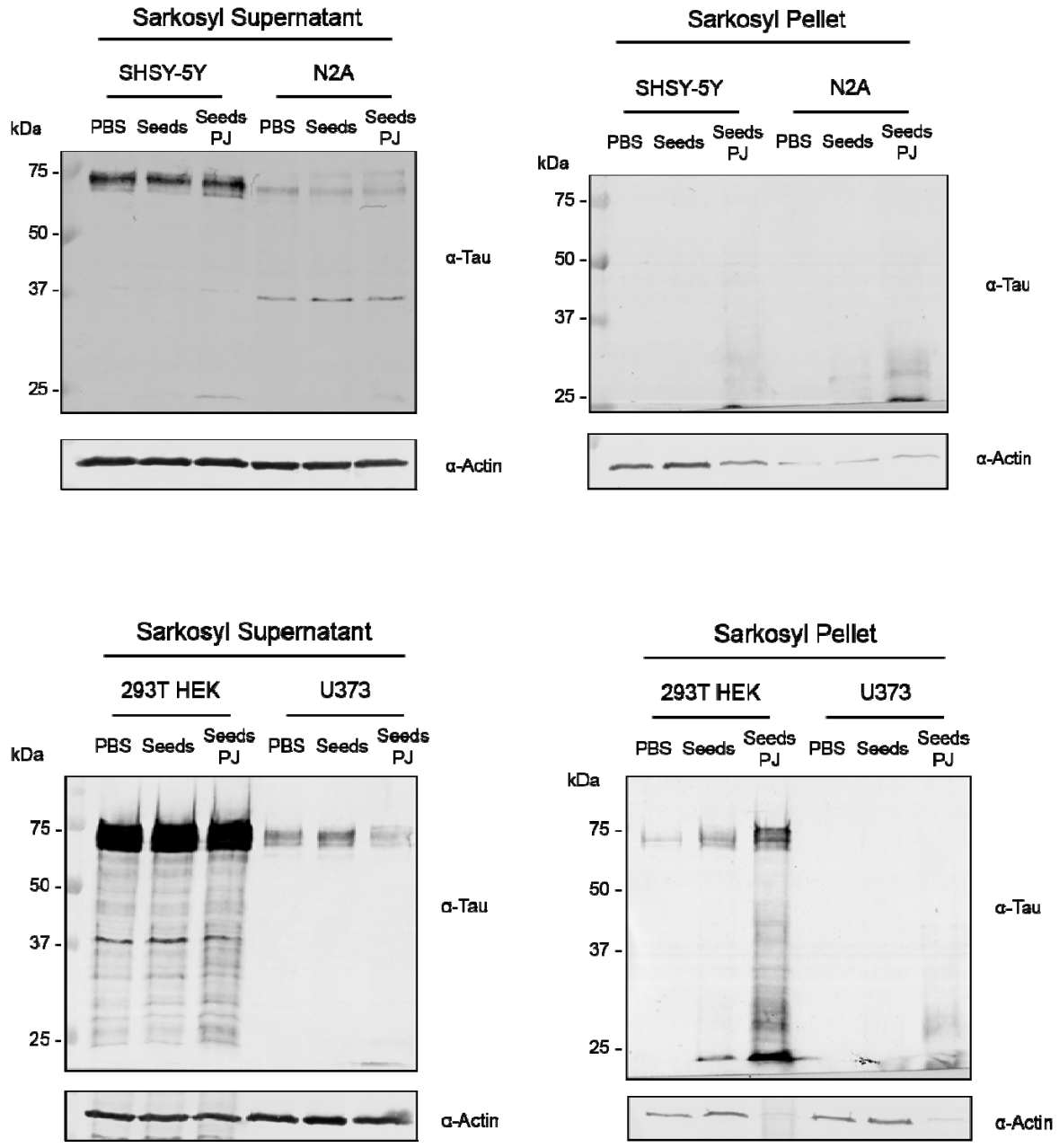

Figure 38 - Test of SHSY-5Y, N2A, HEK-293T and U373 Cells for Seeding of Tau Aggregation

Cells transiently overexpressing HA tagged P301L Tau were treated with PBS (PBS), medium conditioned with MTBD aggregate seeds (Seeds) or were transfected with MTBD seeds using the protein transfection reagent Pro-Ject (Seeds PJ). After Sarkosyl extraction, samples from the Sarkosyl soluble (left panels) and insoluble (right panels) fractions were subjected to SDS PAGE followed by immunoblotting against Tau or Actin (as a loading control).

In the left panels, the Sarkosyl soluble fraction containing the bulk of cellular proteins is shown, which approximately reflects the total amount of overexpressed Tau in the respective cell line. The Sarkosyl insoluble, i.e. aggregated, proteins were analyzed by the immunoblots

shown in the right panel of Figure 38. When comparing the individual cell lines, the HEK-293T cells showed the highest levels of P301L Tau expression, SHSY-5Y and U373 cells expressed P301L Tau at moderate levels, and only little expression was detectable in N2A cells (Figure 38, left panels). It should be noted that it was not possible to precisely compare the cell lines with regard to expression levels based on the immunoblots presented here, because of the growth characteristics and overall protein concentrations which differed considerably between the cell lines. Therefore, different total amounts of protein were subjected to SDS-PAGE and immunoblotting for each cell line (i.e., 15 µg for SHSY-5Y, 35 µg for N2A, 85 µg for HEK-293T and 10 µg for U373 cells), which may in part explain the variations in the amounts of overexpressed Tau. Regarding the amounts of insoluble Tau, however, only the HEK-293T cells showed insoluble Tau with the apparent MW corresponding to full-length P301L Tau (Figure 38, right panels). In this case, there was some Tau in the Sarkosyl pellet after treating the cells with MTBD Tau seeds without the transfection reagent, and considerably more aggregated Tau when the seeds were transfected into the cells using a transfection reagent. In the Sarkosyl insoluble fractions of the other three cell lines, there was some lower MW protein detected by the anti Tau antibody, which supposedly corresponded to the transfected seeds or SDS resistant dimers or oligomers of the MTBD seeds.

Based on these findings, HEK-293T cells were chosen to further establish the model of cytoplasmic Tau aggregation. The subcellular localization as well as the amyloid properties of intracellular, seeded Tau aggregates are important features regarding further analyses and the potential role of HTRA1 in the intracellular aggregation and the clearance of Tau aggregates. Both characteristics were addressed by immunofluorescence of P301L Tau overexpressing HEK-293T cells which were transfected with MTBD Tau seeds to induce intracellular aggregation. For this purpose, the cells were seeded on coated glass coverslips and treated in the 24 well format, allowing fixation and staining was without the need of further trypsinization and replating. The protocol of transient expression of Tau and aggregate seeding was performed as described above (3.5.1), followed by immunostaining against the HA tag of endogenously overexpressed Tau and Thioflavin S (ThS) staining for the specific detection of amyloid aggregates within the cells. Confocal microscopy with serial acquisitions of the individual channels was performed to ensure the imaging of single focal plains while avoiding fluorescence bleed-through.

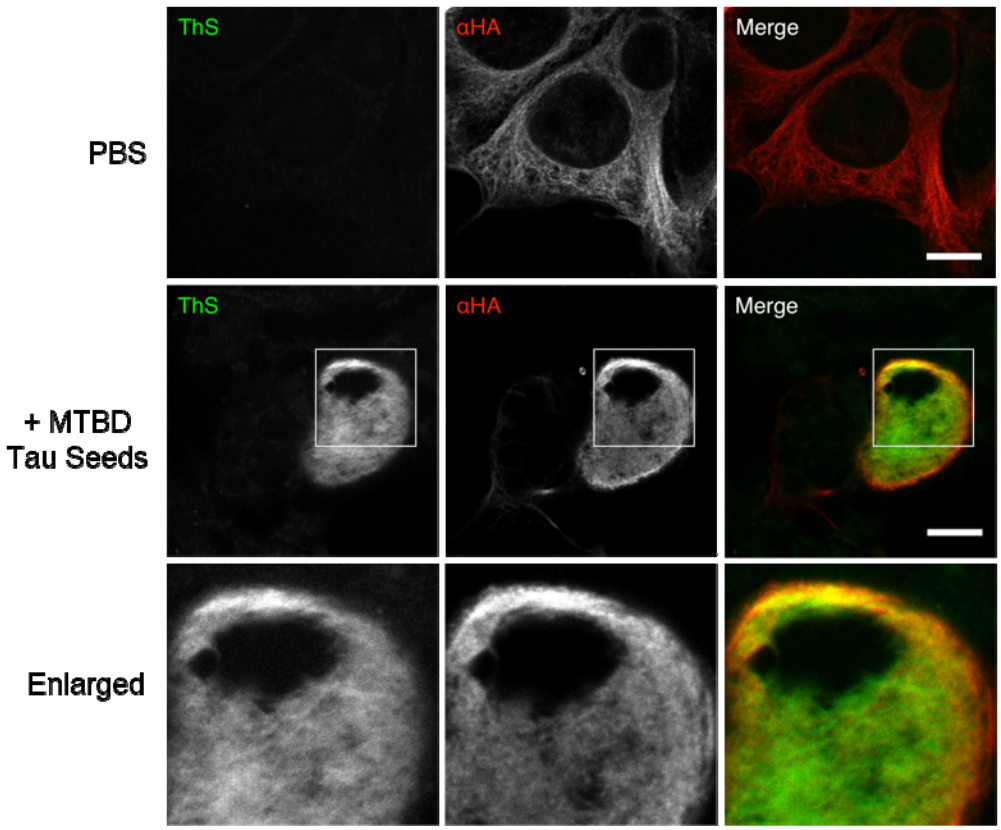

Figure 39 - Immunofluorescence of HEK-293T Cells with Seeded Tau Aggregates

Aggregation of transiently overexpressed P301L Tau was induced by transfection with MTBD Tau seeds, which was followed by 24 h of incubation, fixation and staining with the amyloid specific fluorescent dye ThS (green) and an antibody against the HA tag of overexpressed Tau (red). Control cells were treated with PBS instead of MTBD Tau transfection. Scale bar = 10 µm.

Transient expression of HA-tagged P301L Tau led to high intracellular levels of HA-positive protein which localized to cytoplasmic structures closely resembling the microtubular network, in accordance with the physiological role and microtubule binding properties of the Tau protein (Figure 39, top row). There were no detectable inclusions, aggregates, or ThS positive structures when the HEK-293T cells were treated with PBS only, consistent with reported observations of Tau being largely soluble even when expressed at high levels (Frost et al., 2009a). The levels of Tau expression varied greatly within each sample. This is a common observation when cultured cells are transiently transfected with expression plasmids, which normally leads to a heterogeneous population of cells. Also, not all of the cells were successfully transfected with the P301L Tau-encoding plasmid. Anti-HA immunostaining indicated a transfection efficiency of ca. 60% as estimated on the basis of immunofluorescence images (data no shown).

Upon transfection with MTBD Tau seeds, a fraction of the cells contained large amounts of ThS positive aggregates. All of the cells which were positive for ThS also showed intensive immunostaining with the anti-HA antibody, indicating that high levels of intracellular Tau were the prerequisite of successful seeding. Furthermore, the ThS positive structures were to some extent, but not completely, positive for the HA-tag which also suggests that the aggregates originated from overexpressed, HA-tagged P301L Tau. The overall portion of ThS positive cells was below 1%, which might be explained by the combination of treatments (i.e. transient plasmid transfection and protein transfection of seeds) and the efficiency of templated aggregation once the MTBD Tau seeds have entered the cells, which is probably also below 100% and requires high concentrations of Tau. Cells which were full of ThS positive aggregates tended to lose their characteristic shape and were round and smaller as compared to control cells, an observation which was described in a different cell model before (Bandyopadhyay et al., 2007). However, most of them were positively stained with a nuclear counterstain and could therefore be unambiguously identified as cells and not artefacts on the coverslips. The abnormal cell shape might reflect the considerable stress which is imposed on the cells through the occurrence of large amounts of cytoplasmic aggregates.

3.5.2. Spontaneous Internalization of Recombinant HTRA1 from the Extracellular Space

The experimental modulation of intracellular HTRA1 levels is crucial to the investigation on its role in the process of Tau aggregation and clearance in the cellular context. Transient overexpression of HTRA1 from a plasmid was hampered by the fact that the cellular model of Tau aggregation already required two different transfection procedures. This resulted in a relatively low frequency of cells with aggregates, and the problem of stressing the cells additionally by including another transfection step. Moreover, transfection would only be successful in a subset of cells, further reducing the number of cells with the desired change in HTRA1 levels. To circumvent these problems, an alternative way of titrating HTRA1 into the cells was needed.

The open reading frame of HTRA1 contains a signal sequence for the secretion into the extracellular space. Accordingly, its extracytoplasmic localization and suggested roles, e.g. in the remodeling of the extracellular matrix were reported as physiological features of the

protease. At the same time, localization of HTRA1 in the cytoplasm as well as the cleavage of potential cytoplasmic substrates have been reported (Clausen et al., 2011). However, it is not yet known in which way a cytoplasmic pool of HTRA1 protein might be established by cells. One possible way of doing so would be the uptake of extracellular HTRA1 into the cytoplasm after secretion. Evidence for a corresponding process has been provided for other secreted proteins with assumed intracellular roles (Nellaiappan et al., 2000).

To test whether recombinant HTRA1 could be spontaneously internalized, HEK-293T cells were treated with culture medium conditioned with increasing concentrations of recombinant, purified HTRA1 S328A. Alternatively, cells were treated with a constant concentration of HTRA1 S328A and lysed at various time-points to assess the time-course of internalization. After incubation for the indicated periods of time, the cells were trypsinized, lysed and the lysates were subjected to SDS PAGE followed by immunoblotting for the detection of endogenous and internalized HTRA1.

a

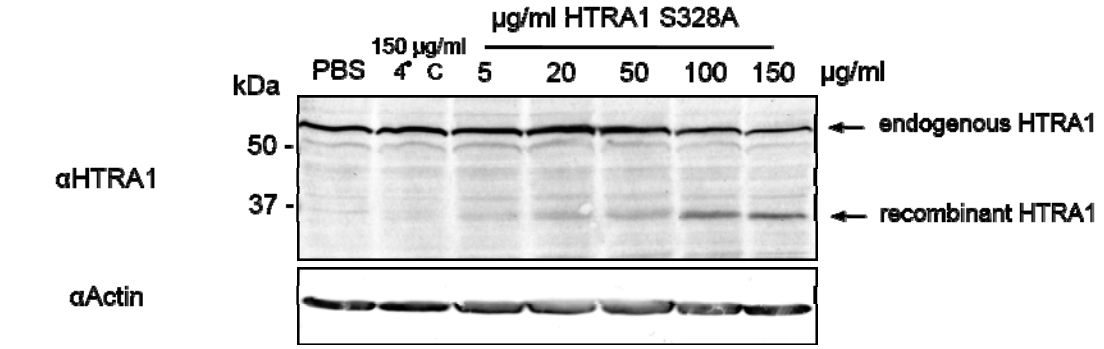

b

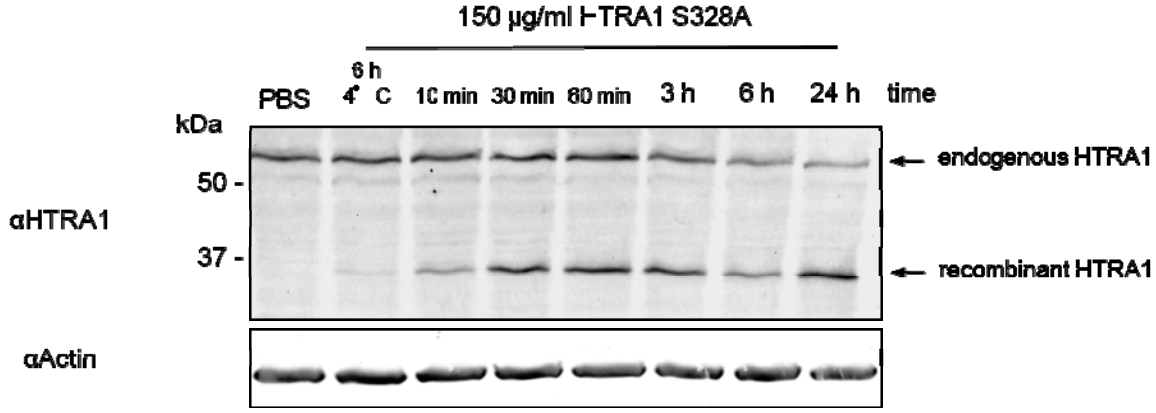

Figure 40 - Internalization of Recombinant HTRA1 S328A by HEK-293T Cells

HEK-293T cells were treated with **a** varying amounts of recombinant HTRA1 S328A for 6 h or **b** with 150 µg/ml HTRA1 S328A for different periods of time, followed by trypsinization, lysis and immunoblotting using a rabbit polyclonal antibody against the PDZ domain of HTRA1, or Actin as a loading control.

After 6 h of incubation, an additional band was detected by immunoblotting against HTRA1, with an apparent MW of ca. 36 kDa which corresponds to the recombinant human HTRA1 S328A construct which was used to treat the cells (Figure 40 a). This band was faintly visible at an HTRA1 concentration of 5 µg/ml, its intensity increased at 20 and 50 µg/ml and reached its maximum at a concentration of 100 µg/ml. These results indicate a concentration dependent uptake of HTRA1 into HEK-293T cells. Furthermore, the lack of intracellular recombinant HTRA1 after the incubation of the cells at 4 °C suggests that HTRA1 is internalized by an active transport mechanism rather than by a passive diffusion based mechanism, as reported e.g. for cell penetrating peptide associated processes. When the

uptake of HTRA1 was monitored over time, the HTRA1 band appeared within 10 min and reached its maximum intensity after 30 min, indicating that the internalization was complete within this time frame (Figure 40 b). The internalized HTRA1 was stable for 24 h, or there was an equilibrium of internalization and intracellular degradation of HTRA1 leading to constant levels of HTRA1 during this period of time.

3.5.3. Immunofluorescence Analysis of Internalized HTRA1 S328A

Confocal fluorescence microscopy was employed for the detection of internalized HTRA1 in order to determine its subcellular localization and the distribution of HTRA1 internalization within a population of treated cells. To identify the portion of recombinant HTRA1 and to distinguish it from the endogenous protein, HTRA1 S328A was labeled with the amine reactive fluorescent dye Alexa Fluor 568 carboxylic acid, succinimidyl ester (AF568). HEK-293T cells were incubated with culture medium containing 50 µg/ml labeled HTRA1 S328A or PBS for 20 h prior to fixation and immunostaining as indicated.

a

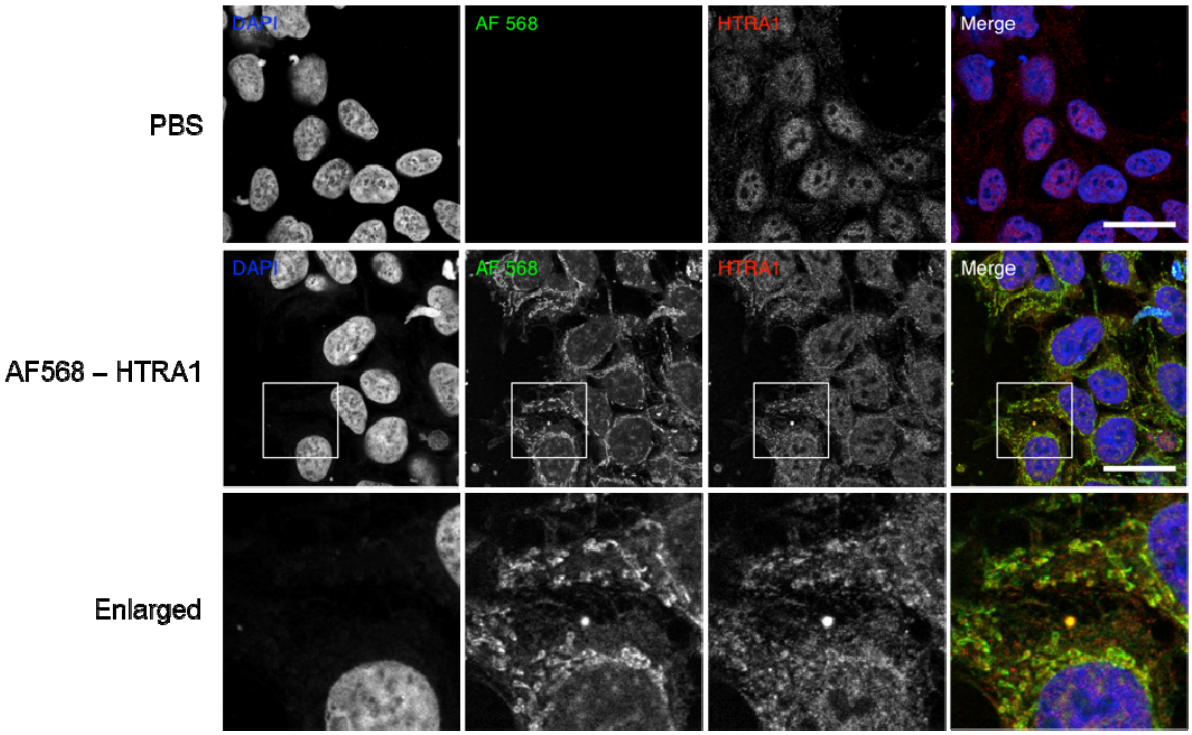

b

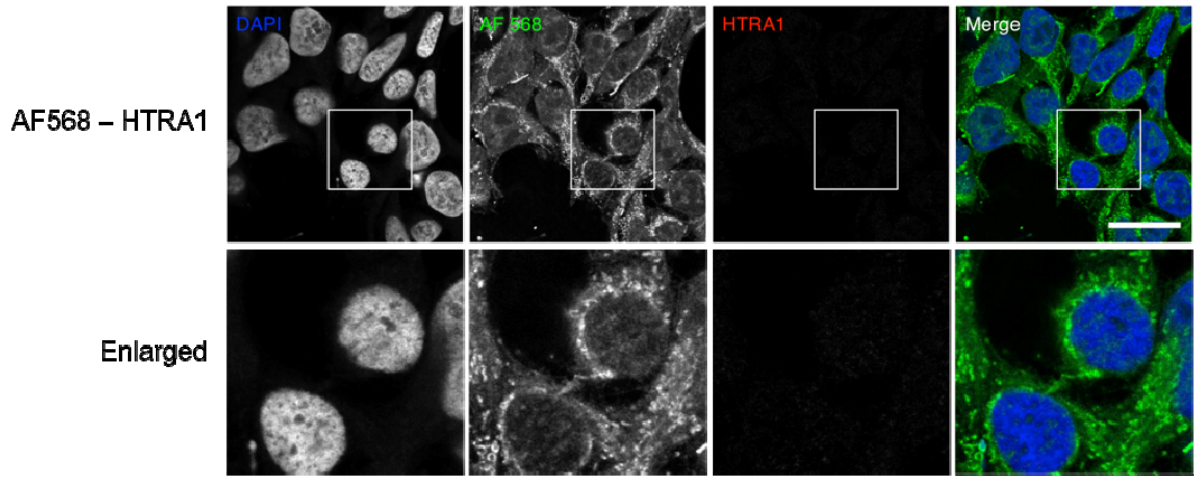

Figure 41 - Subcellular Localization of Internalized Labeled HTRA1 S328A

After incubation with 50 µg/ml recombinant HTRA1 S328A labeled with the fluorescent dye Alexa Fluor 568 (AF568) or PBS at 37 °C for 20 h, the HEK-293T cells were fixed with MeOH and stained with DAPI and **a,** a rabbit polyclonal antibody against the PDZ domain of HTRA1 or **b,** without the primary antibody as control. Scale bar = 25 µm

While in PBS treated HEK-293T cells, there was no signal in the channel specific for the AF568, all of the cells treated with AF568-labeled HTRA1 S328A showed a clear intracellular staining with AF568, indicative of internalized HTRA1 (Figure 41). In addition to some structures of vesicular appearance, fluorescence was also detected in a more diffuse localization within the cytoplasm. Importantly, the AF568 fluorescence almost completely overlapped with the staining using an HTRA1 specific antibody and fluorescently labeled secondary antibodies. This confirmed that the AF568 dye was still linked to the labeled protein and that the recombinant, labeled HTRA1 had not been degraded, which could give rise to a misleading AF568 signal not representing HTRA1. The HTRA1 antibody also stained proteins which were not labeled with AF568, consistent with an endogenous pool of HTRA1, which was also detectable by immunoblotting (Figure 41). To rule out that the staining of labeled HTRA1 with the HTRA1 antibody was due to unspecific binding of the secondary antibody, a control labeling was performed without the primary antibody and using the secondary antibody only (Figure 41 b).

3.5.4. Colocalization of Recombinant HTRA1 and its Substrate Tau

Assuming that recombinant HTRA1 is internalized by HEK-293T cells into the cytoplasm and stays functionally intact, its subcellular localization should coincide with the distribution of its substrates. Tau has been shown to be a substrate of HTRA1 in the cellular context previously (Dissertation A. Tennstädt). Therefore HEK-293T cells transiently overexpressing HA-tagged P301L Tau were treated with labeled recombinant HTRA1 and subsequently fixed and stained with an anti-HA antibody and fluorescently labeled secondary antibodies.

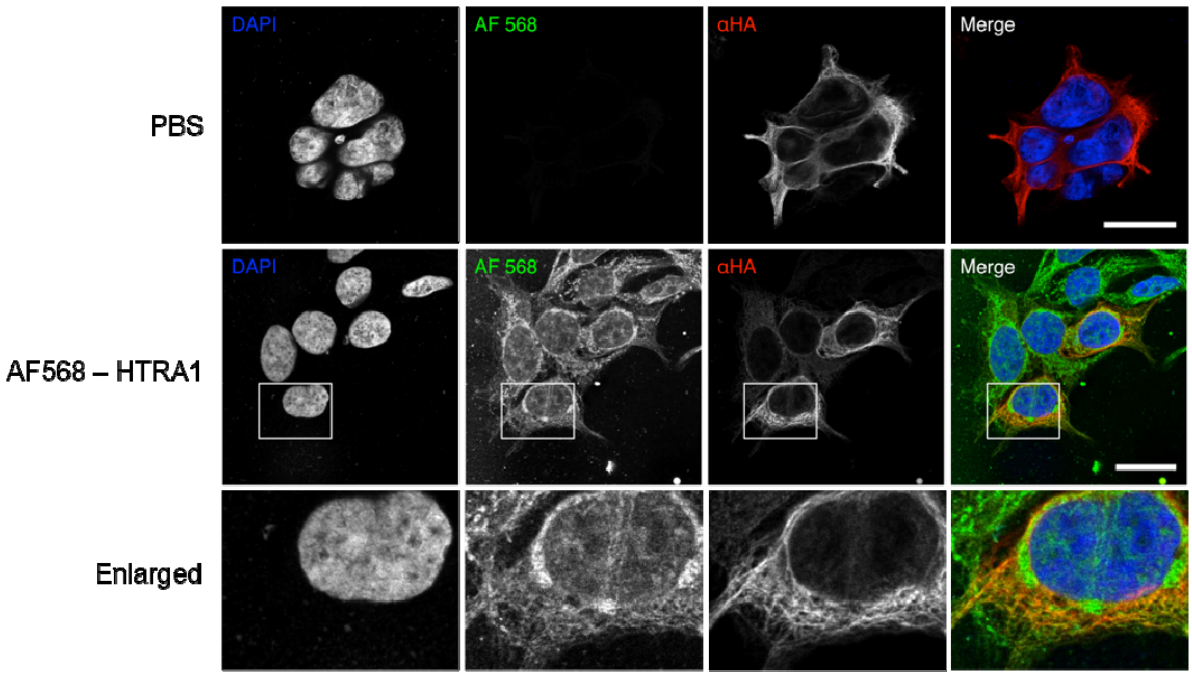

Figure 42 - Colocalization of Internalized HTRA1 with Cytoplasmic Tau

HEK-293T cells transiently overexpressing HA tagged 4R P301L Tau were treated with 50 µg/ml recombinant, AF568 labeled HTRA1 S328A for 20 h, followed by fixation and DAPI stain as well as immunostaining against the HA-tag of overexpressed Tau. Scale bar = 10 µm.

As described above (3.5.1), the HA-antibody marked structures resembling the microtubule network in Tau overexpressing cells. In these cells there was a distinct overlap between the HA staining and the AF568 signal representing the internalized, labeled HTRA1 S328A (Figure 42). This suggests that upon internalization, HTRA1 was still intact after 24 h of incubation and was at least partially localized in the cytoplasm where it was able to interact with its natural substrate Tau.

3.5.5. Localization of Internalized HTRA1 to Cytoplasmic Tau Aggregates

The colocalization of HTRA1 with intracellular Tau aggregates would be a prerequisite for the protease acting on Tau fibrils in the cellular context. To test whether this is the case, the seeding of intracellular Tau aggregation was performed as described above (3.5.1), followed by the treatment with recombinant, labeled HTRA1 S328A. After an incubation time with HTRA1 for 24 h, the cells were fixed and stained with ThS for immunofluorescence analysis. As a control, HEK-293T cells were treated with the isolated AF568 fluorescent dye to rule out a possible internalization of the free dye into HEK-293T cells which would result in a false positive signal in the immunofluorescence analysis.

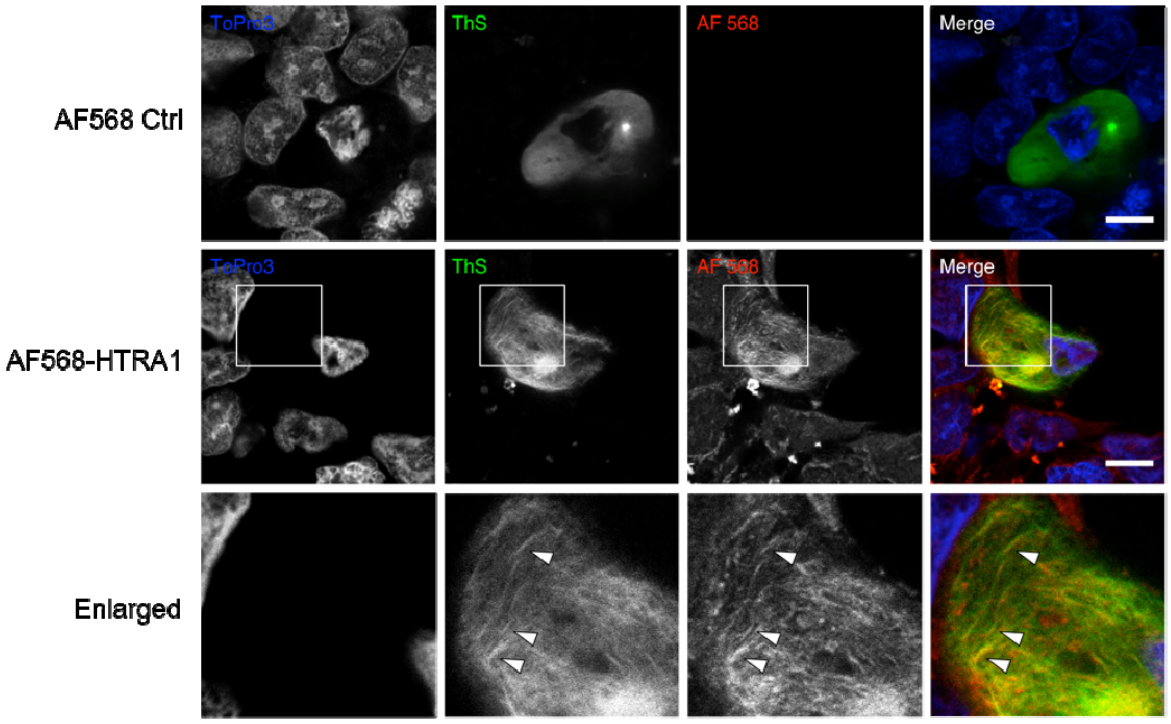

Figure 43 - Localization of Internalized HTRA1 in the Cellular Model of Cytoplasmic Tau Aggregation

The aggregation of cytoplasmic P301L Tau was induced in HEK-293T cells by transfection of MTBD Tau seeds as described above. The seeded cells were treated with 50 µg/ml recombinant, AF568-labeled HTRA1 S328A or the isolated AF568 dye as a control (red channel) for 20 h, followed by MeOH fixation and immunostaining. Amyloid aggregates were stained with ThS (green), the nucleus was stained with To-Pro3 (blue). The arrowheads mark exemplary regions of colocalization between amyloid structures and internalized, labeled HTRA1. Scale bar = 10 µm.

While there was no detectable fluorescence signal in control cells treated with the isolated AF568 fluorescent dye only, AF568-labeled HTRA1 was found to distinctly localize to ThS

positive structures (Figure 43). The overlap of the two channels showing the distribution of cytoplasmic aggregates and internalized recombinant HTRA1 did not overlap completely, which indicates that, in addition to binding intracellular amyloid aggregates, HTRA1 engaged further localizations within the cell. However, as indicated by the arrowheads in Figure 43, regions of prominent ThS staining were also found to be positive for labeled HTRA1, which clearly argues for a physical interaction between HTRA1 and Tau aggregates in the cellular context.

3.5.6. Effect of Internalized wt HTRA1 on the Abundance of Intracellular Tau Aggregates

The colocalization of recombinant, internalized HTRA1 with intracellular Tau aggregates enabled us to experimentally test the effects of increasing intracellular levels of HTRA1 on the total aggregate burden. A good measure of the extent of Tau aggregation is the amount of Tau protein found to be resistant to detergent treatment of cell lysates. The procedure of Sarkosyl extraction was performed earlier (3.5.1) and was applied here to assess the functional impact of HTRA1 internalization on the fibril load of HEK-293T cells. Cells were transfected with P301L Tau plasmids and MTBD Tau seeds as described above (3.5.1), followed by a 20 h incubation period with 150 µg/ml recombinant, proteolytically active HTRA1 or PBS as a control. Subsequently, the cells were trypsinized and lysed, followed by Sarkosyl treatment and ultracentrifugation to isolate the detergent insoluble portion of intracellular Tau.

a

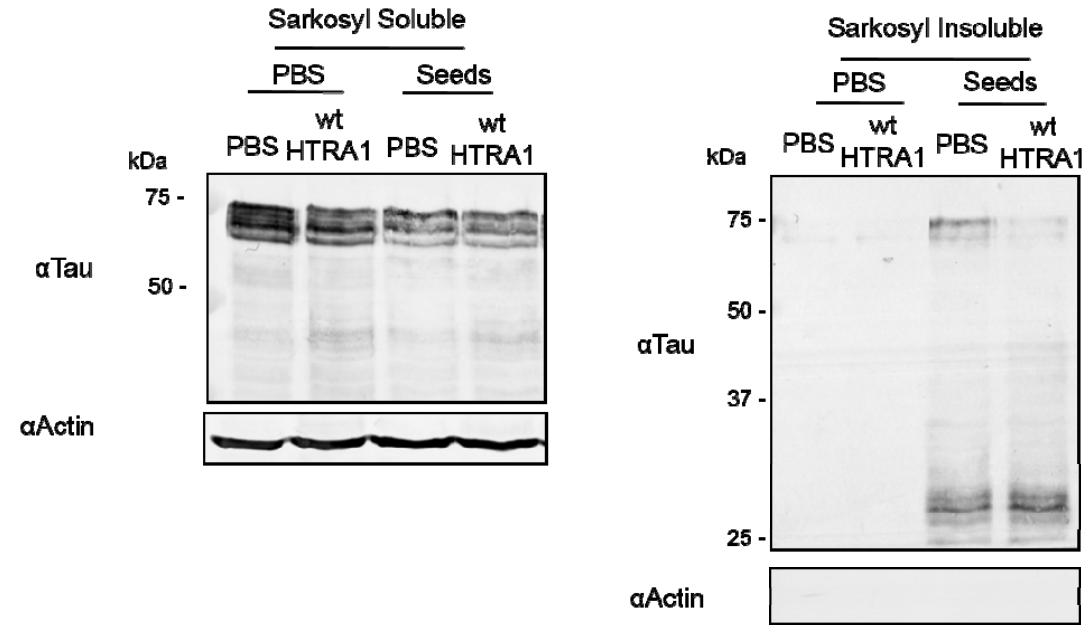

b

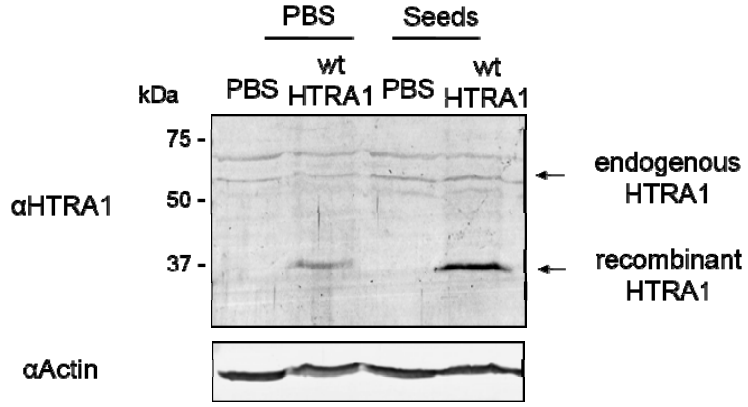

Figure 44 - Sarkosyl Extraction from Cells after Internalization of Recombinant wt HTRA1

Cells containing aggregated cytoplasmic Tau were trypsinized, lysed followed by Sarkosyl extraction to assess the amounts of soluble (**a**, left panel) versus aggregated (**a**, right panel) Tau. **a**, Representative anti-Tau immunoblots of lysates from cells treated with PBS or transfected with MTBD Tau aggregate seeds, which were subsequently treated with 150 µg/ml recombinant wt HTRA1 or PBS for 20 h. **b**, Sarkosyl soluble fractions were immunoblotted against HTRA1 to show internalization of recombinant HTRA1. Actin levels served as loading controls.

Internalized, recombinant wt HTRA1 strongly reduced the total Tau aggregate burden in cultured cells. As indicated by the amounts of insoluble Tau comparing HTRA1 treated and PBS treated cells after seeding, there was a considerable reduction of insoluble Tau in the

presence of internalized wt HTRA1 (Figure 44 a). The increased levels of HTRA1 in the respective samples is illustrated by Figure 44 b, which suggested that the amount of internalized HTRA1 exceeded the concentration of endogenous HTRA1. The Sarkosyl soluble portion of Tau was slightly reduced after seeding, which might reflect the sequestration of soluble Tau into aggregates or increased proteolysis of Tau upon aggregate seeding. In the PBS treated samples, there was a reduced amount of soluble Tau (Figure 44 a, left part of the left panel), which suggests that wt HTRA1 might also degrade soluble Tau in the absence of Tau aggregation. Taken together, increased concentrations of HTRA1 seemed to reduce the aggregate burden in this cell culture model of intracellular Tau aggregation.

3.5.7. Effect of Internalized HTRA1 S328A on the Abundance of Intracellular Tau Aggregates

It has been shown earlier that HTRA1 has disaggregase activity which supports the proteolysis of amyloid Tau aggregates *in vitro*. Based on these findings, it was reasoned that this activity might also lead to a reduction of aggregate burden in the cellular model of Tau aggregation when the proteolytically inactive mutant HTRA1 S328A is added to cells to be internalized. If this was the case, treatment of cells containing seeded Tau aggregates with HTRA1 S328A would lead to a reduction in the amount of Sarkosyl insoluble Tau. To test this experimentally, the aggregate seeding and treatment of HEK-293T cells was performed as before (3.5.6) except that instead of wt HTRA1, recombinant HTRA1 S328A was used.

a

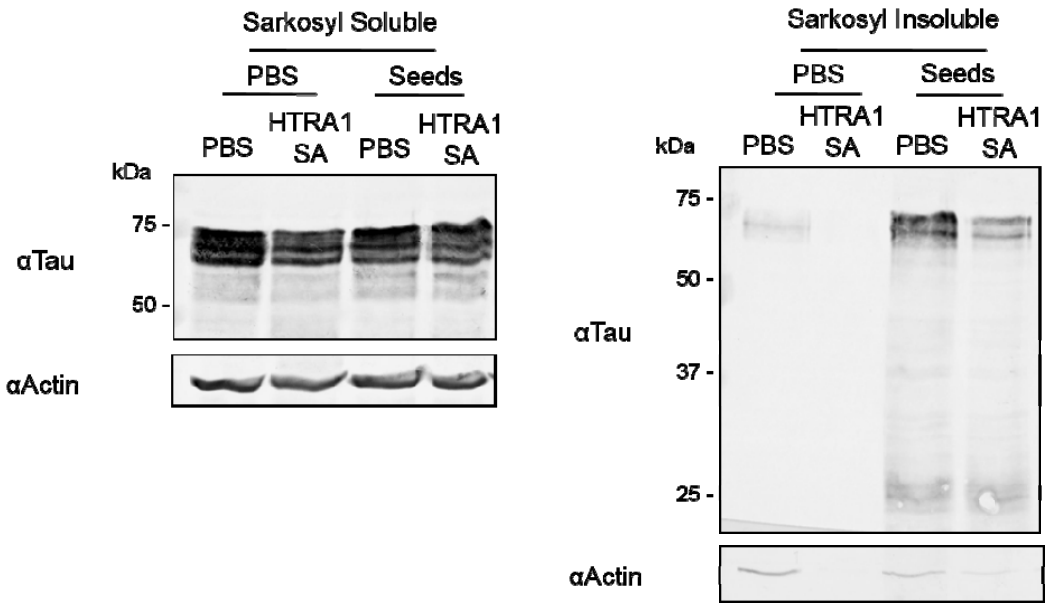

b

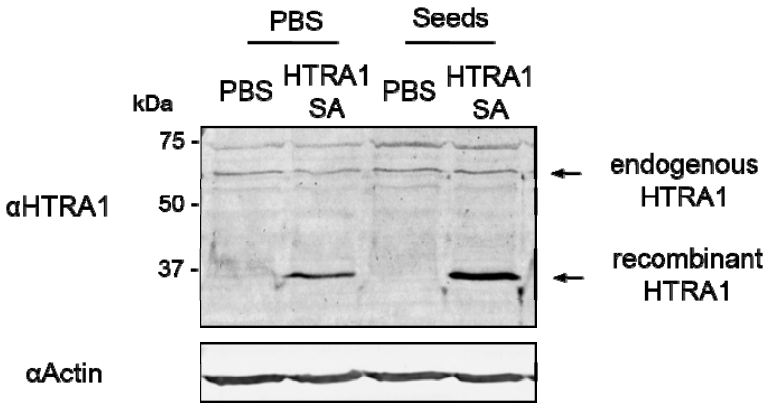

Figure 45 - Sarkosyl Extraction from Cells after Internalization of Recombinant HTRA1 S328A

Cells containing aggregated cytoplasmic Tau were trypsinized, lysed followed by Sarkosyl extraction to assess the amounts of soluble (**a**, left panel) versus aggregated (**a**, right panel) Tau. **a**, Representative anti-Tau immunoblots of lysates from cells treated with PBS or transfected with Tau MTBD aggregate seeds, which were subsequently treated with 150 µg/ml recombinant HTRA1 S328A or PBS for 20 h. **b**, Sarkosyl soluble fractions were immunoblotted with anti-HTRA1 antibodies to show the internalization of recombinant HTRA1. Actin levels served as loading controls.

Whereas the levels of Sarkosyl soluble Tau remained constant (Figure 45 a, left panel, less aggregated Tau was found in the HEK-293T cells after internalization of recombinant HTRA1

S328A (Figure 45 a, right panel). This indicated that, even in the absence of its proteolytic activity, HTRA1 can lead to a decrease of the total Tau aggregate load in cells. These data suggest the presence of disaggregase activity of HTRA1 in cells.

4. Discussion

Members of the HtrA family of serine proteases perform protein quality control functions in bacteria and plants. The roles of their human homolog HTRA1 seems to be more diverse, including functions in cell growth and proliferation. At the same time, HTRA1 has been implicated in AD based on its negative correlation with hallmark lesions and its ability to proteolyze Tau *in vitro* and in cultured cells (dissertation A. Tennstädt). These findings support a protein quality control function of HTRA1 and prompted the question of how these tasks might be accomplished mechanistically. The experimental work presented herein revealed that HTRA1 is not only capable of proteolyzing amyloid aggregates composed of Tau, but employs a heretofore unrecognized, ATP-independent mechanism of disaggregation *in vitro* and in cultured cells. This disaggregase activity facilitates the proteolysis of aggregates by dissolving the tightly packed core of fibrillar Tau assemblies and thereby renders inaccessible regions of the aggregate susceptible to the proteolytic attack by the active site.

4.1. HTRA1 can Proteolyze Tau Aggregates

Previous work showed that Tau is a substrate of HTRA1 *in vitro* as well as in cells. The analysis of cleaved peptide bonds after proteolysis of recombinant protein showed that hydrolysis occurred along the whole primary sequence of Tau, including those regions which confer the self-association into fibrillar aggregates (dissertation A. Tennstädt). To further characterize the proteolytic activity of HTRA1, the degradation of Tau aggregates by HTRA1 was therefore investigated. Initial proteolysis experiments were performed using the shortest isoform of Tau, 3R wt Tau, which was purified by ammonium sulfate precipitation and gave rise to an insoluble and soluble fraction. Biochemical characterization of the two fractions by Thioflavin fluorescence, atomic force microscopy (AFM) and dynamic light scattering (DLS) showed that the insoluble preparation yielded from ultracentrifugation of the purified protein was enriched in large, unstructured aggregates as compared to the soluble fraction (3.2.2). Both soluble and insoluble Tau acquired this way showed strong Thioflavin fluorescence, indicative of β-sheet rich structures such as amyloid aggregates being present in both fractions. *In vitro* proteolysis of these different Tau preparations showed that HTRA1 was able to proteolyze Tau aggregates, but this activity was not restricted to the aggregated state of the protein. Both the soluble and insoluble Tau were readily digested by HTRA1, with

soluble Tau being degraded more efficiently which was probably due to its pronounced flexibility and better availability to the active site of HTRA1 (3.2.3).

Fatty acids such as arachidonic acid (ArA) were reported to promote the formation of amyloid aggregates from recombinant Tau protein *in vitro* (Kuret et al., 2005b). The incubation of soluble 3R wt Tau with ArA led to the *de novo* formation of tightly packed aggregates including heat- and SDS resistant oligomers which were not resolved by SDS PAGE. Although this aggregation strategy did not give rise to classical amyloid aggregates, and no significant further increase in the ThT fluorescence was detected, the formation of SDS resistant oligomers indicated that there was a substantial effect of ArA on the aggregation state of Tau. As a consequence of incubation with ArA, there was an increase in the stability of aggregates marked by the changed migration on SDS gels (3.2.5). HTRA1 efficiently degraded these types of aggregates *in vitro*, which illustrated the ability of HTRA1 to proteolyze even tightly packed aggregates representing particularly dense and inaccessible substrates. However, the majority of tauopathies is characterized by the deposition of paired helical or rod-like Tau fibrils which share the characteristic features of amyloids.

In order to produce aggregates *in vitro* which resemble those forming the deposits found in AD and other tauopathies, the modification of the purification strategy of Tau proved useful. Based on the boiling method to remove the majority of bacterial proteins in the crude extracts, recombinant Tau was further purified by means of chromatographic methods instead of the AS precipitation steps as done before. By using HAP chromatography and SEC, it was possible to isolate soluble Tau protein which did not show significant ThT fluorescence. In contrast to the 3R wt Tau protein purified by boiling followed by AS precipitation, Tau purified by this procedure readily and reproducibly assembled into fibril shaped aggregates the dimensions of which fit those reported for PHFs before (3.3.2). This effect of the modified purification strategy might have several reasons. Tau fragments or other proteins or biomolecules might have impaired the heparin induced aggregation before, e.g. by interaction with the protein and therefore locking it in a conformation which would not allow the formation of fibrils. As an intrinsically disordered protein, Tau can adopt numerous conformations and undergo conformational changes upon interaction with possible ligands. It is a well-known phenomenon that unstructured proteins or unstructured regions of proteins adopt a defined structure upon binding to other proteins specifically (Dunker et al., 2008). The complexity of Tau conformations in solution is vast and has hampered investigations on e.g. the mechanism of induced aggregation in the presence of polyanions (Jeganathan et al., 2008). The same holds true for Tau oligomers and even different types of aggregates which

may represent a collection of various conformational states (Furukawa et al., 2011). These observations underline the importance of elaborating a purification strategy yielding preparations which are devoid of inhibiting substances or fragments and instead contain such conformations that are conformationally flexible enough to adopt the cross-β structure found in Tau fibrils. To allow or reestablish conformational flexibility might be the basis of the advantage of a heat denaturation step before addition of heparin (2.3.13). The ThT fluorescence which was detectable in both the soluble and insoluble fractions of 3R wt Tau after AS precipitation possibly represents cross β-sheet structures which just do not give rise to a fibrillar morphology, but are sequestered as part of an amorphous aggregate. The fluorescence could also arise from the interaction of the isolated Tau protein with contaminant proteins or other biomolecules, which might have been co-purified along with Tau. For example, polyanionic factors such as RNA or DNA could have induced the formation of β-sheet rich structures still present after boiling and AS precipitation, but removable from the preparation by HAP chromatography and SEC as was performed later.

The availability of Tau fibrils made possible studying the proteolytic activity of HTRA1 towards these fibrils and assaying their amyloid features such as their morphology and insolubility. Proteolysis of fibrillar Tau aggregates by HTRA1 was successful, albeit less efficient and at a lower substrate:protease ratio than used for the degradation of soluble protein (3.3.3). This probably reflects the tight interactions giving rise to amyloid fibrils (Eisenberg and Jucker, 2012) which hinder the access to the active site and could therefore necessitate additional mechanisms destabilizing the fibril spine. So far, no relevant proteases have been described to be able to proteolyze amyloid fibrils *in vivo* or under conditions comparable to the physiological situation. The ability of HTRA1 to hydrolyze such highly ordered and stable aggregates underlines its potential importance in the clearance of aggregates and under pathological conditions characterized by the deposition of amyloid Tau aggregates. It should be pointed out that in this, as well as in previous work (dissertation A. Tennstädt), HTRA1 was also shown to proteolyze soluble Tau and is therefore not restricted to the aggregated, pathogenic forms. This means that on one hand, HTRA1 may help maintaining steady-state levels of the Tau protein or reduce the cellular pool of free, soluble Tau, which would otherwise run the risk of aggregating, as has been suggested for the proteaseome (David et al., 2002; Petrucelli et al., 2004) or, under some conditions, Calpain (Delobel et al., 2005). On the other hand, the data collected so far does not imply that proteolysis of Tau aggregates by HTRA1 is limited to stress conditions or the accumulation of

misfolded Tau protein. Both scenarios are possible and both require the faithful regulation of the activity of HTRA1 on the levels of enzymatic activation or subcellular localization.

4.2. Proteolysis of Tau Aggregates by other Proteases

The turnover, i.e. the interplay of synthesis and degradation rates of Tau serves to maintain physiological protein levels and ensure the correct localization and folding state of Tau. Still, little is known about the proteolytic processes targeting Tau under physiological or pathological conditions. The latter would have to include mechanisms of sensing aberrant PTMs, localization or misfolding of Tau to trigger the clearance of otherwise harmful protein. Cellular studies have suggested that the ubiquitin proteasome system might mediate the turnover of Tau, and the pathological Tau in AD PHFs being ubiquitinated might indicate that the aggregation results from failed degradation by the proteasome (Iqbal and Grundkeiqbal, 1991). On the other hand, this observation could reflect attempts of removing misfolded or already aggregated Tau from the cell by targeting to the proteasome, meaning that proteasomal degradation of Tau could be a folding stress induced process which might, for example, be conferred by CHIP mediated ubiquitination of Tau (Petrucelli et al., 2004). In AD, research on the proteolysis has focused on the truncation of Tau, because partial hydrolysis has been implicated in the generation of toxic Tau fragments in the disease process (De Strooper, 2010). One of the mechanisms of toxicity might be the increased tendency of truncated Tau to aggregate. When Tau is processed N- and C-terminally, it was shown to aggregate more readily (Wang et al., 2007), which was proposed to be due to inhibitory conformations by the parts of the protein which lie outside of the MTBD (Jeganathan et al., 2008). Accordingly, work on the proteases Caspase-3 and Calpain, which have been tested in this work, has been limited to their potential role in the generation of fragments of Tau which promote the neurodegenerative processes in AD. Strikingly little work has been dedicated so far to the proteolytic clearance of Tau aggregates, reflecting that so far no physiologically relevant degradation of Tau aggregates by proteases has been observed. Caspase-3 mediated truncation was suggested to take place early in the pathogenesis of AD, preceding tangle formation and therefore potentially favoring the occurrence of tangles (de Calignon et al., 2010; Rissman et al., 2004). In accordance with the limited proteolysis by Caspase 3, only limited fragmentation of Tau aggregates was observed here (3.2.3), and no significant degradation of aggregates. Calpain was implicated in AD in providing a possible mechanistic link between Aβ and Tau because it was argued

that Aβ mediated activation of Calpain leads to the generation of a toxic 17 kDa fragment of Tau (Park and Ferreira, 2005). However, other studies have doubted the both the toxic effects of Calpain mediated Tau hydrolysis and its dependence on Aβ (Garg et al., 2011). In light of the Ca^{2+} dependence of Calpain and disturbed local Ca^{2+} homeostasis in neurons, Calpain activity was also proposed to generally contribute to neuronal death and drive the disease process in AD (Higuchi et al., 2012). Taken together, the significance of these findings and the contribution of Caspase to neurodegeneration remain unresolved questions (Wray and Noble, 2009). It was shown here that Calpain efficiently degraded soluble, as well as aggregated Tau and even fibrillar Tau *in vitro* (3.2.3). This challenges the widely accepted notion that aggregates are protease resistant. At the same time, it still has to be determined under which conditions Calpain might cleave aggregates, whether fibrils are completely removed or only partially degraded and what the mechanism of fibril cleavage might be. *In vivo*, this can only be relevant if Calpain is recruited to aggregates and the local concentration of Ca^{2+} is sufficient to allow proteolytic activity of Calpain. Given the importance of Ca^{2+} for neuronal function, these aspects are crucial when considering a possible relevance of these findings.

4.3. Disaggregation

HTRA1 was shown to degrade Tau aggregates *in vitro*, which closely resembled the pathologically relevant fibrils found in Tauopathies, as measured by their morphology, detergent resistance and characteristic binding of the amyloid specific dye Thioflavin T (3.3.3). These types of aggregates are generally believed to be protease resistant in cells, a feature which probably contributes to their irreversible accumulation in the course of diseases. As illustrated by the impaired proteolysis of aggregated vs. soluble Tau, this in part holds true for HTRA1, showing that the flexibility of the soluble protein supports their engagement and concomitant hydrolysis by the active site, whereas the sequestration of the substrate in the aggregate structure inhibits this process. However, it is still possible for HTRA1 to degrade amyloid aggregates composed of Tau (3.3.3). Chaperone activities have been described for other HtrA members and implicated in their functions as protein quality control factors. For example, the chaperone function of DegP was shown to be temperature dependent (Spiess et al., 1999) and important for the synthesis and correct folding of outer membrane proteins of *E. coli* (Krojer et al., 2008). The plant HtrA DEG1 is important for the correct assembly of a light harvesting complex in *A. thaliana* by assisting in the incorporation of subunits into the

complex (Sun et al., 2010). Supported by these known activities of other HtrAs, it was reasoned that HTRA1 might employ a protein remodeling activity, which would help proteolyzing even tightly packed, insoluble assemblies such as Tau amyloids. Such restructuring would imply that the integrity and amyloid properties of Tau aggregates are changed in order to make the protein accessible for proteolysis.

As a simple way of detecting such an activity, the insolubility of Tau fibrils after incubation with proteolytically inactive HTRA1 was chosen here. The HTRA1 S328A mutant used for these experiments has its active site Ser changed to an Ala and is therefore incapable of proteolysis. Ultracentrifugation after o/n incubation of Tau fibrils with HTRA1 S328A revealed that Tau was completely solubilized by HTRA1, while it remained largely insoluble in the respective buffer or in the presence of a control protein (3.4.1). This led to the assumption that HTRA1 can loosen the aggregate structure in a way that leads to increased solubility. Disaggregation was expected to change fibril morphology or dissolve the fibrillar structure which should be therefore measureable by AFM. When imaging fibril preparations after o/n disaggregation by HTRA1, a marked decrease in the abundance of fibrils was detectable, indicative of less fibrillar structures being in solution (3.4.3). This was not the case after incubation with the isolated PDZ domain of HTRA1, which showed that HTRA1 was able to release the Tau protein from the stable fibrillar structures and helps to explain and complement the findings after ultracentrifugation of Tau fibrils after incubation with HTRA1.

Functionally, the disaggregase activity should be instrumental in the proteolysis of fibrils by supplying the active site with hydrolyzable stretches of polypeptide chains which would be inaccessible when engaged in the core of aggregates. Thus, it was reasoned that disaggregation would enhance subsequent proteolysis by wt HTRA1. As an approach to test this assumption, the successive treatment with HTRA1 S328A and proteolysis by wt HTRA1 was chosen (3.4.4). Fibrillar Tau was much more efficiently degraded by HTRA1 after a period of disaggregation by HTRA1 S328A. Importantly, the increased degradation by HTRA1 was not observed when instead of HTRA1 S328A, MDH was used, showing that high protein concentrations did not unspecifically affect the fibril structure in a way favoring the proteolytic degradation by HTRA1. A possible explanation of these findings is that an excess of HTRA1 S328A might generally increase Tau proteolysis, for example by activating wt HTRA1. However, the incubation of soluble Tau with HTRA1 S328A did not positively affect its proteolysis, it instead slowed down proteolysis, which served to show that the preincubation effect is restricted to Tau aggregates. In accordance with that, using a synthetic peptide substrate to determine the specific activity of HTRA1, no activating effect of an excess of

HTRA1 S328A was detectable (3.4.8). These findings substantiated the assumption that HTRA1 disaggregase activity can functionally support proteolytic degradation of fibrillar Tau. Using a 10 fold higher concentration of wt HTRA1, corresponding to the concentration of HTRA1 S328A in preincubation experiments, led to an observation with potentially interesting implications. Strongly increasing the amounts of active protease only led to enhanced proteolysis of fibrillar, but not soluble Tau (3.4.4). Possibly, the concentration of wt HTRA1, i.e. the number of available active sites was not the rate-limiting factor of the proteolysis of soluble Tau. Instead, it is more likely that the process of binding to the active site and hydrolysis itself were rate limiting and, consequently, the addition of more active protein would not affect the efficiency of degradation but rather leave active sites unoccupied. In contrast, when the concentration of wt HTRA1 was increased 10-fold in the presence of Tau fibrils, their proteolysis was enhanced and even more efficient than the degradation of soluble Tau. This might have several implications. First, adding more active sites means that fibrils are more easily degraded by HTRA1. But the mere presence of more active sites would not necessarily lead to more efficient degradation, as can be seen from the proteolysis of soluble Tau under the same conditions. When high HTRA1 concentrations were applied, the proteolysis of aggregates was even favored over the proteolysis of soluble protein, which is the opposite of what was found at low concentrations, where fibrils were degraded much more slowly. Hence, high HTRA1 concentrations represent conditions under which Tau fibrils are preferably degraded by HTRA1. This means that a simple model where Tau monomers are released from aggregates and subsequently proteolyzed cannot explain this finding. The necessity of disaggregation before proteolysis would rather slow down the proteolytic process. Instead, the presence of fibrils enables HTRA1 to more efficiently degrade Tau, given that there is enough HTRA1 in solution. Several mechanisms might explain this. First, Tau could still be in a conformation which is more readily proteolyzed by HTRA1 and would therefore be cleaved much more efficiently after the fibrils being disassembled. Second, the fibrillar structure or the solution of fibrils could trigger the conversion of HTRA1 into an activated state and by these means enhance proteolysis. But as this alone would not account for the need to have high enough concentrations of HTRA1 available, it is conceivable that, third, HTRA1 converts into higher order oligomers for disaggregation and proteolysis. In support of this hypothesis, the relevant active unit of HTRA1 would be smaller for soluble than for fibrillar Tau, because increasing the concentration of HTRA1 means adding more active units in the case of Tau aggregates, while with soluble Tau as a substrate the solution is already saturated with HTRA1 units. It is tempting to speculate that this was due to the

units being larger, i.e. composed of more HTRA1 building blocks and thus representing higher oligomers which arise in the course of disaggregation.

The proteolysis of fibrils followed by SDS-PAGE might be misleading because the activity is assessed by the presence and intensity of silver stained proteins bands corresponding to full-length monomeric Tau. This could mask a limited proteolysis of fibrils leaving the tightly packed fibril core intact. Therefore, to further assess the effect of disaggregation of the proteolysis of fibrils, the respective preincubation experiments were repeated and followed by AFM analysis to determine fibril abundance after proteolysis. These experiments confirmed what was detected by SDS PAGE. Proteolysis of fibrils led to a decrease in the amounts of fibrils in solution, which was strongly enhanced after incubation with inactive HTRA1, but not the PDZ domain of HTRA1 (3.4.5). Consequently, the proteolysis of fibrils was not limited to the “fuzzy” coat, but led to the complete degradation of fibrillar structures. Even without a previous disaggregation step, wt HTRA1 was able to eliminate fibrillar structures. The differences between SDS-PAGE results showing poor proteolysis by wt HTRA1 only and the AFM results indicating a ca. 50% decrease in total fibril abundance, could be explained by wt HTRA1 disaggregating Tau fibrils without necessarily degrading them, or by the fact that for the AFM experiments, no ultracentrifugation step was performed in order to leave the fibrillar structures intact as far as possible. As a consequence, the solution might still contain oligomers, heparin or activating Tau conformations that might increase proteolysis by HTRA1 in the AFM experiments but not in the experiments followed by SDS-PAGE.

The data discussed so far are evidence for a disaggregase activity which allows HTRA1 to proteolyze tightly packed aggregates, supposedly by facilitating access to stretches of Tau buried in the fibril core. A direct way of testing this is to identify the sites of proteolytic cleavage within the Tau protein after distinct time spans of proteolysis. Peptidic cleavage products were therefore isolated and analyzed by mass spectrometry to assess differences in the cleavage patterns comparing disaggregated samples to those without preincubation with HTRA1 S328A (3.4.6). After 3 h of proteolysis, wt HTRA1 alone only gave rise to a few proteolytic products which all could be mapped to the C-terminal and N-terminal regions of Tau, thus leaving the MTBD of Tau comprising the fibril core intact. In contrast, incubation with HTRA1 S328A for 2 h before adding the active protease led to a strong increase in the total amount of detected peptides and, notably, to the emergence of peptides reflecting cleavage in the fibril core (3.4.6). The C- or N-termini of ca. 40% of all detected peptides were mapped to the MTBD and, consequently, to the tightly packed fibril core. In other words, after disaggregation HTRA1 was able to cleave parts of the Tau protein which were

inaccessible to the wt protease without previous disaggregation. This showed that disaggregation led to a loosening of the aggregate structure and enhanced proteolysis by making available otherwise inaccessible parts of the substrate. In principle, the increased cleavage in the MTBD after disaggregation could simply reflect higher activity of HTRA1 towards fibrils in the presence of high concentrations of HTRA1 S328A and because of that the cleavage of low preference sites. However, proteolytic activity of wt HTRA1 is not increased in the presence of HTRA1 S328A as discussed above, and the sites in the MTBD represent 40% of all cleavage sites and thus not a minority and less preferred sites. Moreover, even after o/n incubation only two cleavage events could be mapped to the MTBD using wt HTRA1 alone, while the pattern of proteolysis after disaggregation changed only mildly, indicating that proteolyzing for a longer period of time did not allow the active protease to access the fibril core to a significant degree under these conditions. When soluble Tau was digested, the differences between preincubated samples and those containing only the active protease were less striking. All in all, the distribution of cleavage sites along the primary sequence of Tau was roughly comparable to the cleavage of fibrillar Tau after disaggregation, when comparing the 3 h time points. However, much more peptides were detected all in all even after 10 min with a preference for sites residing in the most C-terminal part of Tau. Most importantly, cleavage within the MTBD of Tau was observed when using wt HTRA1 only to an extent comparable to the samples after incubation with HTRA1 S328A. Since after 3 h in the presence of HTRA1 S328A, 40% of cleavage sites were found in the MTBD when digesting fibrils and only 27% when using soluble Tau as the substrate, it would be tempting to speculate that the MTBD region is a region which is proteolyzed by HTRA1 preferentially in fibrils, potentially due to its amyloid structure. However, based on the data presented here, this is hard to say because technically, the detection by mass spectrometry was designed to detect peptides in a qualitative rather than quantitative manner, and so it is not recommended to draw these conclusions from the available data yet.

Taken together, it was shown that HTRA1 has disaggregase activity, which is a feature which not only adds to the mechanistic repertoire of HtrAs, but also represents a novel, ATP independent activity of protein disaggregation and aggregate clearance. HTRA1 can disassemble Tau aggregates when proteolytic activity is abolished by mutating the active site and disaggregation was shown to specifically enhance the proteolytic degradation of fibrillar Tau. This enhancement was due to an increase in the accessibility of the tightly interacting core structure of the fibrils and therefore a loosening of the fibril core. Having established that HTRA1 is a disaggregase, a number of questions arise which are to be discussed in the

following. First, it is crucial to learn about the molecular basis, i.e. the mechanism of disaggregation and, secondly, to test the relevance in the cellular context of Tau aggregation.

4.3.1. Mechanism of Disaggregation

Some of the experiments discussed above, in which HTRA1 S328A was used as the disaggregase, can be helpful in explaining aspects of the disaggregation mechanism. Other questions, which concern the involvement of functional parts of HTRA1 in the disaggregation process, can be best addressed by experiments using mutations targeting the regions of the HTRA1 protein in question.

The parts of tau which make up the so-called “fuzzy coat” of the fibrils might in principle help to disaggregate Tau filaments by providing initial contact points for HTRA1. These regions were shown to inhibit the formation of filaments (von Bergen et al., 2000) and thus destabilize aggregates. Binding of HTRA1 could therefore increase this effect and by these means favor the disintegration of aggregates. HTRA1 was able to disaggregate fibrils composed of the MTBD of Tau alone (3.4.2), which indicates that interacting with the parts of Tau lying outside the fibril core is not a prerequisite for disaggregation. Although it might not be necessary, binding to more flexible parts of Tau might still be supportive because higher concentrations of HTRA1 were needed for disaggregating MTBD Tau aggregates. Furthermore, the analysis of cleavage sites within the Tau protein indicated that before proteolyzing the fibril core, HTRA1 cleaved Tau outside of the core region which became particularly apparent in the absence of HTRA1 S328A, i.e. without previous disaggregation (3.4.6). Therefore, it is likely that binding to the flexible, readily accessible part of the aggregates represents a first step in the course of disaggregation and proteolysis of Tau fibrils.

AFM in principle allows for the specific detection of aggregate morphologies and dimensions, which was made use of in previous studies (Wegmann et al., 2010). Here, the focus was on the abundance of fibrillar structures as a measure of disaggregation and proteolysis. Whereas the total amount of aggregates in the sample was assessed by means of the sum of fibril lengths per image, the relative distribution of lengths in the sample might offer clues to the mechanism of disaggregation. When Tau filaments were disaggregated by HTRA1 S328A (3.4.2), only mild changes in the distribution of fibrils were observed, and the overall distribution of lengths was comparable between the disaggregated and the control samples. This precludes a model in which disaggregation is based on a breakage of fibrils into smaller

pieces which are further broken or disaggregated upon interaction with HTRA1. It is also unlikely that HTRA1 prefers a subpopulation of fibrils as substrates for disaggregation with respect to their size, because all sizes seemed to similarly decrease in abundance. Furthermore, a shift of the overall distribution towards shorter fibril lengths was not observed, which suggests that a possible shortening of the fibrils occurred in all fibrils to a similar extent, with those filaments which fall below a certain length not being detected by AFM. Thus, based on the AFM data available so far, two mechanisms are likely. First, HTRA1 might disaggregate the filaments in a progressive manner from their ends. A similar mode of disaggregation has been suggested for the action of sHsp in disaggregating amyloid aggregates (Duennwald et al., 2012) and would be further supported by a study which suggested a dynamic behavior and even monomer exchange at the ends of amyloid fibrils (Carulla et al., 2005). Secondly, HTRA1 could also bind regularly along the filament and destabilize the Tau-Tau interactions within the aggregates until a threshold is reached, which then leads to a collapse of the fibril without intermediate products of disaggregation being detectable by AFM. Given the first possible explanation, it might be surprising that very long fibrils seem to persist in the samples and there is no obvious decrease in the maximum detectable fibril lengths (data not shown). This might be explained by some long fibrils representing conformations which are more resistant to disaggregation than others. This would be a likely scenario because fibril preparations generated from recombinant Tau *in vitro* are known to represent an ensemble of different types and morphologies of filaments (Wegmann et al., 2010). A more detailed analysis using more samples and higher resolution of AFM analysis would be required for further clarifying this issue. Similarly, analyzing the fibril decomposition at higher resolution with respect to both the time course and morphology might be helpful in assessing possible intermediate steps in the course of disaggregation. Apart from the mechanisms suggested here so far, it is also conceivable that HTRA1 shifts a dynamic equilibrium between soluble forms of Tau and oligomers or aggregates towards the soluble species by sequestering or degrading the soluble forms. Even though there might be a dynamic exchange in parts of an amyloid fibre (Carulla et al., 2005) such a mechanism would be rather unlikely given the pronounced stability of amyloids. However, to exclude this possibility, experiments would need to be performed which directly detect the binding of HTRA1 to the fibrillar structure and at the same time prove that this binding is required for successful disaggregation.

4.3.2. Effects of Mutations on the Disaggregase Activity

PDZ domains play diverse roles in the allosteric regulation, oligomerization, substrate recognition and localization of HtrAs (1.3). For HTRA1, however, the exact function of the PDZ domain is not well understood, yet. While it is important for the subcellular localization of the protease (dissertation A. Tennstädt, (Chien et al., 2009c)), the impact of the PDZ domain on the mechanistic action of HTRA1 is yet to be resolved. In contrast to other HtrAs, substrate induced activation of HTRA1 was shown to be independent of the PDZ domain ((Truebestein et al., 2011), this work RES). Given that the PDZ domain is a potential binding platform for interaction partners and substrates (Runyon et al., 2007), and that it displays high *en bloc* mobility, it would be conceivable that the PDZ is mechanistically involved in the disaggregation process. It might, for example, facilitate disaggregation by providing additional binding sites for Tau and upon binding of HTRA1 oligomers to Tau filaments promote the destabilization of intra-aggregate interactions by means of their flexibility and by providing alternative and competing interaction partners for individual Tau monomers. Based on these assumptions, it was reasoned that interfering with the function of the PDZ domain by introducing mutations or deleting the PDZ domain completely would help recognizing its involvement in the disaggregation process. When Tau fibrils were incubated o/n with HTRA1 ΔPDZ S328A, they were dissolved in the same way as compared to HTRA1 S328A, indicating that the PDZ domain is dispensable for the disaggregase activity as judged by this assay (3.4.7). However, there was an impact of the loss of the PDZ domain when performing experiments with disaggregation followed by proteolysis. In these experiments, only preincubation with HTRA1 S328A but not HTRA1 ΔPDZ S328A led to enhanced proteolysis of fibrils. When the preincubation was followed by proteolysis with active HTRA1 ΔPDZ, there was a gradual difference with HTRA1 ΔPDZ S328A having a mildly enhancing effect, but HTRA1 S328A having a strong effect on the subsequent degradation of fibrils. These results indicated that the PDZ was not absolutely required, but advantageous for the dissolution of fibrils. This gradual effect might have been masked in the o/n incubation experiments using the S328A mutant only. The HTRA1 ΔPDZ mutant used here displayed a higher proteolytic activity towards fibrils, in particular after disaggregation by HTRA1 S328A, where fibrils were most rapidly degraded by HTRA1 ΔPDZ. With the mechanistic knowledge about the PDZ domain and the regulation of HTRA1 available so far, it is hard to explain how this is brought about. In a situation where disaggregated fibrils are digested, the PDZ seemed to have an inhibiting effect on the proteolytic activity, but the structural and biochemical basis for this cannot be sufficiently explained here. It can be speculated that in while being instrumental in

the disaggregation process the PDZ domains might hamper proteolytic processing because of remaining occupied with disaggregation. It should be noted that the complete deletion of the PDZ domain leads to the generation of an unnatural mutant of HTRA1 since HTRA1 ΔPDZ has not been observed in cells. Therefore, the relevance of related observations for the function of HTRA1 is questionable.

To obtain additional insights about which elements within the HTRA1 structure might be involved in the disaggregation reaction, point mutations were introduced into the PDZ domain a well as the protease domain of HTRA1, thereby targeting the possible substrate binding to the PDZ domain and the protease domain. In the case of both R302A and I383A, the amino acids which were changed were selected on the basis of available structural data indicating that these residues take part in the interaction of the substrate with the protease and the PDZ domain of HTRA1, respectively. The R302 is located in the L3 loop of HTRA1 which makes up the activation domain with the active site loops L1, L2 and LD in the active state of the protease (Truebestein et al., 2011). Activity assays of these mutants showed that, while the PDZ mutation I383A hardly affected the proteolytic activity of HTRA1, the protease was essentially inactive when the R302A mutation was introduced (3.4.8). This both confirmed the dispensability of the PDZ domain for proteolysis and the need of an intact loop L3 for the setup of a catalytically competent active site. When performing disaggregation experiments followed by ultracentrifugation to monitor the insolubility of Tau upon incubation with wt HTRA1 or the mutants described above, the PDZ mutant I383A was not able to disaggregate Tau filaments, whereas disaggregation was still possible for the R302A mutant (3.4.10). The effects were further tested with respect to the proteolytic degradation of Tau fibrils. Surprisingly, HTRA1 I383A was not impaired in its ability to degrade Tau fibrils, it was even able to proteolyze the Tau fibrils more effectively than wt HTRA1. Preincubation with the L3 mutant HTRA1 R302A led to enhanced proteolysis of fibrils with an efficiency comparable to HTRA1 S328A which was used in previous experiments.

These observations have several possible implications. Regarding the PDZ domain mutation I383A, the disaggregase activity was impaired, whereas proteolysis (and disaggregation which should take place concomitantly) was not compromised. This might point to a mechanistic difference between disaggregation alone on one hand, and disaggregation with simultaneous proteolysis on the other hand. Peptide binding to the mutated PDZ domain has not been tested in this study. Therefore, the mechanistic outcome of an increase or decrease in the affinity of binding of certain peptidic ligands to the PDZ domain remains a matter of speculation, but might turn out to be an important aspect of disaggregation in future studies.

Some interesting aspects of HTRA1 activity were pointed to by using the mutant R302A. First of all, disaggregase activity was shown not to be an artifact generated by the S328A mutation used earlier, but disaggregation could also be performed when the active site Ser was still present and even when the wt HTRA1 protein was used (3.4.10). Furthermore, the loss of proteolytic activity observed for the R302A mutant suggests that the active site is defective when loop L3 is compromised. At the same time, there are structural mechanisms needed for hydrolysis which are obviously not required for disaggregation, which might imply that disaggregation involves different conformational requirements and rearrangements than does proteolysis. Thus, regarding the active site, disaggregation and proteolysis could be mechanistically separable events on the level of the protease domain. Taken together, the data using HTRA1 mutants have allowed some conclusions on the disaggregase activity. The PDZ domain seems to play a role in the disaggregation of Tau aggregates, but it has not become clear how strong the influence of the PDZ domain is or what the mechanistic link between the PDZ and protease domains might look like. Mutating loop L3 has shown that disaggregase activity is a distinct property of HTRA1 which functions in part independently of the proteolytic activity and thus might have evolved as additional feature of the protease while maintaining the proteolytic competence.

4.3.3. Model of Disaggregation

The biochemical data discussed above allow a simple model explaining the disaggregase activity of HTRA1 in combination with the proteolytic degradation of Tau fibrils, as illustrated in Figure 46.

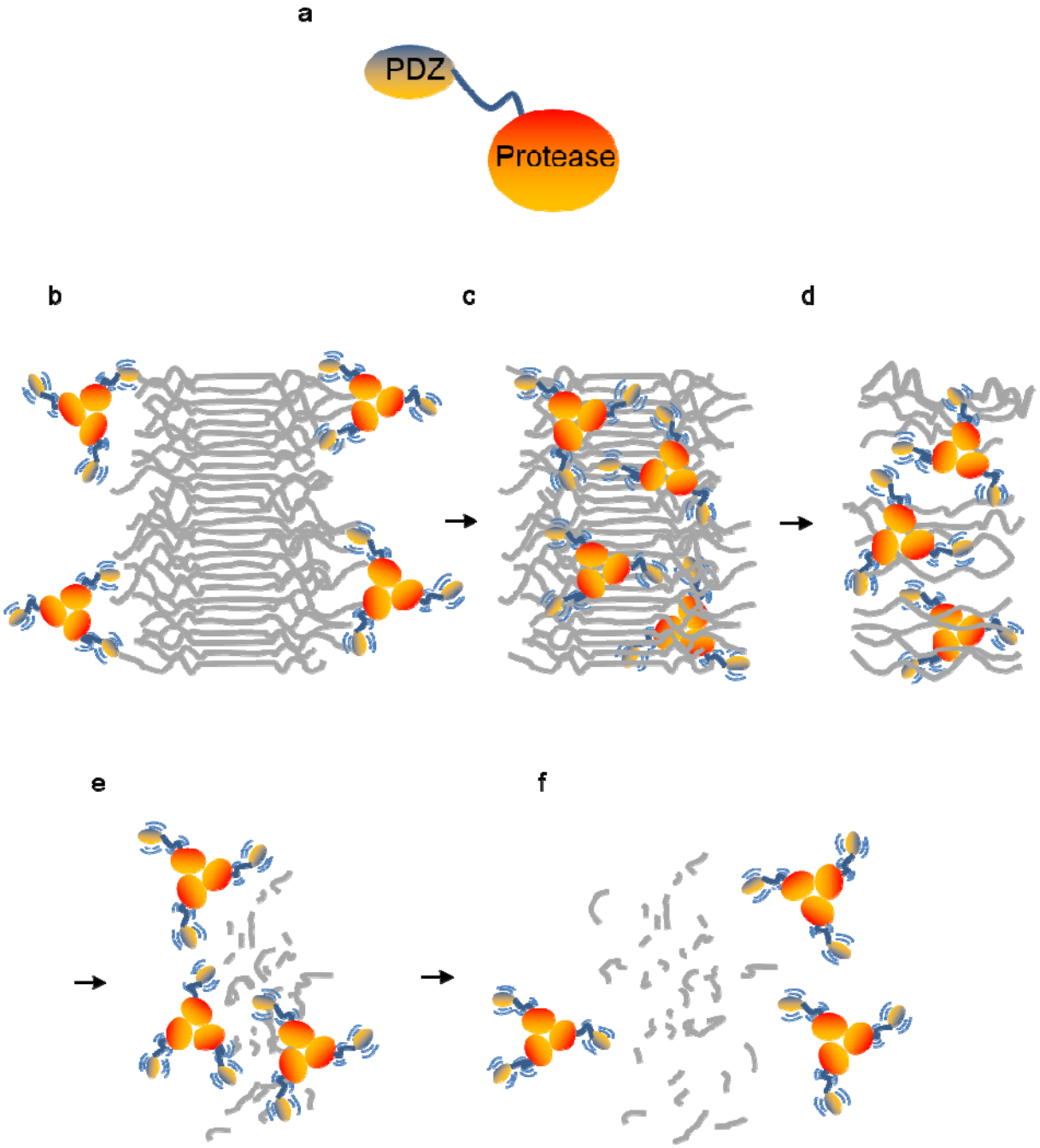

Figure 46 - Model of the Mechanism of Disaggregation and Proteolysis of Tau Fibrils by HTRA1

Cartoon representation summarizing the basic steps assumed to underlie the disaggregase activity of HTRA1. **a**, legend explaining the elements of the schematic HTRA1 representation. The basic steps are **b**, the initial binding, **c**, the tight interaction, **d**, the loosening of the fibril core structure, **e**, the proteolytic degradation of the Tau filament and **f**, the release of HTRA1 after completion of proteolysis as explained in detail in the text.

The schematic Figure 46 summarizes the experimental findings discussed above and combines them in a simple, preliminary model. It should be noted that the mechanistic details

which form the basis of the individual steps will have to be investigated in further studies, some aspects of which will be elaborated on in 4.5. First, upon encountering Tau fibrils, HTRA1 binds to the parts of Tau which protrude from the fibril core and which do not take part in constituting the tightly packed core (Figure 46 b). In this part of the aggregate, the Tau protein is more flexible and, consequently, more easily accessible to the protease, which is supported by the preferred cleavage in the regions flanking the MTBD of Tau at early time points. With each PDZ and protease domain providing a potential binding site for Tau, HTRA1 can engage each fibril with a total of six binding sites per HTRA1 trimer. Successive recruitment of more free binding sites to the Tau filament leads to HTRA1 approaching the core region of the aggregate, allowing interaction with stretches of Tau residing in the fibril core (Figure 46, c). In the following step, HTRA1 causes a disintegration of the core structure, presumably by dynamically interacting with the constituent monomers and by competitively binding to the parts of Tau residing in the fibril core (Figure 46, d). This steps is of particular interest as will be discussed below, because at this point the binding energy which stabilizes the amyloid core structure has to be overcome, therefore representing a crucial stage in thermodynamic terms. Loosening the fibril core structure in turn allows for the protease domain to productively interact with parts of Tau residing in the tightly packed core region, i.e. to hydrolyze peptide bonds within the aggregate core (Figure 46, e). When the proteolytic degradation of Tau is completed, HTRA1 can dissociate from the protein and engage in new cycles of disaggregation and proteolysis (Figure 46, f). The proteolytic cleavage of the substrate Tau makes the reaction irreversible and removes ligands from the solution by destroying them hydrolytically. In this way, substrate release is ensured even if the interactions involved are characterized by high binding affinity and accordingly low dissociation rates. This is worth noting because in the case of many chaperones, the release of substrates is the step which requires ATP hydrolysis to drive conformational changes mediating substrate release.

A striking feature of the disaggregase activity of HTRA1 is its ATP independence. HtrA proteases have evolved to serve functions in the extracytoplasmic protein quality control and therefore act in an ATP independent manner (1.3). In the cytoplasm, the classical tasks of protein quality control such as chaperone functions, the clearance of misfolded proteins as well as disaggregase functions by the Hsp104/ClpB system are typically carried out by ATP hydrolyzing factors. In Hsp104/ClpB, the energy from ATP hydrolysis is directly coupled to the process of disaggregation by generating a pulling force acting on single polypeptide chains which are threaded through a narrow central pore (1.2.3). In other words, ATP

hydrolysis in these cases is needed to break the tight interactions which stabilize the aggregate assembly. Accordingly, the energetic aspect is of particular interest in studying HTRA1 disaggregase activity. Within the model described above, the step in which an energy barrier needs to be surmounted is the loosening of the tight fibril core (Figure 46, d). This step seemed to be independent of subsequent or concomitant proteolysis, as indicated by disaggregation experiments involving HTRA1 S328A alone. As mentioned above, it is possible that HTRA1 competes for with other Tau monomers within the filament for the binding of individual Tau monomers. By doing so at several points along the filament, and taking into account the flexibility of HTRA1 trimers and their PDZ domains, this would lead to the gradual destabilization of the fibril core structure. Binding to both the protease and the PDZ domain of HTRA1 happens via a β-augmentation process, in which a ligand engages with the binding partner by adding a β-strand to a preexisting β-sheet of the interacting protein. It is not unlikely that the high β-sheet content of the amyloid core and the concomitant β-propensity of the regions of Tau within this part of the aggregate favor the interaction with HTRA1 by a β-augmentation process. According to the structure of the amyloid core of Tau fibrils which has been reported (Wiltzius et al., 2009), there are amino acid side chains protruding outwards from the spine of the amyloid, which could in principle interact with the protease or PDZ domain of HTRA1. Whereas the PDZ domain is a classical interaction domain for C-terminal residues of ligands, binding of internal peptide sequences has also been reported (Runyon et al., 2007), so that an involvement of the PDZ domains at this stage would be possible. Furthermore, binding competition of sites of interaction has been proposed to be central to a recently reported mechanism of an ATP independent disaggregase acting on membrane protein aggregates (Jaru-Ampornpan et al., 2013).

Other mechanistic aspects may add up to this initial model, but have not been addressed experimentally, yet. For example, the dynamic interconversion of oligomeric states is a feature of some HtrAs, such as DegP, where it reflects a change in activity and couples substrate sensing to enzymatic activation and the buildup of large particles for proteolytic destruction (1.3.1). Higher order oligomers have also been reported for HTRA1 (Truebestein et al., 2011), but so far little is known about the exact composition, the cues triggering conversion, the oligomer dynamics or the interplay between oligomerization and proteolytic activity. Therefore, a role of oligomerization for the disaggregase activity of HTRA1 can only be speculated here. Some aspects at least point to the possibility of oligomerization being an important aspect of disaggregation. HTRA1 being present in an oligomeric state means that there is a high local concentration of potential binding sites for Tau, which would help

generating enough competitive binding energy for the destabilization of fibrils. A scenario in which oligomer conversion is triggered, for example by binding of the amyloid core of the fibrils, would include extensive conformational changes similar to what was reported for DegP. These changes are energetically sufficient to drive substantial intermolecular rearrangements and might therefore contribute to a partial destabilization of the aggregate core structure. For ClpB, it has been suggested that deoligomerization could be involved in the disaggregation process, because even aggregates in which parts of a protein are aggregated while other domains remain stably folded can be disaggregated, arguing that the polypeptide cannot be completely translocated through the central pore (Haslberger et al., 2008). Although the mechanism of disaggregation differs completely between ClpB and HTRA1, this observation gives a hint that oligomeric regulation might generally be instrumental in such processes. Finally, some experimental findings discussed earlier (4.3) could well be interpreted in a way that the functional unit for aggregate disassembly is larger, i.e. composed of more HTRA1 subunits, than for the degradation of soluble Tau. Therefore, a mechanism involving larger HTRA1 oligomers would be conceivable, but has to be thoroughly addressed, as suggested below (4.5.1).

4.4. Cell Biology of HTRA1 and Tau Aggregates

In the course of testing the potential significance of Tau disaggregation in the cellular context, the uptake of recombinant HTRA1 protein by cultured cells was considered a convenient alternative to additional transfection procedures, which would have imposed additional stress on the cells. HTRA1 was shown to be readily taken up by HEK-293T cells in a concentration dependent manner and within a time span of ca. 30 min to 1 h (3.5.2). Not only was HTRA1 detected in cell lysates, but the colocalization with overexpressed Tau also confirmed the cytoplasmic localization of HTRA1 and its functional intactness following the uptake process (3.5.4). While HTRA1 was reported to have extracellular, as well as cytoplasmic and nuclear localizations, the mechanisms of generating an intracellular pool of HTRA1 remain unknown so far. Alternative splicing giving rise to N-terminally truncated transcripts of the HtrA1 gene are predicted (Vega Genome Browser, http://vega.sanger.ac.uk; gene ID OTTHUMG00000019186), but the relevance of this prediction awaits experimental testing. Another mechanism could be the posttranslational modification of the HTRA1 protein, i.e. the retranslocation into the cytosol, which could in principle occur during stages of the secretory pathway or after secretion, involving

reinternalization of the secreted protein. So far, no mechanisms have been characterized which would mediate such translocation events. In the course of the ER associated protein degradation, misfolded proteins are translocated across the ER membrane, but this is strictly followed by their proteolytic degradation (Meusser et al., 2005). Internalization of proteins from the extracellular space has been reported in other cellular processes. For example, membrane resident receptors are recycled or internalized for regulatory purposes (Maxfield and McGraw, 2004), and the uptake of viral proteins classically involves endocytosis and enzyme catalyzed lysosomal disruption (Greber et al., 1993). However, these mechanisms either do not involve protein release into the cytosol, or they depend on additional mechanisms which do not apply. Tau aggregates have been shown to enter the cytoplasm via bulk endocytosis (Wu et al., 2013), and the secreted protein Lysyl oxidase was reported to be reinternalized into the cytosol and nucleus (Nellaiappan et al., 2000). The exact mechanisms of internalization remain unclear in these cases, but they indicate that for other proteins, reinternalization does take place and might therefore be of general relevance. The results presented here suggest an active uptake mechanism, because the internalization was rapid and did not take place at 4°C (3.5.2). Whether the process of HTRA1 internalization involves specific receptors, how it is regulated and how HTRA1 can enter the cytoplasm will be possible objectives for future research (4.5.2).

Increased intracellular HTRA1 levels led to a decrease in the amount of aggregated Tau in HEK-293T cells (3.5.6), which was observed both for the active protease and the proteolytically inactive, but disaggregation competent HTRA1 S328A mutant. These results show that disaggregation as well as the clearance of aggregates can be mediated by HTRA1 in the cellular context and is not restricted to the *in vitro* situation. This implicates that, for instance, HTRA1 is targeted to the sites of Tau aggregation as supported by the physical association of recombinant, internalized HTRA1 and ThS positive Tau aggregates visualized by immunofluorescence microscopy (3.5.5). Also, it is likely that the disaggregase and proteolytic activity of HTRA1 is specifically targeted to Tau, a process that might involve both additional interaction partners within the cell, as well as rearrangements within HTRA1 that ensure substrate specific degradation. Both processes need further investigation to get an idea of the mechanisms involved in the intracellular action of HTRA1. Also, it is not clear in how far the disassembly or clearance of Tau aggregates is beneficial to the cells. In order to address these questions the cellular model of Tau aggregation probably needs further optimization because so far the rate of successful induction of intracytoplasmic Tau aggregation was relatively low (3.5.1). This might hamper the quantitative analysis of the effects on individual

cells, because only few cells are affected per sample. With regard to the regulation of the internalization of HTRA1, it would be interesting to see whether there is a regulated increase in the intracellular concentration of HTRA1 by means of increased internalization rates from the extracellular space, representing a possible stress response to protein aggregation inside of the cells. While the data obtained so far might indicate that in the presence of Tau aggregates more HTRA1 was taken up (3.5.6), this has to be examined in further detail, in particular because HTRA1 was also taken up without any further manipulation of the cells.

Regarding the physiological role of HTRA1, the possibility of HTRA1 also functioning in the extracellular protein quality control should not be ignored at this point. Earlier evidence indicated that HTRA1 might play a role in the metabolism of Aβ (Grau et al., 2005) and in the clearance of Aβ peptides in the course of AD pathogenesis (dissertation A. Tennstädt). It would therefore not be surprising if the disaggregase activity of HTRA1 also had an impact on the removal of Aβ amyloid aggregates from the extracellular space. Additionally, HTRA1 could as well act as a disaggregase and protease on extracellular Tau aggregates, which have been referred to as ghost tangles (Bancher et al., 1989). With regard to the spreading of Tau pathology across the different brain regions (de Calignon et al., 2012), a tempting idea would be that HTRA1 might sequester, disaggregate or proteolyze amyloid oligomers composed of Tau and by these means reduce their infectiousness and halt the progression of Tau misfolding. In this context, it would be of interest to test the effect of HTRA1 on specific assemblies of Tau with regard to their toxicity, amyloid properties and seeding capacity. Antibodies which inhibit the seeding capacity of Tau aggregation were tested *in vitro* and in a mouse model of Tauopathy, indicating that the process of seeded misfolding might be a promising target of intervention (Yanamandra et al., 2013) which might also hold true for modulating extracellular HTRA1 activity.

Finally, the regulation of HTRA1 in response to Tau aggregation and related protein misfolding stress is of interest when characterizing the role of HTRA1 in the cellular context. This concerns all possible levels of regulation, including transcriptional regulation, but also a possible regulation of secretion, reinternalization, subcellular localization and enzymatic regulation of the protease. Posttranslational modifications of HTRA1 could both affect the turnover and catalytic activity of HTRA1 and would therefore provide possible means of cellular adaptation to protein misfolding stress.

4.5. Conclusion and Future Perspectives

The experimental data provided and discussed here establish HTRA1 as a protein quality control factor combining disaggregase and protease activities in a single protein and employing a novel, ATP independent mechanism of disaggregation. This makes HTRA1 the first HtrA member to be reported to act on protein aggregates, thereby expanding the repertoire of biochemical activities of the HtrA family of serine proteases. HTRA1 is therefore an example of how mechanisms to counteract the toxic process of protein aggregation have evolved in extracytoplasmic factors which consequently act in an ATP independent manner. The spatial limitation to the cytoplasm which is imposed on the dedicated disaggregase and protease machines by their ATP dependence was compensated by the emergence of alternative mechanisms of aggregate clearance as exemplified by HTRA1. Although only a matter of speculation, it is conceivable that HTRA1 can perform its protein quality control function both in the extracellular space and in the cytoplasm, and that cells have elaborated a mechanism of internalization to make use of these functions in the cytoplasm. In conclusion, it will be of great interest to get a more detailed view of the mechanism of disaggregation and proteolysis of aggregates by HTRA1, on both the cellular and the biochemical level. The following sections are aimed at summarizing some of the central questions, outline possible directions of future studies and suggest possible experimental approaches.

4.5.1. Mechanistic Studies

HTRA1 can degrade Tau aggregates by destabilizing their fibrillar structure and by these means gaining access to the tightly packed fibril core. A simple model was suggested to summarize the fundamental aspects of this process and to outline how disaggregation is coupled to proteolysis in an ATP independent manner (Figure 46). This model can serve as a starting point for future work by suggesting critical questions and will be refined and revised by further studies.

When focusing in on the Tau filaments themselves, a few open questions become evident. First, the AFM data available so far do not yet allow any conclusions on how the disassembly process changes the overall structure. It would be interesting to visualize the disaggregation in a time-dependent manner, aiming at capturing intermediate states of disaggregation. This might involve the questions of whether fibrils gradually become loosened or rather collapse in

a rapid manner once a threshold is exceeded, or whether disassembly occurs locally rather than globally. Time resolved AFM or super-resolution microscopic techniques such as total internal reflection fluorescence microscopy (TIRFM) using fluorescently labeled Tau aggregates could help addressing these questions. Imaging of fibrils by TIRFM and confocal fluorescence microscopy has been done in previous studies on the growth dynamics of amyloid fibrils and should therefore be feasible (Ban and Goto, 2006; Inoue et al., 2001; Patil et al., 2011). Similarly, the spatial aspect of disaggregation would be of importance, because HTRA1 could act on the ends of fibrils to progressively disassemble them or all over the length of a Tau filament. Getting an idea of these aspects would help understanding the dynamics and mechanistic details of disaggregation. The use of fluorescently labeled HTRA1 protein in combination with high resolution microscopic techniques could be instrumental in directly demonstrating the binding of HTRA1 and the particular sites of binding. By tracking the disaggregation over time in combination with fluorescent microscopic techniques such as fluorescence recovery after photobleaching (FRAP), insights into the dynamics involved in binding and disengagement of fibrils by HTRA1 could be gained.

As outlined above, little is known about the oligomerization dynamics of HTRA1, while this aspect might be of importance for the disaggregase activity and degradation of aggregates by HTRA1. Some experimental approaches aiming at the determination of the oligomeric state of HTRA1, such as size-exclusion chromatography or chemical cross-linking, are hampered in the presence of large aggregates, which in addition to their size represent a heterogeneous mixture of assemblies. Another way of detecting the dynamic conversion and interplay of HTRA1 oligomers would be fluorescence resonance energy transfer (FRET) which can be used to monitor nanometer scale vicinity of two suitable fluorophores. By using two populations of HTRA1 labeled with different fluorescent dyes and mixing them with Tau fibrils for disaggregation, the interaction of individual oligomers and their dynamics could be monitored in solution. This could ideally even be extended by using e.g. TIRFM combined with FRET measurements and thereby specifying the location of oligomer exchange processes. When observing proteolytically inactive and active HTRA1 in this way, it would be interesting to see whether inactive HTRA1 would engage in oligomers with wt HTRA1 and support proteolytic degradation in the same particle without being proteolytically active themselves. Such experiments could also be helpful in providing an assay for the identification of oligomerization defects in HTRA1 mutants, which could ultimately lead to a better understanding of the mechanism of oligomerization of HTRA1.

Regarding the individual domains and structural elements of HTRA1, distinct roles for the mechanism of disaggregation could not be unambiguously ascribed so far. The mode and place of binding of Tau to the PDZ or the protease domain of HTRA1 is an important aspect, and could be addressed by measuring the binding affinities of model peptides to the respective domains of HTRA1 or mutants with these domains altered. The mutants described in this work might have been not optimally suited, because none of them compromised all aspects of disaggregation and proteolysis in a significant manner. This could be overcome by testing more mutants in search of stronger phenotypes, or by modifying the described assays of disaggregation for a more gradual assessment of disaggregation. By doing so, it might be possible to identify more modest phenotypes of the respective mutants. A more detailed understanding of the sites of interaction between Tau monomers and HTRA1 would help to explain the mechanism of substrate recognition by HTRA1 and in which way competitive binding between Tau and HTRA1 versus intra-aggregate interactions contributes to the ATP independence of the process. It was concluded from the experimental evidence presented here, that proteolysis and disaggregation are in part separable mechanistic processes, indicated by residue R302 being necessary for protease but not disaggregase activities. This assumption points to the fact that HTRA1 harbors various potential mechanisms of loop rearrangements and interactions which ultimately convey catalytic and regulatory processes within the protein. The allosteric regulation of DegP is an example of such intramolecular signaling processes (Merdanovic et al., 2010). Given the simultaneous action as a protease and disaggregase, this illustrates a complex situation in which, for example, disaggregation might precede proteolysis or enhance proteolytic activity or proteolysis might go along with allosteric changes affecting oligomerization or disaggregation and so on. This complexity might explain the seemingly contradictory observations using the HTRA1 mutants described in this study. At the same time it underlines the challenge of appropriately choosing and interpreting mutants and their resulting effects. When considering the novel feature of HTRA1 which is so far unrecognized in other HtrAs, it is very likely that HTRA1 has evolved new mechanisms of substrate recognition and regulation which might dramatically differ from what has been described for other family members such as DegP. Thus, it might be another example of regulatory diversification of homologous proteins which has been proposed to be greatly stimulated by colocalization and oligomerization processes (Kuriyan and Eisenberg, 2007).

Finally, the specificity of the disaggregation process by HTRA1 would be an interesting aspect to further address. As shown here, HTRA1 can proteolyze various types of

aggregates, but it is not known whether in all cases the same mechanisms of disaggregation apply, or whether this activity is limited to the fibrillar, amyloid structure of Tau fibrils. Also, the possibility of generalizing the disaggregase activity of HTRA1 could be the subject of further studies, using other amyloid aggregates such as Aβ or α-synuclein filaments as substrates. The proteolysis of amyloid fibrils could be a hint to a proteolytic activity specifically targeted at substrates which are rich in β-sheets, which would explain aspects of substrate specificity with rather low sequence specificity, as reported for HTRA1.

Given its implication in protein quality control processes and diseases associated with protein aggregation such as AD, HTRA1 is a promising disease modifying factor. HTRA1 might play important roles in the clearance of aggregates, therefore, modulating HTRA1 activity could be a potent strategy of interfering with the disease progression. Establishing easy assays of disaggregation and proteolysis, as well as understanding the underlying mechanisms in as much detail as possible would be of great advantage for studies aimed at identifying small molecule activators or inhibitors of HTRA1. Vice versa, inhibitors and activators could prove valuable tools for elucidating mechanistic aspects of HTRA1 activity and regulation. If it was possible to specifically target the disaggregation and proteolysis of aggregates and leave the proteolysis of other substrates or in other contexts unaffected, this could reduce negative side effects which would occur when unwantedly interfering with different functions of HTRA1.

4.5.2. Cellular Physiology of HTRA1

Both the finding that HTRA1 was internalized by cultured cells through an active mechanism and the impact of increased levels of HTRA1 on the amounts of insoluble Tau prompt a number of further questions. Concerning the uptake of HTRA1, it is important to understand how the recruitment of HTRA1 to the membrane is conferred, i.e. which receptors, if any, serve to recognize HTRA1 and mediate its reimport, as well as which parts of HTRA1 are needed for this process. Immunoprecipitations (IPs) of HTRA1 using membrane fractions of cultured cells or chemical cross-linking of HTRA1 upon interaction with cell membranes followed by mass-spectrometry could serve to identify candidate receptors or other proteins such as adaptors involved in the initial steps of internalization. Specifically interfering with distinct pathways of endocytosis by chemical reagents or the overexpression of dominant negative mutants could help characterizing the relevant endocytic process. The interna-

lization of labeled HTRA1 can be easily quantified by fluorescence activated cell sorting (FACS), providing means of assessing the regulation and dynamics of HTRA1 internalization under various conditions and perhaps in response to certain stresses.

Regarding the cellular functions of HTRA1 there are still many unresolved questions, some of which might gain particular importance in light of the findings presented here. Broadly speaking, the implication of HTRA1 within the protein interaction, modification and regulation network of the cell should be further elaborated. In terms of protein quality control, stress response pathways could regulate HTRA1 on various levels – protein abundance by transcriptional regulators, the turnover of HTRA1 by e.g. ubiquitination or other regulated proteolysis events, the enzymatic activity through interaction partners and PTMs such as phosphorylation, or the localization by regulated secretion or reimport. Each of these regulatory levels can potentially enable cells to adapt to stress situations and make targeted use of the disaggregase and protease activity of HTRA1 to counteract or reverse protein aggregation. In addition to these processes, the intrinsic regulatory properties of the protease could immediately confer the sensing of misfolding independently of other cellular signals. HTRA1 could also engage with other factors of protein quality control or degradative factors and in this way become part of an orchestrated response to aggregation. A candidate interaction partner is Calpain, which was shown here to be able to degrade Tau aggregates and which was shown to form a composite protease complex *in vitro* (dissertation M. Breiden).

The eventual outcome of the disaggregase activity of HTRA1 in the context of amyloid aggregates could be critical for further investigations, because dissolving amyloid aggregates might not necessarily be advantageous for the cell. It is widely recognized that oligomeric and pre-aggregate species of amyloid forming proteins can exert toxic effects on cells, and that the formation of aggregates might therefore be protective in sequestering such species and keeping them from diffusing through the cell (Ross and Poirier, 2004). It is also possible that, under pathophysiological and conditions and in the presence of, e.g. PTMs, HTRA1 only truncates the Tau protein and by these means generates potentially harmful fragments. Although these are diverse points of concern which might well play only minor roles and be difficult to address, they should be considered when working in the cellular or *in vivo* context and, for example, aiming at the pharmacological use of HTRA1 activators. The *in vivo* situation is even more complex and therefore harder to evaluate, but a first step of assessing the significance of HTRA1 disaggregase activity could be the analysis of mouse models of Tauopathy crossed with HtrA knockout mice. If HTRA1 contributes to the clearance of Tau

aggregates *in vivo*, an increasing effect of the loss of HTRA1 on the abundance of pathologically aggregated Tau would be expected.

When looking at the functions which have been suggested for HTRA1, it will be an important issue to define how such diverse aspects can be affected by a single player. Roles in cancer metastasis, cell growth and protein quality control seem to be combined in a single protein. Nevertheless, the implications of HTRA1 in disease and physiological process indicate that this must be in some way controlled. HTRA1 could serve different functions depending on its modifications or localization and, consequently on the interaction partners it associates with under certain conditions. These factors as well as the organ and cell type specific environment could channel the activity of HTRA1 to the various functional tasks it has to complete. For example, in long lived, post-mitotic cells like neurons, protein quality control functions could prevail on the expense of cell proliferation related and developmental roles. How the regulatory complexity of mammalian cells might account for this versatility of a single factor is an interesting aspect of HTRA1 biology.

5. Summary

Loss of normal protein function and the accumulation of aberrantly folded proteins as insoluble aggregates are potential manifestations of the impaired integrity of the cellular proteome. To maintain proteins intact and, consequently, prevent misfolding and aggregation, mechanisms of protein quality control have evolved. Protein quality control factors catalyze the folding of proteins, their transport and assembly into complexes as well as the degradation of damaged or aged proteins, thereby conferring physiological protein abundance, localization and function. Although some protein aggregates such as amyloids are generally considered to resist proteolytic degradation, disaggregases have recently gained attention, which use chemical energy from the hydrolysis of ATP to disrupt aggregates and help to restore or degrade the constituent proteins. Fatal disorders such as Alzheimer's or Parkinson's disease are characterized by the continuous deposition of aggregates, which underlines the importance of learning about the pathways and mechanisms of protein quality control.

HTRA1 is a human member of the conserved family of HtrA serine proteases, many of which are well known players of protein quality control in diverse organisms such as bacteria and plants. Whereas HTRA1 was previously shown to degrade the microtubule-associated protein Tau which forms characteristic amyloid aggregates in so-called Tauopathies, of which Alzheimer's disease (AD) is the most prevalent, the biochemical and cellular implications of these observations remained unclear. Therefore, the aim of this work was to characterize the mechanistic basis of the degradation of Tau by HTRA1 and in particular of Tau aggregates resembling those found in AD.

In vitro proteolysis experiments using recombinant human Tau and HTRA1 showed that HTRA1 was able to proteolyze not only soluble, but also aggregated Tau which was rich in β-sheets characteristic of amyloids. Heparin-induced Tau aggregates resembling amyloid aggregates biochemically and morphologically were also efficiently degraded by HTRA1. This lead to the hypothesis of a potential disaggregase activity which would allow HTRA1 to resolve tightly packed Tau aggregates and render their component monomers susceptible to the proteolytic attack by HTRA1. On the basis of sedimentation experiments and atomic force microscopic studies, it was shown that proteolytically inactive HTRA1 was able to solubilize Tau fibrils. Disaggregation by the inactive HTRA1 S328A mutant facilitated subsequent proteolysis by wt HTRA1 and thus suggested a combined disaggregase and protease function of HTRA1 that involves the loosening of the aggregate core structure. The

hydrolysis of regions of Tau residing in the fibril core was detected on the basis of mass-spectrometric analysis of peptidic products generated by the proteolysis of fibrils after previous disaggregation. Experiments using mutant variants of HTRA1 pointed at a possible role of the PDZ domain of HTRA1, which was, however, not strictly required for disaggregation. The data presented here thus allowed a preliminary model of disaggregation, in which the sequential binding of stretches of the Tau protein in fibrils and the eventual loosening of the aggregate core facilitates the proteolysis tightly packed part of the aggregate.

Cultured human cells spontaneously internalized recombinant HTRA1 from the extracellular space, which on one hand pointed at a possible way of generating a cytoplasmic pool HTRA1, which is normally secreted. On the other hand, this observation allowed for the experimental manipulation of intracellular levels of HTRA1 in a cellular model of cytoplasmic Tau aggregation. Both active and inactive HTRA1 introduced into the cytoplasm of cultured HEK-293T cells led to a reduction of the intracellular aggregate burden, indicating that HTRA1 performs its disaggregase function in the cellular context.

Taken together, these findings suggest a combination of disaggregase and protease activities by HTRA1, which not only expands the known repertoire of protein quality control functions by HtrAs, but also represent a novel mechanism of ATP-independent disaggregation. The model presented here will form the basis of future studies aimed at elucidating the mechanism of disaggregation in further detail.

Zusammenfassung

Mechanismen der Proteinqualitätskontrolle gewährleisten die korrekte Faltung, Lokalisation und Mengen der zellulären Proteine und sichern dadurch die Intaktheit des Proteoms. Wenn dies nicht in ausreichendem Maß gelingt, kann es zur vermehrten Fehlfaltung von Proteinen kommen, was den Verlust ihrer normalen Funktionsweise und die Ansammlung unlöslicher Aggregate zu Folge haben kann. Enzyme der Proteinqualitätskontrolle katalysieren die Faltung von neu synthetisierten und Rückfaltung beschädigter Proteine, den proteolytischen Abbau alter, geschädigter oder fehlgefalteter Proteine, oder das Auflösen von Aggregaten mit folgender Rückfaltung oder Proteolyse. Insbesondere der letztere Prozess, die Disaggregation, stellt besondere Anforderungen an die beteiligten Enzyme, da Protein-aggregate sehr stabile Komplexe sind, deren Auflösung und Proteolyse nach bisherigem Wissensstand den Einsatz chemischer Energie aus der Hydrolyse von ATP erfordert.

HtrA Proteasen sind in ATP unabhängige, hochkonservierte Serinproteasen, deren Rolle für die Proteinqualitätskontrolle in vielen Spezies nachgewiesen und detailliert untersucht werden konnte. Die humanen HtrAs erfüllen offenbar vielfältige Funktionen, da sie mit vielen grundlegenden zellulären Prozessen assoziiert sind, z.B. mit Zellmigration, Wachstum und Apoptose. Eine Assoziation von HTRA1 mit Proteinablagerungen in der Alzheimerschen Krankheit (AD), sowie die durch HTRA1 katalysierte Proteolyse des Mikrotubuli-assoziierten Proteins Tau, das in AD Aggregate ausbildet, ließen eine Rolle von HTRA1 in der Protein-qualitätskontrolle humaner Zellen vermuten. Ziel der vorliegenden Arbeit war es daher, den biochemischen Mechanismus des Abbaus von Tau, insbesondere von amyloiden Tau Aggregaten durch HTRA1 zu charakterisieren, da die Proteolyse von Tau Aggregaten eine Möglichkeit darstellt, wie neuronale Zellen sich vor schädlichen Effekten dieser Ablagerungen schützen könnten.

Es konnte hier gezeigt werden, dass neben löslichem Tau auch verschiedene Formen von Tau Aggregaten durch rekombinantes HTRA1 proteolytisch abgebaut werden konnten. Dies galt auch für solche Aggregate, die spektroskopischen und rasterkraftmikroskopischen Untersuchungen zufolge den fibrillären, mit neurodegenerativen Prozessen assoziierten Tau-Aggregaten entsprachen. Aufgrund dieser Beobachtungen wurde vermutet, dass HTRA1 eine Disaggregaseaktivität aufweist, die das Auflösen von stabilen Tau Aggregaten ermöglicht und damit dazu beiträgt, dass auch aggregiertes Tau durch HTRA1 proteolysiert werden kann. Mithilfe von Ultrazentrifugation und Rasterkraftmikroskopie konnte schließlich gezeigt werden, dass eine proteolytisch inaktive HTRA1-Mutante Tau Fibrillen auflösen

konnte. Diese Disaggregation ermöglichte außerdem einen erleichterten proteolytischen Abbau von Tau Aggregaten nach anschließender Zugabe von proteolytisch aktivem HTRA1. Die massenspektrometrische Analyse der proteolytischen Spaltprodukte verdeutlichte, dass durch die Disaggregation insbesondere diejenigen Bereiche des Tau Proteins vermehrt hydrolysiert wurden, die sich in dem schwer zugänglichen Kern befanden. Somit konnte ein Modell vorgeschlagen werden, demzufolge HTRA1 eine ATP unabhängige Disaggregase-aktivität besitzt, die es der Protease ermöglicht, nach Auflösung der festen Struktur des Kerns der Aggregate auch zu den Bereichen Zugriff zu bekommen, die vermutlich zu der Persistenz von amyloiden Aggregaten unter pathologischen Bedingungen beitragen. Experimente mit HTRA1 Mutanten, deren PDZ Domäne mutiert oder deletiert war, lassen eine Rolle der PDZ Domäne im Prozess der Disaggregation vermuten. Allerdings ist der genaue Mechanismus und das Ausmaß der Beteiligung der PDZ Domäne noch unklar, da auch ohne diesen Teil des Enzyms eine Disaggregation möglich war, wenn auch mit weniger deutlichem Effekt auf die anschließende Proteolyse durch aktives HTRA1.

In Zellkulturexperimenten konnte nachgewiesen werden, dass rekombinantes HTRA1 von kultivierten humanen Zellen aufgenommen wurde und im Zytoplasma mit seinem Substrat Tau kolokalisierte. Dies zeigt zum Einen einen möglichen Weg auf, mit Hilfe dessen das sezernierte HTRA1 Protein auch intrazellulär zur Verfügung gestellt werden könnte. Zum Anderen eröffnete dieses Phänomen die Möglichkeit, in einem experimentellen Modell der intrazellulären Tau Aggregation die Mengen an zytoplasmatischem HTRA1 zu manipulieren. Diese Vorgehensweise wurde genutzt um zu zeigen, dass HTRA1 nicht nur *in vitro*, sondern auch in humanen Zellen Tau Aggregate disaggregieren und proteolysieren konnte, da erhöhte Mengen an intrazellulärem, proteolytisch inaktivem, sowie auch aktivem HTRA1 zu einer Verminderung der Menge an Tau Aggregaten führten.

Zusammenfassend lässt sich also festhalten, dass anhand der hier dargelegten experimentellen Daten ein Mechanismus der Proteinqualitätskontrolle für HTRA1 nachgewiesen wurde, der nicht nur das bis hierher bekannte Repertoire der HtrA Proteasen erweitert, sondern auch einen neuartigen Mechanismus der ATP-unabhängigen Disaggregation zeigt. HTRA1 vereinigt also Protease- und Disaggregasefunktionen in einem Enzym und kann folglich als ein neuer Faktor der Proteinqualitätskontrolle betrachtet werden, der ein interessantes Ziel pharmazeutischer Intervention in neurodegenerativen Erkrankungen wie beispielsweise AD darstellen könnte.

6. References

Ahmed, Z., Cooper, J., Murray, T.K., Garn, K., McNaughton, E., Clarke, H., Parhizkar, S., Ward, M.A., Cavallini, A., Jackson, S.*, et al.* (2014). A novel in vivo model of tau propagation with rapid and progressive neurofibrillary tangle pathology: the pattern of spread is determined by connectivity, not proximity. Acta Neuropathologica *127*, 667-683.

Al-Bassam, J., Ozer, R.S., Safer, D., Halpain, S., and Milligan, R.A. (2002). MAP2 and Tau bind longitudinally along the outer ridges of microtubule protofilaments. Journal of Cell Biology *157*, 1187-1196.

Arriagada, P.V., Growdon, J.H., Hedleywhyte, E.T., and Hyman, B.T. (1992). Neurofibrillary tangles but not senile plaques parallel duration and severity of Alzheimers-disease. Neurology *42*, 631-639.

Augustinack, J.C., Schneider, A., Mandelkow, E.M., and Hyman, B.T. (2002). Specific tau phosphorylation sites correlate with severity of neuronal cytopathology in Alzheimer's disease. Acta Neuropathologica *103*, 26-35.

Auluck, P.K., Chan, H.Y.E., Trojanowski, J.Q., Lee, V.M.Y., and Bonini, N.M. (2002). Chaperone suppression of alpha-synuclein toxicity in a Drosophila model for Parkinson's disease. Science *295*, 865-868.

Avila, J., Lucas, J.J., Perez, M., and Hernandez, F. (2004). Role of tau protein in both physiological and pathological conditions. Physiological Reviews *84*, 361-384.

Avila, J., Santa-Maria, I., Perez, M., Hernandez, F., and Moreno, F. (2006). Tau phosphorylation, aggregation, and cell toxicity. Journal of Biomedicine and Biotechnology.

Babu, J.R., Geetha, T., and Wooten, M.W. (2005). Sequestosome 1/p62 shuttles polyubiquitinated tau for proteasomal degradation. Journal of Neurochemistry *94*, 192-203.

Bachmair, A., Finley, D., and Varshavsky, A. (1986). *In vivo* half-life of a protein is a function of its amino-terminal residue. Science *234*, 179-186.

Baldi, A., De Luca, A., Morini, M., Battista, T., Felsani, A., Baldi, F., Catricala, C., Amantea, A., Noonan, D.M., Albini, A.*, et al.* (2002). The HtrA1 serine protease is down-regulated during human melanoma progression and represses growth of metastatic melanoma cells. Oncogene *21*, 6684-6688.

Ballatore, C., Lee, V.M.Y., and Trojanowski, J.Q. (2007). Tau-mediated neurodegeneration in Alzheimer's disease and related disorders. Nature Reviews Neuroscience *8*, 663-672.

Ban, T., and Goto, Y. (2006). Direct observation of amyloid growth monitored by total internal reflection fluorescence microscopy. In Amyloid, Prions, and Other Protein Aggregates, Pt C, I. Kheterpal, and R. Wetzel, eds. (San Diego: Elsevier Academic Press Inc), pp. 91-102.

Bancher, C., Brunner, C., Lassmann, H., Budka, H., Jellinger, K., Wiche, G., Seitelberger, F., Grundkeiqbal, I., Iqbal, K., and Wisniewski, H.M. (1989). Accumulation of abnormally phosphorylated Tau precedes the formation of neurofibrillary tangles in Alzheimers-disease. Brain Research *477*, 90-99.

Bandyopadhyay, B., Li, G.B., Yin, H.S., and Kuret, J. (2007). Tau aggregation and toxicity in a cell culture model of tauopathy. Journal of Biological Chemistry *282*, 16454-16464.

Barghorn, S., Davies, P., and Mandelkow, E. (2004). Tau paired helical filaments from Alzheimer's disease brain and assembled in vitro are based on beta-structure in the core domain. Biochemistry *43*, 1694-1703.

Bence, N.F., Sampat, R.M., and Kopito, R.R. (2001). Impairment of the ubiquitin-proteasome system by protein aggregation. Science *292*, 1552-1555.

Berg, J.M., Tymoczko, J.L., and Stryer, L. (2002). Biochemistry. 5th Edition. (New York: W.H. Freeman).

Berger, Z., Ravikumar, B., Menzies, F.M., Oroz, L.G., Underwood, B.R., Pangalos, M.N., Schmitt, I., Wullner, U., Evert, B.O., O'Kane, C.J.*, et al.* (2006). Rapamycin alleviates toxicity of different aggregate-prone proteins. Human Molecular Genetics *15*, 433-442.

Berriman, J., Serpell, L.C., Oberg, K.A., Fink, A.L., Goedert, M., and Crowther, R.A. (2003). Tau filaments from human brain and from in vitro assembly of recombinant protein show cross-beta structure. Proceedings of the National Academy of Sciences of the United States of America *100*, 9034-9038.

Braak, H., and Braak, E. (1991). Neuropathological staging of Alzheimer-related changes. Acta Neuropathologica *82*, 239-259.

Bradford, M.M. (1976). Rapid and sensitive method for quantitation of microgram quantities of protein utilizing principle of protein-dye binding. Analytical Biochemistry *72*, 248-254.

Brady, R.M., Zinkowski, R.P., and Binder, L.I. (1995). Presence of tau in isolated-nuclei from human brain. Neurobiology of Aging *16*, 479-486.

Brandt, R., Leger, J., and Lee, G. (1995). Interaction of tau with the neural plasma-membrane mediated by tau amino-terminal projection domain. Journal of Cell Biology *131*, 1327-1340.

Brundin, P., Melki, R., and Kopito, R. (2010). Prion-like transmission of protein aggregates in neurodegenerative diseases. Nature Reviews Molecular Cell Biology *11*, 301-307.

Butner, K.A., and Kirschner, M.W. (1991). Tau protein binds to microtubules through a flexible array of distributed weak sites. Journal of Cell Biology *115*, 717-730.

Campioni, M., Severino, A., Manente, L., Tuduce, I.L., Toldo, S., Caraglia, M., Crispi, S., Ehrmann, M., He, X.P., Maguire, J.*, et al.* (2010). The Serine Protease HtrA1 Specifically Interacts and Degrades the Tuberous Sclerosis Complex 2 Protein. Molecular Cancer Research *8*, 1248-1260.

Carulla, N., Caddy, G.L., Hall, D.R., Zurdo, J., Gairi, M., Feliz, M., Giralt, E., Robinson, C.V., and Dobson, C.M. (2005). Molecular recycling within amyloid fibrils. Nature *436*, 554-558.

Chang, E., Kim, S., Schafer, K.N., and Kuret, J. (2011). Pseudophosphorylation of tau protein directly modulates its aggregation kinetics. Biochimica Et Biophysica Acta-Proteins and Proteomics *1814*, 388-395.

Chen, J., Kanai, Y., Cowan, N.J., and Hirokawa, N. (1992). Projection domains of MAP2 and Tau determine spacings between microtubules in dendrites and axons. Nature *360*, 674-676.

Chiang, K.R., and Koo, E.H. (2014). Emerging Therapeutics for Alzheimer's Disease. In Annual Review of Pharmacology and Toxicology, Vol 54, P.A. Insel, ed. (Palo Alto: Annual Reviews), pp. 381-405.

Chien, J., Aletti, G., Baldi, A., Catalano, V., Muretto, P., Keeney, G.L., Kalli, K.R., Staub, J., Ehrmann, M., Cliby, W.A.*, et al.* (2006). Serine protease HtrA1 modulates chemotherapy-induced cytotoxicity. Journal of Clinical Investigation *116*, 1994-2004.

Chien, J., Campioni, M., Shridhar, V., and Baldi, A. (2009a). HtrA Serine Proteases as Potential Therapeutic Targets in Cancer. Current Cancer Drug Targets *9*, 451-468.

Chien, J., He, X.P., and Shridhar, V. (2009b). Identification of Tubulins as Substrates of Serine Protease HtrA1 by Mixture-Based Oriented Peptide Library Screening. Journal of Cellular Biochemistry *107*, 253-263.

Chien, J., Ota, T., Aletti, G., Shridhar, R., Boccellino, M., Quagliuolo, L., Baldi, A., and Shridhar, V. (2009c). Serine Protease HtrA1 Associates with Microtubules and Inhibits Cell Migration. Molecular and Cellular Biology *29*, 4177-4187.

Cho, J.H., and Johnson, G.V.W. (2003). Glycogen synthase kinase 3 beta phosphorylates tau at both primed and unprimed sites - Differential impact on microtubule binding. Journal of Biological Chemistry *278*, 187-193.

Clausen, T., Kaiser, M., Huber, R., and Ehrmann, M. (2011). HTRA proteases: regulated proteolysis in protein quality control. Nature Reviews Molecular Cell Biology *12*, 152-162.

Clavaguera, F., Akatsu, H., Fraser, G., Crowther, R.A., Frank, S., Hench, J., Probst, A., Winkler, D.T., Reichwald, J., Staufenbiel, M.*, et al.* (2013). Brain homogenates from human tauopathies induce tau inclusions in mouse brain. Proceedings of the National Academy of Sciences of the United States of America *110*, 9535-9540.

Clavaguera, F., Bolmont, T., Crowther, R.A., Abramowski, D., Frank, S., Probst, A., Fraser, G., Stalder, A.K., Beibel, M., Staufenbiel, M.*, et al.* (2009). Transmission and spreading of tauopathy in transgenic mouse brain. Nature Cell Biology *11*, 909-U325.

Conway, K.A., Harper, J.D., and Lansbury, P.T. (2000). Fibrils formed in vitro from alpha-synuclein and two mutant forms linked to Parkinson's disease are typical amyloid. Biochemistry *39*, 2552-2563.

Croce, K., Flaumenhaft, R., Rivers, M., Furie, B., Furie, B.C., Herman, I.M., and Potter, D.A. (1999). Inhibition of calpain blocks platelet secretion, aggregation, and spreading. Journal of Biological Chemistry *274*, 36321-36327.

Crowther, R.A. (1991). Straight and paired helical filaments in Alzheimer-disease have a common structural unit. Proceedings of the National Academy of Sciences of the United States of America *88*, 2288-2292.

Cuervo, A.M., and Dice, J.F. (1998). Lysosomes, a meeting point of proteins, chaperones, and proteases. Journal of Molecular Medicine-Jmm *76*, 6-12.

Dauer, W., and Przedborski, S. (2003). Parkinson's disease: Mechanisms and models. Neuron *39*, 889-909.

David, D.C., Layfield, R., Serpell, L., Narain, Y., Goedert, M., and Spillantini, M.G. (2002). Proteasomal degradation of tau protein. Journal of Neurochemistry *83*, 176-185.

de Calignon, A., Fox, L.M., Pitstick, R., Carlson, G.A., Bacskai, B.J., Spires-Jones, T.L., and Hyman, B.T. (2010). Caspase activation precedes and leads to tangles. Nature *464*, 1201-U1123.

de Calignon, A., Polydoro, M., Suarez-Calvet, M., William, C., Adamowicz, D.H., Kopeikina, K.J., Pitstick, R., Sahara, N., Ashe, K.H., Carlson, G.A.*, et al.* (2012). Propagation of Tau Pathology in a Model of Early Alzheimer's Disease. Neuron *73*, 685-697.

De Strooper, B. (2010). Proteases and Proteolysis in Alzheimer Disease: A Multifactorial View on the Disease Process. Physiological Reviews *90*, 465-494.

Dehmelt, L., and Halpain, S. (2005). The MAP2/Tau family of microtubule-associated proteins. Genome Biology *6*, 10.

Delobel, P., Leroy, O., Hamdane, M., Sambo, A.V., Delacourte, A., and Buee, L. (2005). Proteasome inhibition and Tau proteolysis: an unexpected regulation. Febs Letters *579*, 1-5.

Delobel, P., Mailliot, C., Hamdane, M., Sambo, A.V., Begard, S., Violleau, A., Delacourte, A., and Buee, L. (2003). Stable-tau overexpression in human neuroblastoma cells - An open door for explaining neuronal death in Tauopathies. Apoptosis: from Signaling Pathways to Therapeutic Tools *1010*, 623-634.

Demuro, A., Mina, E., Kayed, R., Milton, S.C., Parker, I., and Glabe, C.G. (2005). Calcium dysregulation and membrane disruption as a ubiquitous neurotoxic mechanism of soluble amyloid oligomers. Journal of Biological Chemistry *280*, 17294-17300.

Dobson, C.M. (2003). Protein folding and misfolding. Nature *426*, 884-890.

Dobson, C.M., Sali, A., and Karplus, M. (1998). Protein folding: A perspective from theory and experiment. Angewandte Chemie-International Edition *37*, 868-893.

Dorval, V., and Fraser, P.E. (2006). Small ubiquitin-like modifier (SUMO) modification of natively unfolded proteins tau and alpha-synuclein. Journal of Biological Chemistry *281*, 9919-9924.

Doyle, S.M., Genest, O., and Wickner, S. (2013). Protein rescue from aggregates by powerful molecular chaperone machines. Nature Reviews Molecular Cell Biology *14*, 617-629.

Duennwald, M.L., Echeverria, A., and Shorter, J. (2012). Small Heat Shock Proteins Potentiate Amyloid Dissolution by Protein Disaggregases from Yeast and Humans. Plos Biology *10*.

Dunker, A.K., Silman, I., Uversky, V.N., and Sussman, J.L. (2008). Function and structure of inherently disordered proteins. Current Opinion in Structural Biology *18*, 756-764.

Ehrnsperger, M., Graber, S., Gaestel, M., and Buchner, J. (1997). Binding of non-native protein to Hsp25 during heat shock creates a reservoir of folding intermediates for reactivation. Embo Journal *16*, 221-229.

Eigenbrot, C., Ultsch, M., Lipari, M.T., Moran, P., Lin, S.J., Ganesan, R., Quan, C., Tom, J., Sandoval, W., Campagne, M.V.*, et al.* (2012). Structural and Functional Analysis of HtrA1 and Its Subdomains. Structure *20*, 1040-1050.

Eisele, Y.S., Obermuller, U., Heilbronner, G., Baumann, F., Kaeser, S.A., Wolburg, H., Walker, L.C., Staufenbiel, M., Heikenwalder, M., and Jucker, M. (2010). Peripherally Applied A beta-Containing Inoculates Induce Cerebral beta-Amyloidosis. Science *330*, 980-982.

Eisenberg, D., and Jucker, M. (2012). The Amyloid State of Proteins in Human Diseases. Cell *148*, 1188-1203.

Ellis, R.J., and Minton, A.P. (2006). Protein aggregation in crowded environments. Biological Chemistry *387*, 485-497.

Ewalt, K.L., Hendrick, J.P., Houry, W.A., and Hartl, F.U. (1997). In vivo observation of polypeptide flux through the bacterial chaperonin system. Cell *90*, 491-500.

Fath, T., Eidenmuller, J., and Brandt, R. (2002). Tau-mediated cytotoxicity in a pseudohyperphosphorylation model of Alzheimer's disease. Journal of Neuroscience *22*, 9733-9741.

Ferrari, A., Hoerndli, F., Baechi, T., Nitsch, R.M., and Gotz, J. (2003). beta-amyloid induces paired helical filament-like tau filaments in tissue culture. Journal of Biological Chemistry *278*, 40162-40168.

Friedhoff, P., Schneider, A., Mandelkow, E.M., and Mandelkow, E. (1998a). Rapid assembly of Alzheimer-like paired helical filaments from microtubule-associated protein tau monitored by fluorescence in solution. Biochemistry *37*, 10223-10230.

Friedhoff, P., von Bergen, M., Mandelkow, E.M., Davies, P., and Mandelkow, E. (1998b). A nucleated assembly mechanism of Alzheimer paired helical filaments. Proceedings of the National Academy of Sciences of the United States of America *95*, 15712-15717.

Frost, B., Hemberg, M., Lewis, J., and Feany, M.B. (2014). Tau promotes neurodegeneration through global chromatin relaxation. Nature Neuroscience *17*, 357-U348.

Frost, B., Jacks, R.L., and Diamond, M.I. (2009a). Propagation of Tau Misfolding from the Outside to the Inside of a Cell. Journal of Biological Chemistry *284*, 12845-12852.

Frost, B., Ollesch, J., Wille, H., and Diamond, M.I. (2009b). Conformational Diversity of Wild-type Tau Fibrils Specified by Templated Conformation Change. Journal of Biological Chemistry *284*, 3546-3551.

Furukawa, Y., Kaneko, K., and Nukina, N. (2011). Tau Protein Assembles into Isoform- and Disulfide-dependent Polymorphic Fibrils with Distinct Structural Properties. Journal of Biological Chemistry *286*, 27236-27246.

Gamblin, T.C., Chen, F., Zambrano, A., Abraha, A., Lagalwar, S., Guillozet, A.L., Lu, M.L., Fu, Y.F., Garcia-Sierra, F., LaPointe, N.*, et al.* (2003). Caspase cleavage of tau: Linking amyloid and neurofibrillary tangles in Alzheimer's disease. Proceedings of the National Academy of Sciences of the United States of America *100*, 10032-10037.

Garg, S., Timm, T., Mandelkow, E.M., Mandelkow, E., and Wang, Y.P. (2011). Cleavage of Tau by calpain in Alzheimer's disease: the quest for the toxic 17 kD fragment. Neurobiology of Aging *32*, 1-14.

Gasteiger, E. (2005). Protein Identification and Analysis Tools on the ExPASy Server. In The Proteomics Protocols Handbook, G.A. Hoogland C., Duvaud S., Wilkins M.R., Appel R.D., Bairoch A., ed. (Humana Press), pp. 571-607.

Glover, J.R., and Lindquist, S. (1998). Hsp104, Hsp70, and Hsp40: A novel chaperone system that rescues previously aggregated proteins. Cell *94*, 73-82.

Goedert, M., and Jakes, R. (1990). Expression of separate isoforms of human Tau protein - correlation with the Tau pattern in brain and effects on tubulin polymerization. Embo Journal *9*, 4225-4230.

Goedert, M., Jakes, R., Spillantini, M.G., Hasegawa, M., Smith, M.J., and Crowther, R.A. (1996). Assembly of microtubule-associated protein tau into Alzheimer-like filaments induced by sulphated glycosaminoglycans. Nature *383*, 550-553.

Goldberg, A.L. (1972). Degradation of abnormal proteins in *Escherichia coli.* Proceedings of the National Academy of Sciences of the United States of America *69*, 422-&.

Goldberg, A.L. (2003). Protein degradation and protection against misfolded or damaged proteins. Nature *426*, 895-899.

Gong, C.X., Liu, F., Grundke-Iqbal, I., and Iqbal, K. (2005). Post-translational modifications of tau protein in Alzheimer's disease. Journal of Neural Transmission *112*, 813-838.

Gotz, J., Chen, F., van Dorpe, J., and Nitsch, R.M. (2001). Formation of neurofibrillary tangles in P301L tau transgenic mice induced by A beta 42 fibrils. Science *293*, 1491-1495.

Grau, S., Baldi, A., Bussani, R., Tian, X.D., Stefanescu, R., Przybylski, M., Richards, P., Jones, S.A., Shridhar, V., Clausen, T.*, et al.* (2005). Implications of the serine protease HtrA1

in amyloid precursor protein processing. Proceedings of the National Academy of Sciences of the United States of America *102*, 6021-6026.

Grau, S., Richards, P.J., Kerr, B., Hughes, C., Caterson, B., Williams, A.S., Junker, U., Jones, S.A., Clausen, T., and Ehrmann, M. (2006). The role of human HtrA1 in arthritic disease. Journal of Biological Chemistry *281*, 6124-6129.

Greber, U.F., Willetts, M., Webster, P., and Helenius, A. (1993). Stepwise dismantling of adenovirus-2 during entry into cells. Cell *75*, 477-486.

Grundkeiqbal, I., Iqbal, K., Quinlan, M., Tung, Y.C., Zaidi, M.S., and Wisniewski, H.M. (1986). Microtubule-associated protein Tau - a component of Alzheimer paired helical filaments. Journal of Biological Chemistry *261*, 6084-6089.

Guo, J.L., Covell, D.J., Daniels, J.P., Iba, M., Stieber, A., Zhang, B., Riddle, D.M., Kwong, L.K., Xu, Y., Trojanowski, J.Q.*, et al.* (2013). Distinct alpha-Synuclein Strains Differentially Promote Tau Inclusions in Neurons. Cell *154*, 103-117.

Guo, J.L., and Lee, V.M.Y. (2011). Seeding of Normal Tau by Pathological Tau Conformers Drives Pathogenesis of Alzheimer-like Tangles. Journal of Biological Chemistry *286*, 15317-15331.

Hagestedt, T., Lichtenberg, B., Wille, H., Mandelkow, E.M., and Mandelkow, E. (1989). Tau protein becomes long and stiff upon phosphorylation - correlation between paracrystalline structure and degree of phosphorylation. Journal of Cell Biology *109*, 1643-1651.

Hanahan, D. (1983). Studies on transformation of *Escherichia coli* with plasmids. Journal of Molecular Biology *166*, 557-580.

Harada, A., Oguchi, K., Okabe, S., Kuno, J., Terada, S., Ohshima, T., Satoyoshitake, R., Takei, Y., Noda, T., and Hirokawa, N. (1994). Altered microtubule organization in small-caliber axons of mice lacking Tau protein. Nature *369*, 488-491.

Hardy, J. (2009). The amyloid hypothesis for Alzheimer's disease: a critical reappraisal. Journal of Neurochemistry *110*, 1129-1134.

Harlin, H., Reffey, S.B., Duckett, C.S., Lindsten, T., and Thompson, C.B. (2001). Characterization of XIAP-deficient mice. Molecular and Cellular Biology *21*, 3604-3608.

Hartl, F.U., Bracher, A., and Hayer-Hartl, M. (2011). Molecular chaperones in protein folding and proteostasis. Nature *475*, 324-332.

Hasenbein, S., Merdanovic, M., and Ehrmann, M. (2007). Determinants of regulated proteolysis in signal transduction. Genes & Development *21*, 6-10.

Haslberger, T., Zdanowicz, A., Brand, I., Kirstein, J., Turgay, K., Mogk, A., and Bukau, B. (2008). Protein disaggregation by the AAA plus chaperone ClpB involves partial threading of looped polypeptide segments. Nature Structural & Molecular Biology *15*, 641-650.

Helbecque, N., Abderrhamani, A., Meylan, L., Riederer, B., Mooser, V., Miklossy, J., Delplanque, J., Boutin, P., Nicod, P., Haefliger, J.A.*, et al.* (2003). Islet-brain1/C-Jun N-terminal kinase interacting protein-1 (IB1/JIP-1) promoter variant is associated with Alzheimer's disease. Molecular Psychiatry *8*, 413-422.

Hershko, A., and Ciechanover, A. (1998). The ubiquitin system. Annual Review of Biochemistry *67*, 425-479.

Heukeshoven, J., and Dernick, R. (1988). Improved silver staining procedure for fast staining in phastsystem development unit. 1. Staining of sodium dodecyl-sulfate gels. Electrophoresis *9*, 28-32.

Higuchi, M., Iwata, N., Matsuba, Y., Takano, J., Suemoto, T., Maeda, J., Ji, B., Ono, M., Staufenbiel, M., Suhara, T.*, et al.* (2012). Mechanistic involvement of the calpain-calpastatin system in Alzheimer neuropathology. Faseb Journal *26*, 1204-1217.

Hoover, B.R., Reed, M.N., Su, J.J., Penrod, R.D., Kotilinek, L.A., Grant, M.K., Pitstick, R., Carlson, G.A., Lanier, L.M., Yuan, L.L.*, et al.* (2010). Tau Mislocalization to Dendritic Spines Mediates Synaptic Dysfunction Independently of Neurodegeneration. Neuron *68*, 1067-1081.

Hou, J., Clemmons, D.R., and Smeekens, S. (2005). Expression and characterization of a serine protease that preferentially cleaves insulin-like growth factor binding protein-5. Journal of Cellular Biochemistry *94*, 470-484.

Hutton, M., Lendon, C.L., Rizzu, P., Baker, M., Froelich, S., Houlden, H., Pickering-Brown, S., Chakraverty, S., Isaacs, A., Grover, A.*, et al.* (1998). Association of missense and 5 '-splice-site mutations in tau with the inherited dementia FTDP-17. Nature *393*, 702-705.

Huvent, I., Kamah, A., Cantrelle, F.X., Barois, N., Slomianny, C., Smet-Nocca, C., Landrieu, I., and Lippens, G. (2014). A functional fragment of Tau forms fibers without the need for an intermolecular cysteine bridge. Biochemical and Biophysical Research Communications *445*, 299-303.

Inoue, Y., Kishimoto, A., Hirao, J., Yoshida, M., and Taguchi, H. (2001). Strong growth polarity of yeast prion fiber revealed by single fiber imaging. Journal of Biological Chemistry *276*, 35227-35230.

Iqbal, K., and Grundkeiqbal, I. (1991). Ubiquitination and abnormal phosphorylation of paired helical filaments in Alzheimers-disease. Molecular Neurobiology *5*, 399-410.

Ittner, L.M., and Gotz, J. (2011). Amyloid-beta and tau - a toxic pas de deux in Alzheimer's disease. Nature Reviews Neuroscience *12*, 67-72.

Jakes, R., Novak, M., Davison, M., and Wischik, C.M. (1991). Identification of 3-repeat and 4-repeat Tau isoforms within the PHF in Alzheimers-disease. Embo Journal *10*, 2725-2729.

Jarrett, J.T., and Lansbury, P.T. (1993). Seeding one-dimensional crystallization of amyloid - a pathogenic mechanism in Alzheimers-disease and Scrapie. Cell *73*, 1055-1058.

Jaru-Ampornpan, P., Liang, F.C., Nisthal, A., Nguyen, T.X., Wang, P.C., Shen, K., Mayo, S.L., and Shan, S.O. (2013). Mechanism of an ATP-independent Protein Disaggregase II. Distinct molecular interactions drive multiple steps during aggregate disassembly. Journal of Biological Chemistry *288*, 13431-13445.

Jeganathan, S., von Bergen, M., Mandelkow, E.M., and Mandelkow, E. (2008). The natively unfolded character of Tau and its aggregation to Alzheimer-like paired helical filaments. Biochemistry *47*, 10526-10539.

Jin, M., Shepardson, N., Yang, T., Chen, G., Walsh, D., and Selkoe, D.J. (2011). Soluble amyloid beta-protein dimers isolated from Alzheimer cortex directly induce Tau hyperphosphorylation and neuritic degeneration. Proceedings of the National Academy of Sciences of the United States of America *108*, 5819-5824.

Johnson, G.V.W., and Stoothoff, W.H. (2004). Tau phosphorylation in neuronal cell function and dysfunction. Journal of Cell Science *117*, 5721-5729.

Johnston, J.A., Ward, C.L., and Kopito, R.R. (1998). Aggresomes: A cellular response to misfolded proteins. Journal of Cell Biology *143*, 1883-1898.

Jucker, M., and Walker, L.C. (2013). Self-propagation of pathogenic protein aggregates in neurodegenerative diseases. Nature *501*, 45-51.

Kampers, T., Friedhoff, P., Biernat, J., and Mandelkow, E.M. (1996). RNA stimulates aggregation of microtubule-associated protein tau into Alzheimer-like paired helical filaments. Febs Letters *399*, 344-349.

Kampinga, H.H., and Craig, E.A. (2010). `The HSP70 chaperone machinery: J proteins as drivers of functional specificity. Nature Reviews Molecular Cell Biology *11*, 579-592.

Keck, S., Nitsch, R., Grune, T., and Ullrich, O. (2003). Proteasome inhibition by paired helical filament-tau in brains of patients with Alzheimer's disease. Journal of Neurochemistry *85*, 115-122.

Keller, J.N., Hanni, K.B., and Markesbery, W.R. (2000). Impaired proteasome function in Alzheimer's disease. Journal of Neurochemistry *75*, 436-439.

Khatoon, S., Grundkeiqbal, I., and Iqbal, K. (1994). Levels of normal and abnormally phosphorylated Tau in different cellular and regional compartments of Alzheimer-disease and control brains. Febs Letters *351*, 80-84.

Khlistunova, I., Biernat, J., Wang, Y.P., Pickhardt, M., von Bergen, M., Gazova, Z., Mandelkow, E., and Mandelkow, M. (2006). Inducible expression of tau repeat domain in cell models of tauopathy - Aggregation is toxic to cells but can be reversed by inhibitor drugs. Journal of Biological Chemistry *281*, 1205-1214.

Kidd, M. (1963). Paired helical filaments in electron microscopy of Alzheimers disease. Nature *197*, 192-&.

King, M.E., Ahuja, V., Binder, L.I., and Kuret, J. (1999). Ligand dependent tau filament formation: Implications for Alzheimer's disease progression. Biochemistry *38*, 14851-14859.

King, R.W., Deshaies, R.J., Peters, J.M., and Kirschner, M.W. (1996). How proteolysis drives the cell cycle. Science *274*, 1652-1659.

Komatsu, M., Waguri, S., Chiba, T., Murata, S., Iwata, J., Tanida, I., Ueno, T., Koike, M., Uchiyama, Y., Kominami, E.*, et al.* (2006). Loss of autophagy in the central nervous system causes neurodegeneration in mice. Nature *441*, 880-884.

Kovacech, B., and Novak, M. (2010). Tau Truncation is a Productive Posttranslational Modification of Neurofibrillary Degeneration in Alzheimer's Disease. Current Alzheimer Research *7*, 708-716.

Krojer, T., Garrido-Franco, M., Huber, R., Ehrmann, M., and Clausen, T. (2002). Crystal structure of DegP (HtrA) reveals a new protease-chaperone machine. Nature *416*, 455-459.

Krojer, T., Sawa, J., Schafer, E., Saibil, H.R., Ehrmann, M., and Clausen, T. (2008). Structural basis for the regulated protease and chaperone function of DegP. Nature *453*, 885-U831.

Kuret, J., Chirita, C.N., Congdon, E.E., Kannanayakal, T., Li, G.B., Necula, M., Yin, H.S., and Zhong, Q. (2005a). Pathways of tau fibrillization. Biochimica Et Biophysica Acta-Molecular Basis of Disease *1739*, 167-178.

Kuret, J., Congdon, E.E., Li, G.B., Yin, H.H., Yu, X., and Zhong, Q. (2005b). Evaluating triggers and enhancers of tau fibrillization. Microscopy Research and Technique *67*, 141-155.

Kuriyan, J., and Eisenberg, D. (2007). The origin of protein interactions and allostery in colocalization. Nature *450*, 983-990.

Laemmli, U.K. (1970). Cleavage of structural proteins during assembly of head of Bacteriophage-t4. Nature *227*, 680-&.

Launay, S., Maubert, E., Lebeurrier, N., Tennstaedt, A., Campioni, M., Docagne, F., Gabriel, C., Dauphinot, L., Potier, M.C., Ehrmann, M.*, et al.* (2008). HtrA1-dependent proteolysis of TGF-beta controls both neuronal maturation and developmental survival. Cell Death and Differentiation *15*, 1408-1416.

Lauren, J., Gimbel, D.A., Nygaard, H.B., Gilbert, J.W., and Strittmatter, S.M. (2009). Cellular prion protein mediates impairment of synaptic plasticity by amyloid-beta oligomers. Nature *457*, 1128-U1184.

Lee, G.J., Roseman, A.M., Saibil, H.R., and Vierling, E. (1997). A small heat shock protein stably binds heat-denatured model substrates and can maintain a substrate in a folding-competent state. Embo Journal *16*, 659-671.

Levine, H. (1993). Thioflavine T interaction with synthetic Alzheimers-disease beta-amyloid peptides - detection of amyloid aggregation in solution. Protein Science *2*, 404-410.

Li, W.K., and Lee, V.M.Y. (2006). Characterization of two VQIXXK motifs for tau fibrillization in vitro. Biochemistry *45*, 15692-15701.

Lim, Y.W., Yoon, S.Y., Choi, J.E., Kim, S.M., Lee, H.S., Choe, H., Lee, S.C., and Kim, D.H. (2010). Maintained activity of glycogen synthase kinase-3 beta despite of its phosphorylation at serine-9 in okadaic acid-induced neurodegenerative model. Biochemical and Biophysical Research Communications *395*, 207-212.

Lipinska, B., Sharma, S., and Georgopoulos, C. (1988). Sequence-analysis and regulation of the htrA gene of *Escherichia coli* - a sigma-32-independent mechanism of heat-inducible transcription. Nucleic Acids Research *16*, 10053-10067.

Love, S., Saitoh, T., Quijada, S., Cole, G.M., and Terry, R.D. (1988). Alz-50, Ubiquitin and Tau-immunoreactivity of neurofibrillary tangles, pick bodies and Lewy bodies. Journal of Neuropathology and Experimental Neurology *47*, 393-405.

Maillard, R.A., Chistol, G., Sen, M., Righini, M., Tan, J., Kaiser, C.M., Hodges, C., Martin, A., and Bustamante, C. (2011). ClpX(P) Generates Mechanical Force to Unfold and Translocate Its Protein Substrates. Cell *145*, 459-469.

Marcus, E.M., and Jacobson, S. (2003). Integrated Neuroscience (Kluwer Academic Publishers).

Maxfield, F.R., and McGraw, T.E. (2004). Endocytic recycling. Nature Reviews Molecular Cell Biology *5*, 121-132.

McClellan, A.J., Tam, S., Kaganovich, D., and Frydman, J. (2005). Protein quality control: chaperones culling corrupt conformations. Nature Cell Biology *7*, 736-741.

Merdanovic, M., Mamant, N., Meltzer, M., Poepsel, S., Auckenthaler, A., Melgaard, R., Hauske, P., Nagel-Steger, L., Clarke, A.R., Kaiser, M.*, et al.* (2010). Determinants of structural and functional plasticity of a widely conserved protease chaperone complex. Nature Structural & Molecular Biology *17*, 837-U884.

Merlini, G., and Bellotti, V. (2003). Molecular mechanisms of amyloidosis. New England Journal of Medicine *349*, 583-596.

Merril, C.R., Dunau, M.L., and Goldman, D. (1981). A rapid sensitive silver stain for polypeptides in polyacrylamide gels. Analytical Biochemistry *110*, 201-207.

Meusser, B., Hirsch, C., Jarosch, E., and Sommer, T. (2005). ERAD: the long road to destruction. Nature Cell Biology *7*, 766-772.

Michalski, A., Damoc, E., Lange, O., Denisov, E., Nolting, D., Mueller, M., Viner, R., Schwartz, J., Remes, P., Belford, M.*, et al.* (2012). Ultra High Resolution Linear Ion Trap Orbitrap Mass Spectrometer (Orbitrap Elite) Facilitates Top Down LC MS/MS and Versatile Peptide Fragmentation Modes. Molecular & Cellular Proteomics *11*.

Min, S.W., Cho, S.H., Zhou, Y.G., Schroeder, S., Haroutunian, V., Seeley, W.W., Huang, E.J., Shen, Y., Masliah, E., Mukherjee, C.*, et al.* (2010). Acetylation of Tau Inhibits Its Degradation and Contributes to Tauopathy. Neuron *67*, 953-966.

Mogk, A., Deuerling, E., Vorderwulbecke, S., Vierling, E., and Bukau, B. (2003). Small heat shock proteins, ClpB and the DnaK system form a functional triade in reversing protein aggregation. Molecular Microbiology *50*, 585-595.

Moisoi, N., Klupsch, K., Fedele, V., East, P., Sharma, S., Renton, A., Plun-Favreau, H., Edwards, R.E., Teismann, P., Esposti, M.D.*, et al.* (2009). Mitochondrial dysfunction triggered by loss of HtrA2 results in the activation of a brain-specific transcriptional stress response. Cell Death and Differentiation *16*, 449-464.

Morimoto, R.I. (2008). Proteotoxic stress and inducible chaperone networks in neurodegenerative disease and aging. Genes & Development *22*, 1427-1438.

Munch, G., Deuther-Conrad, W., and Gasic-Milenkovic, J. (2002). Glycoxidative stress creates a vicious cycle of neurodegeneration in Alzheimer's disease - a target for neuroprotective treatment strategies? Journal of Neural Transmission-Supplement, 303-307.

Munro, S., and Pelham, H.R.B. (1986). An Hsp70-like protein in the ER - identity with the 78 kDa glucose-regulated protein and immunoglobulin heavy-chain binding-protein. Cell *46*, 291-300.

Nellaiappan, K., Risitano, A., Liu, G.M., Nicklas, G., and Kagan, H.M. (2000). Fully processed lysyl oxidase catalyst translocates from the extracellular space into nuclei of aortic smooth-muscle cells. Journal of Cellular Biochemistry *79*, 576-582.

Nelson, R., Sawaya, M.R., Balbirnie, M., Madsen, A.O., Riekel, C., Grothe, R., and Eisenberg, D. (2005). Structure of the cross-beta spine of amyloid-like fibrils. Nature *435*, 773-778.

Nilsson, M.R., Driscoll, M., and Raleigh, D.P. (2002). Low levels of asparagine deamidation can have a dramatic effect on aggregation of amyloidogenic peptides: Implications for the study of amyloid formation. Protein Science *11*, 342-349.

Olsen, J.V., de Godoy, L.M.F., Li, G.Q., Macek, B., Mortensen, P., Pesch, R., Makarov, A., Lange, O., Horning, S., and Mann, M. (2005). Parts per million mass accuracy on an orbitrap mass spectrometer via lock mass injection into a C-trap. Molecular & Cellular Proteomics *4*, 2010-2021.

Pallen, M.J., and Wren, B.W. (1997). The HtrA family of serine proteases. Molecular Microbiology *26*, 209-221.

Park, S.Y., and Ferreira, A. (2005). The generation of a 17 kDa neurotoxic fragment: An alternative mechanism by which tau mediates beta-amyloid-induced neurodegeneration. Journal of Neuroscience *25*, 5365-5375.

Patil, S.M., Mehta, A., Jha, S., and Alexandrescu, A.T. (2011). Heterogeneous Amylin Fibril Growth Mechanisms Imaged by Total Internal Reflection Fluorescence Microscopy. Biochemistry *50*, 2808-2819.

Perkins, D.N., Pappin, D.J.C., Creasy, D.M., and Cottrell, J.S. (1999). Probability-based protein identification by searching sequence databases using mass spectrometry data. Electrophoresis *20*, 3551-3567.

Perutz, M.F., and Windle, A.H. (2001). Cause of neural death in neurodegenerative diseases attributable to expansion of glutamine repeats. Nature *412*, 143-144.

Petrucelli, L., Dickson, D., Kehoe, K., Taylor, J., Snyder, H., Grover, A., De Lucia, M., McGowan, E., Lewis, J., Prihar, G.*, et al.* (2004). CHIP and Hsp70 regulate tau ubiquitination, degradation and aggregation. Hum Mol Genet *13*, 703-714.

Rampelt, H., Kirstein-Miles, J., Nillegoda, N.B., Chi, K., Scholz, S.R., Morimoto, R.I., and Bukau, B. (2012). Metazoan Hsp70 machines use Hsp110 to power protein disaggregation. Embo Journal *31*, 4221-4235.

Rappsilber, J., Mann, M., and Ishihama, Y. (2007). Protocol for micro-purification, enrichment, pre-fractionation and storage of peptides for proteomics using StageTips. Nature Protocols *2*, 1896-1906.

Ratajczak, E., Zietkiewicz, S., and Liberek, K. (2009). Distinct Activities of Escherichia coli Small Heat Shock Proteins IbpA and IbpB Promote Efficient Protein Disaggregation. Journal of Molecular Biology *386*, 178-189.

Ren, P.H., Lauckner, J.E., Kachirskaia, I., Heuser, J.E., Melki, R., and Kopito, R.R. (2009). Cytoplasmic penetration and persistent infection of mammalian cells by polyglutamine aggregates. Nature Cell Biology *11*, 219-U232.

Rideout, H.J., Lang-Rollin, I., and Stefanis, L. (2004). Involvement of macroautophagy in the dissolution of neuronal inclusions. International Journal of Biochemistry & Cell Biology *36*, 2551-2562.

Rissman, R.A., Poon, W.W., Blurton-Jones, M., Oddo, S., Torp, R., Vitek, M.P., LaFerla, F.M., Rohn, T.T., and Cotman, C.W. (2004). Caspase-cleavage of tau is an early event in Alzheimer disease tangle pathology. Journal of Clinical Investigation *114*, 121-130.

Roberson, E.D., Scearce-Levie, K., Palop, J.J., Yan, F.R., Cheng, I.H., Wu, T., Gerstein, H., Yu, G.Q., and Mucke, L. (2007). Reducing endogenous tau ameliorates amyloid beta-induced deficits in an Alzheimer's disease mouse model. Science *316*, 750-754.

Ross, C.A., and Poirier, M.A. (2004). Protein aggregation and neurodegenerative disease. Nature Medicine *10*, S10-S17.

Ross, C.A., and Poirier, M.A. (2005). What is the role of protein aggregation in neurodegeneration? Nature Reviews Molecular Cell Biology *6*, 891-898.

Runyon, S.T., Zhang, Y.G., Appleton, B.A., Sazinsky, S.L., Wu, P., Pan, B., Wiesmann, C., Skelton, N.J., and Sidhu, S.S. (2007). Structural and functional analysis of the PDZ domains of human HtrA1 and HtrA3. Protein Science *16*, 2454-2471.

Salvesen, G.S., and Dixit, V.M. (1997). Caspases: Intracellular signaling by proteolysis. Cell *91*, 443-446.

Sato, S., Tatebayashi, Y., Akagi, T., Chui, D.H., Murayama, M., Miyasaka, T., Planel, E., Tanemura, K., Sun, X.Y., Hashikawa, T.*, et al.* (2002). Aberrant tau phosphorylation by glycogen synthase kinase-3 beta and JNK3 induces oligomeric tau fibrils in COS-7 cells. Journal of Biological Chemistry *277*, 42060-42065.

Sawaya, M.R., Sambashivan, S., Nelson, R., Ivanova, M.I., Sievers, S.A., Apostol, M.I., Thompson, M.J., Balbirnie, M., Wiltzius, J.J.W., McFarlane, H.T.*, et al.* (2007). Atomic structures of amyloid cross-beta spines reveal varied steric zippers. Nature *447*, 453-457.

Schneider, A., Biernat, J., von Bergen, M., Mandelkow, E., and Mandelkow, E.M. (1999). Phosphorylation that detaches tau protein from microtubules (Ser262, Ser214) also protects it against aggregation into Alzheimer paired helical filaments. Biochemistry *38*, 3549-3558.

Schneider, C.A., Rasband, W.S., and Eliceiri, K.W. (2012). NIH Image to ImageJ: 25 years of image analysis. Nature Methods *9*, 671-675.

Schweers, O., Mandelkow, E.M., Biernat, J., and Mandelkow, E. (1995). Oxidation of Cysteine-322 in the repeat domain of microtubule-associated protein Tau controls the *in vitro* assembly of paired helical filaments. Proceedings of the National Academy of Sciences of the United States of America *92*, 8463-8467.

Selkoe, D. (2001). Alzheimer's disease: genes, proteins, and therapy. Physiol Rev *81*, 741-766.

Selkoe, D.J., Ihara, Y., and Salazar, F.J. (1982). Alzheimers-disease - insolubility of partially purified paired helical filaments in sodium dodecyl-sulfate and urea. Science *215*, 1243-1245.

Sheng, M., and Sala, C. (2001). PDZ domains and the organization of supramolecular complexes. Annual Review of Neuroscience *24*, 1-29.

Smith, M.A., Harris, P.L.R., Sayre, L.M., Beckman, J.S., and Perry, G. (1997). Widespread peroxynitrite-mediated damage in Alzheimer's disease. Journal of Neuroscience *17*, 2653-2657.

Soto, C. (2012). Transmissible Proteins: Expanding the Prion Heresy. Cell *149*, 968-977.

Spiess, C., Beil, A., and Ehrmann, M. (1999). A temperature-dependent switch from chaperone to protease in a widely conserved heat shock protein. Cell *97*, 339-347.

Spillantini, M.G., Murrell, J.R., Goedert, M., Farlow, M.R., Klug, A., and Ghetti, B. (1998). Mutation in the tau gene in familial multiple system tauopathy with presenile dementia. Proceedings of the National Academy of Sciences of the United States of America *95*, 7737-7741.

Stetler-Stevenson, W.G., and Yu, A.E. (2001). Proteases in invasion: matrix metalloproteinases. Seminars in Cancer Biology *11*, 143-152.

Strauss, K.M., Martins, L.M., Plun-Favreau, H., Marx, F.P., Kautzmann, S., Berg, D., Gasser, T., Wszolek, Z., Muller, T., Bornemann, A.*, et al.* (2005). Loss of function mutations in the gene encoding Omi/HtrA2 in Parkinson's disease. Human Molecular Genetics *14*, 2099-2111.

Stroud, R.M., Kossiakoff, A.A., and Chambers, J.L. (1977). MECHANISMS OF ZYMOGEN ACTIVATION. Annual Review of Biophysics and Bioengineering *6*, 177-193.

Sun, X.W., Ouyang, M., Guo, J.K., Ma, J.F., Lu, C.M., Adam, Z., and Zhang, L.X. (2010). The thylakoid protease Deg1 is involved in photosystem-II assembly in Arabidopsis thaliana. Plant Journal *62*, 240-249.

Sun, Y., and MacRae, T.H. (2005). Small heat shock proteins: molecular structure and chaperone function. Cellular and Molecular Life Sciences *62*, 2460-2476.

Sunde, M., Serpell, L.C., Bartlam, M., Fraser, P.E., Pepys, M.B., and Blake, C.C.F. (1997). Common core structure of amyloid fibrils by synchrotron X-ray diffraction. Journal of Molecular Biology *273*, 729-739.

Tarcsa, E., Szymanska, G., Lecker, S., O'Connor, C.M., and Goldberg, A.L. (2000). Ca2+-free calmodulin and calmodulin damaged by in vitro aging are selectively degraded by 26 S proteasomes without ubiquitination. Journal of Biological Chemistry *275*, 20295-20301.

Terry, R.D., Masliah, E., Salmon, D.P., Butters, N., Deteresa, R., Hill, R., Hansen, L.A., and Katzman, R. (1991). Physical basis of cognitive alterations in Alzheimers-disease - synapse loss is the major correlate of cognitive impairment. Annals of Neurology *30*, 572-580.

Truebestein, L., Tennstaedt, A., Moonig, T., Krojer, T., Canellas, F., Kaiser, M., Clausen, T., and Ehrmann, M. (2011). Substrate-induced remodeling of the active site regulates human HTRA1 activity. Nature Structural & Molecular Biology *18*, 386-388.

Tyedmers, J., Mogk, A., and Bukau, B. (2010). Cellular strategies for controlling protein aggregation. Nature Reviews Molecular Cell Biology *11*, 777-788.

Vabulas, R.M., Raychaudhuri, S., Hayer-Hartl, M., and Hartl, F.U. (2010). Protein Folding in the Cytoplasm and the Heat Shock Response. Cold Spring Harbor Perspectives in Biology *2*.

Verhagen, A.M., Silke, J., Ekert, P.G., Pakusch, M., Kaufmann, H., Connolly, L.M., Day, C.L., Tikoo, A., Burke, R., Wrobel, C.*, et al.* (2002). HtrA2 promotes cell death through its serine protease activity and its ability to antagonize inhibitor of apoptosis proteins. Journal of Biological Chemistry *277*, 445-454.

Verreault, A., Kaufman, P.D., Kobayashi, R., and Stillman, B. (1996). Nucleosome assembly by a complex of CAF-1 and acetylated histones H3/H4. Cell *87*, 95-104.

Vogelsberg-Ragaglia, V., Bruce, J., Richter-Landsberg, C., Zhang, B., Hong, M., Trojanowski, J.Q., and Lee, V.M.Y. (2000). Distinct FTDP-17 missense mutations in tau produce tau aggregates and other pathological phenotypes in transfected CHO cells. Molecular Biology of the Cell *11*, 4093-4104.

von Bergen, M., Barghorn, S., Li, L., Marx, A., Biernat, J., Mandelkow, E.M., and Mandelkow, E. (2001). Mutations of tau protein in frontotemporal dementia promote aggregation of paired helical filaments by enhancing local beta-structure. Journal of Biological Chemistry *276*, 48165-48174.

von Bergen, M., Friedhoff, P., Biernat, J., Heberle, J., Mandelkow, E.M., and Mandelkow, E. (2000). Assembly of tau protein into Alzheimer paired helical filaments depends on a local sequence motif ((306)VQIVYK(311)) forming beta structure. Proceedings of the National Academy of Sciences of the United States of America *97*, 5129-5134.

Wang, J.Z., GrundkeIqbal, I., and Iqbal, K. (1996). Glycosylation of microtubule-associated protein tau: An abnormal posttranslational modification in Alzheimer's disease. Nature Medicine *2*, 871-875.

Wang, Y.P., Biernat, J., Pickhardt, M., Mandelkow, E., and Mandelkow, E.M. (2007). Stepwise proteolysis liberates tau fragments that nucleate the Alzheimer-like aggregation of full-length tau in a neuronal cell model. Proceedings of the National Academy of Sciences of the United States of America *104*, 10252-10257.

Wang, Y.P., Martinez-Vicente, M., Kruger, U., Kaushik, S., Wong, E., Mandelkow, E.M., Cuervo, A.M., and Mandelkow, E. (2009). Tau fragmentation, aggregation and clearance: the dual role of lysosomal processing. Human Molecular Genetics *18*, 4153-4170.

Wegmann, S., Jung, Y.J., Chinnathambi, S., Mandelkow, E.M., Mandelkow, E., and Muller, D.J. (2010). Human Tau Isoforms Assemble into Ribbon-like Fibrils That Display Polymorphic Structure and Stability. Journal of Biological Chemistry *285*, 27302-27313.

Weibezahn, J., Tessarz, P., Schlieker, C., Zahn, R., Maglica, Z., Lee, S., Zentgraf, H., Weber-Ban, E.U., Dougan, D.A., Tsai, F.T.F.*, et al.* (2004). Thermotolerance requires refolding of aggregated proteins by substrate translocation through the central pore of ClpB. Cell *119*, 653-665.

Wickner, S., Maurizi, M.R., and Gottesman, S. (1999). Posttranslational quality control: Folding, refolding, and degrading proteins. Science *286*, 1888-1893.

Wilken, C., Kitzing, K., Kurzbauer, R., Ehrmann, M., and Clausen, T. (2004). Crystal structure of the DegS stress sensor: How a PDZ domain recognizes misfolded protein and activates a protease. Cell *117*, 483-494.

Wilson, D.M., and Binder, L.I. (1995). Polymerization of microtubule-associated protein Tau under near-physiological conditions. Journal of Biological Chemistry *270*, 24306-24314.

Wiltzius, J.J.W., Landau, M., Nelson, R., Sawaya, M.R., Apostol, M.I., Goldschmidt, L., Soriaga, A.B., Cascio, D., Rajashankar, K., and Eisenberg, D. (2009). Molecular mechanisms for protein-encoded inheritance. Nature Structural & Molecular Biology *16*, 973-U998.

Winkler, J., Tyedmers, J., Bukau, B., and Mogk, A. (2012). Hsp70 targets Hsp100 chaperones to substrates for protein disaggregation and prion fragmentation. Journal of Cell Biology *198*, 387-404.

Winklhofer, K.F., and Haass, C. (2010). Mitochondrial dysfunction in Parkinson's disease. Biochimica Et Biophysica Acta-Molecular Basis of Disease *1802*, 29-44.

Winner, B., Jappelli, R., Maji, S.K., Desplats, P.A., Boyer, L., Aigner, S., Hetzer, C., Loher, T., Vilar, M., Campionic, S*., et al.* (2011). In vivo demonstration that alpha-synuclein oligomers are toxic. Proceedings of the National Academy of Sciences of the United States of America *108*, 4194-4199.

Wischik, C.M., Novak, M., Edwards, P.C., Klug, A., Tichelaar, W., and Crowther, R.A. (1988). Structural Characterization of the Core of the Paired Helical Filament of Alzheimer Disease. Proceedings of the National Academy of Sciences of the United States of America *85*, 4884-4888.

Wisniewski, H.M., Narang, H.K., and Terry, R.D. (1976). Neurofibrillary Tangles of Paired Helical Filaments. Journal of the Neurological Sciences *27*, 173-181.

Wray, S., and Noble, W. (2009). Linking Amyloid and Tau Pathology in Alzheimer's Disease: The Role of Membrane Cholesterol in A beta-Mediated Tau Toxicity. Journal of Neuroscience *29*, 9665-9667.

Wu, J.W., Herman, M., Liu, L., Simoes, S., Acker, C.M., Figueroa, H., Steinberg, J.I., Margittai, M., Kayed, R., Zurzolo, C*., et al.* (2013). Small Misfolded Tau Species Are Internalized via Bulk Endocytosis and Anterogradely and Retrogradely Transported in Neurons. Journal of Biological Chemistry *288*, 1856-1870.

Wyatt, A.R., Yerbury, J.J., Ecroyd, H., and Wilson, M.R. (2013). Extracellular Chaperones and Proteostasis. In Annual Review of Biochemistry, Vol 82, R.D. Kornberg, ed. (Palo Alto: Annual Reviews), pp. 295-322.

Yanamandra, K., Kfoury, N., Jiang, H., Mahan, T.E., Ma, S.M., Maloney, S.E., Wozniak, D.F., Diamond, M.I., and Holtzman, D.M. (2013). Anti-Tau Antibodies that Block Tau Aggregate Seeding In Vitro Markedly Decrease Pathology and Improve Cognition In Vivo. Neuron *80*, 402-414.

Yu, A., Shibata, Y., Shah, B., Calamini, B., Lo, D.C., and Morimoto, R.I. (2014). Protein aggregation can inhibit clathrin-mediated endocytosis by chaperone competition. Proceedings of the National Academy of Sciences of the United States of America *111*, E1481-1490.

Zempel, H., Luedtke, J., Kumar, Y., Biernat, J., Dawson, H., Mandelkow, E., and Mandelkow, E.M. (2013). Amyloid-beta oligomers induce synaptic damage via Tau-dependent microtubule severing by TTLL6 and spastin. Embo Journal *32*, 2920-2937.

Zimmerman, S.B., and Trach, S.O. (1991). Estimation of macromolecule concentrations and excluded volume effects for the cytoplasm of *Escherichia coli*. Journal of Molecular Biology *222*, 599-620.

Appendix

Lebenslauf

Der Lebenslauf ist in der Online-Version aus Gründen des Datenschutzes nicht enthalten.

Erklärung:

Hiermit erkläre ich, gem. § 6 Abs. (2) f) der Promotionsordnung der Fakultäten für Biologie, Chemie und Mathematik zur Erlangung der Dr. rer. nat., dass ich das Arbeitgebiet, dem das Thema „Proteolysis and ATP-independent Disaggregation of Tau Aggregates by the Human Serine Protease HTRA1“ zuzuordnen ist, in Forschung und Lehre vertrete und den Antrag von Simon Pöpsel befürworte und die Betreuung auch im Falle eines Weggangs, wenn nicht wichtige Gründe dem entgegenstehen, weiterführen werde.

Essen, den _____ _____

Unterschrift eines Mitglieds der Universität Duisburg - Essen

Erklärung:

Hiermit erkläre ich, gem. § 7 Abs. (2) c) + e) der Promotionsordnung Fakultäten für Biologie, Chemie und Mathematik zur Erlangung des Dr. rer. nat., dass ich die vorliegende Dissertation selbständig verfasst und mich keiner anderen als der angegebenen Hilfsmittel bedient habe.

Essen, den _____ _____

Unterschrift des/r Doktoranden/in

Erklärung:

Hiermit erkläre ich, gem. § 7 Abs. (2) d) + f) der Promotionsordnung der Fakultäten für Biologie, Chemie und Mathematik zur Erlangung des Dr. rer. nat., dass ich keine anderen Promotionen bzw. Promotionsversuche in der Vergangenheit durchgeführt habe und dass diese Arbeit von keiner anderen Fakultät/ Fachbereich abgelehnt worden ist.

Essen, den _____ _____

Unterschrift des Doktoranden